Reliability of methods to determine arterial oxygen-haemoglobin saturation in immobilized southern white rhinoceros (*Ceratotherium simum simum)*

by

Thembeka Kim Mtetwa

BSc, BHSc (Hons) & MSc (Vet Sci)

Submitted for the degree of Doctor of Philosophy (PhD)

in the Department of Paraclinical Sciences

in the Faculty of Veterinary Science, at the University of Pretoria

PROMOTERS: Prof Leith CR Meyer & Prof Edward P Snelling

09 December 2022

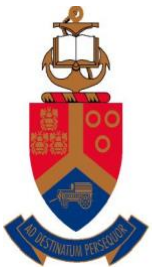

UNIVERSITEIT VAN PRETORIA
UNIVERSITY OF PRETORIA
YUNIBESITHI YA PRETORIA

Declaration

I, Thembeka K Mtetwa, hereby declare that the research presented in this thesis, was conceived and executed by myself, under guidance from my supervisors.

Neither the substance, nor any part of the thesis has been submitted in the past, or is to be submitted for a degree at the University of Pretoria or any other University.

This thesis is presented for fulfilment of the requirements for degree of Doctor of Philosophy (PhD).

Signature: Date: _____

Thembeka K Mtetwa

Ethical statement

I, **Thembeka K Mtetwa** (student no. **u04892497**) declare that ethical standards required in terms of the University of Pretoria's Code of Ethics for Researchers and the Policy guidelines for responsible research were followed accordingly.

The Research Ethics Committee of the Faculty of Veterinary Science (University of Pretoria) granted the research protocol of the present study a clearance with number: **REC246-19**

The author further declares that the ethical standards required in terms of the University of Pretoria's Code of Ethics for researchers and the policy guidelines for responsible research were observed.

Signature: Date:_____

Thembeka K Mtetwa

Acknowledgements

Throughout my PhD I received a great amount of support and assistance from a number of people who I will forever be indebted to. Thank you for your help and assistance during this challenging and enlightening endeavour.

I would first like to acknowledge and thank the following bodies for funding the research: National Research Foundation (NRF) of South Africa, the South African Veterinary Association (Wildlife Group), the Wiederhold Foundation, Dnata Wild-over-Wildlife, South African Government Health and Welfare Sector Education and Training Authority (HWSETA) and Agriculture Sector Education Training Authority (AGRISETA), the Centre for Veterinary Wildlife Research, and the Department of Paraclinical Sciences and the Department of Veterinary Tropical Diseases, in the Faculty of Veterinary Science, at the University of Pretoria.

I want to also thank the Veterinary Wildlife Services, South African National Parks, in the Kruger National Parks for allowing me to access and use their facilities. I am most grateful to their entire animal handling team for their collaboration, caring for the rhinoceros and the many hours they dedicated to animal handling and transportation.

I want to give specific thanks to the Veterinary Wildlife Services team including Tebogo, Guy and Leanna for all their assistance with data collection and sacrificing their time to make my study a success.

I want to thank Dr Peter Buss for his leadership, assistance with data collection, and extremely valuable feedback on my papers.

I also want to thank Prof Robin Gleed from Cornell University and Prof Emma Hooijberg, for your mentorship, support, and guidance during my PhD. You are very much appreciated. Thank you.

A very big thank you to Dr Frederik Pohlin, my friend and colleague. Your work ethic has motivated me greatly. Your support and the fun times we spent during this period made things a whole lot easier for me.

Thank you Drs Marion Lieberich and Luke Michaelides, your support and help during my data collection did not go unnoticed.

A special thank you to Dr Annette Roug and Ashleigh Donaldson who not only took their time to teach themselves the different methods and devices I used for my project but also dedicated their time to helping me to collect most of my data. Thank you so much guys, I appreciate you.

My friends – Valery and Ash.

Ash, thank you for not only being my friend but also my study buddy and helping me with all my data collection, data organization, data interpretation and write-up. Your work ethic and drive has been my greatest motivation. I appreciate you so much.

Valery and Ash, you guys have been with me through and through. Having friends in the same path as me has given me so much strength to push through during the tough days. Taking time out to meet and converse with you guys, the long nights on campus, and countless snack breaks have helped so much when I was overwhelmed. You have helped me to relax and laugh in stressful times, which made it easy for me to get back to my work. I appreciate you greatly. Thank you.

I would like to thank my wonderful supervisors, and mentors, Leith Meyer and Ned Snelling.

Ned, you went beyond your call of duty as my co-supervisor and mentor and became a friend who became an older brother I never had. I will forever be grateful for your support, advice, and encouragement in trying times and the endless coffee breaks made a whole lot of difference in my mood and my drive to finish. I also appreciate the time you took to teach me different skills, your ability to steer me towards the right direction with regards to my future and career. You have been a true blessing in this journey. Thank you so much! I am looking forward to working with you and learning more from you until we both retire!

Leith, I remember the first day I met you in 2016, a day that changed my entire life. After my Honours degree, I had given up on my research career, but you saw something in me that I couldn't see in myself. You did not only make me fall in love with research again but helped me grow in it. Thank you for allowing me to learn from you, pick your brain and to get know you outside of work. You are a true embodiment and definition of a mentor and friend. I know this journey has not been easy for you too, yet you were able to not only offer constructive criticism, but through all my mistakes you were extremely patient with me and not once gave up on me, and for that I will forever be endeared to you. Through you I have the honour to be amongst the best of the best in our field and even though it is

seemingly impossible I can only aim to be half as excellent a mentor to others as you are to me. Thank you so much! I am looking forward to working with you and learning more from you until we both retire!

I also want to thank my beautiful and supportive family: my mother Jennifer Mtetwa and my father Simon Mtetwa who have sacrificed a lot for me to be able to do my PhD. I cannot express my gratitude enough for the values you have instilled in me that have contributed to my work ethic and my level of professionalism. Through small tasks and responsibilities growing up, you have taught me hard work, consistency, kindness, and patience. It is precisely that foundation that you have both laid for me that has allowed me to endure until this level. Thank you very much and I love you.

My siblings Nobantu Mtsweni, Dineo and Ayanda Mtetwa, for your enduring support and words of encouragement when I dedicated most of my years into my career. You have allowed me to be who I am freely without fear or favour and that always helped me to realise my own potential. How you always reminded me what an inspiration I am to you and others made me realise how capable and worthy I am to be where I am today. I could have not asked for better loving, caring and supportive siblings than you. Thank you very much and I love you.

To my son Luthando Mbuyisa and my nieces Zamandala, Nomakhetho and Sthokozile Mtsweni, watching you grow has brought me great joy, motivation, and encouragement to finish my PhD. You are a true definition of the saying “when you want to quit, remember who is looking” knowing that you are the next generation looking up to me has given me no other option but to keep on going. Thank you very much and I love you.

There is a new saying; “behind this successful black woman is an equally successful and supportive black man.” Mr Qiniso Mbuyisa, you carried me through this challenging yet fulfilling time, through the darkest days, happiest days and cheered me on over the finish line. Yes, I am proud to have done the work, but I can honestly say, hand on heart, that I wouldn’t have made it without your unconditional love, support, and patience. Thank you so much S’thandwa sam’, I love you, forever!

Table of contents

Declaration ..... **ii**

Ethical statement ..... **iii**

Acknowledgements ..... **iv**

List of tables ..... **ix**

List of figures ..... **xiii**

List of abbreviations ..... **xviii**

Thesis summary ..... **xx**

CHAPTER 1: **1**

General introduction, literature review and scope of the thesis **1**

1.1 General introduction **1**

1.2 Literature review **3**

1.2.1 Oxygen transport in the blood 3

1.2.2 Techniques to monitor blood oxygenation 17

1.2.3 General anaesthesia techniques used for white rhinoceros 57

1.3 Scope of the thesis **62**

1.3.1 Problem statement 62

1.3.2 Aims of the thesis 62

CHAPTER 2: **67**

Reliability of pulse oximetry, at four different attachment sites, in immobilized southern white rhinoceros (*Ceratotherium simum simum)* **67**

2.1 Abstract **68**

2.2 Introduction **69**

2.3 Materials & methods **70**

2.4 Results **75**

2.5 Discussion **80**

2.6 Conclusion **81**

CHAPTER 3: **82**

Reliability of a pulse oximeter and a pulse co-oximeter, at different attachment sites, to detect hypoxaemia in immobilized southern white rhinoceros (*Ceratotherium simum simum*) **82**

3.1 Abstract **83**

3.2 Introduction **84**

3.3 Materials & methods **87**

3.4 Results **94**

3.5 Discussion....104

3.6 Conclusion....108

CHAPTER 4:....110

Reliability of the Enterprise Point-of-Care (EPOC) blood analyser's calculated arterial oxygen-haemoglobin saturation, in immobilized southern white rhinoceros (*Ceratotherium simum simum*)....110

4.1 Abstract....111

4.2 Introduction....112

4.3 Materials & methods....113

4.4 Results....119

4.5 Discussion....125

4.6 Conclusion....127

CHAPTER 5:....128

Reliability of calculated arterial oxygen-haemoglobin saturation in immobilized southern white rhinoceros (*Ceratotherium simum simum*)....128

5.1 Abstract....129

5.2 Introduction....131

5.3 Materials & methods....134

5.4 Results....142

5.5 Discussion....147

5.6 Conclusion....150

CHAPTER 6:....152

General discussion and conclusions....152

6.1 Thesis limitations....154

6.2 Reliability of pulse oximetry and pulse co-oximetry, at different attachment sites, in immobilized southern white rhinoceros....155

6.3 Reliability of calculated arterial oxygen-haemoglobin saturation in immobilized southern white rhinoceros....159

6.4 Future studies and recommendations....163

6.5 Conclusion....166

References....168

Addendums....206

List of tables

Table 1.1 Summary of the some of the methods commonly used in clinical practice to monitor blood oxygenation [either as arterial partial pressure of oxygen (PaO_2), or arterial oxygen-haemoglobin saturation (SaO_2), or peripheral arterial oxygen-haemoglobin saturation (SpO_2)], and, or tissue oxygenation, perfusion and metabolism. The principle of measurement, variables measured or calculated, the site of measurement, advantages and disadvantages of each method are also summarised. 18

Table 1.2 The maximum and minimum millimolar absorptivity of oxyhaemoglobin (HbO_2) at wavelengths between 400 – 1000 nm. Also represented are the millimolar absorptivities at isosbestic points (the point where the two haemoglobin derivatives have the same millimolar absorptivity) between HbO_2 and the other haemoglobin derivatives [i.e., deoxyhaemoglobin (HHb), carboxyhaemoglobin (HbCO) and methaemoglobin (MetHb)]. These specific wavelengths are used in different spectrophotometric devices to measure the concentration (as the absorptivity or extinction coefficient) of HbO_2 and the other haemoglobin derivates (i.e., HHb, HbCO and MetHb). This table is from Van Kampen & Zijlstra 1983. Reprinted from Van Kampen, E. J., & Zijlstra, W. G. (1983). Spectrophotometry of haemoglobin and haemoglobin derivatives. *Advances in Clinical Chemistry*, *23*, 199-257, Copyright © 1983 Academic Press Inc. Published by Elsevier Ltd.....26

Table 2.1 Standard doses of drugs based on body mass used for white rhinoceros. Animals were weighed during the two-week habituation period and at the end of the immobilization and reversal by encouraging them to enter a crate, which was weighed using a crane balance. Rhinoceros weighed 1145 ± 75 kg [(mean ± standard deviation (SD)]. 71

Table 2.2 Number of time-matched paired measurements of peripheral oxygen-haemoglobin saturation from the pulse oximeters (SpO_2) at the four different attachment sites (third eyelid, cheek, rectum, and tail) compared with arterial oxygen-haemoglobin saturation measured from a benchtop co-oximeter (SaO_2). Presented are the number of paired measurements for all the data before the exclusion criteria was applied ("all data") and their pulse quality (green, amber, and red) are presented. Also presented are the total number of paired measurements that were not excluded ("pass data"), the number of paired measurements excluded ("excluded data"), and the exclusion criteria applied, are also presented. SD, standard deviation. Sample size (*n)*. 77

Table 2.3 Performance of the Nonin PalmSAT 2500A pulse oximeter (SpO_2) at four probe attachment sites (third eyelid, cheek, rectum and tail) compared with a benchtop AVOXimeter 4000 co-oximeter (SaO_2) reference method in eight southern white rhinoceros (*Ceratotherium simum simum*) after exclusion criteria were applied (i.e. table represents only "pass data"). SpO_2, peripheral oxygen-haemoglobin saturation. SaO_2, arterial oxygen-haemoglobin saturation. ARMS, area root mean squares; LOA, limits of agreement (minimum to maximum); *n* represents the sample size of the pass data. 78

Table 3.1 Standard doses of drugs based on body mass used for white rhinoceros. Animals were weighed intermittently during the four-to-six-week habituation period and at the end of each immobilization and reversal, by encouraging them to enter a crate that was weighed using a crane balance. Rhinoceros weighed 1311 ± 115 kg [mean ± standard deviation (SD)]. 88

Table 3.2 Number of time-matched (paired) measurements of the peripheral oxygen-haemoglobin saturation (SpO_2) from the Nonin PalmSAT pulse oximeters and Masimo Radical-7 pulse co-oximeters at the two attachment sites (third eyelid and ear pinna) compared with arterial oxygen-haemoglobin saturation (SaO_2) measured from the benchtop AVOXimeter 4000 co-oximeter. Presented are the number of paired measurements for all the data before the exclusion criteria was applied ("all data") and the Nonin PalmSAT pulse oximeters signal pulse quality (green, amber, and red). Also presented are the total number of paired measurements that were not excluded ("pass data"), the number of paired measurements excluded ("excluded data"), and the exclusion criteria applied. SD, standard deviation. Sample size (*n*).....95

Table 3.3 Performance of the Nonin PalmSAT 2500A pulse oximeters (SpO_2) and Masimo Radical-7 pulse co-oximeters (SpO_2) at two attachment sites (the third eyelid and the ear pinna) compared with a benchtop AVOXimeter 4000 co-oximeter (SaO_2) reference method in eight immobilized southern white rhinoceros (*Ceratotherium simum simum*) after exclusion criteria were applied (i.e., table represents only the "pass data"). SpO_2, peripheral oxygen-haemoglobin saturation. SaO_2, arterial oxygen-haemoglobin saturation. ARMS, area root mean squares; LOA, limits of agreement (minimum to maximum); *n* represents the sample size of the pass data. 99

Table 3.4 Sensitivity, specificity, positive and negative predictive values for the detection of hypoxaemia at the clinical decision limit of ≤92% based on the Nonin PalmSAT 2500A pulse oximeters' and Masimo Radical-7 pulse co-oximeters' SpO_2 measurements at two attachment sites (third eyelid and ear pinna sites) in immobilized southern white rhinoceros. The cut-off values for clinical hypoxaemia (SaO_2 ≤92%) were based on values applied in large animal anaesthesia (Haskins 2012). The area under the curve (AUC) values measured from the receiver operation characteristics (ROC) curves are also represented. SpO_2, peripheral arterial oxygen-haemoglobin saturation. 103

Table 4.1 Standard doses of drugs based on body mass used on white rhinoceros. Animals were weighed during the two-week habituation period and at the end of the immobilization and reversal by encouraging them to enter a crate, which was weighed using a crane balance. Rhinoceros weighed 1145 ± 75 kg (mean ± standard deviation (SD). 115

Table 4.2 Standard doses of drugs based on body mass used for white rhinoceros. Animals were weighed intermittently during the four-to-six-week habituation period and at the end of each immobilization, by encouraging them to enter a crate that was weighed using a

crane balance. Rhinoceros weighed 1311 ± 115 kg [mean ± standard deviation (SD)]. 116

Table 4.3 Bland-Altman and area root mean squares (ARMS) analysis showing the poor agreement within a number of different saturation ranges, between the arterial oxygen-haemoglobin saturation ($cSaO_2$) calculated from the EPOC blood analyser and the arterial oxygen-haemoglobin saturation (SaO_2) measured by a benchtop AVOXimeter 4000 co-oximeter. 121

Table 5.1 Standard doses of drugs based on body mass used for white rhinoceros. Animals were weighed intermittently during the four-to-six-week habituation period and at the end of each immobilization, by encouraging them to enter a crate that was weighed using a crane balance. Rhinoceros weighed 1311 ± 115 kg [mean ± standard deviation(SD)]. 135

Table 5.2 Mean ± [standard deviation (SD)] for arterial oxygen-haemoglobin saturations calculated from the oxygen content equation (method 1 $cSaO_2$) and calculated from the Siggaard-Andersen algorithm (method 2 $cSaO_2$), arterial oxygen-haemoglobin saturations (co-oximeter SaO_2) measured by the benchtop AVOXimeter 4000 co-oximeter, total oxygen content (CaO_2) measured by the method of Tucker (1967), arterial partial pressures of oxygen and carbon dioxide (PaO_2 and $PaCO_2$), pH, packed cell volume (PCV), and haemoglobin concentration [Hb] in immobilized southern white rhinoceros (*n* = 8). ...142

Table 5.3 Performance of arterial oxygen-haemoglobin saturation calculated from the oxygen content equation (method 1 $cSaO_2$), and those calculated from the Siggaard-Andersen algorithm (method 2 $cSaO_2$), in eight immobilized southern white rhinoceros (*Ceratotherium simum simum).* Methods 1 and 2 $cSaO_2$ were compared against the arterial oxygen-haemoglobin saturation measured by a benchtop AVOXimeter 4000 co-oximeter (co-oximeter SaO_2) reference method. ARMS, area root mean squares; LOA, limits of agreement (minimum to maximum); *n* represents the sample size between paired measurements.....144

List of figures

Figure 1.1 The basic structure of adult human haemoglobin molecule consisting of two identical ∝ chains and two identical β chains (a) and each globin chain contain an iron (Fe^{2+}) ion (b) in the centre of each ring responsible for binding to oxygen. Each haemoglobin binds to four oxygen molecules. Reprinted from Marieb, E. N., & Hoehn, K. (2013). The respiratory system. In *Human Anatomy and Physiology* (9th edn) (pp. 1056-1061). Pearson, London, UK, Copyright © 2013 with permission from Pearson Educators Inc.……..5

Figure 1.2 A standard human oxygen-haemoglobin dissociation curve represented by a sigmoidal relationship between the oxygen that is dissolved in the blood [PaO_2 (mmHg)] and the oxygen bound to haemoglobin in the red blood cells [SaO_2 (%)]. The right y-axis values represent the oxygen content (CaO_2), which is the total oxygen that is dissolved and bound to haemoglobin. The steep part of the oxygen-haemoglobin dissociation curve illustrates what happens in the lungs, when oxygen diffuses into the pulmonary circulation down its partial pressure gradient, across the alveolar-capillary interface, into the blood and increasing the PaO_2 (PaO_2 ~40 – 60 mmHg). As PaO_2 increases, one oxygen molecule binds to one Fe^{2+} ion (oxygen binding site) causing another oxygen binding site to be readily available, increasing the affinity of oxygen to haemoglobin. When one or two oxygen molecules are bound to haemoglobin, it becomes partially saturated and SaO_2 is approximately 50%. The plateau part of the curve illustrates what happens when the haemoglobin binds to the third and fourth oxygen molecule and changes from being partially saturated to being fully saturated with oxygen, and SaO_2 is above 75%. The blood colour shifts from dark blue to dark red as PaO_2 and SaO_2 increase in the arterial blood……8

Figure 1.3 Scaling relationship between P_{50} (the partial pressure of oxygen when haemoglobin is 50% saturated with oxygen) and body mass (in grams) of different mammals. The graph is plotted and described by the power function $\boldsymbol{P_{50} = 50.34{M_b}^{-0.054}}$, where P_{50} is measured in mmHg and body mass in grams. Mammals with small body mass have a high P_{50} and mammals with large body mass have a low P_{50}. Small body mass mammals with relatively high mass-specific metabolic rates have haemoglobins that tend to always facilitate oxygen offloading to the tissues (i.e., low oxygen affinities), having oxygen-haemoglobin dissociation curves that are more shifted to the right. Large body mass mammals with relatively low mass-specific metabolic rates have haemoglobins that tend to facilitate oxygen loading at low PaO_2 values (i.e., high oxygen affinities), therefore having oxygen-haemoglobin dissociation curves that are more shifted to the left. Reprinted from Schmidt-Neilsen, K., & Larimer, J. L. (1958). Oxygen dissociation curves of mammalian blood in relation to body size. *American*

Journal of Physiology-Legacy Content, *195*(2), 424-428, Copyright © 1958 with permission from American Physiological Society……...12

Figure 1.4 A conventional spectrophotometer as described by Zwart et al. 1984 used to measure the concentration of haemoglobin in the blood. The spectrophotometer consists of L, the light source [(a) deuterium and tungsten lamp] at wavelengths of 200 – 1000 nm, M, the monochromator (prism) that divides the light into different wavelengths, C, the cuvette that contains a blood sample and D, a light detector that measures the light absorbed by haemoglobin. Reprinted from Zwart, A., Buursma, A., Van Kampen, E. J., & Zijlstra, W. G. (1984). Multicomponent analysis of haemoglobin derivatives with reversed-optics spectrophotometer. *Clinical Chemistry*, *30*(3), 373-379, Copyright © 1984 Oxford University Press with permission from The American Association of Clinical Chemists, Inc……23

Figure 1.5 The extinction coefficients (or millimolar absorptivity) of oxyhaemoglobin and the other haemoglobin derivatives [deoxyhaemoglobin (HHb), carboxyhaemoglobin (HbCO) and methaemoglobin (MetHb)] at the visible and near infrared spectral range (i.e., at wavelengths of 600–1000 nm). These specific wavelengths and their extinction coefficients are used in different spectrophotometric devices to measure the concentration of HbO_2 and the other haemoglobin derivates. Reprinted from Van Kampen, E. J., & Zijlstra, W. G. (1983). Spectrophotometry of haemoglobin and haemoglobin derivatives. *Advances in Clinical Chemistry*, *23*, 199-257, Copyright © 1983 Academic Press Inc. with permission from Elsevier Ltd……...25

Figure 1.6 Calibration curve for the determination of arterial oxygen-haemoglobin saturation [SaO_2 (%)] showing the ratio of optical densities ($\frac{\mathbf{D2}}{\mathbf{D1}}$) in whole haemolysed blood between fully oxygenated (X_{HbO2}) and deoxygenated blood (X_{Hb}) at 505 nm and 605 nm. The curve was derived from blood samples of known oxygen and carbon dioxide partial pressures and the measured optical densities were used to calibrate the method of Nahas (1951) for the measurement of SaO_2. The Figure is from Nahas (1951). Reprinted from Nahas, G. G. (1951). Spectrophotometric determination of haemoglobin and oxyhaemoglobin in whole haemolysed blood. *Science*, *113*(2947), 723-725, Copyright © 1951 with permission from American Association for the advancement of Science.……28

Figure 1.7 Light absorbance between pulsatile arterial blood, non-pulsatile venous blood, soft tissue, skin, and bone (Fig. 1.7a). To determine SpO_2, the light absorbers are divided into alternating current (AC) and direct current (DC) (Fig. 1.7a). Peripheral arterial oxygen-haemoglobin saturation is then estimated from the ratio between the light absorbance of AC and DC at wavelengths of 660 and 940 nm. The relationship between SpO_2 (%) and the red and infrared absorption ratio obtained from empirical data that were collected in vivo from healthy patients with saturation levels between 70-100%, which

represents the calibration curve for pulse oximetry. At saturation levels below 70%, the values were extrapolated from saturation values measured by a benchtop co-oximeter, reference method. The calibration curve is from Pologe (1987) Reprinted from Pologe, J. A. (1987). Pulse oximetry: technical aspects of machine design. *International Anesthesiology Clinics*, *25*(3), 137-153, Copyright © 1987 with permission from Wolters Kluwer Health, Inc……..34

Figure 1.8 The molar extinction coefficient (or molar absorptivity) of oxyhaemoglobin (HbO_2 or O_2Hb) deoxyhaemoglobin (HHb), carboxyhaemoglobin (HbCO or COHb) at the visible and near infrared spectral range (600 – 1000 nm). Deoxyhaemoglobin (HHb) absorbs more light at the red wavelength of 660 nm (indicated by the black and white arrows at 660 nm), compared to oxyhaemoglobin (HbO_2). Oxyhaemoglobin absorbs more light at the infrared region (940 nm), compared to deoxyhaemoglobin (indicated by the black and white arrows at 940 nm) (Wukitsch et al. 1988; Chan et al. 2013). The millimolar coefficients of oxyhaemoglobin and deoxyhaemoglobin at the red and infrared region are used by pulse oximetry to calculate SpO_2. Reprinted from Chan, E. D., Chan, M. M., & Chan, M. M. (2013). Pulse oximetry: understanding its basic principles facilitates appreciation of its limitations. *Respiratory Medicine*, *107*(6), 789-799, Copyright © 2013 with permission from Elsevier Ltd…….36

Figure 1.9 Summary of the signal extraction technology used in Masimo Radical pulse co-oximeters to mitigate some of the limitations present in conventional pulse oximeters such as patient movement, low tissue perfusion and ambient light interference. The signal extraction technology utilizes adaptive filters and discrete saturation transform (DST) to calculate red, infrared and reference signals. Once these signals are known, the adaptive filter and DST identifies the correct arterial saturation and constructs a power curve that corresponds to the different SpO_2 values. Reprinted from Goldman, J. M., Petterson, M. T., Kopotic, R. J., & Barker, S. J. (2000). Masimo signal extraction pulse oximetry. *Journal of Clinical Monitoring and Computing*, *16*(7), 475-483, Copyright © 2000 with permission from Kluwer Academic Publishers……43

Figure 1.10 The Hill plot showing the relationship between arterial oxygen-haemoglobin saturation [SaO_2 or s (%)] and partial pressure of oxygen [PaO_2 or p (mmHg)]] according to the mathematical model of Siggaard-Andersen (1984). The Hill plot is explained by the binding theory when one oxygen molecule binds to haemoglobin until the fourth molecule, giving the S-shape of the oxygen-haemoglobin dissociation curve. The curve is made up of two logarithmic curves 1) a straight line and 2) a hyperbolic tangent curve and can be characterized by three variables: the point of symmetry (p_0, s_0), the slope at the point of symmetry (n_0) and the horizontal or vertical distance between the asymptotes (2h) that are used to construct the curve. Reprinted from Siggaard-Andersen, O. (1977). The van Slyke equation. *Scandinavian Journal of Clinical and*

Laboratory Investigation, *37*(sup146), 15-20, Copyright © 1984 with permission from Oxford University Press……..……54

Figure 2.1 Four Nonin PalmSAT pulse oximeters and 2000T transflectance probes used at four different attachment sites (third eyelid, cheek, rectum, and tail) in eight immobilized white rhinoceroses (*Ceratotherium simum simum*) (Fig. 2.1a) The transflectance probes (Nonin- 2000T) were placed against (Fig 2.1b) the third eyelid towards the medial canthus of the eye, (Fig. 2.1c) the mucosa of the cheek, approximately 90 mm from the commissure of the lip (using a technique described by Reiners et al. 2018), (Fig.2.1d_1) the rectal mucosa, approximately 50 mm into the rectal cavity (d_2 is the temperature probe) and (Fig. 2.1d_3) the ventral midline of the tail where it was secured gently with adhesive tape on a non-pigmented area of the skin……73

Figure 2.2 Bland-Altman plots showing the level of agreement between arterial oxygen-haemoglobin saturation (SaO_2) measured by a benchtop co-oximeter (reference method) and the peripheral arterial oxygen-haemoglobin saturation (SpO_2) measured by the Nonin PalmSAT pulse oximeters and 2000T transflectance probes attached at four different attachment sites in eight immobilized white rhinoceroses (*Ceratotherium simum simum*). The probes were placed against (a) the third eyelid, (b) the mucosa of the cheek, (c) the rectal mucosa and (d) the ventral midline of the tail on a non-pigmented area of the skin. The percent mean difference between SaO_2 and SpO_2 is plotted against the percent mean arterial oxygen-haemoglobin saturation measurements obtained from the co-oximeter and the pulse oximeters (SaO_2 and SpO_2) at the saturation range of 70-100%. The grey shaded regions represent the manufacturer's claimed performance range of 70-100%. The estimated bias is represented by the solid line, and limits of agreement [bias ± 1.96×standard deviation (SD)] is represented by the dashed lines. Each datum point represents the paired measurements taken from the rhinoceroses. The number of paired measurements from each attachment site are as follows: third eyelid (n = 41), cheek (n = 33), rectum (n = 33) and the tail (n = 35)……79

Figure 3.1 A Nonin 2000T transflectance probe (Fig. 3.1a_1) and a Masimo LNCS TF-I AH animal transflectance probe (Fig. 3.1a_2) placed on the third eyelid (nictitating membrane mucosa) of the left and right eye of southern white rhinoceros (*Ceratotherium simum simum*) (Fig. 3.1b_1). The Nonin 2000T transflectance probe was placed before the animal was in a lateral position (either on the left or right side), so that it was always placed on the third eyelid of the eye that the rhinoceros rested on (lower eye). The Masimo LNCS TF-I AH animal transflectance probe was placed on the third eyelid of the upper eye so that it could be regularly checked. A Nonin 2000SL lingual transmission clip probe (Fig. 3.1c_1) and a Masimo LNS YI AH SpO_2 animal multisite transmission clip probe (Fig. 3.1c_2) were placed adjacent to one another on the upper

ear, on the border of the ear pinna (upper helix) after gently scarifying the skin surface by scarping it on both sides of the ear surfaces with a scalpel blade.……91

Figure 3.2 Receiver operating characteristics (ROC) curves showing the sensitivity (%) and 100%-Specificity (or false positive ratio) for the peripheral arterial oxygen-haemoglobin saturation (SpO_2) from the Nonin PalmSAT 2500A pulse oximeters and Masimo Radical-7 pulse co-oximeters, at the two attachment sites (third eyelid and ear pinna) for the detection of hypoxaemia in southern white rhinoceros (*Ceratotherium simum simum*). SpO_2 measurements from the Nonin PalmSAT 2500A pulse oximeter (pink line) and Masimo Radical-7 pulse co-oximeter (purple line) under the third eyelid and the Nonin PalmSAT 2500A pulse oximeter (black line) and Masimo Radical-7 pulse oximeter (green line) on the ear pinna. The ■,∇, ・,and ∆ represent the sensitivity (%) and 100%-Specificity (%) at the cut-off values (≤35%, ≤75%, ≤80%, ≤85%, ≤90%, ≤92%, ≤95% and ≤100%).……102

Figure 4.1 Bland-Altman plot, showing poor agreement between the EPOC's calculated arterial oxygen-haemoglobin saturation ($cSaO_2$) and the co-oximeter's arterial oxygen-haemoglobin saturation (SaO_2) in 16 immobilized white rhinoceros. The difference between $cSaO_2$ and SaO_2 is plotted against the mean arterial oxygen-haemoglobin saturation measurements obtained from the EPOC and the co-oximeter ($cSaO_2$ and SaO_2) across the entire 0-100% saturation range. The bias is represented by the solid line, and the limits of agreement (bias ± 1.96×SD) are represented by the dashed lines. Each datum point represents the difference in the paired $cSaO_2$-SaO_2 measurements (389 paired measurements) taken from the 16 white rhinoceroses in both studies……..120

Figure 4.2 Bland-Altman plots, showing poor agreement between the EPOC's calculated arterial oxygen-haemoglobin saturation ($cSaO_2$) and the co-oximeter's measured arterial oxygen-haemoglobin saturation (SaO_2) in eight immobilized white rhinoceros used in Study 1 and a further eight individuals in Study 2. The difference between $cSaO_2$ and SaO_2 is plotted against the mean arterial oxygen-haemoglobin saturation values obtained from the EPOC and the co-oximeter ($cSaO_2$ and SaO_2) across the entire 0-100% saturation range. The bias is represented by the solid line, and the limits of agreement (bias ± 1.96×SD) are represented by the dashed lines. Each datum point represents the difference in the paired $cSaO_2$-SaO_2 measurements taken from the rhinoceros……..…122

Figure 4.1 Calculated arterial oxygen-haemoglobin saturations ($cSaO_2$) obtained from the EPOC blood gas analyser plotted against arterial oxygen-haemoglobin saturations (SaO_2) measured by the AVOXimeter 4000 co-oximeter in eight immobilized white rhinoceros in Study 1 and a further eight individuals in Study 2. The regression equations for Study 1 (n = 89)

and Study 2 (n = 300) are $cSaO_2$ = 0.9691*SaO_2 - 3.022 and $cSaO_2$ = 1.082*SaO_2 - 13.56, respectively……123

Figure 4.4 Relationship between arterial oxygen partial pressure (PaO_2) and the EPOC's calculated arterial oxygen-haemoglobin saturation ($cSaO_2$) and co-oximeter's arterial oxygen-haemoglobin saturation (SaO_2) at a pH of 7.30 ± 0.1 (mean ± standard deviation), dissolved arterial CO_2 partial pressure ($PaCO_2$) of 73.7 ± 10.5 mmHg, body temperature of 37.4 ± 1.8°C, bicarbonate ion concentration of 35.5 ± 2.8 mmol.L^{-1} and chloride ion concentration of 93.0 ± 4.7 mmol.L^{-1}. The data were plotted and a specific binding with Hill slope model was applied. The dashed line at 50% SaO_2 helps visualize the arterial oxygen partial pressure at which haemoglobin is 50% saturated with oxygen (P_{50}) according to the two curves. Note that a decrease in pH and an increase in $PaCO_2$ leads to a right-shift in both the EPOC's $cSaO_2$ oxygen-haemoglobin dissociation curve (P_{50} ~ 32 mmHg) and the co-oximeter SaO_2 oxygen-haemoglobin dissociation curve (P_{50} ~ 29 mmHg)……..124

Figure 5.1 Relationship between arterial oxygen partial pressures (PaO_2) and the arterial oxygen-haemoglobin saturation measured by a benchtop AVOXimeter 4000 co-oximeter (co-oximeter SaO_2) reference method, the arterial oxygen-haemoglobin saturation calculated from the oxygen content equation (method 1 $cSaO_2$) and those calculated from the Siggaard-Andersen algorithm (method 2 $cSaO_2$) in eight immobilized southern white rhinoceros. The data were plotted using the "specific binding with Hill slope" model in GraphPad Prism version 9.4.1. The dashed line at 50% arterial oxygen-haemoglobin saturation helps visualize the P_{50} (arterial oxygen partial pressure when haemoglobin is 50% saturated with oxygen) of the curves……..146

List of abbreviations

μL.g^{-1}.min^{-1}	-	Microlitre(s) per gram per minute
AC	-	Alternating current
AgapK	-	Anion gap, K^+
ARMS	-	Area root mean squares
ATP	-	Adenosine triphosphate
AUC	-	Area under the curve
BE	-	Base excess
Ca^{2+}	-	Calcium ion(s)
cAMP	-	Cyclic adenosine monophosphate
CaO_2	-	Oxygen content in the arterial blood
CO_2	-	Carbon dioxide
Cl^-	-	Chloride ion(s)
CLIA	-	Clinical Laboratory Improvement Amendments
$cSaO_2$	-	Calculated arterial oxygen-haemoglobin saturation
DC	-	Direct current
DST	-	Discrete saturation transform
EPOC	-	Enterprise Point-of-Care
FST	-	Fast saturation transform
[Hb]	-	Haemoglobin concentration
H^+	-	Hydrogen ion(s)
HbO_2	-	Oxyhaemoglobin
HbCO	-	Carboxyhaemoglobin
HCO_3^-	-	Bicarbonate ion(s)
Hct	-	Haematocrit
HHb	-	Deoxyhaemoglobin
HiCN	-	Cyanmethaemoglobin
ICSH	-	International Committee for Standardization in Haematology
IF	-	Infrared light
K^+	-	Potassium ion(s)
$K_3Fe(CN)_6$	-	Potassium ferricyanide solution
LED	-	Light emitting diode
M	-	Molar mass
mm	-	Millimetre(s)
M_b	-	Body mass

$M^{-1}.cm^{-1}$	-	Per molar mass per centimetre(s)
MetHb	-	Methaemoglobin
$mL.dL^{-1}.mmHg^{-1}$	-	Millilitre(s) per decilitre per millimetre of mercury
$mL.g^{-1}.min^{-1}$	-	Millilitre(s) per gram per minute(s)
$mL.mmHg^{-1}$	-	Millilitre(s) per millimetre of mercury
N/A	-	Not applicable
NIRS	-	Near infrared spectroscopy
OHDC	-	Oxygen-haemoglobin dissociation curve
P_{50}	-	Partial pressure of oxygen when haemoglobin is 50% saturated with oxygen
PAC	-	Pulmonary artery catheter
$PaCO_2$	-	Partial pressure of carbon dioxide in the arterial blood
PaO_2	-	Partial pressure of oxygen in the arterial blood
$P(A\text{-}a)O_2$	-	Alveolar-to-arterial oxygen partial pressure gradient or A-a gradient
$PcvO_2$	-	Central venous partial pressure of oxygen
pH	-	Potential of hydrogen
PO_2	-	Partial pressure of oxygen
POC	-	Point-of-Care
PR	-	Pulse rate
PvO_2	-	Partial pressure of oxygen in the venous blood
ROC	-	Receiver operating characteristics
SaO_2	-	Arterial oxygen-haemoglobin saturation measured directly by co-oximetry
$ScvO_2$	-	Central venous or mixed venous arterial oxygen-haemoglobin saturation
SD	-	Standard deviation
SET	-	Signal extraction technology
SjO_2	-	Jugular bulb vascular oxygen saturation
SpO_2	-	Peripheral arterial oxygen-haemoglobin saturation estimated by pulse oximetry
SpHb	-	Haemoglobin concentration estimated by pulse co-oximetry
SpCO	-	Carboxyhaemoglobin concentration estimated by pulse co-oximetry
SpMet	-	Methaemoglobin concentration estimated by pulse co-oximetry
StO_2	-	Arterial oxygen-haemoglobin saturation at the tissue site
STPD	-	Standard temperature pressure, dry air
SvO_2	-	Venous oxygen-haemoglobin saturation
$\dot{V}O_2$	-	Oxygen consumption rate

Thesis summary

Reliability of methods to determine arterial oxygen-haemoglobin saturation in immobilized southern white rhinoceros (*Ceratotherium simum simum)*

by

Thembeka Kim Mtetwa

PROMOTERS: Prof Leith Meyer & Prof Edward Snelling

The goal of monitoring blood oxygenation during chemical immobilization is to help maintain adequate tissue oxygen delivery for normal organ function. Arterial oxygen-haemoglobin saturation (SaO_2), which accounts for 96-98% of total oxygen content in the arterial blood is an important and informative indicator of blood oxygenation. However, the reliability of arterial oxygen-haemoglobin saturation measured or calculated by blood oxygenation monitoring methods has never been examined in southern white rhinoceros (*Ceratotherium simum simum*), despite their susceptibility to hypoxaemia during chemical immobilization. In this thesis, I aimed to evaluate the reliability of 1) a Nonin PalmSAT 2500A pulse oximeter's and a Masimo Radical-7 pulse co-oximeter's peripheral arterial oxygen-haemoglobin saturation (SpO_2) measurements, at different attachment sites (third eyelid, cheek, ear, rectum, and, or tail) (Chapters 2 & 3), and 2) arterial oxygen-haemoglobin saturation ($cSaO_2$) calculated by four different methods (Chapters 4 & 5). In Chapter 4, I evaluated arterial oxygen-haemoglobin saturation calculated from the Enterprise Point-of-Care (EPOC) blood analyser. In Chapter 5, I evaluated arterial oxygen-haemoglobin saturation calculated from the oxygen content equation using oxygen content (CaO_2) measured by a microrespirometer following the method of Tucker (1967) and those calculated from the Siggaard-Andersen algorithm, modified for the specific characteristics of rhinoceros' blood. As part of two broader studies, a convenience sample of 16 (8×2) rhinoceroses were immobilized by darting with different etorphine-based drug combinations, followed by butorphanol or saline, administered intravenously. Thereafter, insufflated oxygen (15 $L.minute^{-1}$ flow rate) was provided intranasally to improve the animals blood oxygen levels. Nonin PalmSAT 2500A pulse oximeters and Masimo Radical-7 pulse co-oximeters with their probes were secured to their attachment sites (third eyelid, cheek, ear, rectum, and tail). At pre-determined time points, arterial blood samples were drawn

from a catheter inserted into the auricular artery, and near-simultaneous SpO_2 measurements were recorded from the different attachment sites. Blood samples were analysed using a benchtop AVOXimeter 4000 co-oximeter (reference method), the EPOC blood analyser and the Tucker cell microrespirometer. Dissolved arterial partial pressure of oxygen and carbon dioxide (PaO_2 and $PaCO_2$) and pH, measured by the EPOC were used to calculate arterial oxygen-haemoglobin saturation from the three calculation methods (i.e., EPOC, oxygen content equation and Siggaard-Andersen algorithm). Bland-Altman (to estimate bias and precision) and area root mean squares (ARMS) analysis were used to determine the reliability of SpO_2 readings from the pulse oximeter devices, at different attachment sites, and calculated arterial oxygen-haemoglobin saturation measurements ($cSaO_2$), when compared with simultaneous co-oximeter's SaO_2 measurements. SpO_2 measurements from the Nonin 2500A PalmSAT pulse oximeter and a 2000T transflectance probe attached to the third eyelid are reliable, but only at the 70-100% saturation range; the other attachment sites are unreliable across the entire 0-100% saturation range. The Masimo Radical-7 pulse oximeter with a LNCS TF-I AH transflectance probe attached to the third eyelid, and with a LNS YI AH transmission probe attached to the ear pinna are unreliable across the entire 0-100% saturation range. The EPOC's $cSaO_2$ readings are unreliable across the entire 0-100% saturation range. Arterial oxygen-haemoglobin saturation calculated by the oxygen content equation using Tucker-derived CaO_2 is also unreliable across the entire 0-100% saturation range. Arterial oxygen-haemoglobin saturation calculated by the Siggaard-Andersen algorithm, modified for rhinoceros is reliable but only at saturations above 90%; below 90% it is unreliable. I conclude that blood oxygenation and hypoxaemia can be monitored reliably in immobilized southern white rhinoceros using a Nonin PalmSAT 2500A pulse oximeter with a 2000T transflectance probe, attached in the space between the third eyelid and the sclera, facing the third eyelid, and when saturation levels are between 70 and 100%; and below 70%, a benchtop co-oximeter should rather be used.

Keywords chemical immobilization, co-oximetry, calculated oxygen-haemoglobin saturation, pulse co-oximetry, pulse oximetry, Tucker method.

CHAPTER 1:

General introduction, literature review and scope of the thesis

1.1 General introduction

Wildlife capture, through physical restraint or chemical immobilization, is an essential procedure for wildlife conservation and management (Fahlman 2008; Meyer et al. 2010; Haw et al. 2014; Buss et al. 2018; Izwan et al. 2018; Reiners et al. 2019; Pohlin et al. 2020). White rhinoceros are captured for translocations, dehorning, removal of snares, disease surveillance and fitting collars for security and research purposes (Fahlman 2008; Buss et al. 2018; Pohlin et al. 2020). To capture rhinoceros by chemical immobilization, potent opioids (e.g., etorphine or thiafentanil) are primarily used, however, rhinoceros are particularly sensitive to the adverse effects caused by these drugs (Fahlman 2014; Haw et al. 2014; Buss et al. 2018). Opioids compromise the cardio-respiratory system resulting in respiratory depression, compromised oxygen diffusion and functional pulmonary right-to-left shunting (i.e., when deoxygenated blood returns to the systemic circulation after bypassing the lungs without being oxygenated) ultimately leading to severe hypoxaemia (Kock et al. 1995; Haw et al. 2014; Fahlman 2014; Buss et al. 2018; Pohlin et al. 2020). Severe hypoxaemia (inadequate blood oxygenation) can be acutely life-threatening, and, if it is left untreated, it may lead to rapid tissue hypoxia in vital organs including the brain, cardiac and skeletal muscles, ultimately leading to increased risk of morbidity and mortality of white rhinoceros (Fahlman et al. 2010; Fahlman 2014). It is therefore important to find reliable, affordable, and easy-to-use methods to monitor hypoxaemia and blood oxygenation in field settings.

Devices that are commonly used to monitor hypoxaemia (e.g., pulse oximeters and blood analysers) are mostly designed specifically for human subjects. These devices estimate or calculate blood oxygenation [either as partial pressure of oxygen in the arterial blood (PaO_2) or arterial oxygen-haemoglobin saturation (SaO_2) and, or peripheral arterial oxygen-haemoglobin saturation (SpO_2)] using a standard human oxygen-haemoglobin dissociation curve or human haemoglobin light absorption

characteristics, which may represent a problem because white rhinoceros' haemoglobin and its oxygen-haemoglobin dissociation curve are different from that of humans (Baumann et al. 1984; Haymerle et al. 2016). White rhinoceros' P_{50} (partial pressure of oxygen when haemoglobin is 50% saturated with oxygen) is between 15 mmHg (Reiners et al. 2019) and 20 mmHg (Bauman et al. 1984), which is much lower than that of humans (P_{50} of 27 mmHg) (Severinghaus 1979). It is likely that analysis of rhinoceros' blood oxygenation using devices designed specifically for humans provides erroneous data, although whether this is true, and if so, what the exact magnitude of the error is, have not yet been determined. Therefore, it is important to determine how accurate and reliable the commonly used methods or devices are when they are used in white rhinoceros. Furthermore, determining a reliable method for monitoring blood oxygenation in rhinoceros during immobilization will have significant benefits, especially for improving individual health outcomes as well as long-term species conservation.

In this chapter, I review 1) the oxygen transport in the blood and the differences in blood characteristics among mammalian species, 2) the methods used for monitoring blood oxygenation during human and veterinary anaesthesia, focusing on the principles of measurement, practicality, and reliability of each method in different mammalian species and 3) the importance of looking at the reliability of each method, particularly in immobilized white rhinoceros, which are prone to hypoxaemia, and other physiological derangements (i.e., hypercapnia and acidosis that influence blood oxygenation and the position of oxygen-haemoglobin dissociation curve), during immobilization.

1.2 Literature review

1.2.1 Oxygen transport in the blood

Oxygen is a critical component in the aerobic production of adenosine triphosphate (ATP) where it serves as the final electron acceptor in the electron transport chain during the process of oxidative phosphorylation (Popel 1989; Pittman 2011). At rest, this process produces more than 90% of the ATP needed for cell function (Boas & Franceschini 2011; Pittman 2011). During inspiration, air (made up of ~20.94% oxygen) flows into the lungs and then oxygen diffuses into the pulmonary circulation down its partial pressure gradient, across the alveolar-capillary interface, entering the blood stream (Marieb & Hoehn 2013). Oxygen in the blood is then transported to the tissues, then it diffuses across the capillary-cellular interface down its partial pressure gradient and into the tissue's mitochondria, where aerobic respiration takes place (Pittman 2011; Marieb & Hoehn 2013). The blood transports oxygen to the tissues in two ways, i.e., it is dissolved in the plasma, or attached to haemoglobin in the red blood cells.

Partial pressure of oxygen in the arterial blood (PaO_2)

Compared to the other gases (e.g., carbon dioxide), oxygen is not very soluble in solution, therefore only 2-3% of oxygen is dissolved in the blood, and it is this component that exerts a partial pressure (Pittman 2011; Collins et al. 2015). Dissolved oxygen in the arterial blood is measured as the partial pressure of oxygen (PaO_2) and can be converted to a concentration of oxygen according to the Henry's Law, which states that "at a constant temperature, the concentration of oxygen in a liquid, or in aqueous phase, is proportional to the partial pressure of oxygen in the gaseous phase" (Marieb & Hoehn 2013; Collins et al. 2015). The concentration of dissolved oxygen in the blood is expressed using the equation $[O_2] = \alpha P$, where $\propto$ is the solubility of oxygen ($mL.dL^{-1}.mmHg^{-1}$) at standard temperature pressure (STPD, 0ºC, 760 mmHg barometric pressure, dry air) and P is the partial pressure of oxygen (in mmHg). When PaO_2 is 100 mmHg and the solubility of oxygen is 0.003 $mL.dL^{-1}.mmHg^{-1}$, then the concentration of dissolved oxygen in the plasma is 0.3 $mL.dL^{-1}$, making up a small proportion of total oxygen content in blood, which is normally between 20-22 $mL.dL^{-1}$ (Ward 2006).

Arterial oxygen-haemoglobin saturation (SaO_2)

The rest of the oxygen in the arterial blood (which is approximately 96-98%) is transported by the red blood cells, where it is attached to haemoglobin (Popel 1989; Collins et al. 2015). The amount of oxygen bound to haemoglobin in the blood depends on its oxygen carrying capacity. Each mole of haemoglobin can bind up to four oxygen molecules; therefore, the maximum volume of oxygen that can bind to haemoglobin can be estimated, and if haemoglobin concentration [Hb] is known, the oxygen carrying capacity of the blood can also be estimated.

Haemoglobin structure and function

Haemoglobin makes up about 95% of the volume of red blood cells. The word haemoglobin originates from two words: haem meaning blood and globin meaning protein. Haemoglobin is composed of four polypeptide globin chains and each chain is made up of two identical alpha ($\propto$) chains and two non-alpha chains [i.e., beta (β), gamma (γ), delta (δ), or epsilon (ε) chains] (Pittman et al. 2011; Oladokun & Atere 2020). For example, the adult human haemoglobin (haemoglobin A) polypeptide chains are made up of two identical $\propto$ chains and two identical β chains (Fig. 1.1), whereas the foetal haemoglobin (haemoglobin F) polypeptide chain is made up of two $\propto$ alpha and two γ chains (Revsbech & Fago 2017; Oladokun & Atere 2020). In adult and foetal haemoglobin, each polypeptide chain ($\propto$ and β or γ respectively) is made up of 141 and 146 amino acid residues that form eight $\propto$-helices, which are interlinked by non-helical segments and the N- and C-terminal extensions that connect these $\propto$-helices (Perutz 1983; Weber & Campbell 2011). The position of the amino acid residues in the polypeptide chain is used to identify them (Perutz 1983; Weber & Campbell 2011). The polypeptide chains contain an iron (Fe) molecule in the centre of each ring that is responsible for binding to oxygen (Fig. 1.1) (Pittman et al. 2011; Oladokun & Atere 2020). When oxygen combines with the iron ion in a ferrous state (Fe^{2+}), it gives the blood its bright red colour (Oladokun & Atere 2020). The four chains enable one haemoglobin to bind to four oxygen molecules, making it the most common and abundant oxygen carrier.

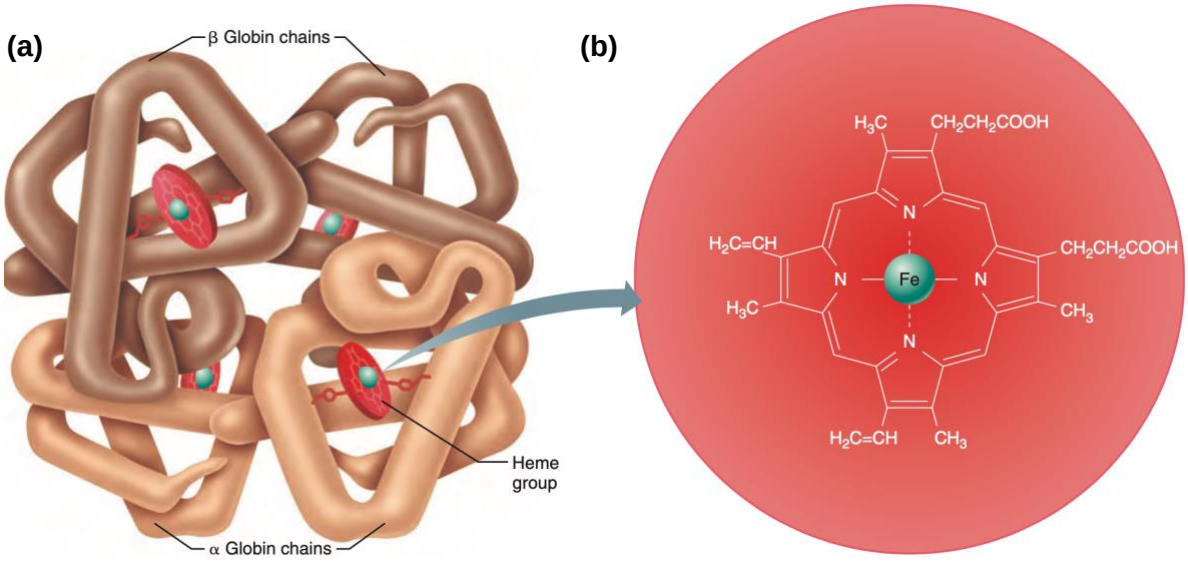

Figure 1.1 The basic structure of adult human haemoglobin molecule consisting of two identical ∝ chains and two identical β chains (a) and each globin chain contain an iron (Fe^{2+}) ion (b) in the centre of each ring responsible for binding to oxygen. Each haemoglobin binds to four oxygen molecules. Reprinted from Marieb, E. N., & Hoehn, K. (2013). The respiratory system. In *Human Anatomy and Physiology* (9^{th} edn) (pp. 1056-1061). Pearson, London, UK, Copyright © 2013 with permission from Pearson Educators Inc.

The ∝ and β chains are arranged in pairs as polypeptide subunits that are held together by stable hydrogen bonds (Pittman 2011; Malte et al. 2021). There are at least two haemoglobin conformations, the tense (T) state, that forms when haemoglobin is not bound to oxygen (deoxyhaemoglobin) and the relaxed (R) state, when haemoglobin is bound to oxygen (oxyhaemoglobin) (Pittman 2011; Malte et al. 2021). These conformations vary depending on the kinds of bonds that hold them together and the distribution of energy of these protomer (subunit) bonds (Monod et al. 1965). The tense state is made up of stable hydrogen bonds and additional intra- and inter-subunit salt-bridges (Malte et al. 2021). In the presence of oxygen, these salt bridges are broken, forming the relaxed state oxyhaemoglobin molecule, held together only by the stable hydrogen bonds (Monod et al. 1965; Pittman 2011; Malte et al. 2021).

Inactive haemoglobin species

Haemoglobin not only reversibly binds to oxygen, but can also reversibly bind to carbon dioxide, carbon monoxide and sulphur, reducing the affinity of oxygen to haemoglobin. Haemoglobin binds to carbon dioxide in its tense state, normally in the tissues and transports it to the lungs, where it is eliminated from the body (Marieb & Hoehn 2013). When carbon dioxide binds to haemoglobin, it binds directly to neutral (uncharged) amino-termini of both the α and β chains (i.e., α1-Val and β1-Val), instead of the Fe^{2+} ion to form carbaminohaemoglobin, which accounts for about 20-25% of the haemoglobin in the red blood cells (Van Kampen & Zijlstra 1983; Marieb & Hoehn 2013). Carbaminohaemoglobin stabilizes the salt-bridges in the tense state, decreasing the oxygen affinity to haemoglobin (Hsia 1998; Malte et al. 2021). In the presence of carbon monoxide, which has a high affinity for haemoglobin compared to oxygen, haemoglobin binds to form carboxyhaemoglobin (HbCO) (Hsia 1998). Sulfhaemoglobin can also form in the presence of sulphur, however, it has been shown to have minor effect on the affinity of oxygen to haemoglobin (Ralston et al. 1991). In other cases (e.g., during exposure to certain drugs and chemicals), Fe^{2+} in the haem-group of haemoglobin can be oxidated to Fe^{3+}, resulting in methaemoglobin (MetHb), which is incapable of binding oxygen (Van Kampen & Zijlstra 1983). Reiners et al. (2019) reported that the white rhinoceros' affinity of oxygen to haemoglobin is unaltered by changes in HbCO and MetHb but the exact cause of this is unknown.

Oxygen-haemoglobin dissociation curve

An oxygen-haemoglobin dissociation curve of whole blood is a sigmoidal curve that serves as a foundation for understanding the relationship between PaO_2 and SaO_2 under normal and abnormal physiological conditions (Fig. 1.2). The shape of the curve is asymmetrically sigmoidal because of the binding nature of oxygen to haemoglobin and shows how PaO_2 can affect the loading and offloading of oxygen by haemoglobin (Marieb & Hoehn 2013). In mammalian lungs that are adequately ventilated and perfused, there is an increase in the partial pressure of oxygen dissolved in the arterial blood, from approximately 40 mmHg at the pulmonary arterial end to 100 mmHg at the pulmonary venule end (Marieb & Hoehn 2013). As the amount of dissolved oxygen increases, there is an increased affinity of oxygen to haemoglobin, resulting in SaO_2 that is at least 95% in normal resting situations. When one

oxygen molecule reversibly binds to one Fe^{2+} (oxygen binding site), the $\alpha\beta$ subunits structure rotates by 12-15º, exposing another oxygen binding site, increasing the oxygen affinity to haemoglobin (Pittman 2011; Malte et al. 2021). When one or two oxygen molecules are bound to haemoglobin, the haemoglobin molecule is partially saturated, and this is shown by the steep part of the oxygen-haemoglobin dissociation curve (Fig. 1.2). When all four oxygen molecules are bound to haemoglobin, the haemoglobin molecule is fully saturated, with SaO_2 that is above 95%, which is represented by the plateau part of the oxygen-haemoglobin dissociation curve (Fig. 1.2). In the tissues, haemoglobin offloads oxygen, releasing it from the red blood cells into the plasma where it is dissolved and then diffuses through the capillary-cellular interface along its partial pressure gradient (Marieb & Hoehn 2013). The offloading (i.e., release) of one oxygen molecule facilitates the offloading of another oxygen molecule and so forth, leading to a decrease in SaO_2 and haemoglobin changes from its relaxed state (oxyhaemoglobin) to its tense state (deoxyhaemoglobin).

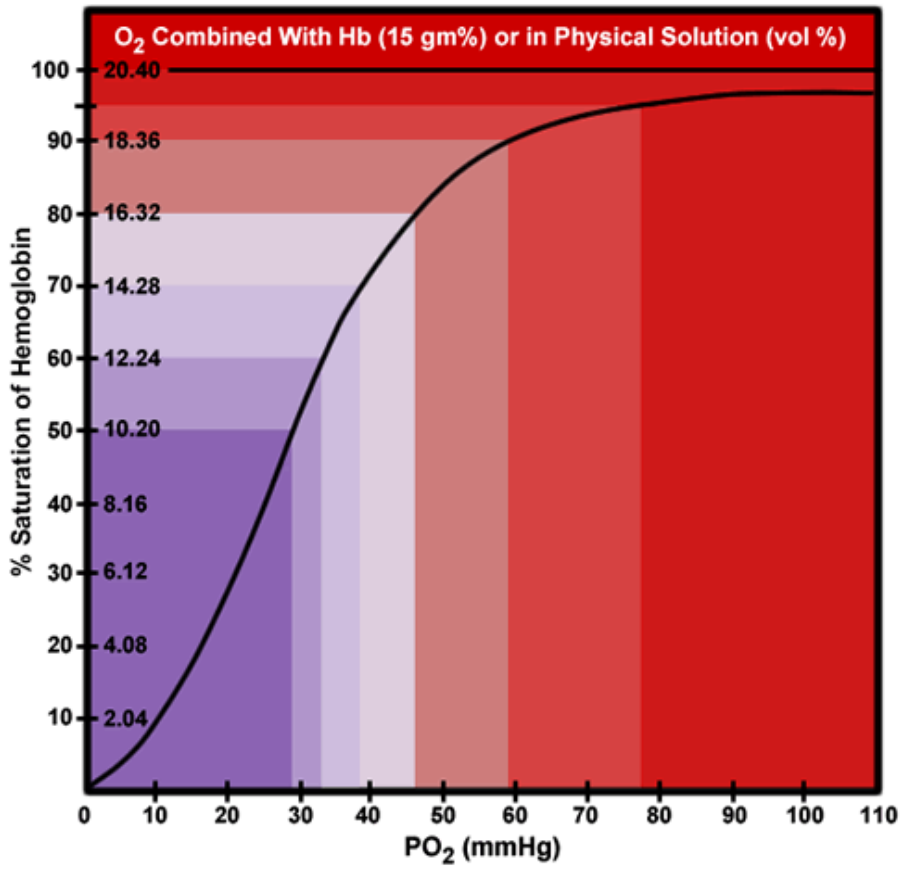

Figure 1.2 A standard human oxygen-haemoglobin dissociation curve represented by a sigmoidal relationship between the oxygen that is dissolved in the blood [PaO_2 (mmHg)] and the oxygen bound to haemoglobin in the red blood cells [SaO_2 (%)]. The right y-axis values represent the oxygen content (CaO_2), which is the total oxygen that is dissolved and bound to haemoglobin. The steep part of the oxygen-haemoglobin dissociation curve illustrates what happens in the lungs, when oxygen diffuses into the pulmonary circulation down its partial pressure gradient, across the alveolar-capillary interface, into the blood and increasing the PaO_2 (PaO_2 ~40 – 60 mmHg). As PaO_2 increases, one oxygen molecule binds to one Fe^{2+} ion (oxygen binding site) causing another oxygen binding site to be readily available, increasing the affinity of oxygen to haemoglobin. When one or two or three oxygen molecules are bound to haemoglobin, it becomes partially saturated and SaO_2 is below 95%. The plateau part of the curve illustrates what happens when the haemoglobin binds to the fourth oxygen molecule and changes from being partially saturated to being fully saturated with oxygen, and SaO_2 is above 95%. The blood colour shifts from dark blue to dark red as PaO_2 and SaO_2 increase in the arterial blood. https://slideplayer.com/slide/12348101/

The first accepted empirical equation that represents the oxygen-haemoglobin dissociation curve was derived by Hill (1910) (Roughton & Severinghaus 1973; Sharan & Singh 1984; Collins et al. 2015). This equation assumed that n molecules of oxygen bind to one molecule of haemoglobin, where n (for molecules of oxygen) is a positive integer value (Hill 1910; Sharan et al. 1989). Adair (1925) demonstrated an empirical relationship between SaO_2 and PaO_2, according to the hypothesis that four molecules of oxygen bind to one molecule of haemoglobin in four steps. Adair's representation was preferred because Hill's equation was inaccurate at low saturation ranges (Sharan et al. 1989). Since these discoveries, oxygen-haemoglobin dissociation curves of different species have been determined.

Variation in oxygen-haemoglobin dissociation curves of different mammals

At rest (pH of 7.4, $PaCO_2$ of 40 mmHg and body temperature of 37°C), the position of the whole blood oxygen-haemoglobin dissociation curve varies among different mammalian species (Schmidt-Neilsen et al.1958; Severinghaus et al.1966; Dhindsa et al. 1979; Bauman et al. 1984; Gustin et al. 1988; Clerbaux et al. 1993; Cambier et al. 2005; Reiners et al. 2019). The position of the curve is usually defined by the P_{50} value, which is the partial pressure of oxygen when haemoglobin is 50% saturated with oxygen (Sharan & Popel 1988; Pittman 2011; Malte et al. 2021). Humans have a P_{50} of approximately 27 mmHg (Severinghaus et al.1966; Clerbaux et al. 1993), which is different from that of other species, such as cats (P_{50} of ~ 34mmHg), dogs of different breeds (P_{50} between 25.8 – 35.8 mmHg), sheep (P_{50} is between 31 – 40 mmHg), pigs (P_{50} of ~33 mmHg), cattle (P_{50} of 24.8 mmHg), horse (P_{50} of 23.8 mmHg), and elephant (P_{50} is between 22 – 24 mmHg) (Schmidt-Neilsen et al.1958; Meschia et al. 1960; Riegel et al. 1967; Novy et al. 1973; Dhindsa et al. 1979; Clearbaux et al. 1993; Moraga et al. 1996). The P_{50} of white rhinoceros was first described by Bauman et al. (1984) who reported a value of 17.1 (pH of 7.20) and 17.4 (pH of 7.40) at a body temperature of 37°C. Reiners et al. (2019) recently constructed an oxygen-haemoglobin dissociation curve from isolated haemoglobin of white rhinoceros and reported P_{50} values of 20.6 mmHg (pH of 7.20) and 15 mmHg (pH of 7.40) at a body temperature of 37°C. Both studies show that the white rhinoceros' curve is normally left shifted compared to that of human. To construct the oxygen-haemoglobin dissociation curves, Baumann et al. (1984) used spectrophotometric methods and calculated the P_{50} value from a Hill plot, whereas Reiners et al. (2019) used a Gill cell but also calculated the P_{50} from a Hill plot.

There are many reasons why oxygen-haemoglobin dissociation curves vary among species. These variations, sometimes called adaptations, are caused by a number of factors including: differences in body mass among species (allometric); differences in the haemoglobin structure (evolutional adaptations); long-term exposure to certain environments and conditions (long-term adaptations); and how haemoglobin and its affinity to oxygen dynamically interacts with different allosteric effectors such as organic phosphates [e.g., 2.3-diphosphoglycerate (2.3-DPG) and ATP], protons (H^+), chloride ions (Cl^-) and temperature (dynamic adaptations)] (Bunn 1980; Berenbrink 2006; Weber & Campbell 2011).

Schmidt-Nielsen & Larimer (1958 & 1970) showed that the position of the oxygen-haemoglobin dissociation curve of different species (represented by the P_{50} values) scales with body mass (Fig.1.3). Mammals with a small body mass tend to have more right-shifted curves (i.e., high P_{50}) whereas mammals with a large body mass have more left-shifted curve (i.e., low P_{50}). This relationship has also been demonstrated in wild mammals that are not represented in Figure 1.3. For example, at rest (37ºC and pH of 7.4), large mammals such as the Asian and African elephants and white rhinoceros have P_{50} values of 25.2 mmHg (Asian), 23.2 mmHg (African) and 15 – 20 mmHg (white rhinoceros) compared to a deer (P_{50} of ~28 mmHg) (Bartels et al. 1963; Dhindsa et al. 1972; Baumann et al.1984; Reiners et al. 2019). The relationship between the P_{50} and body mass is ascribed by the differences in metabolic rate among species of different body mass. The metabolic rate of mammals is expressed by the following equation (Schmidt-Nielsen & Larimer 1958):

$$\dot{V}O_2 = 0.00633\ {M_b}^{-0.27}$$

Where $\dot{V}O_2$ is the oxygen consumption [in millilitres per gram of tissue per minute ($mL.g^{-1}.min^{-1}$)] and M_b is the body mass in grams (g). The equation shows that mass-specific oxygen consumption rate increases with decreasing body mass. A 20 g mouse has an oxygen consumption rate of 28.2 $\mu L.g^{-1}.min^{-1}$ compared to a 700 kg horse with an oxygen consumption rate of 1.72 $\mu L.g^{-1}.min^{-1}$, respectively (Schmidt-Nielsen & Larimer 1958; Lindstedt 2021). Small body mass mammals with relatively high mass-specific metabolic rates have haemoglobins that tend to facilitate oxygen offloading to the tissues

(i.e., low oxygen affinities), having oxygen-haemoglobin dissociation curves that are more shifted to the right compared to large mammals (Schmidt-Nielsen & Larimer 1958; Lindstedt 2021). On the other hand, large body mass mammals with relatively low mass-specific metabolic rates have haemoglobins that tend to limit oxygen offloading to the tissues and facilitate oxygen loading at low PaO_2 values (i.e., high oxygen affinities), therefore having oxygen-haemoglobin dissociation curves that are more shifted to the left compared to small mammals (Schmidt-Nielsen & Larimer 1958; Lindstedt 2021).

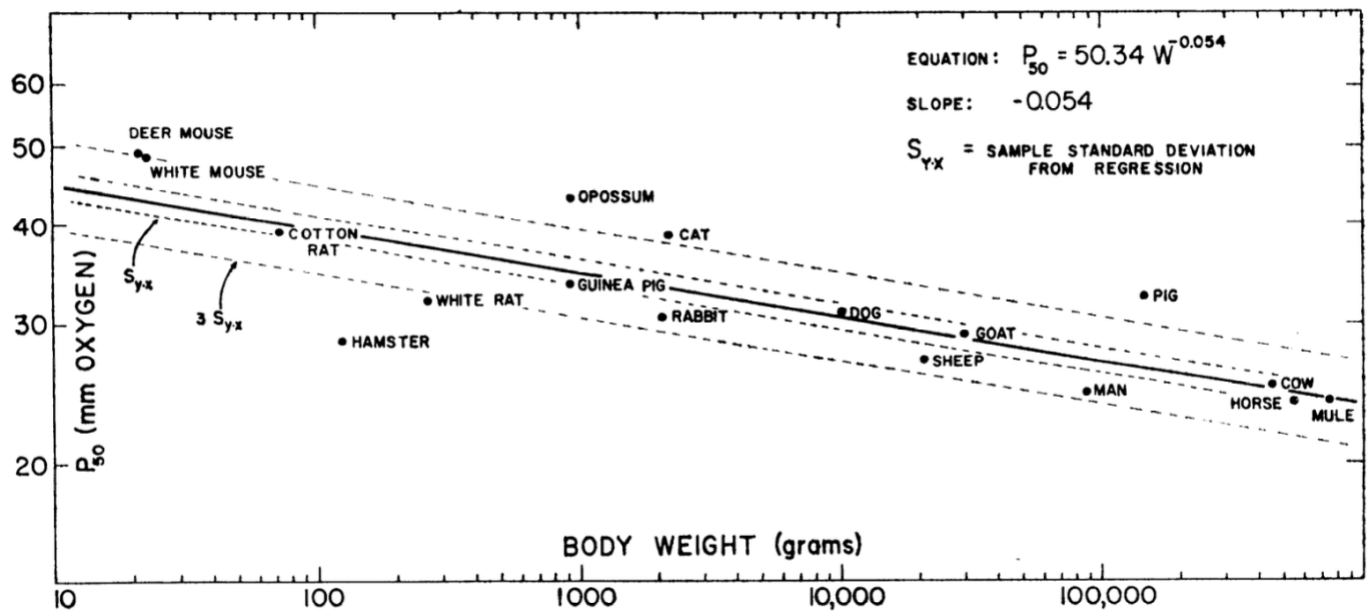

Figure 1.3 Scaling relationship between P_{50} (the partial pressure of oxygen when haemoglobin is 50% saturated with oxygen) and body mass (in grams) of different mammals. The graph is plotted and described by the power function $P_{50} = 50.34{M_b}^{-0.054}$, where P_{50} is measured in mmHg and body mass in grams. Mammals with small body mass have a high P_{50} and mammals with large body mass have a low P_{50}. Small body mass mammals with relatively high mass-specific metabolic rates have haemoglobins that tend to always facilitate oxygen offloading to the tissues (i.e., low oxygen affinities), having oxygen-haemoglobin dissociation curves that are more shifted to the right. Large body mass mammals with relatively low mass-specific metabolic rates have haemoglobins that tend to facilitate oxygen loading at low PaO_2 values (i.e., high oxygen affinities), therefore having oxygen-haemoglobin dissociation curves that are more shifted to the left. This Figure is from Schmidt-Neilsen & Larimer (1958). Reprinted from Schmidt-Neilsen, K., & Larimer, J. L. (1958). Oxygen dissociation curves of mammalian blood in relation to body size. *American Journal of Physiology-Legacy Content*, *195*(2), 424-428, Copyright © 1958 with permission from American Physiological Society.

Haemoglobin function and structure also vary due to evolutional adaptations that are independent of body mass. There is a distinct structure of haemoglobin among all groups of organisms (i.e., plants, bacteria, and vertebrates), and because of these similarities it is evident that this molecule comes from one common ancestral gene (Wells 1999). Therefore, evolution may have been responsible in shaping the role and structure of haemoglobin in all groups of organisms. It has been shown in mammals, that mutations normally occur in the β chain and not the $\propto$ chain, which is considered the "ancestral globin chain" (Wells 1999). For example, the structure of most ruminant haemoglobins differs from those of other mammals, with similar body mass (i.e., the N-terminus of their β chain is hydrophobic and points inwards into the protein moiety, stabilizing its tense state deoxyhaemoglobin molecule) (Weber & Campbell 2011). On the other hand, the haemoglobin of cats and pigs lacks a hydrophobic N-terminal region in its β chain, because it possesses a cluster of three positively charged amino acid residues at position 1 and 2 of the β chain (Weber & Campbell 2011). Equidae, the largest family in the mammalian order Perissodactyla, that include two other families (namely, Taparidae and Rhinocerotidae), has a distinct haemoglobin sequence compared to other mammals (Baumann et al. 1984). Equidae haemoglobin is distinguished by the glutamine, whereas rhinoceros' haemoglobin (from the family Rhinocerotidae) is distinguished by the glutamic acid, at the position β_2, whereas in humans it is occupied by histidine (Baumann et al. 1984). Given the prevalence of mammalian mutations and polymorphisms, there is an assumption that haemoglobin would have responded to selection pressures during evolution to help balance the organism's needs for oxygen with the environment's oxygen supply (Wells 1999). For example, mammals native to hypoxic environments (high-altitude), have high oxygen-haemoglobin affinities (left-shifted curves at rest) compared to their lowland relatives (Moraga et al. 1996; Storz 2007). Adult llama (*Lama glama*) that live in a hypoxic environment (high-altitudes), have a P_{50} between 20.3 – 24.6 mmHg (high oxygen-haemoglobin affinity) compared to their lowland relatives, sheep, with a P_{50} between 31 – 37.5 mmHg (Moraga et al. 1996; Storz 2007). These characteristics allow the mammals living in high altitudes to either increase oxygen uptake in the lungs and improve blood oxygenation at low PaO_2 levels, and, or limit oxygen offloading to the tissues and cope with reduced tissue oxygenation and energy demands (Bunn 1981; Petschow et al. 1977).

Long term exposure to certain environments (long-term adaptations) can alter an animal's phenotype and oxygen-haemoglobin dissociation curve at rest (Moraga et al. 1996; Storz 2007). A well-known

example is seen in foetal and maternal curves across different mammalian species including rats, sheep, humans, and elephants (Riegel et al. 1967; Novy et al. 1973; Bunn 1981; Moraga et al. 1996). The foetus has a higher oxygen-haemoglobin affinity (low P_{50}) than the mother, to permit adequate blood oxygenation in the low PaO_2 uterine environment (Moraga et al. 1996). The differences between foetal and maternal oxygen-haemoglobin affinities can be explained by the fact that foetal haemoglobin (haemoglobin F) is structurally different from adult haemoglobin (haemoglobin A) because it contains serine and not histidine, in position β143, which is one of the positions responsible for binding 2.3-diphosphoglycerate (2.3-DPG) in adults (Bunn 1981). These structural differences may explain the lower concentration of 2.3-DPG found in foetal blood compared to maternal blood (Bunn & Kitchen 1973). It has also been shown that soon after birth, the new-born's 2.3-DPG increases, permanently shifting its curve to the right, decreasing their oxygen-haemoglobin affinity (Bunn 1981). Surprisingly, these differences are not seen in foetal and adult haemoglobins of domestic cats (Novy et al. 1969) or horses (Bunn & Kitchen 1973).

There are also dynamic shifts of the oxygen-haemoglobin dissociation curve caused by changes in the organic phosphate 2.3-DPG, pH, $PaCO_2$, temperature, chloride ions (Cl^-), and haemoglobin derivatives (HbCO and MetHb) (Clerbaux et al. 1993; Chu et al. 2020). These dynamic adaptations, caused by the red cell allosteric effectors depend on the structural properties of haemoglobin and the concentration of the allosteric effectors in the blood (Weber & Campbell 2011). An increase in 2.3-DPG, H^+ and Cl^- ion concentration, $PaCO_2$, temperature and haemoglobin derivatives cause the oxygen-haemoglobin dissociation curve to dynamically shift to the right, to offload oxygen to the tissues. On the other hand, a decrease in these allosteric effectors causes the curve to dynamically shift to the left to limit offloading of oxygen to the tissues. The negative charges on the organic phosphate, 2.3-DPG, form ionic bonds with positive charges of the β_2 chain in haemoglobin, and stabilize the salt-bridges of deoxyhaemoglobin, therefore, reducing the affinity of oxygen to haemoglobin (Bunn 1981; Dhindsa et al. 1972). Cat, sheep, goat, and cow have significantly low levels of 2.3-DPG in their red blood cells and their oxygen-haemoglobin affinities are only partially altered by changes in the concentration of 2.3-DPG (Bunn 1981). Similar findings are reported in pronghorn antelope and giraffe (Dhindsa et al. 1974). According to Baumann et al. (1984), rhinoceros' haemoglobin is also only partially altered by 2.3-DPG because it lacks histidine at position β2, and in humans, histidine is responsible for the binding of 2.3-

DPG (Mazur et al. 1982; Baumann et al. 1984). Mammalian haemoglobin also interacts with H^+ and Cl^- ions (Malte et al. 2021). The H^+ ions bind to oxygen-linked groups (Bohr groups) on the haemoglobin in a tense state (deoxyhaemoglobin), stabilizing its inter-subunit salt bridges, thus reducing the affinity of oxygen to haemoglobin (Malte et al. 2021). The H^+ ions also bind at the C-terminal residues of the β chains, whereas Cl^- ions bind to either one α chain and one β chain (Weber 2007; Weber & Campbell 2011). The P_{50} of white rhinoceros (at pH of 7.2) increased from 7.6 mmHg to 17.1 mmHg when Cl^- ion concentration was increased from 0.01 M to 0.1 M (Bauman et al. 1984). These findings show that there is an effect of Cl^- ions on the rhinoceros' oxygen affinity to haemoglobin and this effect is similar to that in humans (Bauman et al. 1984). Sensitivity to temperature changes depend on the overall enthalpy (total heat) of oxygenation [i.e., the intrinsic heat of haem- oxygenation, the heat of the oxygen solution, the heat of dissociation of the other allosteric effectors (e.g., organic phosphates and H^+ and Cl^- ions) and the heat during the transition of haemoglobin from tense to relaxed state] (Weber & Campbell 2011). Furthermore, the overall effect of temperature on the affinity of oxygen to haemoglobin is reduced by the endothermic release of organic phosphates, H^+ and Cl^- ions (Weber & Campbell 2011). Pig haemoglobin, for example, has a low sensitivity to temperature changes and this can be attributed to several factors. The haemoglobin structure of pigs lacks a hydrophobic N-terminal region and has more 2.3-DPG binding sites compared to other mammalian species (Weber & Campbell 2011). It has also been shown that the red blood cells of pigs have twice as much 2.3-DPG than that in humans, which may reduce the overall effect of temperature on the pig's haemoglobin's oxygen affinity (Weber & Campbell 2011). White rhinoceros' affinity of oxygen to haemoglobin is also unaltered by changes in temperature but the exact reason for this is unknown (Reiners et al. 2019).

The variation in the oxygen-haemoglobin dissociation curves, haemoglobin structure and interaction between haemoglobin and the allosteric effectors among mammals may likely affect the way in which blood oxygenation can be measured in different species as most of the devices are designed specifically for use on human blood.

Oxygen content (CaO_2)

Oxygen content (CaO_2) is the total oxygen that is dissolved and that is bound to haemoglobin in the blood, and it is typically measured in mL of oxygen per dL of blood ($mL.dL^{-1}$) and expressed by the equation:

$$CaO_2 = (\text{Hüfner factor} \times [Hb] \times SaO_2) + (0.003 \times PaO_2)$$

where the Hüfner factor, also known as the oxygen binding capacity of haemoglobin, is the volume of oxygen per gram of haemoglobin ($mL.g^{-1}$) and is between 1.31 – 1.39 $mL.g^{-1}$ (Hüfner 1894; van Slyke 1924; Dijkhuizen et al. 1977; Clerbaux et al. 1986; Shimizu et al. 1986), [Hb] is the haemoglobin concentration, which is the grams of haemoglobin per decilitre of blood ($g.dL^{-1}$) and in humans it averages 13.5 – 18.0 $g.dL^{-1}$ for males and 11.5 – 16.0 $g.dL^{-1}$ for females. SaO_2 is the arterial oxygen-haemoglobin saturation and PaO_2 is the arterial partial pressure of oxygen, with a solubility of 0.003 $mL.dL^{-1}.mmHg^{-1}$ at STPD.

The Hüfner factor is the maximum volume of oxygen carried by 1 gram of haemoglobin (Hüfner 1894). According to Hüfner (1894), the theoretical (estimated) and measured values are both 1.34 $mL.g^{-1}$. It was later shown that the theoretical value (at STPD) should be 1.39 $mL.g^{-1}$ for humans (Braunitzer 1964; Gorelov 2004), 1.38 $mL.g^{-1}$ for dogs (Merlet-Benichou et al. 1974) and between 1.32 – 1.34 $mL.g^{-1}$ for horses (Svedberg & Fahraeus 1926; Boyes-Watson et al. 1947; Perutz 1998) based on the molecular weight of human (64458 g), dog (64898 g) and horse (66700 and 68000 g) haemoglobin. However, in the presence of inactive haemoglobins [deoxyhaemoglobin (HHb), HbCO, MetHb and other unknown inactive haemoglobins], the Hüfner factor (at STPD) is reported to be lower in mice (1.36 $mL.g^{-1}$), dogs (1.34 $mL.g^{-1}$), humans (1.36 – 1.37 $mL.g^{-1}$) and higher in the horse (1.38 $mL.g^{-1}$) (Merlet-Benichou et al. 1974; Dijkhuizen et al. 1977; Clerbaux et al. 1986; Shimizu et al. 1986). Hüfner factors as low as 1.21 – 1.31 $mL.g^{-1}$ have been reported when more than 5.7% of inactive haemoglobins were present in human blood (van Slyke 1924; Dijkhuizen et al. 1977). Surprisingly, Scheerrer and Bachofen (1972) reported a Hüfner factor of 1.39 $mL.g^{-1}$ (*in vivo*) in non-smokers breathing pure oxygen despite the presence of inactive haemoglobins in the blood (0.15% HbCO and 0.20% unknown active haemoglobin). Due to the variation in the Hüfner factor reported in the literature for humans and other

mammals, modern day devices (i.e., benchtop co-oximeters and blood analysers) employ standardized Hüfner factors that fall in the range of 1.30 – 1.39 $mL.g^{-1}$ (Zoff et al. 2019; ITC, Edison, NJ).

1.2.2 Techniques to monitor blood oxygenation

In both human and veterinary medicine, different methods are used to assess blood oxygenation in order to monitor and maintain sufficient tissue oxygenation for the patient's survival. These devices or methods vary according to the measurement technique or principle, the unit of measurement, and the devices' applicability and limitations in clinical and laboratory settings (Table 1.1). Currently, devices that employ spectrophotometry are popular among medical and veterinary professionals because they allow for minimally invasive monitoring of blood oxygenation in patients (Maikala 2010).

Table 1.1 Summary of the some of the methods commonly used in clinical practice to monitor blood oxygenation [either as arterial partial pressure of oxygen (PaO_2), or arterial oxygen-haemoglobin saturation (SaO_2), or peripheral arterial oxygen-haemoglobin saturation (SpO_2)], and, or tissue oxygenation, perfusion and metabolism. The principle of measurement, variables measured or calculated, the site of measurement, advantages and disadvantages of each method are also summarised.

Blood oxygenation method	**Principle of measurement**	**Variables measured/ calculated (unit of measurement)**	**Site of measurement**	**Advantages**	**Disadvantages**
Clark electrodes (reference method)	**Polarographic method** - Based on the principle of oxidation and reduction. - Consists of electrodes with a probe at which the tip is an exposed gold or platinum cathode and a silver anode. The following reaction occurs at the anode: $4Ag \rightarrow 4Ag^{++}4e$ and $4Ag^{++}\ 4Cl^{-} \rightarrow 4AgCl$. This reaction occurs ($O_2 + 2H_2O + 4e \rightarrow 4OH^{-}$) at the cathode. - The current produced by the needle electrode is linearly related to the PO_2 in the blood surrounding the electrode.	PO_2 (mmHg)	Arterial and venous blood (whole blood)	- Quick, easy to use and reliable - Tiny electrodes that can be employed in other blood analysers. - Measures PO_2 reliably	- Invasive - Electrodes consume small amounts of oxygen. - Requires constant calibration. - Measures dissolved oxygen and cannot detect oxygen bound to haemoglobin.
Optodes	**Fluorescence method** - Consist of light-emitting diodes (LEDs) that emits light at wavelengths between 400 – 600 nm - The light is quenched by the presence of oxygen and the fluorescence is converted to PO_2. - PO_2 in the blood that collides with a fluorophore is inversely proportional to the intensity of fluorescence exhibited.	PO_2 (mmHg)	Arterial, venous and capillary blood (whole blood)	- Reliable, easy to use and affordable - Does not consume oxygen - Employed in catheters and can measure PaO_2 in capillaries (i.e., at tissue levels)	- Invasive - Requires constant calibration - Accuracy of the method is affected by the calibration technique and random noise especially at high PO_2 values. - Measures dissolved oxygen and cannot detect oxygen bound to haemoglobin.
Benchtop co-oximeter (reference method)	**Multi-wavelength spectrophotometry** - Utilizing seven or more wavelengths to measure fractional SaO_2 directly from the arterial or venous blood. This device also measures the concentration of HbO_2, HHb, HbCO, and MetHb, respectively.	SaO_2, SvO_2 (%)	Arterial and venous blood (whole blood)	- Quick, easy to use and mostly portable - Measures the different haemoglobin derivatives. - The device is calibrated using blood samples at saturations between 0-100%. Therefore, reliable at the 0-100% saturation range.	- Invasive and noncontinuous; requires blood sample. - No information on tissue oxygenation.

Table 1.1 continued

Blood oxygenation method	Principle of measurement	Variables measured/ calculated (unit of measurement)	Site of measurement	Advantages	Disadvantages
Pulse oximeter	**Dual-wavelength spectrophotometry** - Utilizes the presence of a pulsatile signal generated by the arterial blood vessels and the Beer-Lambert law. - Utilizes probes that use LEDs at two wavelengths (660 nm and 940 nm) based on the absorption spectra of HbO_2 and HHb at 660nm and 940 nm, respectively.	SpO_2 (%)	Peripheral tissue bed. The probes are placed at different sites including ear, lip, tongue, cheek, forehead (in babies), finger (in humans), base of the tail, rectum, vulva, and prepuce	- Non-invasive and provides continuous readings - Portable and can be used in field-settings	- Does not measure other haemoglobin derivatives (i.e., HHb, HbCO and MetHb). - Calibrated on healthy patients with saturations of 70-100%. Therefore, only reliable above 70-100% in all mammals. - No information on tissue oxygenation.
Masimo Radical SET Pulse co-oximeter	**Multi-wavelength spectrophotometry** - Utilizes probes that uses more than seven wavelengths of light (500 nm and 1400 nm) based on the absorption spectra of HbO_2 and the other haemoglobin derivatives. - Utilize signal extraction technology to isolate individual arterial and non-arterial signals that arise from movement and other artefacts to calculate the true arterial signal.	SpO_2 (%)	Peripheral tissue bed. The probes are placed at different sites including ear, lip, tongue, cheek, forehead (in babies), finger (in humans), base of the tail, rectum, vulva, and prepuce	- Non-invasive and provides continuous readings - Measures the different haemoglobin derivatives - Portable and can be used in field-settings - The device is calibrated by measuring a reference signal at saturations between 0-100%. Therefore, reliable at saturation ranges of 0-100%.	- Limited probe types for use in mammals other than human. - No information on tissue oxygenation. - Limited validation studies.
Fibre-optic pulmonary artery or mixed venous catheters	**Dual-wavelength transflectance spectrophotometry** - Based on light absorption spectra of oxyhaemoglobin. - Utilizes two optical fibres that emit light at two or more wavelengths (600 to 900 nm). - One optical fibre sends light into the venous blood and the light absorbed by the blood is reflected back to another fibre that transmits it to a photodiode where it is measured as SjO_2.	SvO_2 (%)	Blood vessels of any organ of choice (e.g., Jugular vein, kidneys and the brain)	- Cerebral blood flow is a global measure of cerebral blood oxygenation - Reflect balance between oxygen supply and consumption. - Reliable in anaesthetized humans.	- Invasive catheters are used - Catheters may cause extracerebral contamination - Monitoring errors - Catheter migration abutment against the vessel wall

Table 1.1 continued

Blood oxygenation method	Principle of measurement	Variables measured/ calculated (unit of measurement)	Site of measurement	Advantages	Disadvantages
Reflectance oximetry	**Multi-wavelength transflectance spectrophotometry** - Based on light absorption spectra of oxyhaemoglobin. - Utilizes fibre-optic probes that send light of different wavelengths (i.e., between 400 to 900 nm) to measure oxyhaemoglobin concentration.	μHbO_2 (%)	Microcirculation (i.e., arterioles and capillaries)	- Non-invasive - Reflect balance between oxygen supply and consumption. - Reliable in anaesthetized humans.	- Probes can impede blood flow to the tissues reducing arterial oxygen-haemoglobin saturation and its reliability. - Pigmentation and movement artefacts affect the SpO_2 readings
Near infrared spectroscopy (NIRS)	**Multi-wavelength transflectance spectrophotometry** - Based on light absorption spectra of oxyhaemoglobin. - Utilizes probes that send near-infrared light (i.e., between 700 to 1000 nm) to the deeper tissues based on the absorption spectra of HbO_2 and HHb. - measures blood flow using the Fick's principle.	HbO_2 (%), HHb (%), cytochrome aa3 and blood flow	Deeper tissues such as muscle, subcutaneous fat, and larger blood vessels at different organs including the brain	- Non-invasive - Cerebral blood flow is a global measure of blood oxygenation - Cytochrome aa3 reflects cellular oxidative metabolism and tissue oxygenation and consumption	- Not easy to validate. - Wavelengths of light used, and algorithms differ between devices, making it hard to validate. - Reliability of this technique is unknown. - Not suitable for superficial tissue because it only uses near-infrared light that penetrates deeper than visible light.

Table 1.1 continued

Blood oxygenation method	Principle of measurement	Variables measured/ calculated (unit of measurement)	Site of measurement	Advantages	Disadvantages
Point-of-care (POC) blood analysers for calculating arterial oxygen-haemoglobin saturation ($cSaO_2$)	**Algorithm employed in blood analysers** - Severinghaus algorithm - Mostly uses the standard human oxygen-haemoglobin curve to calculate SaO_2 as a function of PaO_2 - Measures PaO_2 using a Clark-type electrode - $cSaO_2$ is calculated by the blood analyser after correcting for pH and concentration of bicarbonate (HCO_3^-), of which are also measured directly by the blood analyser.	$cSaO_2$ (%)	Arterial or venous blood (whole blood)	- Portable and easy to use - Measures different blood variables [i.e., pH, PO_2, PCO_2, BE, HCO_3^-, [Hb], glucose, lactate, creatinine, and ion concentrations (i.e., Na+, K+, Cl-) and anion gap potassium (AgapK) and haematocrit (Hct)], respectively. - Reliable measure of PaO_2.	- Invasive and noncontinuous; requires blood sample. - No information on tissue oxygenation. - Uses the standard human oxygen-haemoglobin dissociation curve, which differs from that of other species (including rhinoceros).
Method of Tucker (1967) for calculating $cSaO_2$	**Polarographic method** - Based on the principle that haemoglobin bound oxygen can be released into solution using a potassium ferricyanide solution and the amount of oxygen in the solution can be measured accurately using an oxygen electrode. - Measures the change in PaO_2 (mmHg) before and after injecting the blood sample, then calculate CaO_2 ($mL.dL^{-1}$). Tucker CaO_2 and the oxygen content equation can be used to determine $cSaO_2$.	$cSaO_2$ (%)	Arterial and venous blood (whole blood)	- Simple and reliable method to measure CaO_2 - CaO_2 determination can be quickly self-calculated	- Invasive and noncontinuous; requires blood sample. - Cannot be used easily in field-settings. - Limited validation studies.
Siggaard-Andersen algorithm for calculating $cSaO_2$	**Algorithm employed in blood analysers** - Mathematical model based on Hill plot - Uses standard and non-standard oxygen-haemoglobin curve to calculate SaO_2 as a function of measured PaO_2 - $cSaO_2$ is calculated by the algorithm after correcting for $PaCO_2$, pH and temperature variables measured by a blood analyser.	$cSaO_2$ (%)	Arterial or venous blood (whole blood)	- Standard and non-standard oxygen-dissociation curve - Accounts for changes in variables that affect the position of the oxygen-haemoglobin dissociation curve (i.e., $PaCO_2$, pH, temperature HbCO, MetHb, foetal Hb, base excess and 2.3-DPG)	- Invasive and noncontinuous; requires blood sample. - Complex calculations that require species specific details and time to self-calculate or measure. - Limited validation studies.

1.2.2.1 Spectrophotometry

Spectrophotometry is a measure of the interactions (i.e., absorption, transmission, and reflection) between light and matter, and it is commonly used to measure the concentration of each light-absorbing species in nature (i.e., chromophores) (Maikala 2010). Haemoglobin can absorb and reflect light at different wavelengths (Severinghaus & Astrup 1986). This concept was first discovered by Felix Hoppe Syler in 1825 – 1895 when he showed that haemoglobin absorbs green and blue light from the Soret band (i.e., wavelength of about 400 nm) and found that the colour of blood changes when it is exposed to air (Severinghaus & Astrup 1986). These discoveries first led to the use of spectrophotometric methods to determine the concentration of haemoglobin in the blood (Harboe 1959; Benesch et al. 1973; Van Kampen & Zijlstra 1983).

1.2.2.2 Beer-Lambert Law

Spectrophotometry used to determine blood oxygenation is based on the Beer-Lambert law, which states that the light absorbed by a substance (i.e., haemoglobin) dissolved in a thin solvent (i.e., plasma) is directly proportional to the concentration of the substance and the pathlength of the light penetrating the solution (Wukitsch et al. 1988). The Beer-Lambert law is expressed using the equation:

$$\mathrm{A} = \log\left(\frac{\mathrm{Io}}{\mathrm{I}}\right) = \varepsilon * \mathrm{d} * \mathrm{c}$$

Where A is the absorbance at a specific wavelength (nm) of light, ε is the absorptivity or the extinction coefficient in $M^{-1}.cm^{-1}$, d is the thickness of the medium (or optical path length) in cm, and c is the molar concentration in molar mass (M). When multiple light-absorbing components are present in a solution, the absorbance is measured as the sum of the absorbances of all components present in the solution.

Conventional spectrophotometers (Fig. 1.4) that determine the concentration of haemoglobin in the blood consist of a light source from a deuterium and a tungsten lamp (L), a monochromator (M), a cuvette that contains a blood sample (C), and a detector (D) (Zwart et al. 1984). The light from the lamp is first passed through a monochromator (prism) that divides the light into different wavelengths and each wavelength of light passes through the sample (C). The light absorbed by the sample is detected

and measured (as the absorptivity or extinction coefficient) over the entire visible and near-infrared spectral region (200 and 1000 nm) (Zwart et al. 1984).

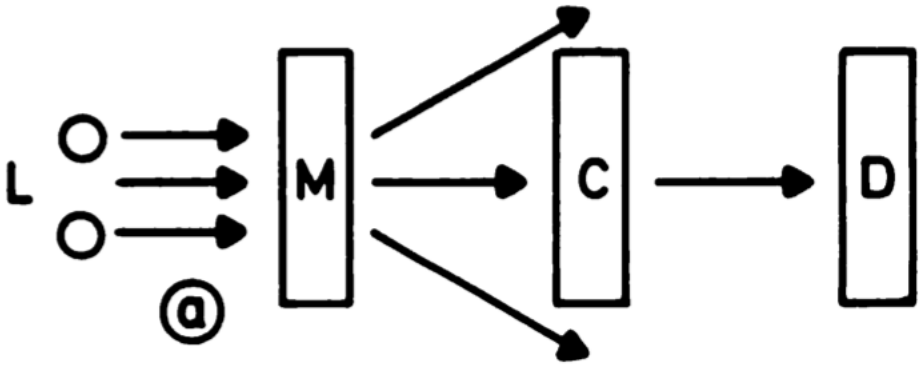

Figure 1.4 A conventional spectrophotometer as described by Zwart et al. 1984 used to measure the concentration of haemoglobin in the blood. The spectrophotometer consists of L, the light source [(a) deuterium and tungsten lamp] at wavelengths of 200 – 1000 nm, M, the monochromator (prism) that divides the light into different wavelengths, C, the cuvette that contains a blood sample and D, a light detector that measures the light absorbed by haemoglobin. Reprinted from Zwart, A., Buursma, A., Van Kampen, E. J., & Zijlstra, W. G. (1984). Multicomponent analysis of haemoglobin derivatives with reversed-optics spectrophotometer. *Clinical Chemistry*, *30*(3), 373-379, Copyright © 1984 Oxford University Press with permission from The American Association of Clinical Chemists, Inc.

Determination of total haemoglobin concentration

Cyanmethaemoglobin (HiCN) method was the first spectrophotometric method to be accepted as the gold-standard by the Standardizing Committee of the European Society of Haematology and the International Committee for Standardization in Haematology (ICSH) (Van Kampen & Zijlstra 1983; Zwart et al. 1984). The HiCN method measures the haemoglobin concentration [Hb] based on the principle that all haemoglobin present in the blood can be converted to HiCN by adding potassium cyanide or ferricyanide to the solution. The amount of light absorbed by HiCN at 540 nm (known as the millimolar absorptivity) can be measured, which represents the total haemoglobin concentration present

in the blood (Van Kampen & Zijlstra 1983; Zwart et al. 1984). Mice, dog, human, cow, and horse HiCN have a similar maximum millimolar absorptivity of 11 $L.mmol^{-1}.cm^{-1}$ at 540 nm, which makes HiCN a reference method for measuring haemoglobin concentration across different species (Van Kampen & Zijlstra 1983; Zijlstra et al. 1994; Zijlstra & Buursma 1997).

The extensive research on the HiCN method became a starting point for more research on the measurement of absorbance spectra of HbO_2 and the other haemoglobin derivates (i.e., HHb, HbCO and MetHb) in the visible and near-infrared spectral range (600 – 1000 nm). Oxyhaemoglobin and the other haemoglobin derivatives absorb light at different wavelengths at the spectral range of 600 – 1000 nm and these differences are shown in Figure 1.5. Therefore, to accurately distinguish between the HbO_2, HHb, HbCO and MetHb; the maximum and minimum millimolar absorptivity at different wavelengths (600 –1000 nm) and their millimolar absorptivity similarities (also known as the isosbestic points) are measured. For example, the human HbO_2 maximum millimolar absorptivity is at wavelengths of 577 and 542 nm and the minimum millimolar absorptivity is at 560 and 510 nm (Van Kampen & Zijlstra 1983). The isosbestic points, which are the points where the two haemoglobin derivatives have the same millimolar absorptivity, for HbO_2 and HHb, are at wavelengths of 315, 506.5, 522, 548.5, 569 and 586 nm (Van Kampen & Zijlstra 1983). The isosbestic points for HbO_2 and HbCO are at wavelengths of 497, 540, 549.5, 572.5, and 592 nm (Van Kampen & Zijlstra 1983) and for HbO_2 and MetHb, the isosbestic points are at wavelengths of 525.5 and 590.5 nm (Van Kampen & Zijlstra 1983). The wavelengths for each millimolar absorptivity of HbO_2, have been summarised in Table 1.2.

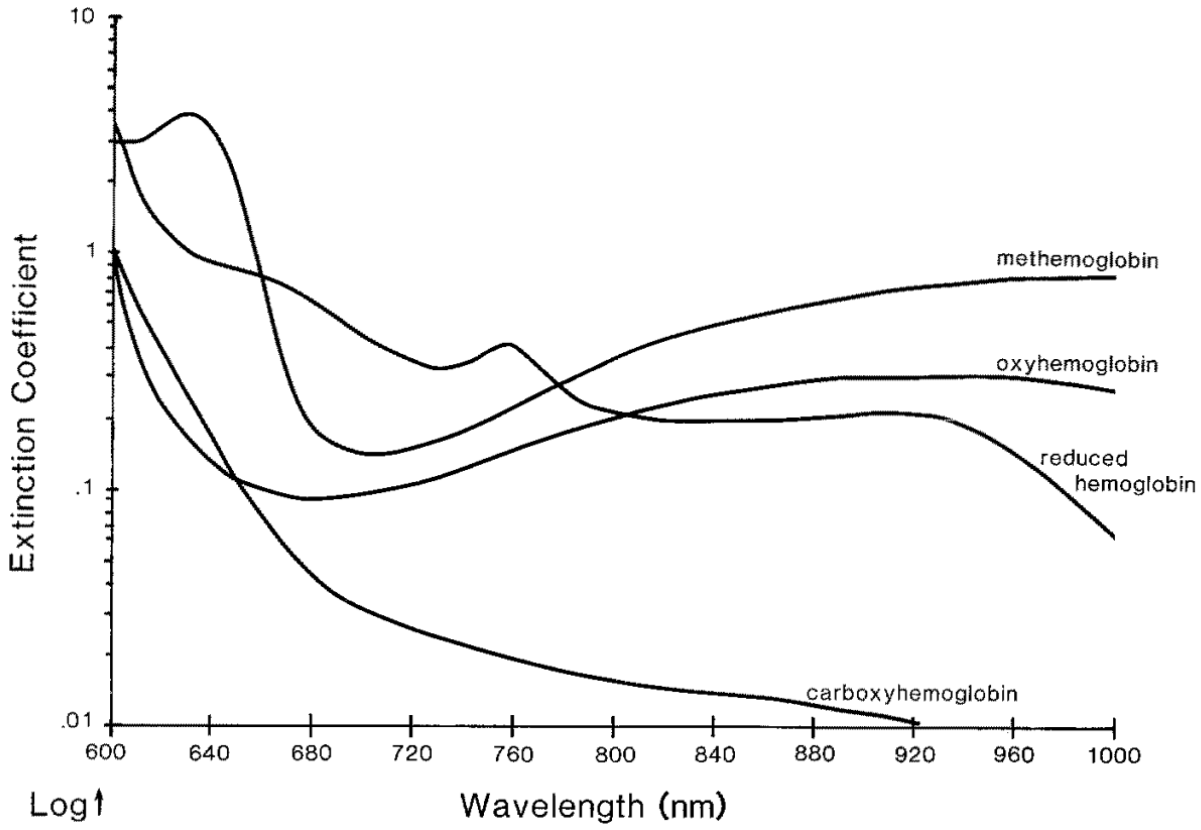

Figure 1.5 The extinction coefficients (or millimolar absorptivity) of oxyhaemoglobin and the other haemoglobin derivatives [deoxyhaemoglobin (HHb), carboxyhaemoglobin (HbCO) and methaemoglobin (MetHb)] at the visible and near infrared spectral range (i.e., at wavelengths of 600–1000 nm). These specific wavelengths and their extinction coefficients are used in different spectrophotometric devices to measure the concentration of HbO_2 and the other haemoglobin derivates. This Figure is from Van Kampen & Zijlstra (1983). Reprinted from Van Kampen, E. J., & Zijlstra, W. G. (1983). Spectrophotometry of haemoglobin and haemoglobin derivatives. *Advances in Clinical Chemistry*, *23*, 199-257, Copyright © 1983 Academic Press Inc. with permission from Elsevier Ltd.

Table 1.2 The maximum and minimum millimolar absorptivity of oxyhaemoglobin (HbO_2) at wavelengths between 400 – 1000 nm. Also represented are the millimolar absorptivities at isosbestic points (the point where the two haemoglobin derivatives have the same millimolar absorptivity) between HbO_2 and the other haemoglobin derivatives [i.e., deoxyhaemoglobin (HHb), carboxyhaemoglobin (HbCO) and methaemoglobin (MetHb)]. These specific wavelengths are used in different spectrophotometric devices to measure the concentration (as the absorptivity or extinction coefficient) of HbO_2 and the other haemoglobin derivates (i.e., HHb, HbCO and MetHb). This table is from Van Kampen & Zijlstra 1983. Reprinted from Van Kampen, E. J., & Zijlstra, W. G. (1983). Spectrophotometry of haemoglobin and haemoglobin derivatives. *Advances in Clinical Chemistry*, *23*, 199-257, Copyright © 1983 Academic Press Inc. Published by Elsevier Ltd.

MILLIMOLAR ABSORPTIVITY OF HbO_2

λ (nm)	ϵ^{λ} (liters $mmol^{-1}$ cm^{-1})	Comments
930	0.31	Maximum
815	0.22	Isobestic with Hb
690	0.07	Minimum
592	2.13	Isobestic with HbCO
590.5	3.62	Isobestic with Hi
586	7.23	Isobestic with Hb
577	15.37	Maximum
572.5	13.50	Isobestic with HbCO
569	11.27	Isobestic with Hb
560	8.47	Minimum
549.5	12.06	Isobestic with HbCO
548.5	12.46	Isobestic with Hb
542	14.37	Maximum
540	14.27	Isobestic with HbCO
525.5	7.72	Isobestic with Hi
522	6.42	Isobestic with Hb
510	4.76	Minimum
506.5	4.81	Isobestic with Hb
497	5.16	Isobestic with HbCO
415	131.0	Maximum

The millimolar absorptivity of foetal (haemoglobin F) and adult (haemoglobin A) human haemoglobin derivatives differ at the red and infrared spectral region (Zijlstra et al. 1991). These differences are mainly observed on the MetHb of haemoglobin F and haemoglobin A at wavelengths of 500 and 640 nm (Zijlstra et al. 1991). These results have prompted some questions regarding the need for additional studies on the haemoglobin absorption spectra of other species (Zijlstra & Buursma 1987; Zijlstra et al. 1994; Grosenbaugh et al. 1997; Zijlstra & Buursma 1997; Reiners et al. 2019). So far, no spectral differences have been observed between adult human and other adult mammalian species (e.g., cat, dog, pig, cow, horse, and white rhinoceros) HbO_2 and HHb at the visible and near infrared spectral region (Zijlstra & Buursma 1987; Zijlstra et al. 1994; Grosenbaugh et al. 1997; Zijlstra & Buursma 1997; Reiners et al. 2019). However, more studies are needed to determine if there are any differences in the absorption spectra of MetHb and HbCO among other mammalian species other than human at the visible and near infrared spectral region.

With the millimolar absorptivity of HbO_2 and the other haemoglobin derivatives known, there was a desire to use spectrophotometry to measure SO_2 from venous or arterial blood samples collected anaerobically. This led to the development of multi-wavelength spectrophotometric methods to measure the concentration HbO_2, the other haemoglobin derivates (i.e., HHb, HbCO and MetHb) and [Hb] in whole blood (Nahas 1951; Zwart et al. 1981). In 1951, Nahas introduced a cuvette that was built to fit a spectrophotometer (Nahas 1951). The method of Nahas (1951) for analysis of SaO_2 depends on the difference in the optical densities (D_1 and D_2) of HbO_2 and HHb at wavelengths of 505 and 605 nm. The wavelength of 505 nm was the isosbestic point for HbO_2 and HHb. Therefore, SaO_2 was calculated using the equation:

$$SaO_2(\%) = \frac{X_{HHb} - X}{X_{HHb} - X_{HbO2}} * 100$$

Where X_{HHb} is the ratio of optical densities $\frac{D2}{D1}$ of fully deoxygenated blood, X is the optical density ratio of an unknown blood sample and X_{HbO2} is the ratio of optical densities $\frac{D2}{D1}$ of fully oxygenated blood.

Blood samples that were controlled for oxygen and carbon dioxide partial pressures were used to measure $\frac{D2}{D1}$ at different saturation ranges (i.e., between 0-100%) and these known ratios were used to calibrate the device as shown in the Figure 1.6 (Nahas 1951).

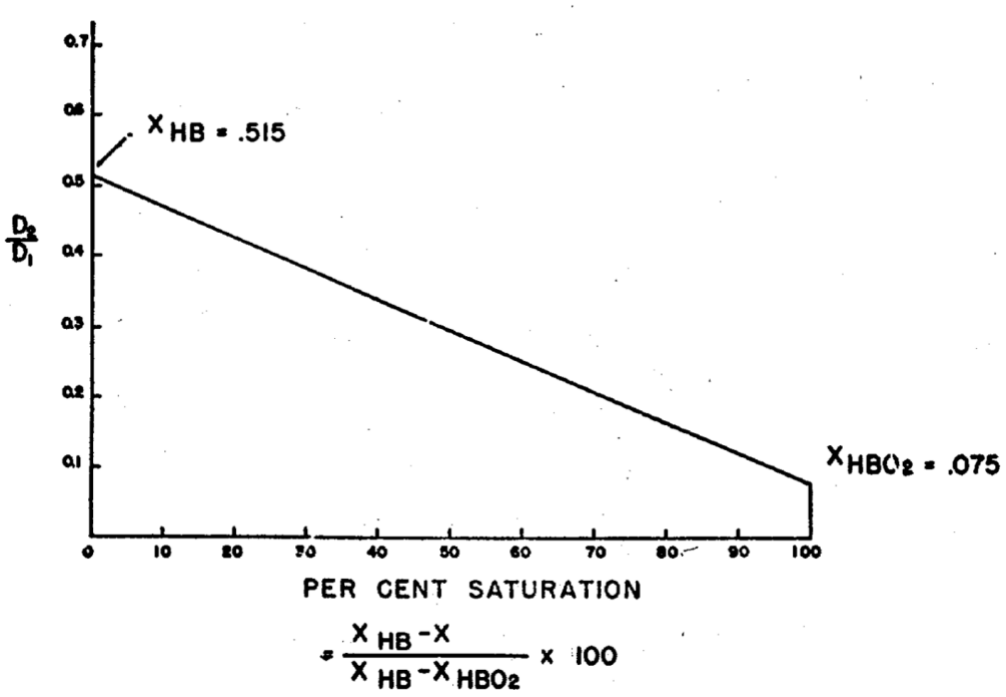

Figure 1.6 Calibration curve for the determination of arterial oxygen-haemoglobin saturation [SaO_2 (%)] showing the ratio of optical densities ($\frac{D2}{D1}$) in whole haemolysed blood between fully oxygenated (X_{HbO2}) and deoxygenated blood (X_{Hb}) at 505 nm and 605 nm. The curve was derived from blood samples of known oxygen and carbon dioxide partial pressures and the measured optical densities were used to calibrate the method of Nahas (1951) for the measurement of SaO_2. Reprinted from Nahas, G. G. (1951). Spectrophotometric determination of haemoglobin and oxyhaemoglobin in whole haemolysed blood. *Science*, *113*(2947), 723-725, Copyright © 1951 with permission from American Association for the advancement of Science.

The SaO_2 measured by the method of Nahas (1951) from 33 human blood samples were accurate (bias or mean difference of 0.2%) and precise (standard deviation of 1.9%) when compared to the SaO_2 measured by the method of Van-Slyke & Neill (1924) (reference method). However, the method of

Nahas (1951) was still not practical because it lacked a readily available cuvette holder and thermostat. Therefore, a special cuvette holder for the Zeiss PMQ spectrophotometer was designed, and then later improved as a thermostated holder to help maintain the temperature of the cuvette and blood sample at 37°C (Siggard-Andersen et al. 1972; Siggaard-Andersen 1977). Later, Siggard-Andersen et al. (1972) developed a method that measured SaO_2, HHb, HbCO, MetHb and [Hb] reliably at wavelengths of 470, 570, 600, and 670 nm, making it a gold-standard method for humans during the 1970s.

1.2.2.3 Co-oximetry

The new technology of spectrophotometry led to the development of automated co-oximeters (multi-wavelength spectrophotometers) for rapid and reliable determination of SaO_2, HHb, HbCO, MetHb in whole blood. In co-oximeters, a blood sample in a syringe is inserted into a cuvette, then the cuvette is inserted into the co-oximeter device where it is automatically mixed, haemolysed and temperature regulated inside the cuvette. Then light at different wavelengths is directed through the cuvette and the amount of light that is absorbed by the blood is automatically measured with results automatically displayed on the device screen (Maas et al. 1970). The co-oximeter device directly measures the concentration of all haemoglobin derivatives (HbO_2, HHb, HbCO, MetHb) present in the blood. From these values, fractional arterial oxygen-haemoglobin saturation (SaO_2), which is the concentration of oxyhaemoglobin divided by the total concentration of the sum of all haemoglobin derivatives present in the blood is calculated (by the co-oximeter) using the equation:

$$\mathrm{SaO_2}(\%) = \frac{\mathrm{HbO_2}}{\mathrm{HbO_2} + \mathrm{HHb} + \mathrm{HbCO} + \mathrm{MetHb}} * 100$$

Where HbO_2, HHb, HbCO and MetHb are the concentrations of oxyhaemoglobin, deoxyhaemoglobin, carboxyhaemoglobin, and methaemoglobin present in the blood.

In the 1970s and 80s, some of the first co-oximeters were designed by the Instrumentation Laboratory (e.g., IL 182, 282; Instrumentation Laboratory Inc., Lexington, USA) and Radiometer (e.g., OSM-1 and OSM-2 hemoximeters/co-oximeter; Radiometer Corporation., Cleveland, OH) (Maas et al. 1970;

Heinemann et al. 1979; Zwart et al. 1987; Burrin et al. 1989; Shiao 2002). These benchtop co-oximeters were calibrated against the gold-standard method of Van-Slyke after equilibration of the blood samples using tonometry at the entire 0-100% saturation range for HbO_2 and HHb (Maas et al. 1970). To measure haemoglobin concentration [Hb], co-oximeters were calibrated against the HiCN method after equilibrating the sample filled with potassium ferricyanide using tonometry (Maas et al. 1970). Advantages of co-oximetry include its ability to reliably differentiate between the different haemoglobin species, and that it is calibrated at the entire 0-100% saturation range, therefore, it can be used to reliably monitor oxygenation of both diseased and healthy patients at any saturation level.

Currently, there are benchtop co-oximeters that utilize up to 128 wavelengths (e.g., Radiometer ABL 720) (Shiao 2002). In 1993, a new technology of a benchtop co-oximetry known as the AVOXimeter was introduced to the market. The first model of these was the AVOXimeter 1000E that measures three variables, namely HbO_2, [Hb] and CaO_2 in whole blood. The current model, introduced in 1996, is the AVOXimeter 4000 that measures HbO_2, the other haemoglobin derivatives (i.e., HHb, HbCO and MetHb), [Hb] and CaO_2 (http://www.pointofcare.net/vendors/avox.htm; AVOXimeter 4000 user manual). These AVOXimeter devices are generally inexpensive, easy to use, have acceptable operation costs, portable (weighs 1.8 kg), and produces results in less than 10 seconds. They also have a battery-powered system, with 8 hours battery life, which can be very convenient especially in field settings when monitoring white rhinoceros. This device does not require sample preparation and only 50 µL of sample is needed to obtain readings. The reliability of SaO_2 reported by the AVOXimeter has been demonstrated in fresh blood of humans when compared with SaO_2 measured from a conventional reference method Radiometer OSM-3 co-oximeter (Freeman & Steinke 1993; Gong 1995; Bailey et al. 1997). However, only one study has used the benchtop AVOXimeter 4000 co-oximeter device as a reference method in wildlife and the study was done in immobilized impala (Mtetwa et al. 2020).

To determine the performance of a spectrophotometric device, it is required that the manufacturers compare the reliability of its measurements against those of a reference or gold standard spectrophotometric device. Co-oximetry has been certified by the US Food and Drug Administration (FDA) and International Organization for Standardization (ISO) as the reference method for monitoring

SaO_2 and all manufacturers must validate their SaO_2 measurements with the SaO_2 reported by a benchtop co-oximeter reference method after it directly measures all haemoglobin derivatives (HbO_2, HHb, HbCO, MetHb) present in the blood (DIN EN ISO 80601-2-61). Pulse oximetry (a dual-wavelength spectrophotometer) is one of the devices used to indirectly measure (estimate) SaO_2, and the FDA and ISO have approved pulse oximetry if its estimates of SaO_2 (known as SpO_2) have a bias (mean difference) $\leq$3% when compared to SaO_2 from a co-oximeter (Batchelder & Raley 2007).

1.2.2.4 Pulse oximetry

From the development of co-oximetry came advancements in monitoring SaO_2 continuously and non-invasively. The first of these non-invasive devices was a pulse oximeter (particularly, an ear oximeter), developed by a biomedical engineer, Takuo Aoyagi in the early 1970s. In 1975, Nakajima and colleagues used Aoyagi's technology to design the first continuous and non-invasive commercial pulse oximeter device, called the Minolta-Mochida Oximet MET 1471, which indirectly measured peripheral oxygen-haemoglobin saturation (SpO_2) and could detect a pulse signal that was dependent only on changes in the arterial blood (Severinghaus et al. 1986; Wukitsch et al. 1988). This device had its limitations, it was very sensitive to movement, therefore could not provide reliable SpO_2 readings. Later, Mendelson and colleagues (1981) investigated the possibility that light (from light emitting diodes and photodiodes) reflected or transmitted on the skin could be used to estimate arterial oxygen-haemoglobin saturation (Mendelson et al. 1983). This device was accurate with a standard deviation of 0.76% at the 89-98% saturation range (Severinghaus et al. 1986). From this research came the successful devices designed by Biox Company followed by Nellcor, both of which still produce the most popularly used pulse oximeters (e.g., Nellcor N200 and datex Ohmeda 3800 pulse oximeter devices) during anaesthesia.

Pulse oximetry, also now called the fourth vital sign, is one of the main devices for monitoring human and veterinary patients (Reiners et al. 2017). It has been shown that pulse oximetry during anaesthesia was able to detect more than 40% of perioperative incidences and anaesthesia related deaths in cats and humans (Brodbelt et al. 2007). Pulse oximetry is a simple, non-invasive, and continuous method

that utilizes peripheral probes to indirectly measure an estimate of SaO_2 (SpO_2) and pulse rate (PR). This device uses plethysmography to indirectly measure SpO_2 and is based on the principle that the light absorbance differs between systole and diastole (Jubran 1999; Proulx 1999; Chan et al. 2013). During systole, the heart pushes blood into the body, including the peripheral tissue bed, increasing the blood volume in the arteries and arterioles, causing them to distend (Jubran 1999; Proulx 1999; Chan et al. 2013). The increased amount of haemoglobin in the distended arteries and arterioles will cause an increase in the light absorbance by haemoglobin in the pulsatile blood (Jubran 1999; Proulx 1999; Chan et al. 2013). During diastole, less blood flows into the skin therefore there is decrease in blood volume and blood pressure in the arteries and arterioles. For that reason, during diastole, the amount of light absorbed is not caused by arterial blood but rather caused by non-pulsatile blood (venous blood), skin, bone, and other tissues as they are also capable of absorbing light (Jubran 1999; Proulx 1999; Chan et al. 2013). For pulse oximetry to work, the light absorbance during systole and diastole must be distinguished. The light absorbance during systole is described as the alternating current (AC), and the light absorbance during diastole as the direct current (DC) as shown in Figure 1.7a (Pologe 1987; Jubran 1999; Chan et al. 2013). The ratio between light absorbance of pulsatile and non-pulsatile blood (including skin, bone, and other tissues) in the red and infrared region can be calculated as follows:

$$R = \frac{A_{red\text{-}AC} / A_{red\text{-}DC}}{A_{IF\text{-}AC} / A_{IF\text{-}DC}}$$

Where A is the ratio between the absorbance of light in the red or the infrared (IF) spectrum by the pulsatile arterial blood (red/IF-AC) and non-pulsatile blood (red/IF-DC). According to this pulse oximeter method, the ratio is empirically related to SpO_2. The ratio is used to compute a calibration curve (Fig. 1.7b) for pulse oximeters, which is stored inside a micro-processor in the pulse oximeter (Pologe 1987; Jubran 1999; Chan et al. 2013) to calculate SpO_2.

Pulse oximeters utilizes non-invasive probes that consist of a light source [i.e., light emitting diodes (LED)] that emit light at wavelengths of 660 nm and 960 nm (Fig. 1.8). The LED is directed through a peripheral tissue bed and the light absorbed by oxyhaemoglobin and deoxyhaemoglobin in the blood is detected by a light detector (photodiode) on the same probe (Schowalter 1997). The photodiode on the

probe generates a current that is proportional to the intensity of LED light absorbed (Schowalter 1997). The current is then converted to a voltage by an analogue amplifier inside the pulse oximeter. Pulse oximetry depends on a microprocessor system to sort the LEDs absorbed light by the pulsatile and non-pulsatile blood and convert them to synchronised readings that are displayed as values on the pulse oximeter.

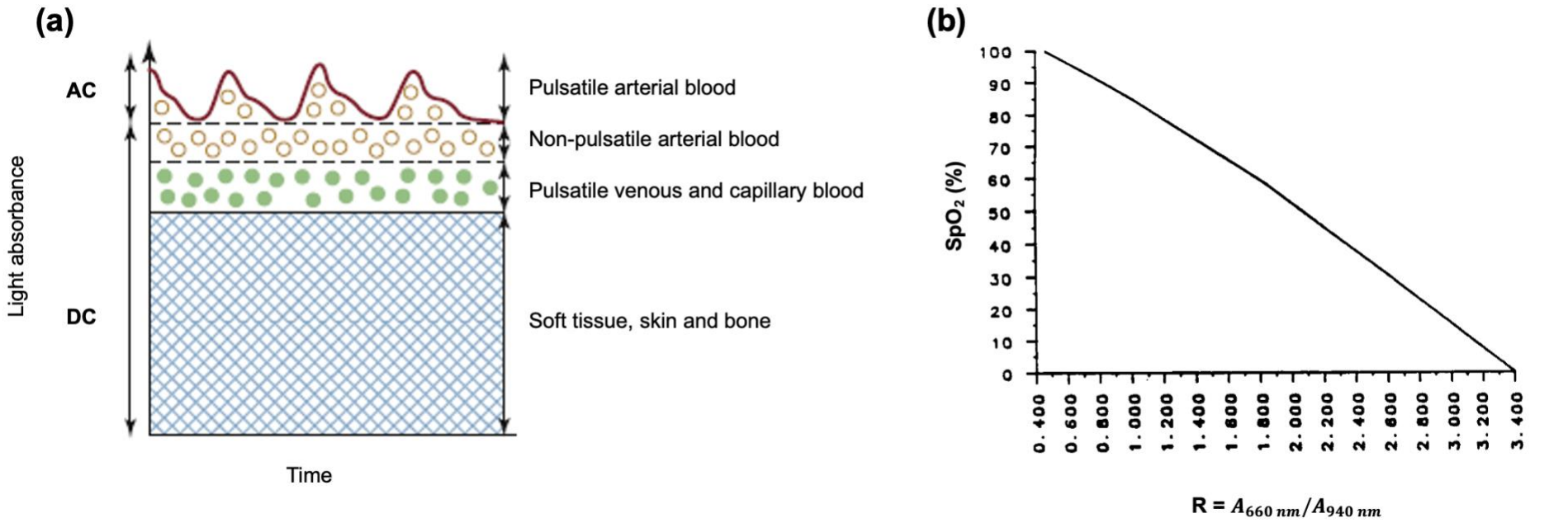

Figure 1.7 Light absorbance between pulsatile arterial blood, non-pulsatile venous blood, soft tissue, skin, and bone (Fig. 1.7a). To determine SpO_2, the light absorbers are divided into alternating current (AC) and direct current (DC) (Fig. 1.7a). Peripheral arterial oxygen-haemoglobin saturation is then estimated from the ratio between the light absorbance of AC and DC at wavelengths of 660 and 940 nm. The relationship between SpO_2 (%) and the red and infrared absorption ratio obtained from empirical data that were collected *in vivo* from healthy patients with saturation levels between 70-100%, which represents the calibration curve for pulse oximetry. At saturation levels below 70%, the values were extrapolated from saturation values measured by a benchtop co-oximeter, reference method. Reprinted from Pologe, J. A. (1987). Pulse oximetry: technical aspects of machine design. *International Anesthesiology Clinics*, *25*(3), 137-153, Copyright © 1987 with permission from Wolters Kluwer Health, Inc.

As a spectrophotometric method, pulse oximetry uses the Lambert-Beer law and the spectral differences of oxyhaemoglobin and deoxyhaemoglobin in the red (660 nm) and infrared (920 – 930 nm) spectral regions (Wukitsch et al. 1988; Jubran 1999; Proulx 1999). Oxyhaemoglobin absorbs more light at the infrared (920 – 930 nm) spectral region compared to deoxyhaemoglobin (Fig. 1.8). Whereas, at the red (660 nm) spectral region, deoxyhaemoglobin absorbs more light compared to oxyhaemoglobin (Wukitsch et al. 1988; Jensen et al. 1998; Jubran 1999; Proulx 1999) (Fig. 1.8). The millimolar coefficients of oxyhaemoglobin and deoxyhaemoglobin (Fig. 1.8) at the red and infrared region are used to calculate SpO_2 (functional arterial oxygen-haemoglobin saturation) as an indirect measurement of SaO_2 as follows:

$$SpO_2(\%) = \frac{\mathrm{HbO_2}}{\mathrm{HbO_2} + \mathrm{HHb}} * 100$$

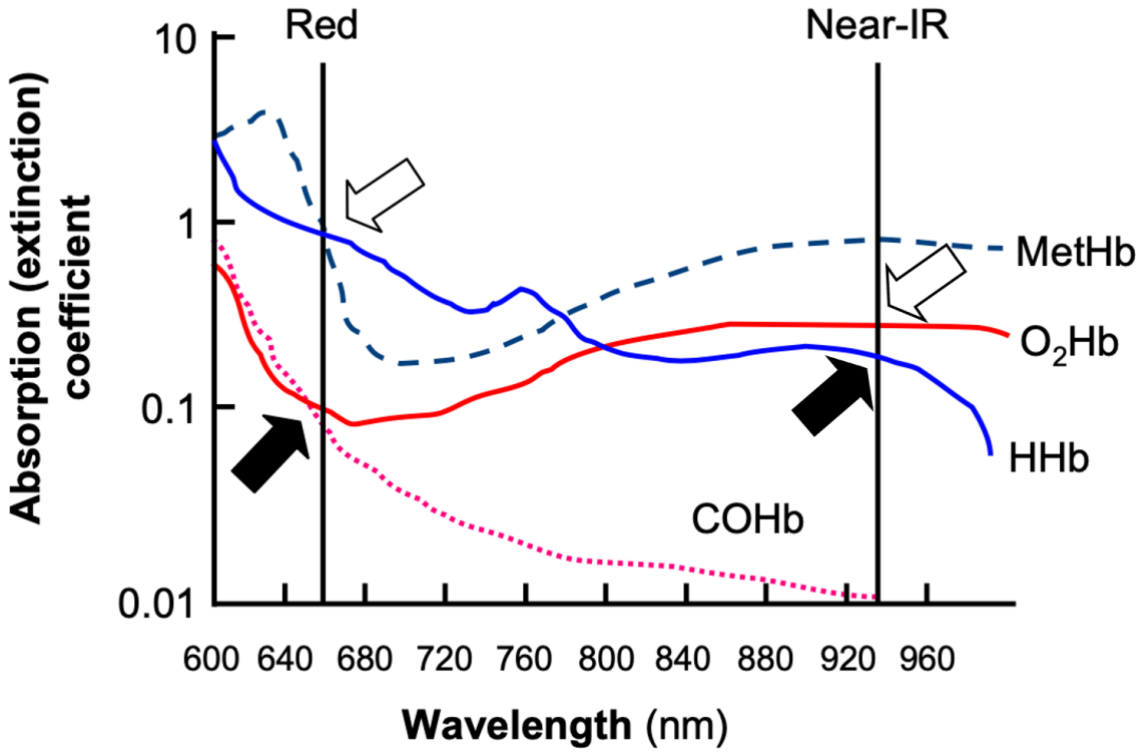

Figure 1.8 The molar extinction coefficient (or molar absorptivity) of oxyhaemoglobin (HbO_2 or O_2Hb) deoxyhaemoglobin (HHb), carboxyhaemoglobin (HbCO or COHb) at the visible and near infrared spectral range (600 – 1000 nm). Deoxyhaemoglobin (HHb) absorbs more light at the red wavelength of 660 nm (indicated by the black and white arrows at 660 nm), compared to oxyhaemoglobin (HbO_2). Oxyhaemoglobin absorbs more light at the infrared region (940 nm), compared to deoxyhaemoglobin (indicated by the black and white arrows at 940 nm) (Wukitsch et al. 1988; Chan et al. 2013). The millimolar coefficients of oxyhaemoglobin and deoxyhaemoglobin at the red and infrared region are used by pulse oximetry to calculate SpO_2. This Figure is from Chan et al. (2013). Reprinted from Chan, E. D., Chan, M. M., & Chan, M. M. (2013). Pulse oximetry: understanding its basic principles facilitates appreciation of its limitations. *Respiratory Medicine*, *107*(6), 789-799, Copyright © 2013 with permission from Elsevier Ltd.

Two types of probes are commonly used for pulse oximetry. Transmission probes that send light through the tissues and that light is detected by a photodiode on the opposite side of the tissue (Reddy 1997; Nixdorff et al. 2021). Transmission probes are the most popularly used probes in humans because of their ease of placement at different attachment sites particularly the finger and ear (Reddy 1997). Finding the ideal attachment site in animals is difficult because of the differences in animal anatomy, tissue and hair thickness, and pigmentation. In cats, dogs, and neonatal foals, transmission probes are usually attached to the tongue and lip (Burns et al. 2006; Giguère et al. 2014; Auckburrally 2016; Cugmas et al. 2019; Mair et al. 2020; Nixdorff et al. 2021). In immobilized impala, neonatal foals, horses, giraffe and white rhinoceros, transmittance probes are usually attached to the ear after shaving off hair or scarifying the ear by scarping with a sharp blade (Boardman et al. 2014; Giguère et al. 2014; Fahlman et al. 2016; Bertelsen et al. 2017; Haymerle et al. 2016; Mtetwa et al. 2020; Meuffels et al. 2022). Other possible attachment sites for veterinary patients include the prepuce and the vulva (Matthews et al. 2003; Reiners et al. 2017).

The other pulse oximeter probe is the transflectance or reflectance probe, which consists of a light source and photodiode positioned on the same side of the probe (Reddy 1997; Reiners et al. 2017). The probe was first described by Brinkman and Zijlstra (1949) and is based on the concept that light is also reflected from the tissues. Therefore, light is transmitted to the tissue and then reflected back and detected by a photodiode on the same side of the probe (Shimada et al. 1991; Reddy 1997; Nixdorff et al. 2021). The design of transflectance probes can make it difficult to find appropriate attachment sites. Therefore, these probes are normally attached to the scalp, forehead, chest wall, foot, the base of the tail (after securing it using a tape) and the rectum in different species (Shimada et al. 1991; Matthews et al. 1994; Chaffin et al. 1996; Nijland et al. 1991; Sugino et al. 2004; Giguère et al. 2014; Farrell et al. 2019; Mtetwa et al. 2020; Nixdorff et al. 2021). In impala and horses, the transmission probes have been placed on the cheek mucosa using a specially designed probe (Reiners et al. 2017; Mtetwa et al. 2020). However, most of these pulse oximeter probes are used without first evaluating their reliability at different attachment sites in different species.

Reliability of pulse oximetry SpO_2 readings

The reliability of pulse oximetry SpO_2 readings has been investigated in cats (Hendricks and King 1993; Matthews et al. 1994), dogs (Sidi et al. 1987; Erhardt et al. 1990; Jacobson et al. 1992; Matthews et al. 1994; Huss et al. 1995; Grosenbaugh and Muir 1998; Burns et al. 2006), neonatal foals (Giguère et al. 2014), pigs (Wideman & Kirby 1995), impala (Mtetwa et al. 2020), sheep (Norton et al. 1998; Coghe et al. 1999), horses (Whitehair et al. 1990; Matthews et al. 1994; Chaffin et al. 1991, Reiners et al. 2017), and giraffe (Bertelsen et al. 2017). The type of probes used by pulse oximeters play a major role in the reliability of the SpO_2 readings. In neonatal foals, the Surgi-Vet (Smiths Medical PM Inc., Norwell, MA) transmission probes placed on the lip (bias -2.3%) and the tongue (bias -5.0%) performed better than the Surgi-Vet transflectance probes placed in the mucosal side of the lower lip (bias -17%) and on the rectal mucosa (bias -23.7%) at saturations above 65.2% (Giguère et al. 2014). In anaesthetized dogs, a Nellcor (Mallinckrodt Inc., Pleasanton, USA) transmission probe placed on the tongue performed better, with low failure rates (i.e., a device's failure to produce a reading), compared to a transflectance probe placed on the tail (Matthews et al. 1994). In immobilized impala, a Nonin (Nonin Medical Inc., North Plymouth, USA) transflectance probe placed on the base of tail performed better (with good pulse signal quality) and provided more reliable SpO_2 measurements (bias 3%) compared to a Nonin transmission probe placed on the ear (bias -6%), at the 90-100% saturation range (Mtetwa et al. 2020). Whereas in cynomolgus monkeys, a Nonin transmission probe placed on the cheek provided reliable SpO_2 measurements at the 70-100% saturation range (Young et al. 2002). In anesthetized horses, a Nonin 200SL transflectance probe, placed on the cheek area, performed well (bias -0.3%) at the 70-100% saturation range (Reiners et al. 2017). In anaesthetized giraffe, the transmission probes placed on the tongue or pinna provided unreliable SpO_2 readings at the 50-100% saturation range (Bertelsen et al. 2017).

After assessing the performance of the different pulse oximeter probes, placed at different attachment sites, it is clear that the attachment site also affects the reliability of the SpO_2 readings in various species. In anaesthetized dogs, the tongue, toe, and prepuce/vulva performed better (with a correlation >0.95%) compared to the lip and the ear when using Nellcor and Surgi-Vet pulse oximeters (Matthews et al. 2003). Surprisingly, in the same study, they found that both models (i.e., Nellcor and Surgi-Vet)

of pulse oximeters at all the attachment sites (tongue, ear, lip, front metacarpus, and hind metatarsus) performed poorly in anaesthetized cats (Matthews et al. 2003). In horses, however, the tongue, nostril, prepuce/vulva, and lip had good correlation compared to the ear when using Nellcor and Surgi-Vet pulse oximeters (Matthews et al. 2003). Reiners et al. (2017) found that the cheek area was a reliable attachment site (bias -0.3% and bias 1.9%) when two Nonin transflectance probes (prototype N1 and N2b) were used in anaesthetized horses at the 70-100% saturation range. Even though the ear was not a reliable attachment site in anaesthetized adult horses (Matthews et al. 2003), it was reliable in anaesthetized neonatal foals at the saturation range of 90-95% (bias -1.4%) and above 95% (bias -3.4%) when using a Nellcor pulse oximeter (Chaffin et al. 1996). However, these findings contrast with those of Giguère et al. (2014), who excluded data taken from the ear of anaesthetized foals using Nellcor and Surgi-Vet pulse oximeters because they had more than 50% failure rates. Nonetheless, the lip or tongue provided the best results in these neonatal foals when using Nellcor and Surgi-Vet pulse oximeters (Giguère et al. 2014). In immobilized impala, the tail was the most reliable (bias 3%) compared to the cheek, ear, and rectum at the 90-100% saturation range when using a Nonin PalmSAT 2500A pulse oximeter (Mtetwa et al. 2020).

The type of device and model used for pulse oximetry can also affect the reliability of the SpO_2 readings (Matthews et al. 2003). For example, in anaesthetized dogs, three Nellcor pulse oximeters (N-395, NPB-190 and NPB-40) had 0% failure rate (I.e., failure to produce SpO_2 readings) compared to a Surgi-Vet (Surgi-Vet Inc., Waukesha, USA) V3304 (20% failure rate) (Matthews et al. 2003). In horses, the failure rate was high when using Nellcor and Surgi-Vet devices with only the Nellcor NPB-290 producing 0% failure rates (Matthews et al. 2003). In cats, Nellcor and Surgi-Vet pulse oximeters, namely, NPB-40 (20%), NPB-190 (0.7%) and V3304 (31.5%) provided high failure rates, with only the Nellcor models N-395 and NPB-290 having 0% failure rate (Matthews et al. 2003). Surprisingly, even with the high failure rates, all the pulse oximeter models provided reliable SpO_2 readings in dogs and horses, but not for cats (Matthews et al. 2003). In the anesthetized dogs, two different pulse oximeters (Dolphin voyager and Nellcor N-180) placed on the tongue, both using transmission probes, had good quality readings with 0% failure rate (Burns et al. 2006). However, regarding the reliability of the SpO_2 readings, the Nellcor N-180 pulse oximeter provided reliable (bias 3.2%) readings compared to the Dolphin voyager (bias 4.3%) in anaesthetized dogs (Burns et al. 2006). In anaesthetized neonatal foals, the Cardell (CAS

Medical Systems Inc., Branford, USA) pulse oximeter provided unreliable SpO_2 readings (bias -7.2%) compared to the Surgi-Vet monitor (bias -2.3%) at saturation ranges below 65.2%, when the probes were both placed on the lip (Giguère et al. 2014). However, at the 65.4-85.4% saturation range, the Cardell (bias -5.5%) performed better than the Surgi-Vet monitor (bias -10.3%), when both probes were placed on the lip (Giguère et al. 2014).

Apart from all these major factors, conventional pulse oximeters have other limitations that apply to all species. Ambient light, electromagnetism, movement, poor tissue perfusion and pigmentation interfere with the pulse signal strength and the light detected by pulse oximetry, thereby affecting the reliability of SpO_2 and pulse rate measurements (Jubran 1999; Proulx 1999). Other limitations include the inability to detect the presence of other haemoglobin derivatives (i.e., MetHb and HbCO) because of the method's limited two-wavelength technology. Furthermore, the molar absorptivity of MetHb and HbCO of mammals other than human, dogs, cats, and horses, have not been extensively studied. This lack of knowledge is problematic as haemoglobin derivatives, MetHb and HHb, absorb the same amount of light at 660 nm, whereas HbCO and HbO_2 absorb the same amount of light at 660 nm (Reynolds et al. 1993; Verhovski et al. 2010; Ayres 2012). Therefore, if there is an increase in MetHb or HbCO in the blood, pulse oximetry may provide unreliable readings because it cannot differentiate between the different haemoglobin derivatives (Reynolds et al. 1993; Verhovski et al. 2010). Fortunately, there is a new technology of pulse oximetry (i.e., Masimo SET Radical pulse co-oximetry) that can differentiate between the different haemoglobin derivates, however, its reliability in different species still needs to be determined.

1.2.2.5 Pulse co-oximetry

An advanced pulse oximetry technology is signal extraction technology (SET) pulse co-oximetry developed by Masimo Corporation (Masimo Corporation., Irvine, USA) This technology addresses the limitations presented in conventional pulse oximeters such as patient movement, low tissue perfusion and ambient light interference. The new technology also uses multiple wavelengths (seven +) of light to differentiate between the different haemoglobin derivatives to obtain more reliable readings. A model

currently used is the Masimo SET Radical-7 pulse co-oximeter that utilizes more than seven wavelengths of light (between 500 – 1400 nm) to indirectly measure SpO_2, HHb (SpHHb), MetHb (SpMet), HbCO (SpCO), haemoglobin concentration (SpHb) and pulse rate (Feiner et al. 2010; Read et al. 2016; Zoff et al. 2019; Tayari et al. 2021). This device also calculates perfusion index (PI), which is the ratio between non-pulsatile and pulsatile absorption. Perfusion index reflects the amplitude of the plethysmography waveform that is used to filter out poor signal pulse quality data and according to the manufacturer, PI determines the ability of the device to provide reliable readings (Keller et al, 2008; Lee et al. 2014).

The SET in these pulse co-oximeters stands for signal extraction technology, which was first investigated in 1989. The Masimo SET technology utilizes a signal processing algorithm that assumes that during motion, the signal that is detected should be the true arterial signal whereas the other signals should come entirely from movement artefacts (non-arterial signal) (Goldman et al. 2000). The devices also use adaptive filters to isolate varying arterial and non-arterial signals and separates them out by evaluating the whole signal and breaking it down to individual “saturation components” using two equations:

$$IR = S * M \quad (1)$$

$$RD = (r_a * S) + (r_v * M) \quad (2)$$

Where IR is the infrared light signal produced by arterial pulsatile blood, S is the signal vector from the arterial pulsatile blood and M is the motion signal vector caused by non-arterial pulsation such as venous blood, skin, bone, muscle, or movement artefacts. RD is the red light signal produced by arterial pulsatile blood, r_a is the optical density ratio that corresponds to arterial saturation at the entire 0-100% saturation range (i.e., this ratio corresponds to SpO_2), r_v is the optical density ratio that corresponds to non-arterial saturation.

Once IR and RD are known, discrete saturation transform (DST) and fast saturation transform (FST) collect the red and infrared signals and calculate the reference signals across the entire 0-100% saturation range as follows:

$$RS = r' * IR – RD \quad (3)$$

Where r' values are equal to the r_a and r_v of which are calculated when the iterative (repetitive) process across the entire saturation range is completed. Once IR and RS are calculated, the DST sends these two signals to the adaptive filters which cancels any frequency that is similar between them. Lastly, the adaptive filter determines that power curve and each peak on the curve corresponds to different SpO_2 values. This process is shown in Figure 1.9.

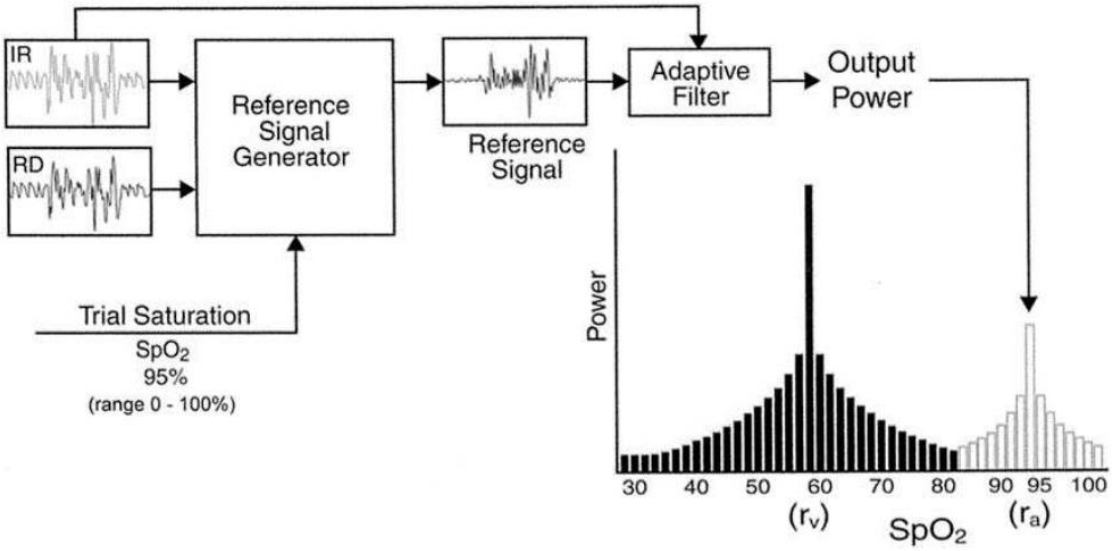

Figure 1.9 Summary of the signal extraction technology used in Masimo Radical pulse co-oximeters to mitigate some of the limitations present in conventional pulse oximeters such as patient movement, low tissue perfusion and ambient light interference. The signal extraction technology utilizes adaptive filters and discrete saturation transform (DST) to calculate red, infrared and reference signals. Once these signals are known, the adaptive filter and DST identifies the correct arterial saturation and constructs a power curve that corresponds to the different SpO_2 values. Reprinted from Goldman, J. M., Petterson, M. T., Kopotic, R. J., & Barker, S. J. (2000). Masimo signal extraction pulse oximetry. *Journal of Clinical Monitoring and Computing*, *16*(7), 475-483, Copyright © 2000 with permission from Kluwer Academic Publishers.

Masimo has two types of probes suitable for the pulse co-oximeter; the adhesive, non-reusable probe for continuous monitoring of the different variables and the reusable probes for spot check assessments (Keller et al. 2008). Both Masimo reusable and non-reusable probes are called low noise optical probes because they help minimize inferences caused by ambient light and movement (Goldman et al. 2000).

Reliability of pulse co-oximetry SpO_2 readings

Studies that have assessed the performance of the Masimo pulse co-oximeter and their probes have only focused on the reliability of haemoglobin concentration (SpHb) measurements in anaesthetized dogs and cats (Read et al. 2016; Mair et al. 2020; Tayari et al. 2021), anaesthetized pregnant sheep

(Quinn et al. 2012), healthy awake or anaesthetized humans (Zaouter & Zavorsky 2012; Chung et al. 2014; Barker et al. 2016; Louie et al. 2018; De Rosa et al. 2020), and anaesthetized horses (Zoff et al. 2019; Tayari et al. 2022). Studies evaluating the reliability of the Radical pulse co-oximeter SpO_2 readings when compared to the SaO_2 reported by a co-oximeter (reference method) are limited and most of them compared SaO_2 and SpO_2 over a narrow saturation range (Kim et al. 2019; Zoff et al. 2019; Tayari et al. 2021; Tayari et al. 2022). Furthermore, studies in anaesthetized humans and animals reported conflicting results on the reliability and usefulness of the Masimo Radical pulse co-oximeter. In children with congenital cyanotic heart failure undergoing anaesthesia, the Radical-7 SpO_2 readings were unreliable (bias -7.4%) when compared to SaO_2 reported by the GEM premier 3000 blood analyser with integrated co-oximetry technology, at all saturation ranges (Kim et al. 2019). A study on anaesthetized pregnant sheep, reported reliability (bias -3%) of the SpO_2 readings when the Masimo probe was placed on the apex of the tongue at saturation above 70% (Quinn et al. 2013). Dawson et al. (2014) showed that the Masimo Radical-4 was reliable (bias 3%) when the probe placed on the limb of anaesthetized neonatal lambs at the 70-100% saturation range. In anaesthetized horses, SpO_2 readings were reliable (bias -1.4%) when the Masimo probes were placed either on the tongue or the lip (Zoff et al. 2019). These findings agree with the findings of Tayari et al. (2021), when the Masimo clip-type probe was placed on the apex of the tongue of anaesthetized horses (bias -1.4%). Zoff et al. (2019) only compared readings at the 92.9-100% saturation range, which is a narrow range to conclude the reliability of this device. In anesthetized dogs, a bias of 0.86% was reported when a Masimo probe was placed on the tongue. However, this study also compared SaO_2 and SpO_2 over a narrow saturation range (85-100%) and used a small, paired sample size (n = 39).

To date, only one study has assessed the performance of the Masimo Radical-5 pulse co-oximeter, at different attachment sites (tongue, upper lip, pinna, knee fold and toe) in anaesthetized cats; but this study only focused on the failure and signal pulse quality rates and not the reliability of SpO_2 readings (Dörfelt et al. 2021). This study found high percentage signal failure rates from the probes placed on the pinna and knee fold compared to those placed on the upper lip and toe (Dörfelt et al. 2021). The probe placed on the tongue struggled to get SpO_2, perfusion index and pulse rate readings, with 4.5% higher failure rates compared to the other attachment sites (Dörfelt et al. 2021). Nonetheless, more

studies are needed to determine the reliability of the SpO_2 readings when the probes are placed at different attachment sites, in animals undergoing anaesthesia.

There are other ways of monitoring arterial oxygen-haemoglobin saturation and they include calculating the arterial oxygen-haemoglobin saturation ($cSaO_2$) from other blood variables (i.e., PaO_2, $PaCO_2$, pH, temperature and Hüfner factor).

1.2.2.6 Calculated arterial oxygen-haemoglobin saturation

1.2.2.6.1 The method of Van-Slyke and Neill (1924) for calculating arterial oxygen-haemoglobin saturation

Arterial oxygen-haemoglobin saturation can be calculated from CaO_2 values measured by the manometric method of Van Slyke and Neill (1924), after correcting for PaO_2 (Sendroy et al. 1934; Lambertsen et al. 1952; Holmgren and Pernow 1959; Weiss and Sinha 1978). The manometric method of Van Slyke and Neill (1924) was the first method used reliably to determine blood oxygenation and it is considered the gold standard method for determining CaO_2, oxygen-carrying capacity and SaO_2 (Lambertsen et al. 1952; Holmgren and Pernow 1959; Weiss and Sinha 1978; Brown 1980). This method is based on the principle that when a solution (in this case, blood) with a known volume and atmospheric pressure, is exposed to air, the solution can be mixed with the air by shaking and the amount of gas in the solution can be measured from the pressure exerted on a manometer (Van Slyke & Neill 1924). This laboratory method is a closed system that consists of a pipette, that is closed at the top by a stopcock and connected to an insulated water-jacket that is maintained at a constant temperature (normally 20 ± 0.1°C) (Van Slyke & Neill 1924). Below, the pipette descends for 800 mm and is connected to a glass tube that turns at a right angle (Van Slyke & Neill 1924). At the end of the glass tube is a levelling bulb and a mercury manometer used to measure the partial pressure of oxygen in the blood (Van Slyke & Neill 1924). The reagent [potassium ferricyanide, $K_3Fe(CN)_6$] that is used to release or free oxygen bound to haemoglobin, at a known volume, is inserted into the chamber over the mercury and shaken for approximately 3 minutes and then the gases in the solution are removed by opening the stopcock (Van Slyke & Neill 1924). The blood sample, at a known volume, is then mixed

with the de-gassed $K_3Fe(CN)_6$, by shaking for approximately 3 minutes. The reaction between the $K_3Fe(CN)_6$ and the blood causes HbO_2 to release oxygen, and HbO_2 is then converted to MetHb (Cook 1928). The change in pressure (P) from before (p_1) to after (p_2) the $K_3Fe(CN)_6$ has caused haemoglobin to release oxygen to the solution is measured on the manometer at STPD. The method makes the assumptions that the temperature and barometric pressure are constant at reading time.

To calculate arterial oxygen-haemoglobin saturation; firstly, CaO_2 and oxygen-carrying capacity of blood are directly measured by the method of Van Slyke & Neill (1924). Oxygen-carrying capacity is measured by exposing the blood to air for 10 minutes and then measuring the pressure of the oxygen gas exerted on the manometer (Lambertsen et al. 1952; Holmgren and Pernow 1959; Weiss and Sinha 1978; Brown 1980). Partial pressure of oxygen in the arterial blood (PaO_2) is corrected for based on an assumption that dissolved oxygen in the blood is proportional to the blood's water content at a given temperature and barometric pressure (Van Slyke & Neill 1924). Partial pressure of oxygen can also be determined by extracting the oxygen from the blood sample in a vacuum without adding $K_3Fe(CN)_6$ solution (Sendroy et al. 1932). Once PaO_2 is corrected for, or measured, it is subtracted from CaO_2 and oxygen-carrying capacity of blood to calculate arterial oxygen-haemoglobin saturation from this equation:

$$SaO_2\ (\%) = \frac{(oxygen\ content - dissolved\ oxygen)}{(oxygen\ capacity - dissolved\ oxygen)} * 100$$

Where oxygen content is the total concentration of oxygen exerted on the manometer ($mL.dL^{-1}$) of the blood, dissolved oxygen is the PaO_2 (mmHg) and oxygen carrying capacity of blood ($mL.dL^{-1}$) is the ideal amount of oxygen that can be bound to haemoglobin, at a given [Hb] and PaO_2.

Even though this method is the most reliable method, the time it takes to obtain the readings for p_1 and p_2 is approximately more than 4 minutes and the apparatus needs to be cleaned between each step of the analyses, making this method time-consuming as it takes more than 30 minutes for one analysis. Furthermore, the method also requires that the operator has a certain skill (that develops over time) to accurately measure the oxygen content and oxygen-carrying capacity.

1.2.2.6.2 Method of Tucker (1967) for calculating arterial oxygen-haemoglobin saturation

Alternatively, a quicker and reliable way to determine CaO_2 is by the method developed in 1967 by Vance Tucker (Tucker 1967). This method utilizes Clark-type oxygen electrode to determine total oxygen content in the blood and can also be used to determine the oxygen-haemoglobin dissociation curves of different species (Tucker 1967). Because oxygen bound to haemoglobin does not exert a partial pressure, the method of Tucker (1967), like the method of Van Slyke & Neill (1924), is based on the principle that haemoglobin bound oxygen can be released into solution using a potassium ferricyanide solution. Thereafter, the total amount of oxygen in the solution can be determined accurately from PaO_2 directly measured using an oxygen electrode, instead of the manometer used by Van Slyke & Neill (1924).

Oxygen electrodes, designed by Clark in 1959, are so far the most reliable and easy way to measure PaO_2 in blood. Clark-electrodes are easier to use because they are small and can be incorporated in different devices (Severinghaus & Astrup 1986). Clark electrodes measure PaO_2 based on the principles of oxidation and reduction reactions that occur in aqueous solutions when exposed to a specific voltage. These electrodes consist of a probe at which the tip is an exposed gold or platinum cathode and a silver anode. The anode and cathode are polarized so that the cathode is kept at a voltage of -0.6 to -0.8 volts (V) relative to the anode and is connected via a solution of electrolytes such as KCl. The following reaction occurs at the anode: $4Ag \rightarrow 4Ag^{+} + 4e$ and $4Ag^{+} + 4Cl^{-} \rightarrow 4AgCl$. Simultaneously, when oxygen is dissolved in a solution at a voltage (-0.6 to -0.8 V), this reaction occurs ($O_2 + 2H_2O + 4e \rightarrow 4OH^{-}$). For each oxygen molecule reduced, 4 electrons of current flow in the circuit and oxygen is continually 'consumed' as it is reduced to OH^{-}. The current produced by the needle electrode is linearly related to the PaO_2 in the blood surrounding the electrode.

The oxygen electrode (Clark electrode) serves as the primary measuring device in Tucker chambers. This electrode is housed in a water-jacketed glass chamber that can accommodate up to 500 µL solution (Strathkelvin Instruments Ltd., North Lanarkshire, Scotland). To maintain the chambers at a constant temperature, the chamber is also connected to a circulating water bath (normally between 20

– 35ºC) (Tucker 1967; Strathkelvin Instruments Ltd., North Lanarkshire, Scotland). The chamber is sealed at the top by an acrylic stopper that has a 2 mm opening in the middle, which is used to insert the blood sample (Tucker 1967). After inserting the blood sample, the opening on the middle of the stopper is closed by a 2 mm glass ball to prevent contamination and flow of gases into and out of the chamber (Tucker 1967; Strathkelvin Instruments Ltd., manual North Lanarkshire, Scotland).

To calculate CaO_2 based on the PaO_2 directly measured by the method of Tucker, a degassed potassium ferricyanide ($K_3Fe(CN)_6$) solution is inserted into the chamber and magnetic stirrers are used to mix the solution and given one or two minutes to allow to equilibrate with the chamber temperature. Once a stable degassed oxygen trace is achieved, approximately 4 – 8 µL of blood is inserted into the Tucker chamber and given sufficient time to mix thoroughly into the degassed $K_3Fe(CN)_6$ solution until it is in equilibrium. Oxygen that is bound to haemoglobin is released into the physical solution by the degassed $K_3Fe(CN)_6$ solution that is responsible for the conversion of oxyhaemoglobin to methaemoglobin (Cook 1928). The total dissolved oxygen, which exerts a partial pressure will increase and the change in PO_2 (ΔPO_2), before and after injecting the blood sample into the $K_3Fe(CN)_6$ filled chamber, is measured**.** The change in PO_2 (ΔPO_2) is used to calculate the CaO_2 (in $mL.dL^{-1}$) at standard temperature, dry air (STPD) using the equation:

$$\mathrm{CaO_2} = \frac{\Delta \mathrm{PO_2}}{760} \times \propto \times \mathrm{V_C} \times \frac{100}{\mathrm{V_b}}$$

Where $\propto$ is the oxygen solubility coefficient (0.0252 $mL.dL^{-1}.mmHg^{-1}$) of $K_3Fe(CN)_6$ at 32 °C, V_c is the volume of the chamber (in mL), V_b is the volume of the blood sample (in mL).

The method by Tucker (1967) has been used to determine CaO_2 in small and large mammals (Tucker 1968; Karas et al. 1987; Jones et al. 1989; Smale and Butler 1994) and fish (Weber & Wells 1989; Speers-Roesch et al. 2012; Harter et al. 2015a). The CaO_2 measurements are accurate (mean difference of 0.03 $mL.dL^{-1}$) and precise (standard deviation of 0.14 $mL.dL^{-1}$) when compared to CaO_2 measured by the reference method of Van Slyke & Neill (1924) in human blood (Tucker 1967). Bridges et al. (1979) looked at the reliability of Tucker CaO_2 measurement in blood containing hemocyanin when compared to the CaO_2 measurements from the method of Van Slyke & Neill (1924) and reported a

standard deviation of 0.064 $mL.dL^{-1}$ of blood. Therefore, the method of Tucker (1967) can be used reliably in species with different haemoglobin structures, as shown by the reliability in both studies that measured CaO_2 in blood with different respiratory pigments (haemoglobin and hemocyanin) (Bridges et al. 1979).

Compared to the method of Van Slyke and Neill (1924), the method of Tucker (1967) is simple, requires no special skill and it is quick; it takes up to 5 to 10 minutes to determine CaO_2. The method of Tucker (1967) also requires a small sample to determine CaO_2, however, unlike the method of Van Slyke and Neill, Tucker CaO_2 measurements have been used multiple times (e.g., in fish, amphibians, reptiles and birds) to calculate arterial oxygen-haemoglobin saturation values (Boutilier et al. 1984; Andersen & Wang 2002; Harter et al. 2015; Bautista et al. 2021). In fish and bar-headed goose, arterial oxygen-haemoglobin saturation was calculated from the Tucker CaO_2 by subtracting PaO_2 and then dividing this result by the theoretical maximal carrying capacity of haemoglobin based on [Hb] measured by the HiCN method (Boutilier et al. 1984; Harter et al. 2015a; Harter et al. 2015b). These variables were then used in fish and bar-headed goose to calculate arterial oxygen-haemoglobin saturation values, that were then used as the reference values to determine the reliability of arterial oxygen-haemoglobin saturation calculated by an i-STAT blood analyser (Harter et al. 2015a; Harter et al. 2015b). However, further research is needed to determine whether arterial oxygen-haemoglobin saturation calculated from the Tucker CaO_2 measurements are reliable. Furthermore, one still needs to consider that the method of Tucker (1967) is a laboratory-based technique that requires training, attention to detail and it is not easy to use in the field.

1.2.2.6.3 Severinghaus equation for calculating arterial oxygen-haemoglobin saturation

Pioneering work of Hill (1910) and Adair (1925), have improved ways to demonstrate the relationship between PaO_2 and SaO_2 (Buerk and Bridges 1986). The oxygen-haemoglobin dissociation curve has been used to construct algorithms that can estimate or calculate arterial oxygen-haemoglobin saturation as a function of PaO_2 (Lutz et al. 1975; Severinghaus 1979; Gabel 1980; Siggaard-Andersen et al. 1984; Siggaard-Andersen et al. 1988; Smale et al. 1994; Serianni et al. 2003; Dash et al. 2016). In

1979, Severinghaus modified the Hill's equation to fit the standard human oxygen-haemoglobin dissociation curve and corrected for the misfit at low saturations to match the curve at rest (pH of 7.40 and body temperature of 37°C). The algorithm has been used as a reference to calculate arterial oxygen-haemoglobin saturation and incorporates the effects of $PaCO_2$, pH and temperature on the curve. After adjusting for these measured variables (i.e., $PaCO_2$, pH and temperature), arterial oxygen-haemoglobin saturation can then be calculated as follows:

$$cSaO_2(\%) = (((PaO_2)^3 + 150PaO_2)^{-1} * 23400) + 1)^{-1} * 100$$

Where PaO_2 (mmHg) is the partial pressure of oxygen measured by a blood analyser.

The algorithm had a maximum error of 0.55% at saturations between 0-98.77% and the P_{50} value calculated from this algorithm was 26.86 mmHg compared to the 26.67 mmHg calculated from the standard curve of Hill (1910) and Adair (1925) (Severinghaus 1979). When Breuer et al. (1989) calculated arterial oxygen-haemoglobin saturation from the Severinghaus algorithm, there was a strong agreement (correlation and regression coefficients of 0.91 and 0.90) between $cSaO_2$ and SaO_2 reported by a co-oximeter (OSM2 Radiometer) in 528 arterial samples, at the 53–98.4% saturation range. Collins et al. (2015) used 3524 blood gas results at pH between 7.35 and 7.44 to calculate arterial oxygen-haemoglobin saturation from the Severinghaus algorithm and compared these $cSaO_2$ values with SaO_2 reported by a co-oximeter (Collins et al. 2015). The study by Collins et al. (2015) found that the $cSaO_2$ values were reliable (bias 0.16%) at PaO_2 below 56.6 mmHg. The study also found that at low pH values, the oxygen-haemoglobin dissociation curve shifted to the right and at high pH values, the curve shifted to the left (Collins et al. 2015). Therefore, this algorithm considers the shifts caused by the change in pH at a normal body temperature of 37°C. The modified-Hill equation by Severinghaus (1979) is now used in numerous blood analysers including the Enterprise Point-of-Care (EPOC) (Epocal Inc., ON, Canada) and the i-STAT (Abbot Point of Care Inc., Princeton, NJ, USA) blood analysers (Breuer et al. 1989; i-STAT Technical Bulletin 2013; EPOC system manual).

There are two types of blood analysers, a benchtop and point-of-care (POC) blood analyser. Benchtop blood analysers are suitable for use in the laboratory, and some have incorporated co-oximetry technology to determine SaO_2, CaO_2, [Hb], MetHb and HbCO. In field settings, POC blood analysers are normally used because they are easy to use and yield results quickly. The human Enterprise Point-of-Care (EPOC) and I-Stat blood analysers are widely used in the field and have been used to monitor respiration and blood oxygenation of immobilized wildlife including impala (Mtetwa et al. 2020), blesbok (Semjonov et al. 2018; Gaudio et al. 2020; Pfitzer et al. 2021), serval (Blignaut et al. 2021), African elephant (Chelopo et al. 2022) and white rhinoceros (Buss et al. 2018; Boesch et al. 2018; Pohlin et al. 2020; Meuffels et al. 2022). Some of these POC blood analysers (e.g., EPOC and i-STAT) use cartridges that contain miniaturized microsensors used to determine these blood variables [i.e., pH, PO_2, PCO_2, base excess (BE), concentration of bicarbonate (HCO_3^-), haemoglobin, glucose, lactate, creatinine, and ion concentrations (Na^+, K^+, Cl^-) and anion gap, potassium (AgapK) and haematocrit (Hct)]. These analysers mostly calculate arterial oxygen-haemoglobin saturation ($cSaO_2$) by incorporating the Severinghaus algorithm and the standard human oxygen-dissociation curve using the following equations:

$$cSaO_2(\%) = \left(X^3 + \frac{150X}{(X^3+150X+23400)}\right) \quad (1)$$

$$X = PO_2 * 10^{\left(0.48(pH-7.4)-0.0013\left(HCO^{3-}-25\right)\right)} \quad (2)$$

Where PO_2 (arterial or venous partial pressure of oxygen), pH and concentration of bicarbonate (HCO_3^-) are blood variables that are measured directly by a blood analyser and used to calculate arterial oxygen-haemoglobin saturation ($cSaO_2$).

In 2006, the Food and Drug Administration (FDA) and Clinical Laboratory Improvement Amendments (CLIA) of 1988 regulations have certified EPOC blood analysers for monitoring arterial blood gas variables in humans (Argarwal et al. 2014). However, there are no acceptable reference intervals available for some of the variables reported by these POC blood analysers (i.e., ionised calcium, bicarbonate, BE and $cSaO_2$). Animal studies have used $cSaO_2$ from the POC blood analysers as reference for the comparison with pulse oximetry SpO_2 measurements despite no guidelines available for clinical acceptability for $cSaO_2$ reported by these devices (Koenig et al. 2003; Uystepruyst et al.

2000). In addition, since POC blood analysers mostly use the human oxygen-haemoglobin dissociation curve to calculate arterial oxygen-haemoglobin saturation, it is important to evaluate the EPOC's $cSaO_2$ on species with different curves. Only a few studies have validated $cSaO_2$ values reported by the human EPOC or i-STAT blood analyser in animals. The first study ran 100 equine samples on the EPOC blood analyser and a Radiometer ABL 77 blood analysers (with co-oximetry) and reported good agreement between the EPOC's $cSaO_2$ and the SaO_2 measurements (Bardell et al. 2017). The study in immobilized impala also reported on the reliability of $cSaO_2$ values (bias -1%) from the human EPOC blood analyser when compared to SaO_2 reported by a reference method, AVOXimeter 4000 co-oximeter, at the 16.3 to 99.3% saturation range (Mtetwa et al. 2020). These findings suggests that the EPOC is likely only reliable in species, like impala, that presumably have similar oxygen-haemoglobin dissociation curves to that of humans. IDEXX Laboratories (manufacturer of VetStat® blood analysers (IDEXX Laboratories Inc., Westbook, USA) introduced veterinary blood analysers for canine, feline and equine patients. The VetStat® blood analyser calculate SaO_2 using dual spectrophotometry (VetStat operators guide). The VetStat® SaO_2 sensor is made up of one LED and two laser diodes that send red and infrared light through a cassette containing a blood sample. The light is partially absorbed before being reflected back to the sensor, where the output signal is converted to an SaO_2 value (VetStat® operators guide). However, the reliability of the $cSaO_2$ reported by these species-specific POC devices is not reported in the literature.

Besides the Severinghaus algorithm used in blood analysers to calculate arterial oxygen-haemoglobin saturation from the oxygen-haemoglobin dissociation curve, there are other algorithms that can be used (Lutz et al. 1975; Severinghaus 1979; Smale et al. 1994; Anstey 2000; Serianni et al. 2003). These algorithms include the Siggaard-Andersen algorithm that constructs standard and non-standard oxygen-haemoglobin dissociation curves of different species and calculate arterial oxygen-haemoglobin saturation as a function of PaO_2 (Siggaard-Andersen et al. 1984).

1.2.2.6.4 Siggaard-Andersen algorithm for calculating arterial oxygen-haemoglobin saturation

The Siggaard-Andersen algorithm, applied in modern blood analysers (Radiometer), is based on the binding theory of oxygen to haemoglobin according to the Hill plot and is represented as an oxygen-haemoglobin dissociation curve (Hill plot) to calculate arterial oxygen-haemoglobin saturation using the following equations (Fig. 1.10):

$$s = \frac{e^y}{1+e^y} \quad (1)$$

$$y = y_0 + x - x_0 + h \tanh\left(k(x - x_0)\right) \quad (2)$$

Where $y = \ln\left[\frac{s}{(1-s)}\right]$, $x = \ln(PaO_2)$, x_0 and y_0 are the points of symmetry, h is the vertical or horizontal asymptote and $k = \frac{n_0 - 1}{h}$ where n_0 is the slope of the points of symmetry. These variables are used to construct the curve (Siggaard-Andersen et al. 1984) as shown in Figure 1.10. Arterial oxygen-haemoglobin saturation is calculated as a function of PaO_2 after correcting for these blood gas variables (i.e., $PaCO_2$, pH), body temperature, P_{50}, and the Bohr coefficient (Siggaard-Andersen et al. 1984; Haymerle et al. 2016; Reiners et al. 2019). This algorithm, unlike others (e.g., Heck, Kelman, Severinghaus, and Lutz algorithms), also corrects for changes in the concentration of COHb, MetHb, foetal Hb, base excess and 2.3-DPG (Siggaard-Andersen et al. 1984; Breuer et al. 1990). Siggaard-Andersen in 1984 assumed that the effect of pH, base excess and 2.3-DPG is only evident in the lower asymptote (h) of the curve while the upper asymptote remains unaffected. Another assumption is that these effectors are linear and additive, i.e., their effect is dependent on the quantity (Siggaard-Andersen et al. 1984).

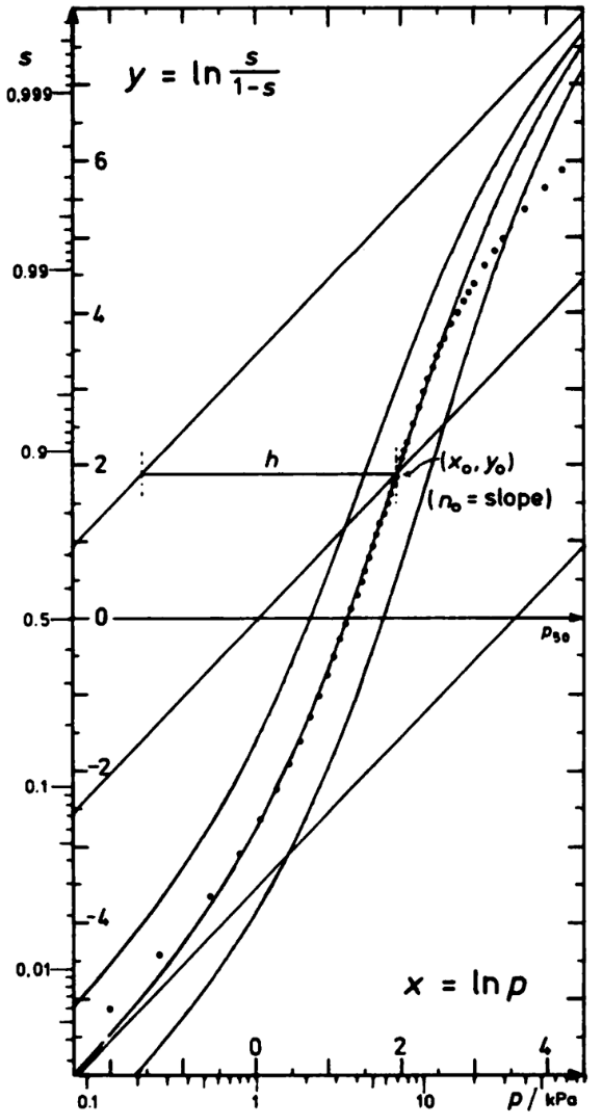

Figure 1.10 The Hill plot showing the relationship between arterial oxygen-haemoglobin saturation [SaO_2 or s (%)] and partial pressure of oxygen [PaO_2 or p (mmHg)]] according to the mathematical model of Siggaard-Andersen (1984). The Hill plot is explained by the binding theory when one oxygen molecule binds to haemoglobin until the fourth molecule, giving the S-shape of the oxygen-haemoglobin dissociation curve. The curve is made up of two logarithmic curves 1) a straight line and 2) a hyperbolic tangent curve and can be characterized by three variables: the point of symmetry (p_0, s_0), the slope at the point of symmetry (n_0) and the horizontal or vertical distance between the asymptotes (2*h*) that are used to construct the curve. Reprinted from Siggaard-Andersen, O. (1977). The van Slyke equation. *Scandinavian Journal of Clinical and Laboratory Investigation*, *37*(sup146), 15-20, Copyright © 1984 with permission from Oxford University Press.

The Siggard-Andersen algorithm fitted well with the model and data of Severinghaus and other models (Winslow et al. 1978; Siggaard-Andersen et al. 1984). For example, Sigaaard-Andersen (1984) used tabulated values that were used to construct the Severinghaus oxygen-haemoglobin dissociation curve of healthy humans and reported a difference of -0.0043% between the $cSaO_2$ (by Severinghaus algorithm) and $cSaO_2$ (by Siggaard-Andersen algorithm) (Severinghaus 1979; Siggaard-Andersen 1984). A study on 528 human arterial blood samples with measured pH, $PaCO_2$, PaO_2, 2.3-DPG, and base excess were used to calculate arterial oxygen-haemoglobin saturation from the Siggaard-Andersen algorithm and the study reported good agreement (correlation and regression coefficients of 0.91 and 0.89) when compared with SaO_2 reported by the OSM-2 Radiometer co-oximeter at the 53.0 to 98.4% saturation range (Breuer et al. 1990). This algorithm has been used to calculate arterial oxygen-haemoglobin saturation in white rhinoceros (Haymerle et al. 2016; Reiners et al. 2019). Haymerle and colleagues (2016) adapted the algorithm for calculating rhinoceros specific $cSaO_2$ values by using P_{50} and the Bohr effect reported by Bauman et al. (1984) and physiological variables (normal temperature and $PaCO_2$ of rhinoceros) reported by Citino & Bush (2007) without changing the shape of the curve. It was reported that ATP and 2.3-DPG have little effect on the shift or the position of the curve (Bauman et al. 1984) and this algorithm allows for the exclusion of these variables from the model. To prevent overestimating $cSaO_2$, the model for white rhinoceros was adjusted and the curve was shifted to the left (low P_{50}), and because of this shift, the Hill curve was flattened by lowering the h variable (distance between the asymptotes) to 3.0 instead of 3.5 (Siggaard-Andersen et al. 1984; Haymerle et al. 2016). Reiners et al. (2019) recently constructed the oxygen dissociation curve of the white rhinoceros and did experiments on white rhinoceros' blood to directly determine rhinoceros-specific variables, which were incorporated in the Siggaard-Andersen algorithm. The variables that change include the point of symmetry (x_0, y_0), asymptote (h), $k = \frac{n_0 - 1}{h}$ and only work under certain measuring conditions (i.e., specified pH, temperature, and salt concentration) (Reiners et al. 2019). Nonetheless, no study has ever validated the reliability of the arterial oxygen-haemoglobin saturation calculated from the rhinoceros modified Siggaard-Andersen algorithm, in immobilized white rhinoceros, despite their susceptibility to hypoxaemia (low blood oxygenation), and other physiological derangements, during anaesthesia or immobilization.

The literature mentioned above describes potential approaches to monitoring blood oxygenation, but more methods are still needed to monitor whether the oxygen is efficiently utilized by the tissues and can meet the tissue's oxygen demands. Therefore, methods that can directly monitor tissue oxygenation, perfusion, and metabolism, to better monitor animal's overall health and disease, are needed. There are promising methods that monitor blood oxygenation and, or tissue oxygenation, perfusion, metabolism, and consumption (Table 1.1), but because they go beyond the scope of the thesis, they will not be discussed in depth here. These methods include fibre-optic pulmonary artery and mixed venous catheters, reflectance oximetry and near infrared spectroscopy (NIRS). Fibre-optic pulmonary artery catheters (PAC) or mixed venous catheters measures venous oxygen saturation in different organs (i.e., brain and kidneys) which can help assess the imbalances between oxygen supply and consumption at the tissue site (Nakajima et al. 1993; Schell & Cole 2000; Sakr 2010). However, this method is still very invasive, sensitive and there are limited validation studies in species other than human. NIRS is a research device, that has been recently introduced mainly in human hospitals to measure tissue oxygenation (StO_2), deoxyhaemoglobin and cytochrome aa3 non-invasively, at tissue level (Sakr 2010). NIRS can also measure cerebral blood flow using the Fick's principle in the presence of a tracer (e.g., indocyanine green dye) that is capable of absorbing near-infrared light. NIRS device measures an estimate of tissue oxygenation (StO_2), deoxyhaemoglobin and cytochrome aa3 using the Beer-Lambert law and use optodes/probes (optical sensors) that have a light source that sends red and near-infrared light through biological tissues (Ferrari et al. 2004; Sakr 2010). The absorption of red and near-infrared light by oxyhaemoglobin and deoxyhaemoglobin in the blood vessels (arterioles, capillaries, and venules) of the tissue is then measured (Ferrari et al. 2004; Sakr 2010). Cytochrome aa3, an enzyme that reacts with oxygen in the electron transport chain during aerobic respiration helps monitor tissue oxygen use or consumption (Sakr 2010). Because tissue myoglobin makes up about 10% of light absorbing chromophores in the tissue, it is challenging for NIRS to differentiate between haemoglobin and myoglobin, making it difficult to reliably monitor StO_2. Currently, there is no reference method for monitoring tissue oxygenation, therefore, there is still a lot of work to be done to help validate the performance of these existing devices (Ferrari et al. 2004; Sakr 2010). NIRS is not easy to validate because of the differences in algorithm and wavelengths used in the various NIRS devices (Ferrari et al. 2004; Sakr 2010). These NIRS devices differ significantly in the methodologies and assumptions

used to calculate their tissue oxygenation measures and so far, no study has been done to validate these techniques in humans and other mammals, including wildlife.

1.2.3 General anaesthesia techniques used for white rhinoceros

South Africa has the highest numbers of rhinoceros horn poaching globally, with the population reduced by 60% since 2013 (Save the Rhino 2022). The poaching numbers call for improved conservation and management plans to ensure the long-term viability of rhinoceros' populations, including the southern white rhinoceros (*Ceratotherium simum simum*). White rhinoceros are immobilized mainly for anti-poaching measures like dehorning, translocation to better protected habitats, wound treatments after poaching, removal of snares, surgical and diagnostic procedures, fitting tracking devices and for research purposes (Buss et al. 2016; van Zijll Langhout et al. 2016; Meyer et al. 2018; Pohlin et al. 2020; Mueffels et al. 2022). For successful immobilization, especially in the field, the use of potent opioids is necessary (Portas 2004; Pohlin et al. 2020; Mosing et al. 2020; Mueffels et al. 2022).

The term "opioid" refers to a class of drugs that works by binding to opioid G-protein coupled receptors, mainly mu (μ), kappa (κ), delta (δ), and non-classified nociception receptors, located throughout the central and peripheral nervous system and the body (McDonald & Lambert 2005; Pattinson 2008; Boom et al. 2012). When opioids bind to opioid receptors, they cause several molecular effects and intracellular changes that occur at different tissue sites (Pattinson 2008; Boom et al. 2012). These molecular effects include adenylyl cyclase inhibition, decreased formation of cyclic adenosine monophosphate (cAMP), inhibition of the opening of calcium (Ca^{2+}) channels in the presynaptic neurons, decreased release of excitatory neurotransmitters (e.g., glutamate and substance P) and increased cellular potassium (K^{+}) concentration (Pattinson 2008; Boom et al. 2012). The spinal cord, which is abundant in μ, κ, δ-opioid receptors, is sensitive to opioids as they inhibit presynaptic release of neurotransmitters and postsynaptic hyperpolarization of spinal neural membrane leading to decreased excitability, causing analgesia (Pattinson 2008). The respiratory centres in the brainstem, particularly the pre-Bötzinger complex, also contain many opioid receptors, which play an important role in controlling breathing patterns (McDonald & Lambert 2005; Pattinson 2008; Boom et al. 2012; Izwan et al. 2018). When opioids bind to receptors in the pre-Bötzinger complex, they inhibit the activation of

the respiratory neurons by reducing the formation of cAMP. The reduction of cAMP causes an increase in the excitatory drive of motor neurons and intercostal interneurons, increasing chest wall rigidity and decreasing thoracic wall compliance potentially leading to reduced respiratory rates and depth (Pattinson 2008; Boom et al. 2018). Low respiratory rates of between 6 to 10 breaths.minute^{-1} have been recorded in white rhinoceros immobilized with the potent opioid, etorphine, which is lower than their normal respiratory rates (16 to 23 breaths.minute^{-1} at rest) (Citino & Bush 2007; Haw et al. 2014; Buss et al. 2015; Buss et al. 2018; Meyer et al. 2018).

Chemoreceptors, mainly the central and peripheral chemoreceptors also contain many opioid receptors (Pattinson 2008; Kimura & Haji 2014). Central chemoreceptors located in the central medulla of the brainstem, regulate ventilation by sensing changes in H^+ ion concentration caused by changes in CO_2 in the cerebral fluid (Pattinson 2008; Kimura & Haji 2014). Opioids alter normal ventilatory responses by reducing the ability of these chemoreceptors to detect these H^+ ion changes (Shook et al. 1990; Kimura & Haji 2014). Opioids also depress the peripheral chemoreceptors, located in the aortic and carotid bodies, that detect any changes in PaO_2 and $PaCO_2$, suppressing the ventilatory responses to hypercapnia and hypoxaemia (Shook et al. 1990; Pattinson 2008; Kimura & Haji 2014). In etorphine-immobilized white rhinoceros, PaO_2 below 30 mmHg and $PaCO_2$ above 65 mmHg have been reported, with no improvement in ventilation during the immobilization period (Buss et al. 2016; van Zijlt Langhout et al. 2016; Buss et al. 2018; Meyer et al. 2018).

Semi-synthetic and synthetic opioids that are mainly used for immobilization of rhinoceros include etorphine hydrochloride, thiafentanil and butorphanol. Etorphine hydrochloride and thiafentanil are highly potent opioid agonists with an analgesic potency of about 1000 to 3000-times that of morphine with greater affinity to opioid receptors than morphine (Portas 2004). Even though etorphine provides rapid and reversible immobilization in rhinoceros, it causes dose-dependent side effects including hypertension, tachycardia, and respiratory depression and compromise (Meyer et al. 2015), which results in hypercapnia, acidosis, and severe hypoxaemia. Recently, butorphanol, a partial μ-antagonist and μ- and κ- agonist, with three to five times the potency of morphine has been used during etorphine immobilization to mitigate etorphine-induced respiratory depression in rhinoceros (Buss et al. 2017;

Buss et al. 2018; Meyer et al. 2018; Mosing et al. 2020). When butorphanol was administered to rhinoceros immobilized with etorphine, there was rapid improvement in PaO_2 and reduced oxygen consumption, carbon dioxide production and muscle tremors (Buss et al. 2018; Meyer et al. 2018). However, this drug combination does not completely reverse hypoxaemia because rhinoceros remained clinically and severely hypoxaemic (PaO_2 of less than 80 mmHg) (Haw et al. 2014; Buss et al. 2018; Meyer et al. 2018). The potent opioids are often combined with butyrophenone tranquilizers like azaperone, and sedatives like medetomidine, midazolam or xylazine to achieve a degree of muscle relaxation and for smooth inductions and recovery (Portas 2004; Wenger et al. 2007; Buss et al. 2016; van Zijll Langhout et al. 2016; Gaudio et al. 2019; Mueffels et al. 2022). However, even with the addition of these "synergic" drugs, white rhinoceros immobilized with etorphine-based drug combinations still show signs of respiratory depression and compromise (van Zijll Langhout et al. 2016; Buss et al. 2017; Pohlin et al. 2020).

1.2.3.1 Hypoxaemia in chemically immobilized white rhinoceros

Hypoxaemia, defined as low blood oxygenation, can be classified as mild, moderate, or severe hypoxaemia. According to the World Health Organization, in humans and presumably animals of similar body mass (e.g., cats and dogs); hypoxaemia begins when SaO_2 is at 95% (which is equivalent to PaO_2 of about 80 mmHg at sea level), clinical hypoxaemia when SaO_2 is below 90% (equivalent to $PaO_2 \leq$ 60 mmHg at sea level) and severe hypoxaemia occurs when SaO_2 is below 80% and (equivalent to $PaO_2 < 40$ mmHg at sea level) (Robertson & Bailey 2002; Read 2003; Fahlman 2008; Haskins 2012; Humm & Kellett-Gregory 2016). In horses and other large mammals, including rhinoceros, SaO_2 at a specific PaO_2 value, may be slightly higher compared to humans and other similar body mass mammals, because of their haemoglobin's ability to bind to oxygen at low PaO_2 (i.e., horses and other large mammals have higher oxygen affinities compared to humans) (Haskins 2012). Severe hypoxaemia has been mostly reported in free ranging and captive white rhinoceros immobilized with etorphine in combination with other "synergic" drugs, with PaO_2 values as low as 20-25 mmHg (Heard et al. 1992; Haw et al. 2014; Buss et al. 2015; Buss et al. 2017).

1.2.3.2 Other causes of hypoxaemia during immobilization of white rhinoceros

Hypoxaemia results primarily from opioid-induced respiratory depression, but other side effects caused by these opioids may further exacerbate hypoxaemia. For example, alveolar-arterial (A-a) partial pressure gradients (i.e., difference between $PAO_2 - PaO_2$) are elevated in etorphine immobilized white rhinoceros, with gradient above 40 mmHg, compared to 10 mmHg reported for horses at rest (Buss et al. 2018). An increased A-a gradient is an indicator of ventilation-perfusion mismatch, physiological right-left shunting of the lung, and, or inadequate oxygen diffusion, which all cause hypoxaemia (Meyer et al. 2015). White rhinoceros immobilized with etorphine may also have pulmonary hypertension, which also contributes to hypoxaemia (Meyer et al. 2015; Buss et al. 2018; Boesch et al. 2018). Etorphine-induced pulmonary hypertension leads to pulmonary congestion accompanied by interstitial oedema and impaired gas exchange across the alveoli, reducing the amount of oxygen crossing the alveoli into the blood stream, leading to hypoxaemia (Meyer et al. 2015; Buss et al. 2018; Boesch et al. 2018). Increased oxygen consumption (approximately 8 $mL.kg^{-1}.min^{-1}$) has also been reported in rhinoceros immobilized with etorphine (Buss et al. 2018). Even though the normal VO_2 of white rhinoceros is unknown, 8 $mL.kg^{-1}.min^{-1}$ seems very high compared to oxygen consumption of a resting horse, which is around 3 $mL.kg^{-1}.min^{-1}$ (Buss et al. 2018). Increased oxygen consumption in etorphine immobilized rhinoceros is caused by an increase in skeletal muscle activity, seen mainly as muscle tremors, which may deplete limited oxygen reserves, further exacerbating hypoxaemia (Buss et al. 2017; De Lange et al. 2017; Nasr et al. 2021). Lateral recumbency also leads to inadequate ventilation of the dependent lung and rhinoceros' large abdominal organs press against the diaphragm, restricting its movement and lung expansion, and therefore impairing ventilation and worsening the hypoxaemia (Haw et al. 2014; Buss et al. 2017; Buss et al. 2018; Mosing et al. 2020).

Consequences of Hypoxaemia

The brain highly depends on a constant supply of oxygen because neurons cannot store oxygen for future use (Auckburally & Nyman 2017). Therefore, prolonged hypoxaemia causes tissue hypoxia in the brain and anaerobic respiration takes over, leading to lactic acid build-up, which causes brain damage. Humans with prolonged hypoxaemia show signs of dizziness, loss of balance and coordination, blurred vision, and weakness, all of which are symptoms of brain hypoxia and damage

(Auckburally & Nyman 2017). Furthermore, the body's response to tissue hypoxia also causes a decrease in intracellular calcium ion release and reuptake in the sarcoplasmic reticulum of muscle cells, causing skeletal muscle damage (Auckburally & Nyman 2017), which may affect white rhinoceros' ability to stand following immobilization. In addition, when oxygen supply to the heart is impaired, there is an increase in lactate production in the myocardial tissue, which interrupts the metabolic, mechanical, and electrical function of the myocardium resulting in a decrease in contractility and cardiac output (Heusch 1998; Auckburally & Nyman 2017). Wounds and infections may heal slower following immobilization, particularly after invasive procedures when oxygen is diverted to the brain, instead of the wound, to prevent brain damage (Auckburally & Nyman 2017). Therefore, it is important to find reliable ways to reliably monitor blood and tissue oxygenation in rhinoceros, in a non- or minimally invasive way, in the field to detect and treat hypoxaemia early before it leads to morbidity and mortality.

1.3 Scope of the thesis

1.3.1 Problem statement

Illegal poaching of white rhinoceros has resulted in declining population numbers since the 1990s. This decline has driven an increasing need for dehorning and relocating vulnerable individuals to better protected places, but to achieve this, and other management practices, requires chemical immobilization using potent opioids. Unfortunately, these opioids often cause severe hypoxaemia in rhinoceros, increasing the risk of morbidity and mortality. When hypoxaemia is not properly managed, tissue hypoxia, organ failure and death can occur. Therefore, it is important to understand and improve the methods used to monitor hypoxaemia and blood oxygenation during chemical immobilization to accurately and reliably detect and treat hypoxaemia early before it is detrimental. Current methods used to monitor hypoxaemia are mostly designed for human use as they either use a human oxygen-haemoglobin dissociation curve or human haemoglobin light absorption characteristics to calculate or estimate arterial oxygen-haemoglobin saturation. This approach represents a problem because white rhinoceros' haemoglobin, and their oxygen-haemoglobin dissociation curve, are different to that of humans. Therefore, it is important to validate the reliability of these methods in white rhinoceros. Determining the magnitude of the potential error and the repeatability of the measurements will help identify reliable methods for measuring or calculating arterial oxygen-haemoglobin saturation in rhinoceros during immobilization and will have significant indirect benefits for their conservation.

1.3.2 Aims of the thesis

This thesis is aimed at assessing 1) if the standard pulse oximetry and the multi-wavelength pulse co-oximeter can reliably (accurately and precisely) measure arterial oxygen-haemoglobin saturation, 2) which attachment site of the pulse oximeter and pulse co-oximeter probes provides the most reliable measure of peripheral arterial oxygen-haemoglobin saturation (SpO_2), an estimate of arterial oxygen-haemoglobin saturation, and 3) whether calculated arterial oxygen-haemoglobin saturation values are reliable indicators of arterial oxygen-haemoglobin saturation in immobilized white rhinoceros. To assess

the reliability of these methods, a benchtop co-oximeter will be used as a reference method for the measurement of arterial oxygen-haemoglobin saturation in line with the US Food and Administration (FDA) and International Organization for Standardization (ISO) guidelines. Below is a brief outline of how each chapter advances our understanding of the reliability of the different methods used to measure, estimate, or calculate arterial oxygen-haemoglobin saturation in immobilized white rhinoceros. Chapters 2 & 3 will address the reliability of a pulse oximeter and a pulse co-oximeter that measure peripheral arterial oxygen-haemoglobin saturation (SpO_2) and show the most reliable attachment site of their probes. Chapter 4 will show the level of reliability of the Enterprise Point-of-Care (EPOC) blood analyser's calculated arterial oxygen-haemoglobin saturation. Lastly, Chapter 5 will show the level of reliability of arterial oxygen-haemoglobin saturation calculated from the oxygen content equation and from the Siggaard-Andersen algorithm in immobilized southern white rhinoceros.

Chapter 2: Reliability of pulse oximetry, at four different attachment sites, in immobilized southern white rhinoceros (Ceratotherium simum simum)

Pulse oximetry has become a popular method for the early detection of hypoxaemia in veterinary medicine (Grubb & Andersen 2017; Mtetwa et al. 2020). However, studies on selected domestic and wild animals have shown that reliable measurement highly depend on the probe attachment site and this location can vary among species (Grubb & Anderson 2017). In llamas and alpacas, pulse oximetry is reliable when the probe is placed on the tongue (Grubb & Anderson 2017), whereas in cattle (Coghe et al. 1999) and impala (Mtetwa et al. 2020), it is reliable at the base of the tail, and in horses (Reiners et al. 2018) and cynomolgus monkeys (Young et al. 2002) the most reliable site is the cheek. Apart from the theoretical-based work of Haymerle and colleagues (2016), no study has investigated the reliability of pulse oximetry and probe attachment site in immobilized white rhinoceros. In this study, a convenience sample of eight white rhinoceros were immobilized by darting with etorphine and in combination with other drugs. Four pulse oximeters (Nonin 2500A PalmSAT) with transflectance probes were fixed securely to the following attachment sites: third eyelid, cheek, rectum, and tail. Thereafter, arterial blood samples were drawn, approximately every 10 minutes and at the same time, near-simultaneous pulse oximetry measurements were recorded from the four attachment sites. The blood samples were analysed using a benchtop AVOXimeter 4000 co-oximeter (reference method). The SpO_2

measurements at each of the four attachment sites were compared with near-simultaneous SaO_2 measurements and these comparisons were interpreted.

Chapter 3: Reliability of a pulse oximeter and a pulse co-oximeter, at different attachment sites, to detect hypoxaemia in immobilized southern white rhinoceros (Ceratotherium simum simum)

Non-invasive methods of monitoring blood oxygenation, such as pulse oximetry and pulse co-oximetry, are popular among medical practitioners because they are non-invasive, affordable, and easy-to-use. A Nonin 2500A PalmSAT pulse oximeter is a dual-wavelength spectrophotometric method that measures peripheral arterial oxygen-haemoglobin saturation (SpO_2) noninvasively. However, pulse oximetry only uses two wavelengths of light (660 and 920 nm) to measure SpO_2, which may provide unreliable SpO_2 measurements in the presence of other haemoglobin derivatives (Reynolds et al. 1993; Verhovski et al. 2010). However, a Radical-7 pulse co-oximeter is a non-invasive multi-wavelength spectrophotometric method that uses seven+ wavelengths of light (between 500 – 1400 nm) to measure SpO_2 and the other haemoglobin derivatives (methaemoglobin and carboxyhaemoglobin). But the Masimo Radical-7 pulse co-oximeter SpO_2 measurements have never been validated in immobilized white rhinoceros. Pulse oximetry and pulse co-oximetry probes are commonly affixed to scarified ears in rhinoceros (Boardman et al. 2014; Fahlman et al. 2016; Haymerle et al. 2016; Meuffels et al. 2022) without validating how reliable this area is as an attachment site. So far, no study that has assessed the reliability of the pulse oximetry and pulse co-oximetry SpO_2 measurements when the probes are attached to the ear of immobilized white rhinoceros has been performed. In this study, a convenience sample of eight white rhinoceros were immobilized by darting with etorphine and in combination with other drugs. Two Nonin 2500A PalmSAT pulse oximeters and two Masimo Radical-7 pulse co-oximeter with transflectance, and transmission probes were fixed securely to the following attachment sites: third eyelid and the ear pinna. Thereafter, arterial blood samples were drawn, approximately every 10 minutes and at the same time, near-simultaneous pulse oximetry and pulse co-oximetry measurements were recorded from the two attachment sites. The blood samples were analysed using a benchtop, AVOXimeter 4000 co-oximeter (reference method). The SpO_2 measurements at each of the two attachment sites were compared with near-simultaneous SaO_2 measurements and these comparisons were interpreted.

Chapter 4: Reliability of the Enterprise Point-Of-Care (EPOC) blood analyser's calculated arterial oxygen-haemoglobin saturation ($cSaO_2$), in immobilized southern white rhinoceros (Ceratotherium simum simum)

Blood gas analysis is used routinely in wildlife veterinary practice to assess the ventilatory, acid-base and blood oxygenation status of chemically immobilized white rhinoceros, which suffer from opioid-induced cardiorespiratory derangements that results in severe hypoxaemia (Buss et al. 2018; Pohlin et al. 2020). Arterial oxygen-haemoglobin saturation (SaO_2) is an important indicator of blood oxygenation, particularly in animals susceptible to developing hypoxaemia during chemical immobilization and anaesthesia (Buss et al. 2018; Pohlin et al. 2020). A commonly used device that reports the SaO_2 is the Enterprise Point-of-Care (EPOC) blood analyser. However, the EPOC does not measure SaO_2 directly, but measures dissolved arterial oxygen partial pressure (i.e., PaO_2) and uses this variable to calculate arterial oxygen-haemoglobin saturation ($cSaO_2$) by applying the human-specific equation, based on the human oxygen-haemoglobin dissociation curve (Severinghaus 1979; West et al. 2014), which is significantly right-shifted compared to that of white rhinoceros. Therefore, there are concerns over the reliability of the EPOC's $cSaO_2$ for use in white rhinoceros. In this study, a convenience sample of 16 white rhinoceros were immobilized by darting with etorphine and a combination with other "synergistic" drugs. Arterial blood samples were drawn, at pre-determined time points, from a catheter inserted into the auricular artery and analysed using the EPOC blood analyser and a benchtop AVOXimeter 4000 co-oximeter. Using the benchtop AVOXimeter 4000 co-oximeter (reference method), the EPOC's $cSaO_2$ measurements were compared with simultaneous co-oximeter's SaO_2 readings and these comparisons were interpreted.

Chapter 5: Reliability of calculated arterial oxygen-haemoglobin saturation ($cSaO_2$) in immobilized southern white rhinoceros (Ceratotherium simum simum).

Arterial oxygen-haemoglobin saturation is one of the most important variables used to monitor blood oxygenation because it accounts for approximately 96 to 98% of the total oxygen (oxygen content – CaO_2) carried in the arterial blood (Collins et al. 2015). The reliability of calculated arterial oxygen-haemoglobin saturation ($cSaO_2$) has never been validated in chemically immobilized southern white rhinoceros (*Ceratotherium simum simum*), despite hypoxaemia being a major issue during immobilization. Oxygen content can be reliably measured using the method of Tucker (1967), but these measurements have never been used to calculate arterial oxygen-haemoglobin saturation in wildlife, including rhinoceros. Alternatively, the Siggaard-Andersen algorithm, integrated in Radiometer blood analysers (Radiometer Corporation., Copenhagen, Denmark) can be used to calculate arterial oxygen-haemoglobin saturation as a function of partial pressures of oxygen (PaO_2) after adjustable corrections for partial pressures of carbon dioxide ($PaCO_2$), pH and temperature are applied (Siggaard-Andersen et al. 1984; Siggaard-Andersen et al. 1988; Anstey 2000). Even though the Siggaard-Andersen algorithm has been used in white rhinoceros (Haymerle et al. 2016; Reiners et al. 2019), the reliability of its $cSaO_2$ values, modified for white rhinoceros, have never been validated in chemically immobilized rhinoceros. In this study, a convenience sample of eight rhinoceros were immobilized by darting with etorphine-based drug combinations. Thereafter, arterial blood samples were drawn, approximately every 10 minutes and used to measure PaO_2, $PaCO_2$ and pH using an Enterprise Point-of-Care (EPOC) blood analyser, CaO_2 using the method of Tucker (1967) and SaO_2 using a benchtop AVOXimeter 4000 co-oximeter. Oxygen content, haemoglobin concentrations [Hb] and PaO_2 were used to calculate arterial oxygen-haemoglobin saturation from the oxygen content equation (method 1 $cSaO_2$). Arterial oxygen-haemoglobin saturation was also calculated from the Siggaard-Andersen algorithm (method 2 $cSaO_2$) after correcting for EPOC measured PaO_2, $PaCO_2$ and pH. Using the benchtop AVOXimeter 4000 co-oximeter (reference method), Methods 1 & 2 $cSaO_2$ measurements were compared with simultaneous co-oximeter's SaO_2 readings and these comparisons were interpreted.

CHAPTER 2:

Reliability of pulse oximetry, at four different attachment sites, in immobilized southern white rhinoceros (*Ceratotherium simum simum*)

Thembeka K Mtetwa, Leith CR Meyer & Edward P Snelling

From the Department of Paraclinical Sciences (Mtetwa, Meyer), Department of Anatomy and Physiology (Snelling), Faculty of Veterinary Science, University of Pretoria, Private Bag X04, Onderstepoort, 0110, South Africa.

Reporting status:

Publication:	Journal of Veterinary Anaesthesia and Analgesia
	https://doi.org/10.1016/j.vaa.2022.08.006
	*Article has been adjusted to this thesis format
	Authors: Thembeka K Mtetwa, Edward P Snelling, Peter Buss, Gareth E Zeiler & Leith CR Meyer
Presentations	Oral: Wildlife Congress 2021, Virtual Event and Expo, 11-13 March 2021
	Oral: Faculty Day, Faculty of Veterinary Science, University of Pretoria; October 2021

2.1 Abstract

Chemically immobilized white rhinoceros require accurate monitoring of their oxygen status to reduce the chances of morbidity and mortality. The objectives of this study were to determine the reliability of peripheral oxygen-haemoglobin saturation (SpO_2), measured by a Nonin PalmSAT 2500A pulse oximeter with 2000T transflectance probes at four attachment sites (third eyelid, cheek, rectum, and tail), by comparing these measurements to arterial oxygen-haemoglobin saturation (SaO_2) measured by a benchtop AVOXimeter 4000 co-oximeter reference method in immobilized southern white rhinoceros (*Ceratotherium simum simum*). As part of a broader study, a convenience sample of eight wild-caught male white rhinoceros were immobilized with etorphine (0.0026 ± 0.0002 $mg.kg^{-1}$, mean ± standard deviation) intramuscularly, after which the pinna was aseptically prepared for arterial blood sample collection, and four pulse oximeters with transflectance probes were fixed securely to their attachment sites (third eyelid, cheek, rectum, and tail). Thirty minutes following recumbency from the etorphine administration, the animals were given either butorphanol (0.026 ± 0.0001 $mg.kg^{-1}$) or an equivalent volume of saline intravenously. Sixty minutes following recumbency, insufflated oxygen (15 $L.minute^{-1}$ flow rate) was provided intranasally. In total, the SpO_2 paired measurements from the third eyelid (n = 80), cheek (n = 67), rectum (n = 59) and tail (n = 76) were compared with near-simultaneous SaO_2 measurements using Bland-Altman plots to assess bias (accuracy) and precision, and the area root mean squares (ARMS) method. When compared with SaO_2, SpO_2 measurements from the third eyelid were reliable (i.e., accurate and precise) above a saturation range of 70% (bias 1%, precision 3%, ARMS 3%). However, SpO_2 measurements from the cheek, rectum and tail were unreliable (i.e., inaccurate, or imprecise) across the entire 0-100% saturation range. We concluded that a Nonin PalmSAT 2500A pulse oximeter with a 2000T transflectance probe inserted into the space between the third eyelid and the sclera provides reliable SpO_2 measurements when SaO_2 is above 70%, in immobilized white rhinoceros.

Keywords chemical immobilization, co-oximetry, oxygen-haemoglobin saturation, pulse oximetry.

2.2 Introduction

Hypoxaemia is a life-threatening complication that often accompanies chemical immobilization of white rhinoceros (*Ceratotherium simum*) (Reiners et al. 2019). If untreated, hypoxaemia can cause organ failure, leading to morbidity and mortality. Hence, reliable, and field-friendly techniques are needed to monitor hypoxaemia, for early detection and treatment in rhinoceros.

Arterial oxygen-haemoglobin saturation (SaO_2) is a useful index of blood oxygenation that can be indirectly estimated by pulse oximetry, or directly measured by co-oximetry. Co-oximetry is a spectrophotometric method that directly measures SaO_2 and is regarded as a 'reference method' for humans. Although untested in rhinoceros, the spectrophotometric characteristics of haemoglobin (i.e., infrared absorbance of oxy- and deoxyhaemoglobin) are almost identical among humans, horse (Grosenbaugh et al. 1997) and rhinoceros (Reiners et al. 2019), suggesting that co-oximetry algorithms are likely transferable to the rhinoceros. Unlike co-oximetry, pulse oximetry measures peripheral arterial oxygen-haemoglobin saturation (SpO_2), non-invasively and continuously, making it a more convenient method to indirectly monitor blood oxygenation in mammals (Reiners et al. 2018). Apart from the theoretical-based work of Haymerle et al. (2016), no study has investigated the reliability of pulse oximetry and probe attachment sites in immobilized white rhinoceros.

In this study, a benchtop co-oximeter was used to directly measure SaO_2 and thereby assess the reliability of pulse oximetry at different attachment sites - specifically the third eyelid, cheek, rectum, and tail. We hypothesized that pulse oximetry, when used with appropriate probe placement, can reliably measure SaO_2 in immobilized white rhinoceros.

2.3 Materials & methods

Experimental animals

This study was approved by the University of Pretoria Animal Ethics Committee (V035-17) and the South African Nation Parks Animal Use and Care Committee (001/16). All procedures were conducted at the Veterinary Wildlife Services, Kruger National Park, South Africa (23° 49' 60 S, 31° 30' 0 E; altitude ~320 m). A convenience sample of eight wild-caught male southern white rhinoceros (*Ceratotherium simum simum*) (4-5 years-old) were captured and relocated to a holding facility (bomas) at Veterinary Wildlife Services where they were used for the study. The animals were fed lucerne and teff, and water was provided *ad libitum* and their adaptation to captivity observed closely by trained staff (Miller et al. 2016).

Immobilization

Data were collected during a larger investigation into the effects of etorphine, with and without butorphanol (Boesch 2019). Animals were immobilized twice with etorphine – once to test the effects of butorphanol on etorphine-immobilization and once for control (saline) purposes – in a random order (www.randomiser.org), with a 2-week washout period between treatments. Etorphine (M99; Voluplex., Mnandi, South Africa), was administered intramuscularly in the nuchal hump using a 3 mL dart with 60 mm uncollared needle propelled by a compressed air rifle (DAN-INJECT International SA, Skukuza, South Africa). Butorphanol (Butonil; Wildlife Pharmaceuticals Pty Ltd., South Africa), or an equivalent volume of saline, was administered intravenously after 30 minutes following recumbency from the etorphine administration. See dose calculations based on body mass in Table 2.1 Insufflated oxygen was provided intranasally (15 L.minute^{-1} flow rate) after 60 minutes through a nasogastric tube, inserted into one nostril to the level of the medial canthus of the eye, coupled to an oxygen tank with a pressure regulator and a flow meter.

Table 2.1 Standard doses of drugs based on body mass used for white rhinoceros. Animals were weighed during the two-week habituation period and at the end of the immobilization and reversal by encouraging them to enter a crate, which was weighed using a crane balance. Rhinoceros weighed 1145 ± 75 kg [(mean ± standard deviation (SD)].

Rhinoceros body mass (kg)	**Etorphine (mg)[a]**	**Butorphanol (mg)[b]**	**Naltrexone (mg)[c]**
1000 - 1250	2.5	25	50
1250 - 1500	3.125	31.25	62.5

[a]Etorphine (0.02 $mg.kg^{-1}$)

[b]Butorphanol (10× etorphine dose, mg)

[c]Naltrexone (20× etorphine dose, mg)

Pulse oximetry data collection

A 25 cm, 22-gauge IV catheter (Nipro Medical Corporation., NJ, USA) was inserted into the medial auricular artery for arterial blood collection. Four Nonin PalmSAT 2500A pulse oximeters with Nonin 2000T transflectance pulse oximeter probes (Fig. 2.1a) were placed at the following attachment sites:

a) Third eyelid (nictitating membrane mucosa), where the probe was covered in lubricant gel and gently inserted (after applying gentle pressure onto the eye orbit through the upper eyelid) into the space between the third eyelid and sclera of the eye, away from the cornea and towards the medial canthus, such that it apposed the third eyelid (Fig. 2.1b). Once the probe was in place, the eyes were covered with a blind fold.

b) Cheek (buccal mucosa), where the probe was attached to a modified pair of tongs (Reiners et al. 2018) and inserted inside the mouth so that it lay against the buccal mucosa, approximately 90 mm from the commissure of the lip (level with the maxillary premolars). The tongs were gently clamped to secure the probe (Fig. 2.1c).

c) Rectum (rectal mucosa), where the probe was inserted approximately 50 mm into the rectal cavity (Fig. 2.1d_1) and secured in position against the rectal wall alongside a rectal temperature probe (Fig. 2.1d_2).

d) Tail (ventral tail skin), where the probe was secured gently with adhesive tape, with the probe apposing, a non-pigmented area of the skin, on the ventral midline of the tail base (Fig. 2.1d_3).

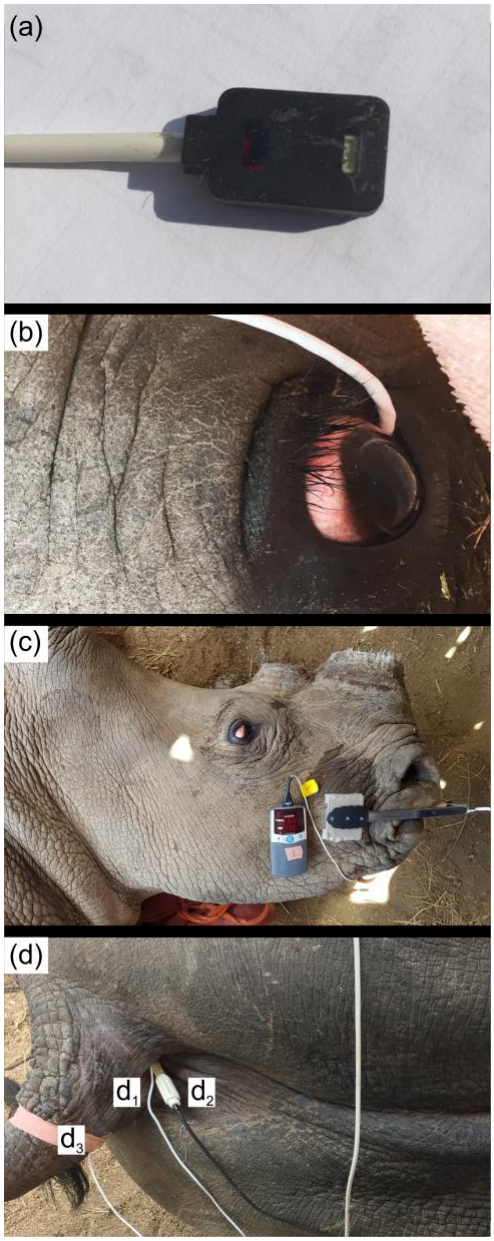

Figure 2.1 Four Nonin PalmSAT pulse oximeters and 2000T transflectance probes used at four different attachment sites (third eyelid, cheek, rectum, and tail) in eight immobilized southern white rhinoceroses (*Ceratotherium simum simum*) (Fig. 2.1a) The transflectance probes (Nonin- 2000T) were placed against (Fig 2.1b) the third eyelid towards the medial canthus of the eye, (Fig. 2.1c) the mucosa of the cheek, approximately 90 mm from the commissure of the lip (using a technique described by Reiners et al. 2018), (Fig.2.1d_1) the rectal mucosa, approximately 50 mm into the rectal cavity (d_2 is the temperature probe) and (Fig. 2.1d_3) the ventral midline of the tail where it was secured gently with adhesive tape on a non-pigmented area of the skin.

We had convenient access to these attachment sites as our study was conducted concurrently with another study.

SpO_2 values, pulse rate and pulse quality were recorded in sets of three (i.e., triplicate), from each of the four pulse oximeters. Pulse quality (signal strength) was indicated by a flashing-coloured light emitting diode (LED), where green indicates good, amber intermediate and red poor quality. Pulse oximetry measurements were recorded in this order: third eyelid, cheek, rectum, tail. A 10 second averaging time was applied for each pulse oximeter reading.

Benchtop co-oximetry analysis

Arterial blood samples, for measurement of SaO_2, were collected within 30 seconds of recording SpO_2 measurement. Yellow and orange optical filters (cuvettes) were used to perform optical quality control for calibration of the co-oximeter. The same optical filters were used to verify that the optics used for measurements were not obscured by blood or debris (AVOXimeter 4000 user manual). The benchtop co-oximeter uses 488.4, 520.1, 562.4, 585.2, 597.5, 621.7 and 671.7 nm wavelengths of light to measure SaO_2, carboxyhaemoglobin (HbCO) and methaemoglobin (MetHb) (AVOXimeter 4000 user manual). Blood samples were analysed within 15 minutes using a benchtop co-oximeter (AVOXimeter 4000; Surgical Innovations., South Africa) and were used as a reference method for comparisons with the SpO_2 measurements (Batchelder & Raley 2007).

Arterial blood sample collection

Animals were instrumented immediately following recumbency. The first arterial blood sample (1 mL) was collected after instrumentation and the remaining six samples were collected approximately every 10 minutes thereafter until reversal. Blood samples were collected anaerobically into heparinised syringes and immediately stored on ice for co-oximeter measurements. At the same time, pulse oximetry measurements were recorded from the four attachment sites.

Data handling

Mean and standard deviation (SD) were calculated for the triplicate SpO_2 measurements. “Pass data” comprised of triplicate SpO_2 measurements, where the pulse quality was indicated by a green (good) or amber light (intermediate), and the SD between the triplicate SpO_2 measurements was <3%, indicating stable and consistent measurements. “Excluded data” consisted of triplicate SpO_2 measurements, where poor pulse quality was indicated by a red light or the SD between the triplicate SpO_2 measurements was ≥3%, indicating unstable and variable measurements.

Statistical analyses

The Bland-Altman method for multiple observations was performed on “pass data” to compare the mean SpO_2 measurements at the four attachment sites with SaO_2 (Bland & Altman 2007). The Bland-Altman method determined the bias (accuracy), precision between the different devices (SD), and the limits of agreement (LOA) between the paired measurements (bias ± 1.96×SD). For Bland-Altman method analysis to meet 80% power at an α of 0.05 and β of 0.90, a minimum of 17 paired data sets (SpO_2-SaO_2) were required. Area root mean squares (ARMS), a combined measure of accuracy and precision, was also calculated between the paired measurements to determine the overall reliability of pulse oximeter measurements (Batchelder & Raley 2007).

2.4 Results

Immobilizations were effective, and animals recovered successfully upon reversal (Boesch et al. 2019).

Quality of pulse oximetry data

The pulse quality of the pulse oximetry data was mostly acceptable at each probe attachment site (Table 2.2). Despite data from the cheek and rectal probes showing good and intermediate pulse quality, compared to the other attachment sites, there was greater variability in the SpO_2 measurements (triplicate SpO_2 measurements with SD ≥3%). Whereas the tail had some SpO_2 measurements that

indicated poor pulse quality (Table 2.2). Thus, most of the SpO_2 data were excluded from the rectum (29%) and cheek (15%), with the least data excluded from the third eyelid (8%) and tail (4%) (Table 2.2).

Reliability of pulse oximetry data

The performance of pulse oximetry is reported in Table 2.3 and Figure 2.2. Pulse oximetry measurements from the third eyelid were accurate, but imprecise over the entire 0-100% saturation range. However, at the manufacturer's claimed performance range of 70-100%, the measurements were accurate and precise (Fig. 2.2), whereas at values <70%, the measurements were inaccurate and imprecise. Between 80-89%, the measurements were accurate but imprecise, however the ARMS indicated overall reliability. Between 70-79%, and 90-100%, the measurements were accurate and precise. In contrast, SpO_2 measurements from the cheek, rectum and the tail were found to be unreliable (i.e., inaccurate, or imprecise) across all saturation ranges.

Table 2.2 Number of time-matched paired measurements of peripheral oxygen-haemoglobin saturation from the pulse oximeters (SpO_2) at the four different attachment sites (third eyelid, cheek, rectum, and tail) compared with arterial oxygen-haemoglobin saturation measured from a benchtop co-oximeter (SaO_2). Presented are the number of paired measurements for all the data before the exclusion criteria was applied ("all data") and their pulse quality (green, amber, and red) are presented. Also presented are the total number of paired measurements that were not excluded ("pass data"), the number of paired measurements excluded ("excluded data"), and the exclusion criteria applied, are also presented. SD, standard deviation. Sample size (*n)*.

Attachment site	All data (*n*)	Pulse quality indicator light (% of total readings)	Excluded data sample size (*n*) and the exclusion criteria *		Pass data (*n*)†
			Triplicate (i.e., three) SpO_2 with SD > 3%	Red light (poor pulse quality)	
Third eyelid	87	Green = 90% Amber = 10% Red = 0 %	7 (8%)	0 (0%)	80 (92%)
Cheek	79	Green = 84% Amber = 16% Red = 0%	12 (15%)	0 (0%)	67 (85%)
Rectum	83	Green = 92% Amber = 8% Red = 0%	24 (29%)	0 (0%)	59 (71%)
Tail	79	Green = 87% Amber =11% Red = 2%	0 (0%)	3 (4%)	76 (96%)

* Excluded data are triplicate SpO_2 readings where the pulse quality was poor (red light) or the standard deviation is ≥3%. † Pass data are triplicate SpO_2 readings where the pulse quality was good or intermediate (green or amber light) and the standard deviation is <3%.

Table 2.3 Performance of the Nonin PalmSAT 2500A pulse oximeter (SpO_2) at four probe attachment sites (third eyelid, cheek, rectum and tail) compared with a benchtop AVOXimeter 4000 co-oximeter (SaO_2) reference method in eight southern white rhinoceros (*Ceratotherium simum simum*) after exclusion criteria were applied (i.e. table represents only "pass data"). SpO_2, peripheral oxygen-haemoglobin saturation. SaO_2, arterial oxygen-haemoglobin saturation. ARMS, area root mean squares; LOA, limits of agreement (minimum to maximum); *n* represents the sample size of the pass data.

Probe site	Ranges	*n*	Bias (%)	Precision (%)	ARMS (%)	LOA
Third eyelid	0-100	80	2*	10	10	21 - 18
	70-100†	41	-1*	3*	3*	5 - 8
	<70	39	5	13	17	30 - 20
	70-79	13	-1*	2*	2*	3 - 4
	80-89	13	0*	4	4*	8 - 8
	90-100	15	-3*	3*	4*	3 - 5
Cheek	0-100	67	-10	16	19	42 - 21
	70-100†	33	0*	10	10	19 - 20
	<70	34	-20	15	25	49 - 9
	70-79	13	-5	5	7	15 - 5
	80-89	10	-3*	10	10	1 22
	90-100	10	8	11	12	13 - 28
Rectum	0-100	59	23	20	30	62 - 16
	70-100†	33	9	11	14	30 - 11
	<70	26	40	14	43	12 68
	70-79	11	20	5	21	11 29
	80-89	10	9	7	11	23 - 5
	90-100	12	0*	5	5	9 - 10
Tail	0-100	76	34	21	40	76 - 8
	70-100†	35	14	8	16	30 - 1
	<70	41	51	12	52	27 74
	70-79	12	22	5	23	12 33
	80-89	11	15	3*	15	10 21
	90-100	12	6	3*	6	12 - 1

†The manufacturers' claimed performance range (70-100%). *Results that are considered acceptable for the Nonin PalmSAT 2500A pulse oximeters (bias ≤ ±3%, precision ≤3%, ARMS ≤4%) according to manufacturer guidelines (Nonin Medical Inc., Minnesota, USA), the United States Food and Drug Administration (FDA) and the International Organization for Standardization (DIN EN ISO 80601-2-61).

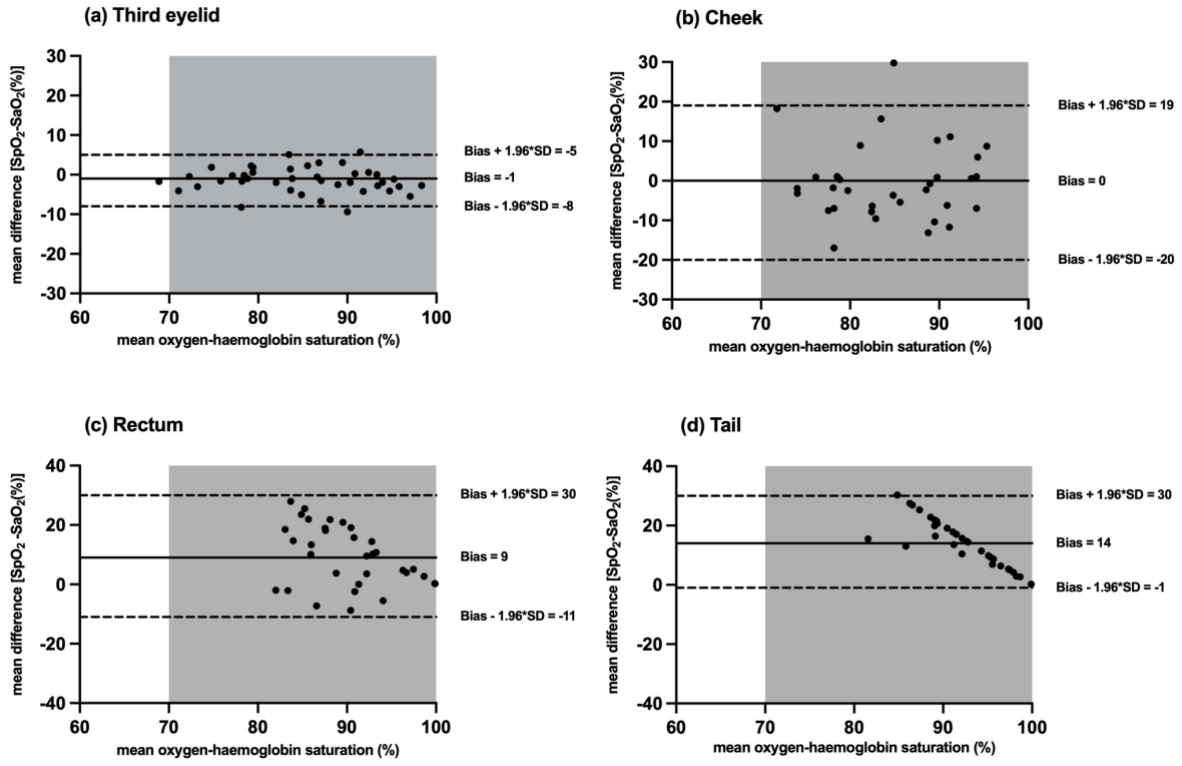

Figure 2.2 Bland-Altman plots, showing the level of agreement between arterial oxygen-haemoglobin saturation (SaO_2) measured by a benchtop co-oximeter (reference method) and the peripheral arterial oxygen-haemoglobin saturation (SpO_2) measured by the Nonin PalmSAT pulse oximeters and 2000T transflectance probes attached at four different attachment sites in eight immobilized southern white rhinoceroses (*Ceratotherium simum simum*). The probes were placed against (a) the third eyelid, (b) the mucosa of the cheek, (c) the rectal mucosa and (d) the ventral midline of the tail on a non-pigmented area of the skin. The percent mean difference between SaO_2 and SpO_2 is plotted against the percent mean arterial oxygen-haemoglobin saturation measurements obtained from the co-oximeter and the pulse oximeters (SaO_2 and SpO_2) at the saturation range of 70-100%. The grey shaded regions represent the manufacturer's claimed performance range of 70-100%. The estimated bias is represented by the solid line, and limits of agreement [bias ± 1.96×standard deviation (SD)] is represented by the dashed lines. Each datum point represents the paired measurements taken from the rhinoceroses. The number of paired measurements from each attachment site are as follows: third eyelid (n = 41), cheek (n = 33), rectum (n = 33) and the tail (n = 35).

2.5 Discussion

In immobilized white rhinoceros, the Nonin PalmSAT 2500A pulse oximeter with a 2000T transflectance probe placed between the third eyelid and the sclera reliably measures arterial oxygen-haemoglobin saturation at the manufacturer's claimed performance range of 70-100%. Although mostly good pulse quality measurements were obtained across all sites, the reliability of pulse oximetry was poor when the probes were placed on the cheek area, rectal mucosa, and the skin of the tail. There were no triplicate SpO_2 with SD >3% (no variability) from the tail and the highest variability was from the rectum (29%). Differences in the reliability and variability of the pulse oximeter measurements between sites highlights the importance of probe placement when assessing blood oxygenation in immobilized white rhinoceros.

Pulse oximetry requires the detection of a pulse to measure SpO_2, so some studies compare pulse oximetry pulse rate with heart rate to exclude potentially erroneous SpO_2 data, as a weak pulse signal may also indicate an error in SpO_2 measurements (Reiners et al. 2018). In this study, I did not measure heart rates simultaneously with pulse oximetry measurements, but instead used the internal pulse quality indicator and variability of the SpO_2 measurements (within the reading time) as exclusion criteria.

In humans, the US Food and Drug Administration (FDA) and International Organization for Standardization (ISO) have certified pulse oximetry as reliable when the comparisons with co-oximetry are $\leq \pm 3\%$ for bias, $\leq 3\%$ for precision and $\leq 4\%$ for ARMS across the 70-100% saturation range (Batchelder & Raley 2007). In immobilized white rhinoceros, this thesis chapter shows that at SaO_2 values <70%, the SpO_2 measurements were unreliable, which was unsurprising given that ISO has set a limit that pulse oximetry devices can only be calibrated at high saturation levels (Weininger 2007). The reliability of pulse oximetry also depends on probe attachment sites in different species. In llamas, and alpacas, pulse oximetry is reliable when the probe is placed on the tongue (Grubb & Anderson 2017). In thick-tongued cattle (Coghe et al. 1999) and impala (Mtetwa et al. 2020), it is reliable at the base of the tail. In horses (Reiners et al. 2018) and cynomolgus monkeys (Young et al. 2002), the most reliable site is the cheek. It is possible that site-specific differences between attachment sites (e.g., skin

and coat thickness, pigmentation, and vascular perfusion), and possibly the effect of ambient light and movement, explain the variation in reliability of pulse oximetry measurements (Reiners et al. 2018). Furthermore, because the reference method (i.e., benchtop AVOXimeter 4000 co-oximeter) is not yet verified for rhinoceros, it may have also contributed to the source of error and unreliability of pulse oximetry at the other different attachment sites (i.e., cheek, rectum and tail). Additional measurement error may have occurred when flushing the catheter before taking an arterial sample, despite discarding the initial blood from the catheter, therefore affecting the quality of our blood samples used to measure SaO_2 from the benchtop AVOXimeter 4000 co-oximeter.

To my knowledge, this is the first study to validate pulse oximetry at different attachment sites in white rhinoceros and we show that the third eyelid is the most reliable attachment site. The mucous membrane of the third eyelid has a well-perfused vascular bed with little pigmentation, which probably facilitates reliable measurement. The probe was also held in secured position by the surrounding tissues and shielded from ambient light. The animals tolerated the probe well during immobilization, and no adverse effects to the eye were observed over the study period, or for 2 weeks thereafter. The transflectance probe used was an appropriate size with smooth edges, for ease of placement without causing abrasion to the surface of the eye.

2.6 Conclusion

In conclusion, the Nonin PalmSAT 2500A device with a 2000T transflectance probe placed under and on the mucous membrane of the third eyelid can be used reliably in white rhinoceros at saturation levels between 70 and 100%. The cheek, rectum and tail attachment sites were unreliable. Furthermore, if saturation levels <70% are expected, then alternative methods such as co-oximetry should be used.

CHAPTER 3:

Reliability of a pulse oximeter and a pulse co-oximeter, at different attachment sites, to detect hypoxaemia in immobilized southern white rhinoceros (*Ceratotherium simum simum*)

Thembeka K Mtetwa, Edward P Snelling & Leith CR Meyer

From the Department of Paraclinical Sciences (Mtetwa, Meyer), Centre for Veterinary Wildlife Research (Mtetwa, Snelling, Meyer), and Department of Anatomy and Physiology (Snelling), Faculty of Veterinary Science, University of Pretoria, Private Bag X04, Onderstepoort, 0110, South Africa.

3.1 Abstract

Reliable monitoring of blood oxygenation during chemical immobilization is essential as southern white rhinoceros (*Ceratotherium simum simum*) are susceptible to opioid-induced hypoxaemia. For this purpose, the reliability of a Nonin PalmSAT 2500A pulse oximeter and a Masimo Radical-7 pulse co-oximeter, at two attachment sites (third eyelid and ear pinna) were evaluated by comparing their peripheral oxygen-haemoglobin saturation (SpO_2) measurements to arterial oxygen-haemoglobin saturation (SaO_2) measured by a benchtop AVOXimeter 4000 co-oximeter (a reference method). As part of a broader study, a convenience sample of eight rhinoceroses were immobilized four times each, at two-week intervals, with different drug combinations (etorphine + saline, etorphine + azaperone, etorphine + midazolam, etorphine + medetomidine). Twelve minutes after recumbency, butorphanol was administered intravenously and at 40 minutes after recumbency, oxygen was administered via intra-nasal insufflation. Once recumbent, the inner surface of the upper ear was aseptically prepared for blood collection and pulse oximeter and pulse co-oximeter probes were secured at their attachment sites (third eyelid and ear pinna). The SpO_2 measurements from the pulse oximeter devices and arterial blood samples for co-oximetry were taken concurrently at 10, 15, 20, 30, 40, 45 and 50 minutes after recumbency. Bland-Altman and area root mean squares (ARMS) methods were used to assess the reliability of the SpO_2 measurements from each pulse oximeter device when compared with simultaneous benchtop co-oximeter SaO_2 measurements. Receiver operating characteristics (ROC) curves, sensitivity, specificity, and positive and negative predictive values were also evaluated to detect clinical hypoxaemia. When compared with SaO_2, the Nonin PalmSAT 2500A pulse oximeter SpO_2 measurements with the 2000T transflectance probe attached to the third eyelid were reliable above the saturation range of 70% (bias -1%, precision 4%, ARMS 4%), consistent with the findings of Chapter 2. Although the bias was low, the Nonin PalmSAT 2500A pulse oximeter with a 2000SL transmission probe placed on the ear pinna, and the Masimo Radical-7 pulse co-oximeter with the transflectance and transmission probes placed on the third eyelid and the ear pinna provided unreliable SpO_2 measurements that had poor precision across the entire 0-100% saturation range. Nonetheless, both the pulse oximeter devices (Nonin & Masimo), at the two attachment sites, can detect hypoxaemia at SaO_2 ≤92%. The Nonin PalmSAT 2500A pulse oximeter with 2000T transflectance probe is best suited for appropriately monitoring blood oxygenation in immobilized white rhinoceros at saturations between 70-100%.

Keywords chemical immobilization, oxygen saturation, wildlife

3.2 Introduction

The goal of monitoring blood oxygenation during chemical immobilization is to ensure adequate oxygen delivery to the tissues to maintain normal organ function. Southern white rhinoceros (*Ceratotherium simum simum*) are susceptible to hypoxaemia (low oxygen levels in the blood), caused by immobilizing drugs, such as etorphine, with arterial oxygen partial pressures (PaO_2) dropping to 25 mmHg in some cases (Haw et al. 2014; Buss et al. 2017; Buss et al. 2018). Hypoventilation, indicated by an increase in arterial carbon dioxide partial pressures ($PaCO_2$ of 80-100 mmHg) is not the only cause of hypoxaemia in rhinoceros; ventilation-perfusion mismatching, impairment in gas exchange and pulmonary blood shunting may also contribute to hypoxaemia during immobilization (Buss et al. 2018; Boesch et al. 2019; Mosing et al. 2020; Meuffels et al. 2022). White rhinoceros also develop muscle tremors and hypermetabolism, which exacerbates hypoxaemia by depleting limited oxygen reserves (Buss et al. 2017; Buss et al. 2018; Boesch et al. 2019; Meuffels et al. 2022). When hypoxaemia is left untreated in white rhinoceros, it can cause organ failure, resulting in morbidity and mortality (Fahlman 2014). Therefore, the availability of affordable, continuous, and non-invasive methods to monitor arterial oxygen-haemoglobin saturation (SaO_2) reliably will aid in the early detection of hypoxaemia, thereby reducing the risk for tissue hypoxia and death.

A conventional pulse oximeter measures peripheral arterial oxygen-haemoglobin saturation (SpO_2) continuously and non-invasively, making it a convenient ‘go-to’ method to monitor the blood oxygen status of mammals, including wildlife (Louw et al. 2001; Young et al. 2002; Giguere et al. 2014; Haymerle et al. 2016). These devices utilise non-invasive probes that emit two wavelengths of light (infrared- and red-light at 660 nm and 960 nm, respectively) through superficial tissue to estimate SaO_2 (Chan et al. 2013; Grubb & Andersen 2017). Pulse oximetry is commonly used in immobilized rhinoceros and the probes are usually attached to the ear pinna after the skin surface is scarified (Zeiler et al. 2012; Buss et al. 2015; Buss et al. 2017; Haymerle et al. 2016; Buss et al. 2018; Boesch et al.

2018; Reiners et al. 2019; Meuffels et al. 2022). However, there is little evidence on the reliability of this device and approach in immobilized rhinoceros. Haymerle et al. (2016) investigated the reliability of pulse oximetry in white rhinoceros and used algorithms to calculate arterial oxygen-haemoglobin saturation to compare with pulse oximetry SpO_2 measurements. These algorithms may be inaccurate, under certain situations, because many blood variables that change during immobilization influence the dynamic relationship between PaO_2 and SaO_2 (Reiners et al. 2019; Chu et al. 2020). Our recent findings show that the Nonin PalmSAT 2500A pulse oximeter SpO_2 measurements when compared to SaO_2 measured by the benchtop AVOXimeter 4000 co-oximeter reference method are reliable when the probe is placed under the third eyelid in immobilized white rhinoceros (Mtetwa et al. 2022). Nonetheless, more studies are needed in white rhinoceros to ascertain the real-time reliability of pulse oximetry SpO_2 measurements obtained when a pulse oximeter probe is attached to a scarified ear pinna, particularly when compared to SaO_2 measured by a reference method, benchtop co-oximeter.

Benchtop co-oximeters, measure arterial oxygen-haemoglobin saturation (SaO_2), haemoglobin concentration [Hb] and other haemoglobin species (carboxyhaemoglobin and methaemoglobin) using multi-wavelength spectrophotometry. These co-oximeters are regarded as the reference method for the measurement of SaO_2 in humans. Even though benchtop co-oximeters have not been tested in rhinoceros, its algorithms are likely suitable for use in rhinoceros as the spectrophotometric characteristic of haemoglobin (i.e., infrared absorbance of oxy- and deoxyhaemoglobin) are similar among humans, horses (Equidae) and white rhinoceros (Reiners et al. 2019). Benchtop co-oximeters are more reliable because they are calibrated by the manufacturer using blood samples at saturations levels between 0-100% (Gehring et al. 2007). On the other hand, pulse oximetry calibration requires a live patient with a pulse and for obvious ethical reasons, it can only be calibrated at saturations between 70-100%. Another limitation of pulse oximetry is that its two-wavelength technology cannot distinguish between different haemoglobin species (Zijlstra et al. 1991; Feiner et al. 2010). This is a problem as the light absorption spectra of oxyhaemoglobin (HbO_2) and carboxyhaemoglobin (HbCO) are similar at the infrared spectral region (at 940 nm), which may affect the reliability of SpO_2 measurements when using the pulse oximetry (Feiner et al. 2010).

A potentially better alternative is the Masimo Rainbow signal extraction technology (SET) Radical-7 pulse co-oximeter (Masimo Corporation., Irvine, California) that uses probes that emit seven + multi-wavelengths of light (between 500 – 1400 nm) to continuously and noninvasively measure SpO_2, haemoglobin concentration (as SpHb), carboxyhaemoglobin (as SpCO) and methaemoglobin (as SpMet) (Feiner et al. 2010; Read et al. 2016; Zoff et al. 2019; Tayari et al. 2021). To date, only a few studies compared the SpO_2 measurements from the Masimo Radical-7 pulse co-oximeter and SaO_2 measured by the reference method, co-oximeter. These studies were done in anaesthetized sheep (Quinn et al. 2013), dogs (Tayari et al. 2021) and horses (Zoff et al. 2019; Tayari et al. 2022) and found conflicting results. In anaesthetized dogs and horses, there was good agreement between the SpO_2 and SaO_2 measurements when the probes were placed on the tongue or the lip (Zoff et al. 2019; Tayari et al. 2021; Tayari et al. 2022). Whereas, in anaesthetized sheep, there was poor agreement between the SpO_2 and SaO_2 measurements when the probe is placed on tongue (Quinn et al. 2013). There have been no similar studies done in wildlife, including rhinoceros.

Therefore, we aimed to assess the reliability of the Nonin PalmSAT 2500A pulse oximeter and the Masimo Radical-7 pulse co-oximeter, and their probes, by comparing their SpO_2 measurements to arterial oxygen-haemoglobin saturation (SaO_2) measurements obtained from a reference method, using a benchtop AVOXimeter 4000 co-oximeter. To achieve these aims, two probe attachment sites, the inner surface of the third eyelid of the left and right eye and the ear pinna of the rhinoceros, were used. For the two oximeter devices and probes, at the two attachment sites, we also aimed to determine their receiver operating characteristics (ROC) curves, sensitivities, and specificities for detecting hypoxaemia (SaO_2 ≤92%) in immobilized white rhinoceros. We hypothesized that the traditional pulse oximeter (Nonin PalmSAT 2500A) and the new multi-wavelength pulse co-oximeter (Masimo Radical-7), at the two attachment sites, could reliably estimate SaO_2, and detect hypoxaemia, in immobilized southern white rhinoceros under field conditions.

3.3 Materials & methods

Experimental animals

The study was approved by the University of Pretoria Animal Ethics Committee (REC246-19) and the South African National Parks Animal Use and Care Committee (no. 012/20). A convenience sample of eight wild-caught male southern white rhinoceros (*Ceratotherium simum simum*) (4 – 5 years-old) were brought to dedicated holding facilities (bomas) at Veterinary Wildlife Services, Skukuza, Kruger National Park, South Africa (23° 49' 60 S, 31° 30' 0 E; altitude ~320 m elevation) where they were habituated to boma-captivity for 4 – 6 weeks. The animals were fed lucerne (*Medicago sativa*) and teff hay (*Eragrostis tef*) and water was provided *ad libitum*.

Immobilization

Data for this study were collected during an unrelated prospective, randomized, controlled crossover study on the effects of different drug combinations on white rhinoceros (REC011-21). Rhinoceros were subjected to four immobilizing protocols each; etorphine (M99; Voluplex., Mnandi, Centurion, South Africa) and injectable saline, etorphine and azaperone (Stresnil; Elanco., ON, Canada), etorphine and midazolam (Dazonil; Wildlife Pharmaceuticals Pty Ltd., White River, South Africa) and etorphine and medetomidine (Metonil; Wildlife Pharmaceuticals Pty Ltd), with a two-week washout period between immobilizations. See dose calculations based on body mass in Table 3.1. The order in which each rhinoceros was subjected to each drug protocol was determined using an online randomizer (www.randomiser.org). The drug protocols were administered intramuscularly using a 3 mL plastic dart with 60 mm uncollared needle propelled by a compressed air rifle (Dan-Inject International SA., Skukuza, South Africa). For each immobilization, animals were given butorphanol intravenously (Butonil; Wildlife Pharmaceuticals Pty Ltd) at ten-times the etorphine dose,12 minutes after recumbency and were insufflated with oxygen intranasally (15 $L.min^{-1}$ flow rate) at 40 minutes after recumbency to obtain a wide range of blood oxygen levels.

Table 3.1 Standard doses of drugs based on body mass used for white rhinoceros. Animals were weighed intermittently during the four-to-six-week habituation period and at the end of each immobilization and reversal, by encouraging them to enter a crate that was weighed using a crane balance. Rhinoceros weighed 1311 ± 115 kg [mean ± standard deviation (SD)].

Rhinoceros body mass range (kg)	**Etorphine (mg)**	**Azaperone (mg)**	**Midazolam (mg)**	**Medetomidine (mg)**	**Butorphanol (mg)**	**Naltrexone (mg)**
750 – 1000	2.0	10.0	10.0	5.0	40.0	40.0
1000 – 1250	2.5	12.5	12.0	6.25	50.0	50.0
1250 – 1500	3.0	15.0	15.0	7.5	60.0	60.0

[a]Etorphine (~0.002 $mg.kg^{-1}$)

[b]Azaperone (~0.01 $mg.kg^{-1}$)

[c]Midazolam (~0.01 $mg.kg^{-1}$)

[d]Medetomidine (~0.005 $mg.kg^{-1}$)

[e]Butorphanol (10×etorphine dose)

[f]Naltrexone (20×etorphine dose)

Pulse oximetry and pulse co-oximetry data collection

A Nonin PalmSAT 2500A pulse oximeter with a 2000T transflectance probe (Nonin Medical Inc., North Plymouth, USA) (Fig. 3.1.a_1) and a Masimo Radical-7 pulse co-oximeter with a LNCS TF-I AH animal transflectance probe (Masimo Corporation., Irvine, USA) (Fig. 3.1a_2) were each placed under the third eyelid (nictitating membrane mucosa) of the left and right eye of the rhinoceros (Fig. 3.1b). Since the Nonin 2000T transflectance probe had previously been studied (Mtetwa et al. 2022), it was inserted prior to the animal being placed in a lateral position (either on the left or right side), so that it was always placed on the third eyelid of the eye on which the rhinoceros rested (lower eye). The Masimo Radical-7 probe was placed on the third eyelid of the upper eye so that it could be regularly checked. The probes were covered in lubricant gel and gently inserted into the space between the third eyelids and sclerae after applying gentle pressure to the eye orbits through the upper eyelids. The probe's light emitting diode (LED) and the photodiode (Fig 3.1a) faced the third eyelids away from the sclera and towards the medial canthus. Once the probes were in place, the eyes were blindfolded using a towel.

When the rhinoceros was recumbent and placed in a lateral position, with its head supported by a cushion, the upper ear was prepared for instrumentation. A 2000SL lingual transmission probe (Fig. 3.1c_1), connected to another Nonin PalmSAT 2500A pulse oximeter, and a LNS YI AH SpO_2 animal multisite transmission probe (Fig. 3.1c_2), connected to another Masimo Radical-7 pulse co-oximeter, were secured to the upper ear pinna of the rhinoceros. The probes were placed adjacent to one another, at the border of the ear pinna (upper helix) after gently scarifying the skin by scraping it on both sides of the ear surfaces with a scalpel blade.

Peripheral arterial oxygen-haemoglobin saturation (SpO_2), pulse rate and signal pulse quality data were recorded in sets of three (i.e., triplicate), from the Nonin PalmSAT 2500A pulse oximeters. Signal pulse quality (signal pulse strength) was indicated by a flashing-coloured LED built into the Nonin PalmSAT pulse oximeters, where green indicates good, amber intermediate and red a poor signal pulse quality. The SpO_2 and pulse rate were also recorded in triplicate from the Masimo Radical-7 pulse co-oximeters. Signal pulse quality from the pulse co-oximeters was indicated by the signal identification and quality indicator (signal IQ) that corresponds to the peak of an arterial pulsation. The SpO_2 and pulse rate

readings were only taken when the vertical line (positive deflection) of the Signal IQ was consistently at its highest peak, indicating that the measurements displayed were of a good signal pulse quality. The sensitivity mode on the Masimo pulse co-oximeters was set at APOD, which is recommended when there is movement at the probe attachment site to reduce erroneous SpO_2 and pulse rate readings when the sensor is not adequately attached. The pulse oximeter and pulse co-oximeter readings were collected within 30 seconds of collecting arterial samples and recorded in the following order: 1) Nonin PalmSAT third eyelid, 2) Masimo Radical-7 third eyelid, 3) Nonin PalmSAT ear, and 4) Masimo Radical-7 ear. The set averaging time for each SpO_2 measurement was 10 seconds.

Arterial blood sample collection

After the oximeter devices were placed at each attachment site, the inner surface of the upper ear was aseptically prepared and a 25 cm, 22 Gauge over-the-needle intravenous (IV) catheter (Introcan; B Braun Medical Inc., Melsungen, Germany) was inserted into the medial auricular artery for blood sample collection. The catheter lines were flushed (rinsed out) using heparinised saline (0.9% sodium chloride) and were allowed sufficient washout of saline or blood clots before taking the blood sample. Approximately 3 mL of arterial blood was collected anaerobically at 10, 15, 20, 30, and 40 minutes of immobilization into 3 mL heparinised syringes (BD Present A-Line, BD Medical., New Jersey, USA). After insufflated oxygen was provided, additional arterial blood samples were collected at 45 and 50 minutes. All blood samples were immediately placed on ice and analysed with a benchtop co-oximeter within 15 minutes of collection.

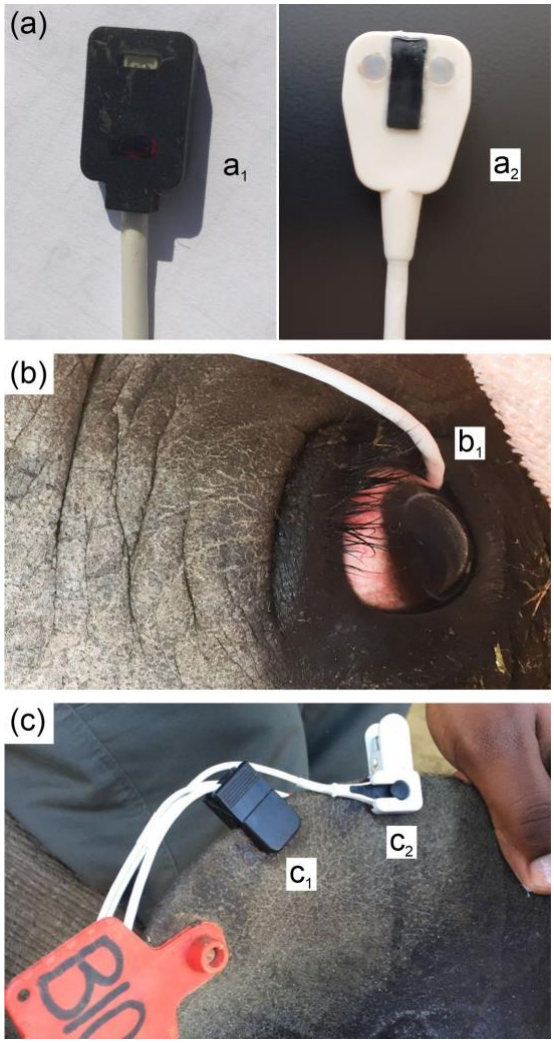

Figure 3.1 A Nonin 2000T transflectance probe (Fig. 3.1a_1) and a Masimo LNCS TF-I AH animal transflectance probe (Fig. 3.1a_2) placed on the third eyelid (nictitating membrane mucosa) of the left and right eye of southern white rhinoceros (*Ceratotherium simum simum*) (Fig. 3.1b_1). The Nonin 2000T transflectance probe was placed before the animal was in a lateral position (either on the left or right side), so that it was always placed on the third eyelid of the eye that the rhinoceros rested on (lower eye). The Masimo LNCS TF-I AH animal transflectance probe was placed on the third eyelid of the upper eye so that it could be regularly checked. A Nonin 2000SL lingual transmission clip probe (Fig. 3.1c_1) and a Masimo LNS YI AH SpO_2 animal multisite transmission clip probe (Fig. 3.1c_2) were placed adjacent to one another on the upper ear, on the border of the ear pinna (upper helix) after gently scarifying the skin surface by scarping it on both sides of the ear surfaces with a scalpel blade.

Benchtop co-oximetry analysis

Fractional arterial oxygen-haemoglobin saturation (SaO_2) was measured from the arterial blood samples using a benchtop co-oximeter (AVOXimeter 4000; Surgical Innovations., Johannesburg, South Africa) and test cuvettes (Surgical Innovations). An optical quality control was performed using yellow and orange optical filters (cuvettes) to calibrate the co-oximeter and to verify that the optics used for measurements were not hidden by blood or debris (AVOXimeter 4000 user manual). This benchtop co-oximeter uses multiple wavelengths of light (488.4, 520.1, 562.4, 585.2, 597.5, 621.7 and 671.7 nm) to measure SaO_2, carboxyhaemoglobin (HbCO) and methaemoglobin (MetHb) (AVOXimeter 4000 user manual). The SaO_2 measurements were used as reference measurements and compared with simultaneous SpO_2 measurements from the oximeter devices, at the two attachment sites.

Data handling

Means and standard deviations (SD) were calculated for the triplicate SpO_2 measurements at each time point and exclusion criteria were applied to exclude SpO_2 measurements that were recorded when there was poor signal pulse quality ("excluded data"). For the Nonin PalmSAT devices, "pass data" comprised of SpO_2 measurements where the signal pulse quality was indicated by a green or amber light (good and intermediate pulse quality, respectively) and the SD between the triplicate SpO_2 measurements was <3%, which indicated stable and consistent measurements. "Excluded data" comprised of SpO_2 measurements where the signal pulse quality was indicated by a red light (poor pulse quality) or the SD between the triplicate SpO_2 measurements was ≥3%, which indicated unstable and variable measurements.

All the readings from the Masimo Radical-7 were of good signal pulse quality (i.e., the readings were only taken when there was a consistent positive deflection of the vertical line of the signal IQ). Therefore, "pass data" comprised of SpO_2 measurements where the SD between the triplicate SpO_2 measurements was <3%, which indicated stable and consistent measurements. "Excluded data" comprised of SpO_2 measurements where the SD between the triplicate SpO_2 measurements was ≥3%, which indicated unstable and variable measurements.

Statistical analyses

The Bland-Altman method for multiple observations (Bland & Altman 2007) was performed on the "pass data" to compare the SpO_2 measurements at the two attachment sites with SaO_2 measurements from the benchtop co-oximeter (i.e., SpO_2-SaO_2). The Bland-Altman method determined the accuracy (bias), precision of the measurements of the pulse oximeter devices at their attachment sites (SD; standard deviation), and the limits of agreement (LOA) between the paired (i.e., SpO_2-SaO_2) measurements (bias ± 1.96×SD). Bias is the mean difference, and precision, is a measure of the variability (SD) of the paired measurements. For Bland-Altman method analysis to meet 80% power at an α of 0.05 and β of 0.90, a minimum of 17 paired data sets of SpO_2-SaO_2 were required. Area root mean squares (ARMS) was also calculated to determine the overall reliability of pulse oximetry (Batchelder & Raley 2007) by combining the accuracy and precision using the equation:

$$\mathrm{ARMS} = \sqrt{\frac{\sum_{i=n}^{n}(\mathrm{SpO_2} - \mathrm{SaO_2})^2}{n}}$$

The guidelines by the US Food and Drug Administration (FDA) and the International Organization for Standardization (ISO) have certified pulse oximetry as reliable when the comparisons with co-oximetry are ≤±3% for bias, ≤3% for precision and ≤±4% for ARMS (Batchelder & Raley 2007).

Multiple cut-off values (≤35%, ≤75%, ≤80%, ≤85%, ≤90%, ≤92%, ≤95% and ≤100%) we chosen to construct receiver operating characteristics (ROC) curves for both the pulse oximeter devices, at the two attachment sites. The ROC curves represent the relationship between sensitivity (%) and 100%-Specificity (or false positive ratio) (Mallett et al. 2012). Sensitivity is the percentage of white rhinoceros with hypoxaemia who are correctly identified as hypoxaemic by the pulse oximeter devices and specificity is the percentage of white rhinoceros without hypoxaemia who are correctly identified as not hypoxaemic by the pulse oximeter devices at the attachment sites. False positive ratio is the number of false positive values divided by false positive and true negative values. Area under the curve (AUC) values were derived from the ROC curves. To determine the accuracy for detecting hypoxaemia, the

following guidelines were applied: 0.50 <AUC ≤ 0.70 indicated low, 0.70 < AUC ≤ 0.90 moderate and 0.90 < AUC ≤ 1.00 indicated high accuracy (Swets 1988).

The SaO_2 or SpO_2 of ≤92% is defined as clinically relevant hypoxaemia in large mammals (Haskins 2012). Therefore, SaO_2 or SpO_2 of ≤92% was used as the best cut-off value to calculate sensitivity, specificity, and positive and negative predictive values for the detection of hypoxaemia by the oximeter devices, at their attachment sites. A positive predictive value is the percentage of rhinoceros testing positive for hypoxaemia (SpO_2 of ≤92%) and a negative predictive value is the percentage of rhinoceros testing negative for hypoxaemia (SpO_2 of >92%) among rhinoceros with and without hypoxaemia.

Statistical analyses were performed using GraphPad Prism version 9.3.1 for Windows (GraphPad Software, La Jolla, California 92073, USA). P value of <0.05 was considered statistically significant.

3.4 Results

Signal pulse quality of the data

There were more acceptable signal pulse quality readings (i.e., signal pulse quality indicated by a green or amber light) from the Nonin PalmSAT probe placed under the third eyelid (99.7%) compared to the Nonin PalmSAT probe placed on the ear (93%) (Table 3.2). All readings from the Masimo Radical-7 probes placed under the third eyelid and on the ear were of a good signal pulse quality (i.e., readings were only taken when there was a consistent positive deflection of the vertical line of the signal IQ).

Minimum variability in the triplicate SpO_2 readings were from the Nonin PalmSAT probe placed under the third eyelid (5.7%), with the most variability (i.e., triplicate readings with SD>3%) from the Masimo Radical-7 probe placed on the ear (17%) (Table 3.2). Overall, fewer data were excluded from the third eyelid [Nonin PalmSAT (6%) and Masimo Radical-7 (13%)] with the most data excluded from the ear [Nonin (18%) and Masimo Radical-7 (17%)].

Table 3.2 Number of time-matched (paired) measurements of the peripheral oxygen-haemoglobin saturation (SpO_2) from the Nonin PalmSAT pulse oximeters and Masimo Radical-7 pulse co-oximeters at the two attachment sites (third eyelid and ear pinna) compared with arterial oxygen-haemoglobin saturation (SaO_2) measured from the benchtop AVOXimeter 4000 co-oximeter. Presented are the number of paired measurements for all the data before the exclusion criteria was applied ("all data") and the Nonin PalmSAT pulse oximeters signal pulse quality (green, amber, and red). Also presented are the total number of paired measurements that were not excluded ("pass data"), the number of paired measurements excluded ("excluded data"), and the exclusion criteria applied. SD, standard deviation. Sample size (*n*).

Device (attachment site)	All data (*n*)	Pulse signal quality indicator light (% of total readings)	Excluded data (*n*) and the exclusion criteria		Pass data (*n*)
			Triplicate (i.e., three) SpO_2 with SD >3%	Poor pulse signal quality (red)	
Nonin PalmSAT (third eyelid)	283	Green = 76.0% Amber = 23.7% Red = 0.3%	16 (5.7%)	1 (0.3%)	266 (94.0%)*
Masimo Radical-7 (third eyelid)	291		39 (13.0%)	N/A	252 (87.0%)†
Nonin PalmSAT (ear)	255	Green = 74.0% Amber = 19.0% Red = 7.0%	26 (10.0%)	21 (8.0%)	208 (82.0%)*
Masimo Radical-7 (ear)	251		43 (17.0%)	N/A	208 (83.0%)†

*For the Nonin PalmSAT devices, “pass data” comprised of SpO_2 measurements where the signal pulse quality was indicated by a green or amber light (good and intermediate signal pulse quality) and the SD between the triplicate SpO_2 measurements was <3%. †For the Masimo Radical-7 devices, all the readings were of a good signal pulse quality (i.e., all readings were taken only when there was a consistent positive deflection the vertical line of the signal IQ), therefore, “pass data” comprised of triplicate SpO_2 measurements with a SD <3%.

Reliability of SpO_2 measurements at the two attachment sites

The Nonin PalmSAT 2500A placed under the third eyelid allowed for 266-paired SpO_2-SaO_2 measurements for comparisons. The mean SpO_2 measurements recorded from this device at this attachment site ranged from 34% to 100% and the corresponding SaO_2 measurements ranged from 12% to 100%. The SpO_2 measurements were accurate (low bias), and although imprecise, had an acceptable overall reliability (acceptable ARMS) at the manufacturers' claimed performance range of 70-100% and at the 80-89% and 90-100% saturation ranges (Table 3.3). The SpO_2 measurements were accurate but imprecise and unreliable at the entire 0-100% saturation range and within the 70-79% saturation range. Below 70%, the SpO_2 measurements were inaccurate, imprecise, and unreliable.

The Masimo Radical-7 placed under the third eyelid allowed for 252-paired SpO_2-SaO_2 measurements for comparisons. The mean SpO_2 measurements recorded from this device at this attachment site ranged from 19% to 99% and the corresponding SaO_2 measurements ranged from 30% to 100%. The SpO_2 measurements were accurate but imprecise and unreliable at the entire 0-100% saturation range and within the 70-100%, 70-79%, 80-89% and 90-100% saturation ranges (Table 3.3). Below 70%, the SpO_2 measurements were inaccurate, imprecise, and unreliable.

The Nonin 2500A PalmSAT placed on the ear pinna allowed for 208-paired SpO_2-SaO_2 measurements for comparisons. The mean SpO_2 measurements recorded from this device at this attachment site ranged from 55% to 100% and the corresponding SaO_2 measurements ranged from 35% to 100%. The SpO_2 measurements were accurate but imprecise and unreliable across the entire 0-100% saturation range and within the 70-100%, 80-89% and 90-100% saturation ranges. Below 70% and at the 70-79% saturation range, the SpO_2 measurements were inaccurate, imprecise, and unreliable.

The Masimo Radical-7 placed on the ear pinna allowed for 208-paired SpO_2-SaO_2 measurements for comparisons. The mean SpO_2 measurements recorded from this device at this attachment site ranged from 21% to 100% and the corresponding SaO_2 measurements ranged from 26% to 100%. The SpO_2 measurements were accurate but imprecise and unreliable at the entire saturation range (0-100%) and

within the 70-100% and 80-89% saturation ranges (Table 3.3). Below 70% and at the 90-100% saturation range, the SpO_2 measurements were inaccurate, imprecise, and unreliable.

Table 3.3 Performance of the Nonin PalmSAT 2500A pulse oximeters (SpO_2) and Masimo Radical-7 pulse co-oximeters (SpO_2) at two attachment sites (the third eyelid and the ear pinna) compared with a benchtop AVOXimeter 4000 co-oximeter (SaO_2) reference method in eight immobilized southern white rhinoceros (*Ceratotherium simum simum*) after exclusion criteria were applied (i.e., table represents only the "pass data"). SpO_2, peripheral oxygen-haemoglobin saturation. SaO_2, arterial oxygen-haemoglobin saturation. ARMS, area root mean squares; LOA, limits of agreement (minimum to maximum); *n* represents the sample size of the pass data.

Device (attachment site)	Ranges (%)	Sample size, n	Bias (%)	Precision (%)	ARMS (%)	LOA
Nonin PalmSAT (third eyelid)	0-100	266	1*	6	6	-12 to 13
	70-100†	226	-1*	4	4*	-9 to 8
	<70	40	8	10	16	-11 to 28
	70-79	25	2*	5	6	-8 to 13
	80-89	92	0*	4	4*	-8 to 8
	90-100	109	-2*	4	4*	-10 to 6
Masimo Radical-7 (third eyelid)	0-100	252	-1*	9	8	-17 to 16
	70-100†	230	-1*	6	6	-14 to 11
	<70	23	8	19	20	-29 to 45
	70-79	24	-1*	11	11	-23 to 22
	80-89	91	0*	6	6	-12 to 12
	90-100	114	-2*	4	5	-11 to 6
Nonin PalmSAT (ear)	0-100	208	1*	7	7	-13 to 14
	70-100†	196	0*	7	7	-13 to 13
	<70	12	10	8	13	-5 to 26
	70-79	20	4	4	6	-4 to 13
	80-89	76	1*	6	6	-11 to 13
	90-100	100	-2*	7	7	-15 to 12
Masimo Radical-7 (ear)	0-100	208	-2*	11	11	-22 to 19
	70-100†	193	-3*	8	9	-19 to 14
	<70	15	13	21	24	-28 to 55
	70-79	19	1*	7	7	-13 to 15
	80-89	73	0*	7	7	-14 to 13
	90-100	101	-5	9	10	-23 to 12

†The manufacturers' claimed performance range (70-100%). *Results that are considered acceptable for the Nonin PalmSAT 2500A pulse oximeters (bias ≤ ±3%, precision ≤ 3%, ARMS ≤ 4%) and Masimo Radical-7 pulse co-oximeter (ARMS ≤ 3%) according to manufacturer guidelines (Nonin Medical Inc., Minnesota, USA and Masimo Corp., Irvine, California), the United States Food and Drug Administration (FDA) and the International Organization for Standardization (DIN EN ISO 80601-2-61).

Ability of the oximeter devices to detect hypoxaemia

There was high accuracy (0.90 < AUC ≤ 1.00) in detecting hypoxaemia from the pulse oximeter (AUC 0.93) and pulse co-oximeter (AUC 0.92) placed under the third eyelid. There was moderate accuracy (0.70 < AUC ≤ 0.90) in detecting hypoxaemia from the pulse oximeter (AUC 0.87) and pulse co-oximeter (AUC 0.83) placed on the ear (Fig. 3.2 and Table 3.4).

At the clinical decision limit of ≤92%, the sensitivity and specificity at detecting clinical hypoxaemia were high for both the oximeter devices, at both attachment sites (Table 3.4). The highest sensitivity and specificity were from the Nonin PalmSAT pulse oximeter (sensitivity 88%, specificity of 85%) and Masimo Radical-7 pulse co-oximeter (sensitivity 87%, specificity 83%) placed under the third eyelid. Generally, the positive predictive values were higher than the negative predictive values, for all the oximeter devices, at each attachment site (Table 3.4). Positive predictive values were high from the Nonin PalmSAT pulse oximeter (96%), and the Masimo Radical-7 pulse co-oximeter (94%) placed under the third eyelid and the Masimo Radical-7 pulse co-oximeter placed on the ear (92%) compared to the Nonin PalmSAT pulse oximeter placed on the ear (86%). The negative predictive value was high (75%) from the Nonin PalmSAT pulse oximeter placed on the ear compared to the other oximeter devices, at their attachment site, with the lowest negative predictive value from the Masimo Radical-7 probe placed on the ear (50%).

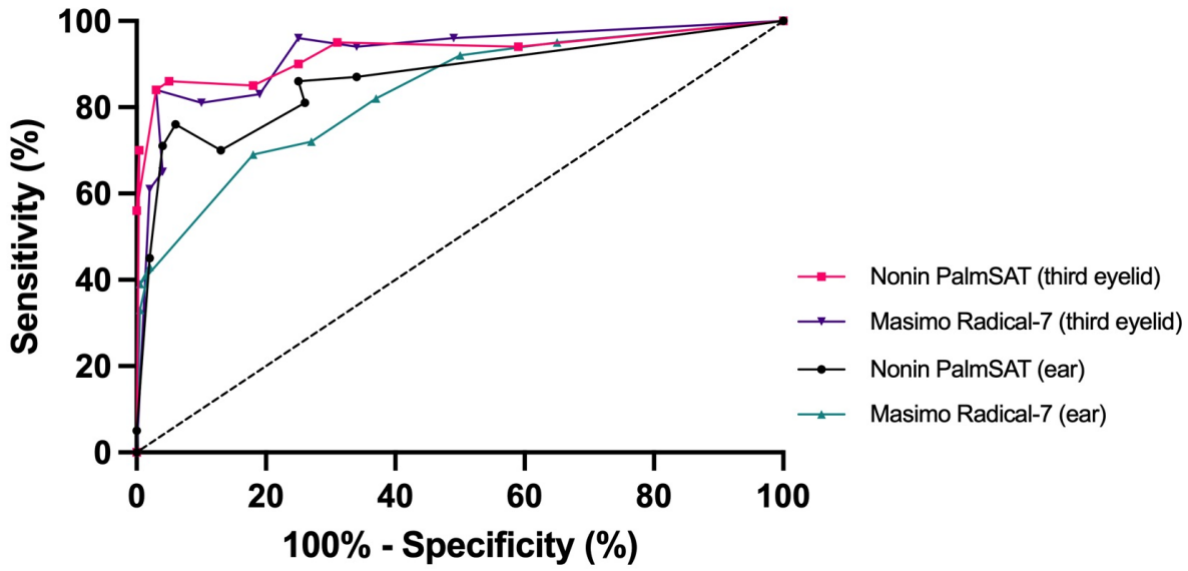

Figure 3.2 Receiver operating characteristics (ROC) curves showing the sensitivity (%) and 100%-Specificity (or false positive ratio) for the peripheral arterial oxygen-haemoglobin saturation (SpO_2) from the Nonin PalmSAT 2500A pulse oximeters and Masimo Radical-7 pulse co-oximeters, at the two attachment sites (third eyelid and ear pinna) for the detection of hypoxaemia in southern white rhinoceros (*Ceratotherium simum simum*). SpO_2 measurements from the Nonin PalmSAT 2500A pulse oximeter (pink line) and Masimo Radical-7 pulse co-oximeter (purple line) under the third eyelid and the Nonin PalmSAT 2500A pulse oximeter (black line) and Masimo Radical-7 pulse oximeter (green line) on the ear pinna. The ■, ∇, •, and Δ represent the sensitivity (%) and 100%-Specificity (%) at the cut-off values (≤35%, ≤75%, ≤80%, ≤85%, ≤90%, ≤92%, ≤95%, and ≤100%).

Table 3.4 Sensitivity, specificity, positive and negative predictive values for the detection of hypoxaemia at the clinical decision limit of ≤92% based on the Nonin PalmSAT 2500A pulse oximeters' and Masimo Radical-7 pulse co-oximeters' SpO_2 measurements at two attachment sites (third eyelid and ear pinna sites) in immobilized southern white rhinoceros. The cut-off values for clinical hypoxaemia (SaO_2 ≤92%) were based on values applied in large animal anaesthesia (Haskins 2012). The area under the curve (AUC) values measured from the receiver operation characteristics (ROC) curves are also represented. SpO_2, peripheral arterial oxygen-haemoglobin saturation. CI, confidence intervals.

Device (attachment site)	Clinical decision limit	Sensitivity (95% CI) (%)	Specificity (95% CI) (%)	Positive Predictive value (95% CI) (%)	Negative Predictive value (95% CI) (%)	AUC* (95% CI)	P value
Nonin PalmSAT (third eyelid)	SaO_2 ≤92%	88 (82 to 91)	85 (74 to 92)	96 (90 to 98)	69 (58 to 78)	0.93 (0.84 to 1.00)[§§]	<0.0001
Masimo Radical-7 (third eyelid)		87 (81 to 90)	83 (72 to 90)	94 (90 to 97)	66 (55 to 75)	0.92 (0.83 to 1.00)[§§]	<0.0001
Nonin PalmSAT (ear)		86 (79 to 91)	76 (66 to 84)	86 (79 to 91)	75 (65 to 84)	0.87 (0.76 to 0.98)[††]	<0.0001
Masimo Radical-7 (ear)		75 (68 to 80)	78 (65 to 87)	92 (85 to 95)	50 (39 to 61)	0.83 (0.73 to 1.00)[††]	<0.0001

*For the interpretation of ROC's area under the curve (AUC) values, the following guidelines have been proposed: low 0.50 < AUC ≤ 0.70**, moderate 0.70 <AUC ≤ 0.90[††] and high 0.90 < AUC ≤ 1.00[§§] accuracy in detecting hypoxaemia (Swets 1988)

3.5 Discussion

In immobilized southern white rhinoceros, the Nonin PalmSAT 2500A pulse oximeter with a 2500T transflectance probe placed under the third eyelid provided generally reliable SpO_2 measurements at the manufacturers' claimed performance range of 70-100%. The Nonin PalmSAT 2500A pulse oximeter with a 2000SL lingual transmission probe placed on the ear pinna provided unreliable SpO_2 measurements, that had discernibly poor precision indicated by a SD of 7%, at the 70-100% saturation range. The signal pulse quality from the Nonin transflectance probe placed under the third eyelid was good compared to the Nonin transmission probe placed on the ear pinna, with readings from the ear comprising of poor signal pulse quality. The Masimo Radical-7 pulse co-oximeter with the LNCS transflectance and LNS transmission probes placed on the third eyelid and on the ear pinna, respectively, provided unreliable SpO_2 measurements that were accurate (low bias) but imprecise at the 70-100% saturation range. The SpO_2 measurements from the Masimo Radical-7 probe placed on the third eyelid had discernibly poor precision, indicated by a SD of 6%, at the 70-100% saturation range. In addition, the SpO_2 measurements from the Masimo Radical-7 probe placed on the ear were associated with discernibly poor precision, indicated by a SD of 8%, at the 70-100% saturation range. The Masimo Radical-7 pulse co-oximeter, at both attachment sites (the third eyelid and the ear pinna), mostly provided good signal pulse quality readings (i.e., displayed readings that mostly had a consistent positive deflection for the signal IQ and only these were recorded). Triplicate SpO_2 measurements from the Nonin PalmSAT probes placed under the third eyelid and the ear pinna were more stable (i.e., triplicate with SD <3%) compared to the triplicate SpO_2 measurements from the Masimo Radical-7 probes placed at similar attachment sites (third eyelid and ear pinna). Both pulse oximeter devices (Nonin PalmSAT and Masimo Radical-7), with the probes placed on the third eyelid, provided high accuracy ($0.90 < AUC \leq 1.00$), and with the probes placed on the ear, provided moderate accuracy ($0.70 < AUC \leq 0.90$) in detecting hypoxaemia. However, both pulse oximeter devices, at the two attachment sites, were sensitive and specific at detecting clinical hypoxaemia (SaO_2 ≤92%) in immobilized white rhinoceros.

Studies on the reliability of pulse oximetry often compare pulse rates detected by the oximeter devices to heart rates measured from an electrocardiograph (ECG) or intra-arterial blood pressure monitor to

exclude poor quality SpO_2 measurements (Bohnhorst et al. 2002; Young et al. 2002; Reiners et al. 2018). A good agreement between these rates suggests that the pulse oximeter is measuring a pulse rather than movement artefacts, therefore, potentially yielding SpO_2 readings of a good signal quality (Bohnhorst et al. 2002; Young et al. 2002; Reiners et al. 2018). In this study, heart rates were recorded from an intra-arterial blood pressure device (IntraTorr, IntraVitals, UK) a minute before taking arterial blood samples and pulse oximetry readings. Due to this mismatch in timing, we did not use heart rates to exclude poor signal quality measurements. However, using heart rate alone to exclude poor signal quality readings can have its limitations as simultaneous heart rate from an ECG and the pulse rate from pulse oximeters have been shown to differ substantially in cats, dogs, and horses (Matthews et al. 2003). Therefore, in our study, to exclude poor signal quality readings, we excluded SpO_2 readings with a poor signal pulse quality (shown by a red LED light) and triplicate SpO_2 readings that had high variability (i.e., triplicate SpO_2 with a SD >3%). In addition, since the Masimo Radical-7 pulse co-oximeter uses signal identification or quality indicator (signal IQ) to help identify good signal quality data, we only took measurements when there was a consistent positive deflection of the vertical line of the signal identification or quality indicator (Signal IQ) within the reading time and excluded triplicate SpO_2 measurements that had a high variability.

The performance and reliability of pulse oximetry varies depending on the probe attachment site (Young et al. 2002; Giguere et al. 2014; Grubb & Anderson 2017; Mtetwa et al. 2020). To date, only two studies have looked at the reliability of pulse oximetry at different attachment sites in wildlife [Mtetwa et al. 2020; Mtetwa et al. 2022 (Chapter 2)]. The study in immobilized impala assessed four attachment sites (cheek, ear, rectum, and tail) and showed that the Nonin PalmSAT 2500A pulse oximeter was reliable (bias 4% precision 3%, ARMS 4%) when a 2500T transflectance probe was attached to the base of the tail but only at a narrower 90-100% saturation range (Mtetwa et al. 2020). As shown in Chapter 2 where four attachment sites were evaluated (third eyelid, cheek, rectum and tail), the Nonin PalmSAT 2500A pulse oximeter was reliable (bias 1% precision 3%, ARMS 3%) when a 2500T transflectance probe was attached under the third eyelid at a broader 70-100% saturation range (Mtetwa et al. 2022). Similarly, here, in this study, we also found that the Nonin PalmSAT 2500A pulse oximeter was reliable (bias -1%, ARMS 4%) when the 2500T transflectance probe was placed under the third eyelid at a 70-100%

saturation range. Results from these two studies corroborate that the third eyelid is a good attachment site for pulse oximetry measurements in immobilized white rhinoceros.

In the field, it is common practice to attach the pulse oximeter probe on the ear pinna of the rhinoceros with no knowledge of how reliable this attachment site is in this species (Boardman et al. 2014; Fahlman et al. 2016; Haymerle et al. 2016; Meuffels et al. 2022). In this study, we determined the reliability of the Nonin PalmSAT 2500A pulse oximeter and the Masimo Radical-7 pulse co-oximeter with their transmission probes placed on the scarified ear pinna of the rhinoceros. We found that the scarified ear pinna is an unreliable attachment site, with SpO_2 measurements that are accurate, but overall unreliable because of the poor precision from both the pulse oximeter devices. The skin on the ear pinna of white rhinoceros is thick and pigmented; therefore, it is common to scarify the skin by scraping it with a sharp object to obtain pulse oximetry readings (Boardman et al. 2014; Fahlman et al. 2016; Haymerle et al. 2016). However, skin scarification results in bleeding, which exposes the blood to air and thus influences the precision of the readings, which is a possible reason for the findings in this study. Furthermore, since the human benchtop AVOXimeter 4000 co-oximeter (reference method) used in this study has not yet been verified in rhinoceros, it might have also been a source of error, resulting in unreliable SpO_2 readings. Additionally, the quality of the arterial blood samples used to measure SaO_2 may have been compromised, especially when flushing the catheter before taking an arterial sample, despite discarding the initial blood from the catheter, therefore affecting the reliability of the SpO_2 readings.

Apart from the site- and species-specific variations, the reliability of pulse oximetry may also be affected by the manufacturer and model of the pulse oximeter. A study showed that the Cardell 9402 and Surgi-Vet V9004 pulse oximeters performed differently in anaesthetized foals (Giguere et al. 2014). In our study, the Masimo Radical-7 pulse co-oximeter performed poorly compared to the Nonin pulse oximeter. Although the Masimo Radical-7 pulse co-oximeter generally gave accurate readings at both attachment sites [third eyelid (bias -1%) and ear (bias -3%)], these readings were unreliable due to poor precision [third eyelid (precision 6%) and ear (precision 8%)]. These findings are similar to those reported in anaesthetized sheep (bias -2%, precision 6%) when a LNCS TC-1 Masimo probe was attached to the

tongue (Quinn et al. 2013). However, our findings are in contrast with those reported in anaesthetized horses (Zoff et al. 2019; Tayari et al. 2022) and dogs (Tayari et al. 2021), where the SpO_2 readings were reliable, with good precision when the Masimo probes were attached on the lip or apex of the tongue. The Masimo Radical-7 pulse co-oximeter uses a signal extraction technology that is not found in traditional pulse oximeters (Masimo Corporation 2007; Causey et al. 2011; Quinn et al. 2013). The signal extraction technology applies adaptive filters that separate the true arterial signal from signals caused by different physiologic artefacts (e.g., motion and light artefacts) and separate them out by evaluating the whole signal and breaking it down into its fundamental components (Masimo Corporation 2007; Causey et al. 2011; Quinn et al. 2013). Furthermore, the Masimo Radical-7 pulse co-oximeter uses multi-wavelength technology, which is similar to that of the benchtop co-oximeter, that is regarded a reference method. Therefore, the Masimo Radical-7 pulse co-oximeter should perform better than the Nonin 2500A pulse oximeter, especially in immobilized white rhinoceros with low blood perfusion and excessive movement (tremors) caused by the chemical immobilization. The lack of reliability (specifically precision) of the Masimo Radical-7, especially when the transflectance probe was placed on the third eyelid, an attachment site shown to be reliable in rhinoceros (Mtetwa et al. 2022), could be attributed to the probe size, as it kept on slipping out of place and was not always easy to secure.

The most commonly used pulse oximeter probes are transmission probes because they can be easily attached to a variety of attachment sites including the ear, finger, and tongue (Chaffin et al. 1996; Quinn et al. 2013; Zoff et al. 2019; Tayari et al. 2021; Tayari et al. 2022). Transmission probes are different from transflectance probes in that the red and infrared LED light that is transmitted through the superficial tissue is detected and recorded by the photodiode positioned on the opposite side of the tissue (Chaffin et al. 1996). In our study, the Nonin and Masimo transmission probes attached to the ear pinna provided accurate (good bias) but overall unreliable SpO_2 measurements due to the poor precision. The results are similar to those reported by Giguere et al. (2014), who found that the SpO_2 readings from the ear, using Cardell 9402 and Surgi-Vet V9004 transmission probes were unreliable in anaesthetized neonatal foals. The reasons behind the poor performance of the transmission probe on the ear are unknown, however, the transmission probes used in our study were clip-type probes that were relatively short and at times did not adhere well to the large ears of the rhinoceros, thus may have resulted in poor tissue contact.

During immobilization of white rhinoceros, the detection of hypoxaemia is crucial for decision making to prevent organ failure and potential morbidity and mortality (Reiners et al. 2019; Meuffels et al. 2022). In this study, the ROC curves' AUC values were evaluated to determine the level of diagnostic accuracy in detecting hypoxaemia during chemical immobilization. The Nonin PalmSAT pulse oximeter and the Masimo Radical-7 pulse co-oximeter, when the probes are placed on the third eyelid, had a high accuracy (0.90 <AUC ≤ 1.00) for detecting hypoxaemia compared to the probes placed on the ear pinna, that only had moderate accuracy (0.71 <AUC ≤ 0.90). Similar findings (AUC 0.71) were reported in anaesthetized giraffe when pulse oximeter transmission probes were placed on the ear or the lip (Bertelsen et al. 2017). At the cut-off value of ≤92%, defined as clinical hypoxaemia in large mammals under anaesthesia, the pulse oximeter devices, at both the attachment sites had high sensitivities, specificities, and positive predictive values. The high sensitivities and positive predictive values show that more than 86% of the immobilized white rhinoceros were correctly identified as hypoxaemic by the pulse oximeter devices, at the two attachment sites. However, at the same cut-off value (SaO_2 ≤92%), the Masimo Radical-7 probe placed on the ear had a low negative predictive value of 50%, which meant that half of the immobilized white rhinoceros were mistaken as normoxic when they were hypoxaemic. Nonetheless, a high positive predictive value is more important than a high negative predictive value during immobilization. This means that it is better to correctly identify hypoxaemia and miss normoxia, to help detect the risks associated with hypoxaemia during in immobilized white rhinoceros.

3.6 Conclusion

We have shown that the Nonin PalmSAT 2500A pulse oximeter with a 2000T transflectance probe placed under the third eyelid provided the most reliable SpO_2 measurements in immobilized white rhinoceros when compared to the reference method, a benchtop AVOXimeter 4000 co-oximeter, at a 70-100% saturation range in immobilized white rhinoceros. Although the bias was low, the Nonin PalmSAT 2500A pulse oximeter with a 2000SL transmission probe placed on the ear pinna, and the Masimo Radical-7 pulse co-oximeter with the probes placed on the third eyelid and the ear pinna provided unreliable SpO_2 measurements that had poor precision across the entire 0-100% saturation

range. Both the oximetry devices, at the two attachment sites, can accurately detect hypoxaemia (SaO_2 ≤92%), however, the Nonin PalmSAT 2500A pulse oximeter with a 2000T transflectance probe placed on the third eyelid is preferred as its measurement are not only sensitive and specific for detecting clinical hypoxaemia, but are also accurate and acceptably reliable. Since reliability differs between devices and probe attachment sites, clinicians should select pulse oximeters, and their probe placements, carefully in order to monitor blood oxygenation reliably, and accurately detect hypoxaemia. Until other devices and probes are properly assessed, the Nonin PalmSAT 2500A pulse oximeter with 2000T transflectance probe is best suited for appropriately monitoring blood oxygenation in immobilized white rhinoceros when SaO_2 measurements are expected to be between 70-100%.

CHAPTER 4:

Reliability of the Enterprise Point-of-Care (EPOC) blood analyser's calculated arterial oxygen-haemoglobin saturation, in immobilized southern white rhinoceros (*Ceratotherium simum simum*)

Thembeka K Mtetwa, Leith CR Meyer & Edward P Snelling

From the Department of Paraclinical Sciences (Mtetwa, Meyer), Department of Anatomy and Physiology (Snelling), Faculty of Veterinary Science, University of Pretoria, Private Bag X04, Onderstepoort, 0110, South Africa.

Reporting status:

Publication:	Veterinary Clinical Pathology (in press)
	Article DOI: 10.1111/vcp.13236
	*Article has been adjusted to this thesis format
	Authors: Thembeka K. Mtetwa, Edward P. Snelling, Ashleigh C. Donaldson, Peter Buss, Leith C. R. Meyer
Presentations	Poster: Faculty Day, Faculty of Veterinary Science, University of Pretoria; October 2022

4.1 Abstract

Enterprise Point-of-Care (EPOC) blood analysis is used routinely in wildlife veterinary practice to monitor blood oxygenation, but the reliability of the EPOC's calculated arterial oxygen-haemoglobin saturation ($cSaO_2$) has never been validated in southern white rhinoceros (*Ceratotherium simum simum*), despite their susceptibility to hypoxaemia during chemical immobilization. The study's objective is to evaluate the reliability of EPOC's $cSaO_2$, by comparison with arterial oxygen-haemoglobin saturation (SaO_2) measured by a benchtop AVOXimeter 4000 co-oximeter (reference method) in immobilized white rhinoceros. As part of two broader studies, a convenience sample of 16 white rhinoceros from the two studies (both n = 8) were immobilized by darting with different etorphine-based drug combinations, followed by butorphanol or saline (administered intravenously). Animals in both studies received oxygen via intra-nasal insufflation after 60 min. Blood samples were drawn, at predetermined time points, from a catheter inserted into the auricular artery and analysed using the EPOC and a benchtop AVOXimeter 4000 co-oximeter. Bland-Altman and area root mean squares (ARMS) were used to determine the reliability of the EPOC's $cSaO_2$ when compared with simultaneous co-oximeter's SaO_2 readings. The rhinoceros were acidaemic [pH of 7.30 ± 0.1 (mean ± standard deviation)], hypercapnic ($PaCO_2$ of 73.7 ± 10.5 mmHg) and normothermic (body temperature of 37.4 ± 1.8°C). In total, 389 paired $cSaO_2$-SaO_2 measurements were recorded ($cSaO_2$ ranged between 13.2 – 99.0% and SaO_2 ranged between 11.8 – 99.9%). The EPOC's $cSaO_2$ readings were unreliable across the entire 0-100% saturation range (bias -6%, precision 5%, ARMS 8%). The EPOC's $cSaO_2$ is unreliable and should not be used to monitor blood oxygenation in immobilized white rhinoceros.

Keywords blood gas analysis, hypoxaemia, oxygen saturation, wildlife

4.2 Introduction

Enterprise Point-of-Care (EPOC) blood analysers are used routinely in wildlife veterinary practice to monitor ventilatory, acid-base and blood oxygenation status of chemically immobilized white rhinoceros, which are susceptible to opioid-induced cardiorespiratory derangements that can result in severe hypoxaemia (Buss et al. 2018; Pohlin et al. 2020). To assess blood oxygenation, the EPOC blood analyser measures arterial oxygen partial pressures (PaO_2) with a single-use test card comprising of a Clark-type oxygen sensing electrode, a reference electrode, a counter electrode, and a fluid used for self-calibration (EPOC system manual). Although the Clark-type electrode used in blood analysis reliably measures PaO_2, dissolved oxygen accounts only for about 2-4% of oxygen in the total blood oxygen content (EPOC system manual; Collins et al. 2015). Conversely, oxygen bound to haemoglobin (SaO_2), which does not exert a partial pressure, accounts for the remaining 96-98%, making it a more informative indicator of blood oxygenation (Collins et al. 2015). Thus, the EPOC uses the measured PaO_2 to calculate arterial oxygen-haemoglobin saturation, but it does so by using an equation based on a typical human oxygen-haemoglobin dissociation curve (EPOC system manual).

The relationship between the oxygen bound to haemoglobin and the partial pressure of oxygen in the blood is represented by the oxygen-haemoglobin dissociation curve, and since the characteristics of haemoglobin differs between species, especially when considered across a broad range of body mass, so too does this curve (Schmidt-Neilsen & Larimer 1958; Reiners et al. 2019). The partial pressure of oxygen at which haemoglobin is 50% saturated (P_{50}) is used to quantify the position of the oxygen-haemoglobin dissociation curve under normal physiological resting state (body temperature of 37°C and pH of 7.4) (Collins et al. 2015). When compared to the human curve, which typically has an average P_{50} of 26.7 mmHg at rest (Severinghaus 1979), the P_{50} of white rhinoceros is between 15 mmHg (Reiners et al. 2019) and 20 mmHg (Baumann et al. 1984), indicating a more left-shifted oxygen-haemoglobin dissociation curve. Because the EPOC blood analysers is calibrated specifically for human use, any differences in the oxygen-haemoglobin dissociation curve from that of humans may affect the reliability of the EPOC's $cSaO_2$ values.

Oxygen-haemoglobin dissociation curves also shift dynamically with changes in the partial pressure of carbon dioxide ($PaCO_2$), pH, 2.3-diphosphoglycerate (2.3-DPG), chloride ions (Cl^-) and temperature of the blood (Collins et al. 2015; Clerbaux et al. 1993). Immobilized white rhinoceros often develop hypercapnia and acidaemia, both of which tend to shift their oxygen-haemoglobin dissociation curve to the right, and therefore closer to that of a healthy human at rest (Buss et al. 2018; Reiners et al. 2019; Pohlin et al. 2020). For this reason, it is important that the reliability of the EPOC's $cSaO_2$ is assessed based on the specific physiological conditions under which the analyser is used on different species.

The reliability of the EPOC's $cSaO_2$ can be assessed by comparing against the SaO_2 measured by co-oximetry, which is considered a 'reference method' according to the US Food and Drug Administration (FDA) and International Organization for Standardization (ISO) (Batchelder & Raley 2007). For example, a recent study on immobilized impala (*Aepyceros melampus*), showed that the EPOC's $cSaO_2$ was indeed reliable when compared against a co-oximeter's SaO_2 across the entire 0-100% saturation range (Mtetwa et al. 2020). However, there has been no research on the reliability of the EPOC's $cSaO_2$ readings in white rhinoceros, despite their susceptibility to hypoxaemia during chemical immobilization. In this study, we therefore assessed the reliability of EPOC's $cSaO_2$ by comparing it against a co-oximeter's SaO_2 in immobilized white rhinoceros.

4.3 Materials & methods

Experimental animals

Studies were approved by the University of Pretoria Animal Ethics Committee (V035-17 and REC246-19), and the South African National Parks Animal Use and Care Committee (001/16 and 012/20). A convenience sample of 16 sub-adult male white rhinoceroses (*Ceratotherium simum*), were captured from the wild and relocated to holding facilities (bomas) at the Veterinary Wildlife Services, Kruger National Park, South Africa (23° 49' 60 S, 31° 30' 0 E; ~320 m altitude), where they were habituated for 4-6 weeks. Animals were fed lucerne (*Medicago sativa*) and teff hay (*Eragrostis tef*), with water provided *ad libitum* and their adaptation to captivity observed closely by trained staff (Miller et al. 2016).

Immobilization

Data were collected and pooled from two separate studies on the physiological effects of etorphine-based immobilization to maximize the sample size. Immobilizing drugs were administered intramuscularly using a 3 mL plastic dart with 60 mm uncollared needle launched by a compressed air rifle (DAN-INJECT International SA., Skukuza, South Africa). In the first study (Study 1), rhinoceroses were immobilized twice with etorphine (M99; Voluplex., Mnandi, Centurion, South Africa), and then given either butorphanol (Butonil; Wildlife Pharmaceuticals Pty Ltd., White River, South Africa)] or 0.9% sodium chloride (NaCl) saline solution (control) at 30 minutes into recumbency and then intra-nasal oxygen insufflation (15 $L.min^{-1}$ flow rate) at 60 minutes. In the second study (Study 2), rhinoceroses were immobilized four times using different immobilizing drugs: etorphine (M99) and 0.9% NaCl saline solution (control); etorphine and azaperone (Stresnil; Elanco., ON, Canada); etorphine and midazolam (Dazonil; Wildlife Pharmaceuticals Pty Ltd); and etorphine and medetomidine (Metonil; Wildlife Pharmaceuticals Pty Ltd). Butorphanol was then administered at 12 minutes into recumbency, and intra-nasal oxygen insufflation (15 $L.min^{-1}$ flow rate) at 60 minutes to obtain a wide range of saturation values. See dosage calculations based on body mass in Tables 4.1 and 4.2.

Table 4.1 Standard doses of drugs based on body mass used on white rhinoceros. Animals were weighed during the two-week habituation period and at the end of the immobilization and reversal by encouraging them to enter a crate, which was weighed using a crane balance. Rhinoceros weighed 1145 ± 75 kg (mean ± standard deviation (SD).

Rhinoceros body mass (kg)	**Etorphine (mg)[a]**	**Butorphanol (mg)[b]**	**Naltrexone (mg)[c]**
1000 - 1250	2.5	25	50
1250 - 1500	3.125	31.25	62.5

[a]Etorphine (0.02 $mg.kg^{-1}$)

[b]Butorphanol (10× etorphine dose, mg)

[c]Naltrexone (20× etorphine dose, mg)

Table 4.2 Standard doses of drugs based on body mass used for white rhinoceros. Animals were weighed intermittently during the four-to-six-week habituation period and at the end of each immobilization, by encouraging them to enter a crate that was weighed using a crane balance. Rhinoceros weighed 1311 ± 115 kg [mean ± standard deviation (SD)].

Rhinoceros body mass (kg)	**Etorphine (mg)[a]**	**Azaperone (mg)[b]**	**Midazolam (mg)[c]**	**Medetomidine (mg)[d]**	**Butorphanol (mg)[e]**	**Naltrexone (mg)[f]**
750 -1000	2.0	10.0	10.0	5.0	40	40
1000 -1250	2.5	12.5	12.0	6.25	50	50
1250 – 1500	3.0	15.0	15.0	7.5	60	60

[a]Etorphine (0.002 $mg.kg^{-1}$)

[b]Azaperone (0.01 $mg.kg^{-1}$)

[c]Midazolam (0.01 $mg.kg^{-1}$)

[d]Medetomidine (0.005 $mg.kg^{-1}$)

[e]Butorphanol (10×etorphine dose)

[f]Naltrexone (20×etorphine dose)

Arterial blood sample collection

Once the immobilized rhinoceros was recumbent, the concave (inner) surface of the ear pinna was aseptically prepared, and a 25 mm, 22 Gauge over-the-needle intravenous (IV) catheter (Introcan; B Braun Medical Inc., Melsungen, Germany) was inserted into the medial auricular artery for blood sample collection. A digital thermometer (HI 98509 Checktemp 1; Hanna Instruments., Woonsocket, USA) with a protective sheath over the probe, was inserted into the rectum to measure body temperature. Once instrumented, arterial blood samples were collected anaerobically into 3 mL heparinised syringes (BD Present A-Line; BD Medical., New Jersey, USA) at 30, 40, 50 and 60 minutes into recumbency in Study 1 and at 10, 15, 20, 30, and 40 minutes into recumbency in Study 2. After 60 minutes, up to six additional arterial blood samples were collected at random times during oxygen insufflation.

Visible air bubbles were immediately removed from the collected blood samples and then it was placed on ice. Within 15 minutes, the sample was assessed in a laboratory, under controlled temperature, using an EPOC blood analyser (EPOC Software version 3.35.4 with sensor configuration version 39.2; Epocal Inc., Ottawa, Canada) with single-use, self-calibrated test cards (BGEM3; Epocal Inc) (EPOC system manual) and a benchtop co-oximeter (AVOXimeter 4000; Surgical Innovations., Johannesburg, South Africa) with test cuvettes (ITC QV8; Surgical Innovations). The benchtop co-oximeter was calibrated daily using calibration cuvettes (Surgical Innovations) (ITC AVOXimeter 4000 user manual). Just prior to measurement, the blood sample was re-mixed by gently rolling the syringe back and forth for approximately 20 seconds. Ensuring no visible air bubbles were introduced, blood was carefully injected into the test card and cuvette, which were then introduced into the EPOC and co-oximeter, respectively, for analyses. Because of limited supplies, we did not take repeated measurements per blood sample.

The EPOC measures dissolved arterial oxygen partial pressures (PaO_2) and pH and then calculates the arterial oxygen-haemoglobin saturation ($cSaO_2$) using an equation based on the human oxygen-haemoglobin dissociation curve, pre-programmed into the blood analyser (Severinghaus 1979). Conversely, the benchtop co-oximeter measures fractional arterial oxygen-haemoglobin saturation (SaO_2), methaemoglobin (MetHb) and carboxyhaemoglobin (HbCO) using multiple wavelengths of light

(488.4, 520.1, 562.4, 585.2, 597.5, 621.7 and 671.7 nm) and was used as the reference method in this study (ITC AVOXimeter 4000 user manual). Although co-oximetry has not been tested in rhinoceros, the spectrophotometric characteristics of haemoglobin derivatives (i.e., infrared absorbance of oxy- and deoxyhaemoglobin) are nearly identical among humans, white rhinoceros, and the closely related horse (Equidae), indicating that the algorithms used in co-oximetry are likely also suitable for use in rhinoceros (Reiners et al. 2019).

Statistical analyses

Using the method-comparison approach of Jensen & Kjelgaard-Hansen (2006), data were plotted using simple linear regression and Deming (Model II) linear regression analysis (Jensen & Kjelgaard-Hansen 2006) to determine proportional and constant error between the EPOC's $cSaO_2$ and the co-oximeter's SaO_2 in Study 1 and Study 2. Acceptability and agreement between the EPOC's $cSaO_2$ and the co-oximeter's SaO_2 was assessed based on inherent imprecision of the two methods (Jensen & Kjelgaard-Hansen 2006) using Bland-Altman analysis for multiple observations. The Bland-Altman analysis determined the accuracy (bias), precision [standard deviation (SD)], and the 95% limits of agreement (LOA) between the paired $cSaO_2$ and SaO_2 measurements (Bland & Altman 2007). Bias is the mean difference between the paired measurements, precision is a measure of the variability (SD) between the paired measurements and the 95% LOA (bias ± 1.96×SD) is an estimate of the interval within which 95% of the differences between measurements lie. An area root mean squares (ARMS), which is a combined estimate of accuracy (bias) and precision (SD), was also calculated to determine the overall agreement between $cSaO_2$ and SaO_2 measurements (Batchelder & Raley 2007). To perform Bland-Altman method at an $\alpha=0.05$ and $\beta= 0.90$, a minimum of 17 paired $cSaO_2$-SaO_2 measurements (taken from eight individuals) is required to obtain sufficient statistical power when the expected bias is 3%, precision is 3% and the LOA is ±10%. Guidelines for clinical acceptability are not available for $cSaO_2$ reported by blood analysers, and so for this study we followed the ISO performance requirements for pulse oximetry, which states that the device is clinically reliable (acceptable) only when the comparisons with co-oximetry are $\leq\pm3\%$ for accuracy (bias), $\leq3\%$ for precision (SD) and $\leq4\%$ for ARMS (Batchelder & Raley 2007).

The relationship between PaO_2 and the EPOC's $cSaO_2$ and co-oximeter's SaO_2 measurements were plotted using a specific binding with Hill slope model. The model was also used to determine the least squares regression fit equations from the plots (i.e., oxygen-haemoglobin dissociation curves). Partial pressure of oxygen when haemoglobin is 50% saturated with oxygen (P_{50}) were calculated from each plot using the least squares regression fit equation.

4.4 Results

The mean pH of rhinoceros arterial blood was 7.30 ± 0.1 (mean ± standard deviation) indicating acidaemia, $PaCO_2$ was 73.7 ± 10.5 mmHg indicating hypercapnia and the body temperature was 37.4 ± 1.8°C indicating normothermia. In total, 389 paired $cSaO_2$-SaO_2 measurements were used for comparisons. The EPOC's $cSaO_2$ readings ranged from 13.2% to 99.0% and the co-oximeter's SaO_2 readings ranged from 11.8% to 99.9%. Based on the Bland-Altman analysis, there was poor agreement between the EPOC's $cSaO_2$ and the co-oximeter's SaO_2 across the entire saturation range (Fig. 4.1 and Table 4.3) and within other narrower ranges analysed in both studies (Table 4.3). When Study 1 and Study 2 were analysed separately (Fig. 4.2), a similar lack of agreement was found [Study 1 (bias -5% precision 4% ARMS 7%) and Study 2 (bias -7% precision 5% ARMS 8%)], justifying combining the data. Nonetheless, there was no proportional or constant error between EPOC's $cSaO_2$ and co-oximeter's SaO_2 in Study 1 (slope = 0.969 with 95% CI = 0.931 to 1.008, y intercept = -3.022 with 95% CI = -6.051 to 0.007 $P < 0.0001$). However, in Study 2, there was no proportional error but there was constant error between EPOC's $cSaO_2$ and co-oximeter's SaO_2 (slope = 1.082 with 95% CI = 1.035 to 1.029, y intercept = -13.560 with 95% CI = -17.640 to -9.490 $P < 0.0001$) (Fig. 4.3). Within the 70-79% saturation range, the EPOC's $cSaO_2$ readings were unreliable (inaccurate, precise, poor ARMS). Below 70% and at the other saturation ranges (70-100%, 80-89% and 90-100%), the EPOC's $cSaO_2$ readings were overall unreliable (inaccurate, imprecise, poor ARMS). Across the entire 0-100% saturation range, the EPOC's $cSaO_2$ readings underestimated the SaO_2 by a mean difference of 6% and with a poor precision of 5%. Each rhinoceros was immobilized successfully according to the different drug combinations, and all made full recoveries at the end of each trial. The P_{50} value for the oxygen-haemoglobin dissociation curve derived from the EPOC's $cSaO_2$ is ~29 mmHg and from co-oximeter's SaO_2 is ~32 mmHg (Fig. 4.4).

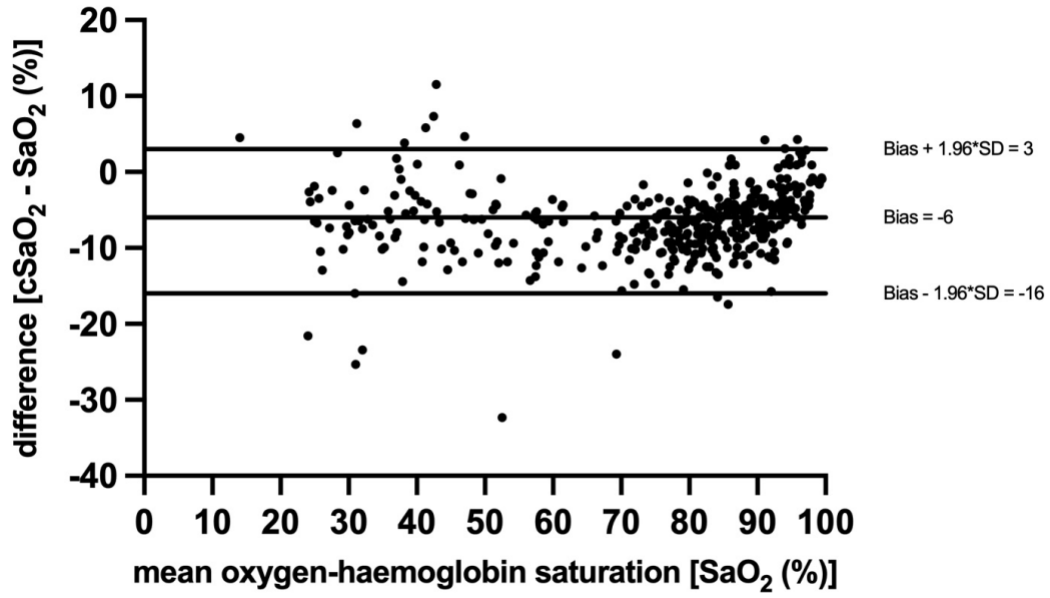

Figure 4.1 Bland-Altman plot, showing poor agreement between the EPOC's calculated arterial oxygen-haemoglobin saturation ($cSaO_2$) and the co-oximeter's arterial oxygen-haemoglobin saturation (SaO_2) in 16 immobilized white rhinoceros. The difference between $cSaO_2$ and SaO_2 is plotted against the mean arterial oxygen-haemoglobin saturation measurements obtained from the EPOC and the co-oximeter ($cSaO_2$ and SaO_2) across the entire 0-100% saturation range. The bias is represented by the solid line, and the limits of agreement (bias ± 1.96×SD) are represented by the dashed lines. Each datum point represents the difference in the paired $cSaO_2$-SaO_2 measurements (389 paired measurements) taken from the 16 white rhinoceroses in both studies.

Table 4.3 Bland-Altman and area root mean squares (ARMS) analysis showing the poor agreement within a number of different saturation ranges, between the arterial oxygen-haemoglobin saturation ($cSaO_2$) calculated from the EPOC blood analyser and the arterial oxygen-haemoglobin saturation (SaO_2) measured by a benchtop AVOXimeter 4000 co-oximeter.

Saturation range (%)	*n*	Bias (%)	Precision (%)	LOA (%)	ARMS (%)
0-100	389	-6*	5*	3 to -16	8*
<70	100	-7*	6*	6 to -19	9*
70-100†	289	-6*	4*	1 to -14	8*
70-79	40	-8*	3	-2 to -14	8*
80-89	112	-7*	4*	1 to -15	8*
90-100	137	-5*	4*	3 to -13	7*

†The manufacturers' claimed performance range (70-100%) *Guidelines for clinical acceptability are not available for $cSaO_2$ reported by blood analysers, and so for this study we followed the ISO performance requirements for pulse oximetry, which states that the device is clinically reliable (acceptable) only when the comparisons with co-oximetry are ≤±3% for accuracy (bias), ≤3% for precision (SD) and ≤4% for ARMS (Batchelder & Raley 2007). *Result that are considered unreliable according to these (ISO) guidelines; n, sample size; ARMS, area root mean squares; LOA, limits of agreement (maximum and minimum).

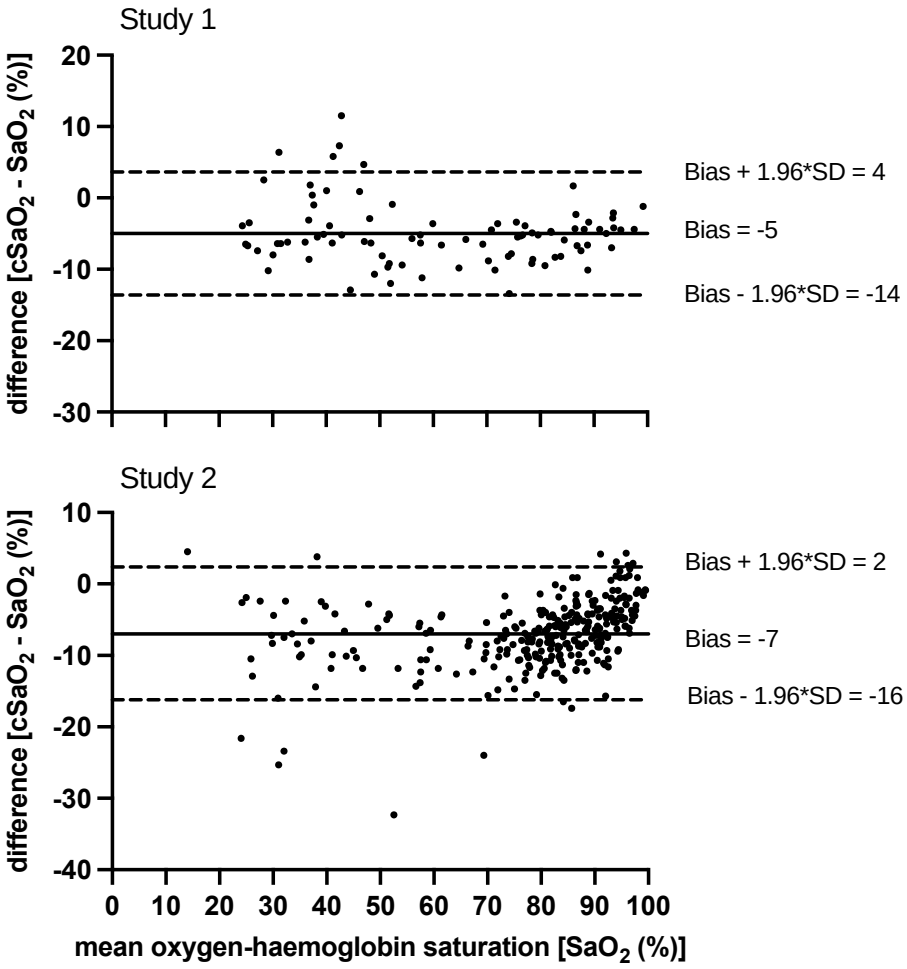

Figure 4.2 Bland-Altman plots, showing poor agreement between the EPOC's calculated arterial oxygen-haemoglobin saturation ($cSaO_2$) and the co-oximeter's measured arterial oxygen-haemoglobin saturation (SaO_2) in eight immobilized white rhinoceros used in Study 1 and a further eight individuals in Study 2. The difference between $cSaO_2$ and SaO_2 is plotted against the mean arterial oxygen-haemoglobin saturation values obtained from the EPOC and the co-oximeter ($cSaO_2$ and SaO_2) across the entire 0-100% saturation range. The bias is represented by the solid line, and the limits of agreement (bias ± 1.96×SD) are represented by the dashed lines. Each datum point represents the difference in the paired $cSaO_2$-SaO_2 measurements taken from the rhinoceros.

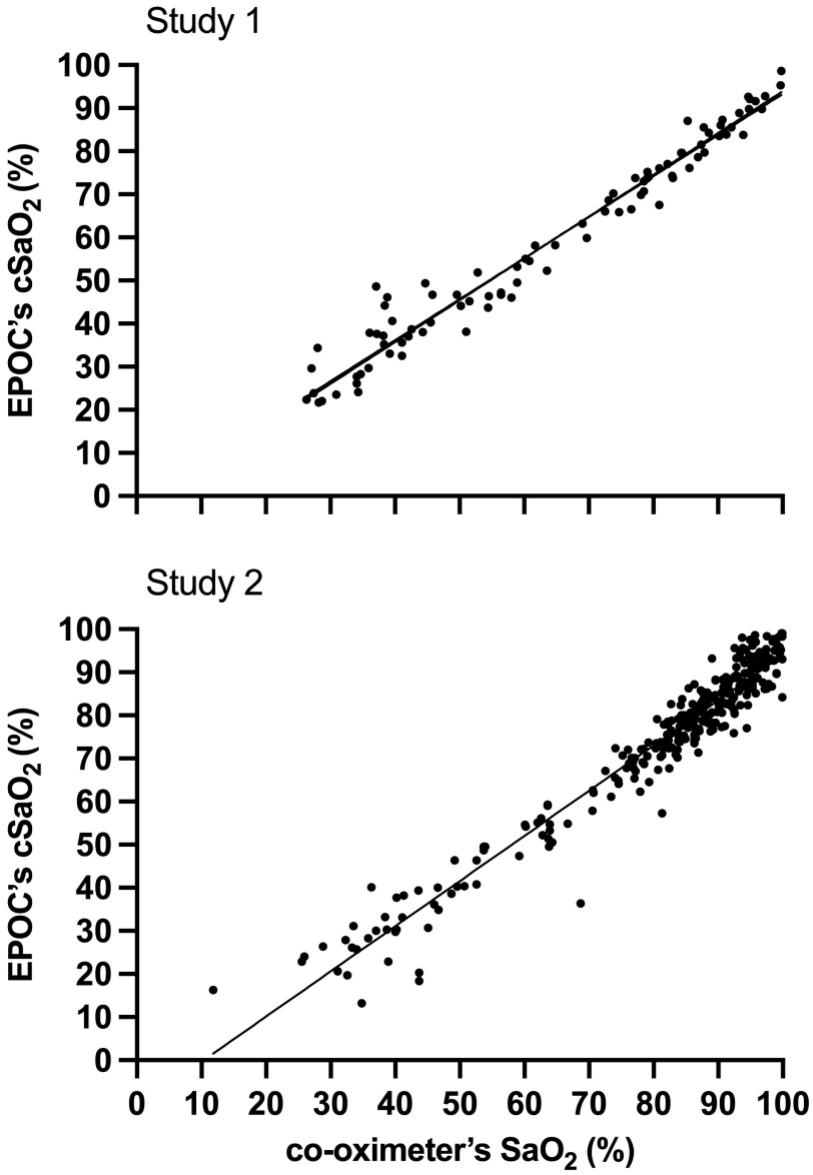

Figure 4.3 Calculated arterial oxygen-haemoglobin saturations ($cSaO_2$) obtained from the EPOC blood gas analyser plotted against arterial oxygen-haemoglobin saturations (SaO_2) measured by the AVOXimeter 4000 co-oximeter in eight immobilized white rhinoceros in Study 1 and a further eight individuals in Study 2. The regression equations for Study 1 (n = 89) and Study 2 (n = 300) are $cSaO_2 = 0.9691*SaO_2 - 3.022$ and $cSaO_2 = 1.082*SaO_2 - 13.56$, respectively.

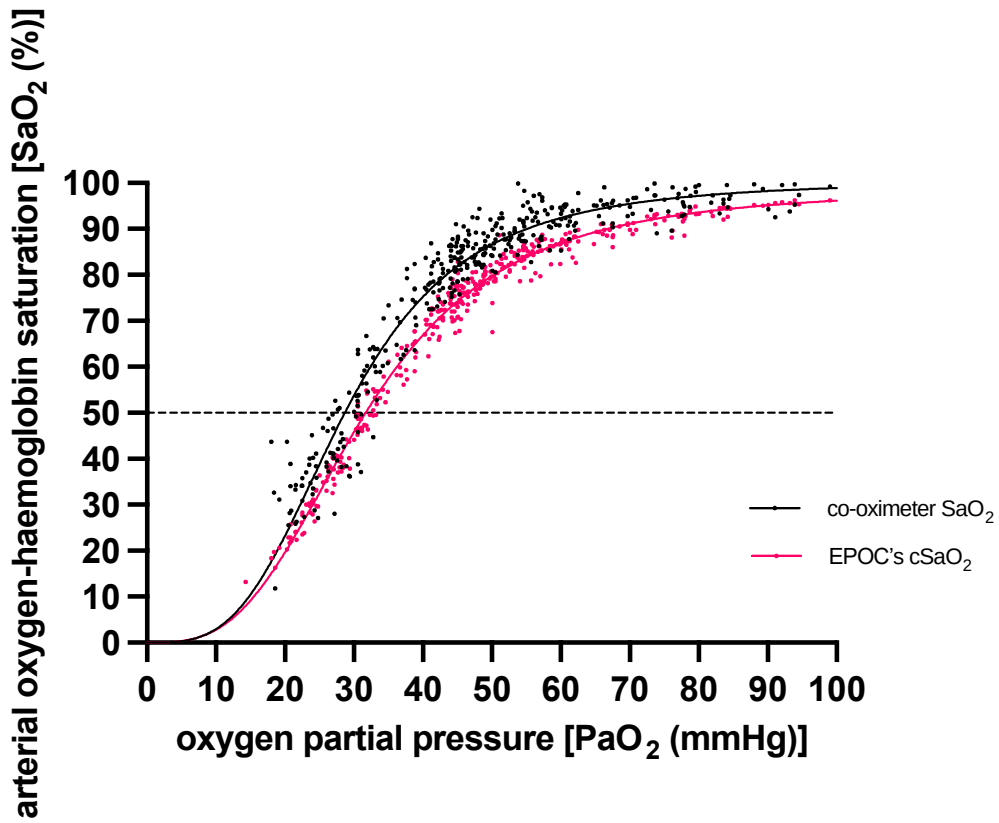

Figure 4.4 Relationship between arterial oxygen partial pressure (PaO_2) and the EPOC's calculated arterial oxygen-haemoglobin saturation ($cSaO_2$) and co-oximeter's arterial oxygen-haemoglobin saturation (SaO_2) at a pH of 7.30 ± 0.1 (mean ± standard deviation), dissolved arterial CO_2 partial pressure ($PaCO_2$) of 73.7 ± 10.5 mmHg, body temperature of 37.4 ± 1.8°C, bicarbonate ion concentration of 35.5 ± 2.8 $mmol.L^{-1}$ and chloride ion concentration of 93.0 ± 4.7 $mmol.L^{-1}$. The data were plotted and a specific binding with Hill slope model was applied. The dashed line at 50% SaO_2 helps visualize the arterial oxygen partial pressure at which haemoglobin is 50% saturated with oxygen (P_{50}) according to the two curves. Note that a decrease in pH and an increase in $PaCO_2$ leads to a right-shift in both the EPOC's $cSaO_2$ oxygen-haemoglobin dissociation curve (P_{50} ~ 32 mmHg) and the co-oximeter SaO_2 oxygen-haemoglobin dissociation curve (P_{50} ~ 29 mmHg).

4.5 Discussion

In immobilized white rhinoceros, the EPOC blood analyser, which uses the human oxygen-haemoglobin dissociation curve to calculate arterial oxygen-haemoglobin saturation, provided an unreliable (inaccurate, imprecise, poor ARMS) estimate of arterial oxygen-haemoglobin saturation across the entire 0-100% saturation range. The EPOC's $cSaO_2$ readings underestimated the co-oximeter's SaO_2 readings, by an average of 6%, and was associated with discernibly poor precision indicated by the SD of 5%, across the entire 0-100% saturation range.

The EPOC blood analyser and the benchtop AVOXimeter 4000 co-oximeter utilize two different methodologies to calculate or measure arterial oxygen-haemoglobin saturation. The EPOC measures the PaO_2, $PaCO_2$, pH, and together with body temperature and the input of the human oxygen-haemoglobin dissociation curve to calculate functional arterial oxygen-haemoglobin saturation (EPOC System manual; Severinghaus 1979). By comparison, the co-oximeter uses six different wavelengths of light to estimate 'fractional' arterial oxygen-haemoglobin saturation by measuring the light absorbance of oxyhaemoglobin present in the blood (ITC AVOXimeter 4000 user manual). Functional arterial oxygen-haemoglobin saturation refers to the percentage haemoglobin capable of carrying oxygen, whereas the fractional arterial oxygen-haemoglobin saturation is the proportion of total haemoglobin that is oxygenated, compared to other fractions such as MetHb and HbCO. In this study, low levels of MetHb (1.1 ± 0.5%) and HbCO (<1.0%) were reported, meaning that functional and fractional arterial oxygen-haemoglobin saturations are effectively equivalent.

Using the ISO guidelines for reliability (i.e., $\leq \pm 3\%$ for bias, $\leq 3\%$ for precision and $\leq 4\%$ for ARMS) (Batchelder & Raley 2007), we found that the EPOC blood analyser performed poorly in immobilized white rhinoceros, with the $cSaO_2$ underestimating the co-oximeter's SaO_2 across the entire 0-100% saturation range (bias -6%, precision 5%, ARMS 8%). These findings differ from those reported in immobilized impala where, the EPOC's $cSaO_2$ readings were reliable when compared to the co-oximeter's SaO_2 measured across the entire 0-100% saturation range (bias -1%, precision 3%, ARMS 3%) (Mtetwa et al. 2020). This finding suggests that the EPOC is likely only reliable in species, like

impala, with presumably similar oxygen-haemoglobin dissociation curves to that of humans, and less reliable in species with markedly different curves, like rhinoceros (Schmidt-Neilsen & Larimer 1958; Reiners et al. 2019). Furthermore, since I did not test for repeatability (i.e., taking repeated measurements per blood sample) for both the human co-oximeter and EPOC devices, the reference method (human co-oximeter) might have also introduced error in my findings, resulting in unreliable $cSaO_2$ measurements. Measurement error could have occurred from flushing the catheter before taking each arterial sample, despite discarding the initial blood from the catheter, therefore affecting the quality of the arterial blood samples, resulting in unreliable measurements.

The oxygen-haemoglobin affinity varies not only among different species of mammal under normal physiological conditions, especially as a function of body mass (Schmidt-Neilsen & Larimer 1958), but it also varies dynamically, responding to acute changes in pH, $PaCO_2$, temperature, 2.3-diphosphoglycerate (2.3-DPG) and chloride ions (Cl^-) (Baumann et al. 1984; Clerbaux et al. 1993). These acute changes invoke dynamic and reversible shifts in the oxygen-haemoglobin dissociation curve, and the magnitude of these shifts could also vary depending on sensitivity among species (Baumann et al. 1984; Clerbaux et al. 1993). For example, the position of the white rhinoceros' oxygen-haemoglobin dissociation curve is apparently unaffected by the presence of 2.3-DPG, but instead responds to changes in Cl^- concentration (Baumann et al. 1984). The negligible effect of 2.3-DPG on the oxygen-haemoglobin affinity is attributed to the unique structure of the rhinoceros' haemoglobin, which contains a glutamic acid (GLU) at position β_2, instead of histidine which is a position responsible for binding 2.3-DPG (Baumann et al. 1984). In the present study, the acidaemia (pH = 7.30) and hypercapnia ($PaCO_2$ = 73.7 mmHg) of the immobilized rhinoceros appears to have right-shifted both the EPOC's $cSaO_2$ and the co-oximeter's SaO_2 (Fig. 4.4) because the P_{50} of EPOC's $cSaO_2$ oxygen-haemoglobin dissociation curve (P_{50} ~ 32 mmHg) and that of the co-oximeter SaO_2 (P_{50} ~ 29 mmHg) are higher than the resting P_{50} of white rhinoceros. Nonetheless, the systematic bias of the EPOC remains because it uses the human oxygen-haemoglobin dissociation curve (and its specific sensitivity to pH and $PaCO_2$), which is too dissimilar to the rhinoceros' curve, and thus results in the observed bias even under the acidotic and hypercapnic conditions elicited during immobilization.

4.6 Conclusion

The immobilization of white rhinoceros is associated with substantial morbidity and mortality risks associated with severe hypoxaemia (Buss et al. 2018; Reiners et al. 2019). Therefore, there is an urgent clinical need to understand the reliability of tools used to monitor blood oxygen levels in this species. We speculate that the poor reliability of the EPOC is primarily explained by its use of the human oxygen-haemoglobin dissociation curve, which is significantly right shifted compared to that of the rhinoceros. The bias persists even under the acidotic and hypercapnic conditions elicited during immobilization. Therefore, a co-oximeter should rather be used to determine arterial oxygen-haemoglobin saturation in immobilized white rhinoceros.

CHAPTER 5:

Reliability of calculated arterial oxygen-haemoglobin saturation in immobilized southern white rhinoceros (*Ceratotherium simum simum*)

Thembeka K Mtetwa, Edward P Snelling & Leith CR Meyer

From the Department of Paraclinical Sciences (Mtetwa, Meyer), Centre of Veterinary Wildlife Research (Mtetwa, Snelling, Meyer), and Department of Anatomy and Physiology (Snelling), Faculty of Veterinary Science, University of Pretoria, Private Bag X04, Onderstepoort, 0110, South Africa.

5.1 Abstract

The reliability of calculated arterial oxygen-haemoglobin saturation ($cSaO_2$) for monitoring blood oxygenation has never been validated in chemically immobilized southern white rhinoceros (*Ceratotherium simum simum*), despite hypoxaemia being a major issue during immobilization. We aimed to determine the reliability of arterial oxygen-haemoglobin saturation calculated using two methods; method 1 calculates arterial oxygen-haemoglobin saturation from the oxygen content equation and method 2 calculates arterial oxygen-haemoglobin saturation from the Siggaard-Andersen algorithm. Methods 1 & 2 $cSaO_2$ were compared to arterial oxygen-haemoglobin saturation (SaO_2) measured by a benchtop AVOXimeter 4000 co-oximeter (reference method). As part of a broader study, a convenience sample of eight rhinoceroses were immobilized four times each, with different drug combinations (etorphine + saline, etorphine + azaperone, etorphine + midazolam, etorphine + medetomidine) and given butorphanol at 12 minutes. Arterial blood samples were drawn from an auricular artery catheter at 10, 15, 20, 30, and 40 minutes after recumbency to measure partial pressures of oxygen and carbon dioxide (PaO_2 and $PaCO_2$), and pH using an Enterprise Point-of-Care (EPOC) blood analyser, oxygen content (CaO_2) using a microrespirometer following the method of Tucker (1967) and SaO_2 using a benchtop AVOXimeter 4000 co-oximeter. Method 1 $cSaO_2$ was calculated from the oxygen content equation using Tucker CaO_2, haemoglobin concentration [Hb] and PaO_2. Method 2 $cSaO_2$ was calculated from the Siggaard-Andersen algorithm using measured PaO_2, $PaCO_2$ and pH. Bland-Altman and area root mean squares (ARMS) methods were used to assess the reliability of Methods 1 & 2 $cSaO_2$ when compared with simultaneous co-oximeter SaO_2 measurements. Oxygen-haemoglobin dissociation curves were plotted using “specific-binding with Hill slope” and least square regression and the regression equation was used to calculate P_{50} (PaO_2 when haemoglobin is 50% saturated with oxygen). Although the bias was low (bias 1%), method 1 $cSaO_2$ values were unreliable (precision 13%, ARMS 13%), across the entire 0-100% saturation range. Method 2 $cSaO_2$ values were only reliable (bias 3%, precision 2%, ARMS 4%), at the 90-100% saturation range, but unreliable (bias 10%, precision 7%, ARMS 12%) across the entire 0-100% saturation range. Compared to P_{50} of rhinoceros at rest (between 15 and 20 mmHg), P_{50} values derived from co-oximeter SaO_2 (27 mmHg) and method 1 $cSaO_2$ (28 mmHg) were higher than those derived from method 2 $cSaO_2$ (20 mmHg). Method 2 $cSaO_2$ can only be used to estimate SaO_2 reliably at saturation above 90%; but

below 90%, a co-oximeter should rather be used to reliably monitor blood oxygenation in immobilized southern white rhinoceros.

Keywords chemical immobilization, calculated oxygen-haemoglobin saturation, co-oximetry, wildlife

5.2 Introduction

Arterial oxygen-haemoglobin saturation is one of the most important variables used to monitor blood oxygenation because it accounts for approximately 96 to 98% of the total oxygen (oxygen content – CaO_2) carried in the arterial blood (Collins et al. 2015). The manometric method of Van Slyke & Neill (1924) (Holmgren & Pernow 1959; Dominguez de Villota et al. 1976; Brown 1980) and the spectrophotometric methods (i.e., co-oximetry) (Dominguez de Villota et al. 1976; Breuer et al. 1990; Katz et al. 2016) are regarded as the reference methods for the measurement of arterial oxygen-haemoglobin saturation (SaO_2) in human and veterinary medicine. The manometric method directly measures CaO_2 before and after the sample is equilibrated with air and uses the CaO_2 to calculate SaO_2, after correcting for PaO_2 (Van Slyke & Neill 1924; Sendroy et al. 1934; Lambertsen et al. 1952; Holmgren & Pernow 1959; Weiss & Sinha 1978).

Oxygen content can also be measured by the method of Tucker (1967), a method that shows good agreement with the manometric method (Tucker 1967; Bridges et al. 1979). The method of Tucker (1967) is based on the principle that oxygen bound to haemoglobin can be released into a physical solution (a potassium ferricyanide solution) and the change in partial pressure of oxygen (ΔPO_2), can be measured by a Clark-type oxygen electrode before and after the introduction of blood to determine the blood's total oxygen content (Tucker 1967). The method has been used in small and large mammals (Tucker 1968; Karas et al. 1987; Jones et al. 1989; Smale & Butler 1994) and fish (Wells et al. 1986; Weber & Wells 1989; Speers-Roesch et al. 2012; Harter et al. 2015a).The Tucker CaO_2 measurements were used in fish to calculate arterial oxygen-haemoglobin saturation, and the $cSaO_2$ values were then used as the reference to determine the reliability of arterial oxygen-haemoglobin saturation calculated by an i-STAT blood analyser (Harter et al. 2015a). Whether arterial oxygen-haemoglobin saturation calculated from the Tucker CaO_2 measurements is reliable remains to be determined. Furthermore, the Tucker CaO_2 measurements have never been used to calculate arterial oxygen-haemoglobin saturation in mammals, including wildlife.

Arterial oxygen-haemoglobin saturation can also be calculated from algorithms integrated in i-STAT and Enterprise Point-of-Care (EPOC) blood analysers (i-STAT Technical Bulletin 2013; Severinghaus 1979). These devices use measured PaO_2 to calculate arterial oxygen-haemoglobin saturation from the Severinghaus algorithm designed to construct the human oxygen-haemoglobin dissociation curve, while considering the dynamic shifts of the curve induced by physiological variables like $PaCO_2$, pH and body temperature (Severinghaus 1979). These algorithms are, however, based on the standard human oxygen-haemoglobin dissociation curve, which differs from the oxygen-haemoglobin dissociation curve of white rhinoceros, primarily due to the differences in the haemoglobin characteristics, which may be scaled with body mass (Schmidt-Neilsen & Larimer 1958; Bauman et al. 1984; Reiners et al. 2019). The position of the oxygen-haemoglobin dissociation curve is quantified by P_{50} (the partial pressure of oxygen when haemoglobin is 50% saturated with oxygen) and at rest (body temperature of 37ºC and pH of 7.40) the human P_{50} is 26.7 mmHg (Severinghaus 1979), and the white rhinoceros P_{50} is between 15 mmHg (Reiners et al. 2019) and 20 mmHg (Bauman et al. 1984). Therefore, using the algorithms from i-STAT and EPOC blood analysers to calculate arterial oxygen-haemoglobin saturation of white rhinoceros may result in inaccurate and unreliable $cSaO_2$ values.

Alternatively, the Siggaard-Andersen algorithm, integrated in Radiometer blood analysers (Radiometer Corporation., Copenhagen, Denmark) is used to calculate arterial oxygen-haemoglobin saturation as a function of PaO_2 after adjustable corrections for $PaCO_2$, pH and temperature where necessary (Siggaard-Andersen et al. 1984; Siggaard-Andersen et al. 1988; Anstey 2000). The algorithm's advantage is that it is suitable for both standard (human) and non-standard oxygen-haemoglobin dissociation curves because it can incorporate species-specific haemoglobin variables such as P_{50} and Bohr effect (Siggaard-Andersen et al. 1984; Siggaard-Andersen et al. 1988; Reiners et al. 2019). In humans, the Siggaard-Andersen algorithm is accurate at saturations between 0-97% (Anstey 2000). Previous research in white rhinoceros have used this algorithm to calculate arterial oxygen-haemoglobin saturation (Haymerle et al. 2016; Reiners et al. 2019). Haymerle and colleagues (2016) replaced some of the human blood variables in this algorithm with those of white rhinoceros including a P_{50} of 20 mmHg, Bohr effect of -0.62 (Baumann et al. 1984), physiological $PaCO_2$ of 49.0 mmHg and physiological body temperature of 36.8°C (Citino & Bush 2007) to calculate arterial oxygen-haemoglobin saturation in white rhinoceros. Later, Reiners et al. (2019) collected experimental data

from white rhinoceros' blood to further improve the algorithm to better suit the blood characteristics of white rhinoceros. Even though the Siggaard-Andersen algorithm has been used in white rhinoceros (Haymerle et al. 2016; Reiners et al. 2019), the reliability of its $cSaO_2$ values have never been validated in this species.

When etorphine is used to immobilize white rhinoceros, hypoxaemia, accompanied by hypercapnia and acidosis usually develops (Haw et al. 2014; Buss et al. 2018; Mueffels et al. 2022). For this reason, finding the most reliable method of calculating arterial oxygen-haemoglobin saturation, that accounts for these physiological changes in white rhinoceros is crucial. Therefore, using SaO_2 measured from a benchtop AVOXimeter 4000 co-oximeter, reference method, we aimed to determine the reliability of two methods that can be used to calculate arterial oxygen-haemoglobin saturation in immobilized white rhinoceros. Method 1 calculates arterial oxygen-haemoglobin saturation using measured Tucker CaO_2 and EPOC PaO_2 and the oxygen content equation. Method 2 (method 2 $cSaO_2$) calculates arterial oxygen-haemoglobin saturation using EPOC measured PaO_2, $PaCO_2$ and pH and the Siggaard-Andersen algorithm. We also derived oxygen-haemoglobin dissociation curves of immobilized white rhinoceros from the co-oximeter SaO_2 measurements and the $cSaO_2$ values from the two calculation methods. We hypothesize that the two methods used to calculate arterial oxygen-haemoglobin saturation, can be used to reliably to determine SaO_2 in immobilized southern white rhinoceros for monitoring purposes. Additionally, we hypothesize that oxygen-haemoglobin dissociation curves derived from the two calculation methods consider the dynamic shifts that are attributed to some of the physiological effects of chemical immobilization on the animal's physiology.

5.3 Materials & methods

Experimental animals

This study was approved by the University of Pretoria Animal Ethics Committee (REC246-19) and the South African National Parks Animal Use and Care Committee (no. 012/20). Eight wild-caught male southern white rhinoceros (*Ceratotherium simum simum*) (4 – 5 years old) were brought to a rhinoceros holding facility (bomas) at the Veterinary Wildlife Services, Kruger National Park, South Africa [23° 49' 60 S, 31° 30' 0 E; altitude ~320 m altitude; barometric pressure 745.3 ± 1.2 (mean ± standard deviation) mmHg], where they were habituated to boma-captivity for 4 – 6 weeks. The animals were fed lucerne (*Medicago sativa*) and teff hay (*Eragrostis tef*) and water was provided *ad libitum*.

Immobilization

Data for this study were collected during an unrelated prospective, randomized, controlled crossover study on the effects of different drug combinations in white rhinoceros (REC011-21). A convenience sample of eight rhinoceros were subjected to four immobilizing protocols each; etorphine (M99; Voluplex., Mnandi, Centurion, South Africa) and injectable saline, etorphine and azaperone (Stresnil; Elanco., ON, Canada), etorphine and midazolam (Dazonil; Wildlife Pharmaceuticals Pty Ltd., White River, South Africa), and etorphine and medetomidine (Metonil; Wildlife Pharmaceuticals Pty Ltd), with a two-week washout period between immobilizations. Doses (in mg) calculated based on body mass are shown in Table 5.1. The protocols were administered intramuscularly using a 3 mL dart with 60 mm uncollared needle propelled by a compressed air rifle (DAN-INJECT International SA., Skukuza, South Africa). For each immobilization, animals were given butorphanol (intravenously; Butonil; Wildlife Pharmaceuticals Pty Ltd) at 10 x the etorphine dose, 12 minutes after recumbency (Table 5.1).

Table 5.1 Standard doses of drugs based on body mass used for white rhinoceros. Animals were weighed intermittently during the four-to-six-week habituation period and at the end of each immobilization, by encouraging them to enter a crate that was weighed using a crane balance. Rhinoceros weighed 1311 ± 115 kg [mean ± standard deviation(SD)].

Rhinoceros body mass range (kg)	**Etorphine (mg)**	**Azaperone (mg)**	**Midazolam (mg)**	**Medetomidine (mg)**	**Butorphanol (mg)**	**Naltrexone (mg)**
750 – 1000	2.0	10.0	10.0	5.0	40.0	40.0
1000 – 1250	2.5	12.5	12.0	6.25	50.0	50.0
1250 – 1500	3.0	15.0	15.0	7.5	60.0	60.0

[a]Etorphine (~0.002 $mg.kg^{-1}$)

[b]Azaperone (~0.01 $mg.kg^{-1}$)

[c]Midazolam (~0.01 $mg.kg^{-1}$)

[d]Medetomidine (~0.005 $mg.kg^{-1}$)

[e]Butorphanol (10×etorphine dose)

[f]Naltrexone (20×etorphine dose)

Experimental procedures

Once the rhinoceros was in lateral recumbency, a digital thermometer with a modified protective sheath (HI 98509 Checktemp 1; Hanna Instruments., Woonsocket RI, USA) was placed inside the rectum to measure core body temperature.

Arterial blood sample collection

The inner surface of an ear was aseptically prepared and a 25 cm, 22 Gauge over-the-needle intravenous (IV) catheter (Introcan; B Braun Medical Inc., Melsungen, Germany) was inserted into the medial auricular artery for blood sample collection. Before each sample was taken, the catheter lines were flushed (rinsed out) with heparinised saline (0.9% sodium chloride) and drained long enough to sufficiently wash out any saline or blood clots. Approximately 3 mL of arterial blood was collected anaerobically at 10, 15, 20, 30, and 40 minutes after recumbency into 3 mL heparinised syringes (BD Present A-Line, BD Medical, New Jersey, USA) and immediately sealed, placed on ice, and analysed within 15 minutes of collection.

Benchtop co-oximetry analysis

Arterial oxygen-haemoglobin saturation (SaO_2) was measured from the arterial blood samples using a calibrated benchtop co-oximeter (AVOXimeter 4000; Surgical Innovations Pty Ltd., South Africa) and test cuvettes (Surgical Innovations Pty Ltd). Calibration was performed daily using yellow and orange optical filters (cuvettes). These optical filters also performed optical quality control to verify whether the optics used for measurements were not hidden by blood or debris (AVOXimeter 4000 user manual). The blood was mixed by gently rolling the syringe back and forth for approximately 20 seconds before it was inserted into the test cuvettes for co-oximetry analysis. The benchtop AVOXimeter 4000 uses multiple wavelengths of light (488.4, 520.1, 562.4, 585.2, 597.5, 621.7 and 671.7 nm) to measure fractional arterial oxygen-haemoglobin saturation (SaO_2), carboxyhaemoglobin (HbCO) and methaemoglobin (MetHb) (AVOXimeter 4000 user manual). Fractional arterial oxygen-haemoglobin saturation (SaO_2) measurements were used as reference measurements of SaO_2 to compare with

calculated arterial oxygen-haemoglobin saturation values calculated from the oxygen content equation (method 1 $cSaO_2$) and those calculated from the Siggaard-Andersen algorithm (method 2 $cSaO_2$).

Blood gas analysis

Arterial oxygen partial pressures (PaO_2), arterial carbon dioxide partial pressures ($PaCO_2$), and pH were measured from the blood samples using an Enterprise Point-of-Care (EPOC) blood analyser (EPOC Software version 3.35.4 with sensor configuration version 39.2; Epocal Inc., Ottawa, Canada) and test cards (BGEM3, Epocal Inc) within 15 minutes of arterial blood sample collection. The test cards are single use cards that were automatically self-calibrated before each analysis. The test cards comprise of a Clark-type oxygen sensing electrode (for the measurement of PaO_2), a pH sensing electrode (for the measurement of pH), and a pH sensing electrode, covered with specific silicone and glass membranes (for the measurement of $PaCO_2$). The test cards also comprise of reference electrodes, counter electrodes, and fluids of known PaO_2, pH and $PaCO_2$ used for self-calibration (EPOC system manual). Blood was carefully injected into the test cards that were placed inside the EPOC blood analyser while making sure there were no visible air bubbles introduced.

Measurement of total oxygen content (CaO_2)

A two-chamber, dual-channel, dissolved oxygen measuring system or microrespirometer (Strathkelvin Instruments Ltd., North Lanarkshire, Scotland) was used to measure total oxygen content (CaO_2) of arterial blood using the method of Tucker (1967). Two “Tucker” chambers (chamber volume: 0.4996 mL and 0.4676 mL), housing two Clark-type oxygen electrodes (no. 1083 and 1085), were water-jacketed and connected to a circulating water bath that was maintained at 32°C. The outputs of the oxygen electrodes were connected to a 782 meter that amplifies the signal currents from the oxygen electrodes and converts the current to digital values. The 782 meter was also connected to a laptop running a dedicated software (928-software program, Serial no. 2650, 782 HID, Version 4.1) that recorded the change in PaO_2 (ΔPaO_2). The oxygen electrodes were calibrated daily, before analysis, using a 0% oxygen solution (2 g of sodium sulphite dissolved in 100 mL of distilled water) and a 100%

oxygen solution or aerated distilled water prepared by mixing air and water in a syringe for approximately 20 minutes and then allowed to stand for 5 minutes.

To measure CaO_2, the chambers were filled with degassed potassium ferricyanide [$K_3Fe(CN)_6$] solution [0.6 g of $K_3Fe(CN)_6$ dissolved in 100mL distilled water] and magnetic stirrers were used to mix the solution and allow it to equilibrate with the chamber temperature. Once a stable degassed oxygen trace was achieved, 8 µL (4 µL × 2) of blood was drawn from the 3 mL heparinised syringe using a 10 µL micro-syringe (SGE syringes; Trajan Scientific and Medical., Ringwood, Australia). The blood was drawn slowly from the middle of the heparinised syringe and into the micro-syringe to prevent any visible air bubbles from entering the micro-syringe. Four µL × 2 was then carefully inserted into the two chambers and mixed thoroughly into the degassed $K_3Fe(CN)_6$ solution until in equilibrium. Oxygen that is bound to haemoglobin is released into the physical solution by the degassed $K_3Fe(CN)_6$ solution that is responsible for the conversion of oxyhaemoglobin to methaemoglobin (Cook 1928). The total dissolved oxygen exerting a partial pressure increases, and the change in PO_2 (ΔPO_2) before and after injecting the blood sample in the chamber filled with $K_3Fe(CN)_6$ was measured. This ΔPO_2 was used to calculate the oxygen content (CaO_2 in $mL.dL^{-1}$) at standard temperature dry air (STPD) using the equation

$$\mathrm{CaO_2} = \frac{\Delta \mathrm{PO_2}}{760} \times \propto \times \mathrm{V_C} \times \frac{100}{\mathrm{V_b}}$$

Where $\propto$ is the oxygen solubility coefficient (0.0252 $mL.mL^{-1}$) of $K_3Fe(CN)_6$ at 32 °C, V_c is the volume of the chamber (in mL), V_b is the volume of the blood sample (in mL).

A duplicate analysis of each arterial sample was performed simultaneously, in the two chambers, to minimise systematic error and analytical variation. The two CaO_2 measurements were then averaged to calculate a mean CaO_2.

Haemoglobin concentration [Hb]

Packed cell volume (PCV) of each arterial sample was determined manually using the micro-haematocrit method by spinning the sampled blood in a centrifuge (Model HKT-400, Gemmy Industrial Corporation, Taipei, Taiwan; 15,000 *g*, 5 min). PCV is the height of the red blood cell column in the micro-haematocrit tube and is measured as a percentage or fraction of red blood cells in the blood. A duplicate PCV analysis of each arterial sample was performed simultaneously, to minimise systematic error and analytical variation. Then the two PCV measurements were averaged to calculate a mean PCV. The mean PCV was used to calculate haemoglobin concentration [Hb] ($g.dL^{-1}$) using a linear regression equation $[\mathrm{Hb}] = 0.2528 \times \mathrm{PCV} + 4.013$ previously derived from 214 white rhinoceroses blood samples (Boesch 2019).

Calculation of arterial oxygen-haemoglobin saturation

Method 1 $cSaO_2$ using the oxygen content and its equation

Arterial oxygen-haemoglobin saturation (method 1 $cSaO_2$) was calculated using the oxygen content equation as follows:

$$\text{Method 1 } \mathrm{cSaO_2} = \frac{\mathrm{CaO_2} - (0.003 * \mathrm{PaO_2})}{1.383 * [\mathrm{Hb}]} * 100$$

Where CaO_2 ($mL.dL^{-1}$) is the mean CaO_2 measured by the method of Tucker (1967), PaO_2 (mmHg) measured by the EPOC blood analyser, and 1.383 $mL.g^{-1}$ is the Hüfner constant derived for horses. To date, no Hüfner constant has been reported for rhinoceros, therefore, in this study we used the value used for horses, close relatives of rhinoceros (horses and rhinoceroses are in the same mammalian order Perissodactyla) (Baumann et al. 1984).

Method 2 $cSaO_2$ using blood gas variables applied to the Siggaard-Andersen algorithm

Arterial oxygen-haemoglobin saturation (method 2 $cSaO_2$) was calculated using the modified Siggaard-Andersen algorithm for white rhinoceros (Reiners et al. 2019). Human blood variables were replaced with the blood characteristics and physiological variables of the white rhinoceros: P_{50} of 15 mmHg (2.00 kPa), Bohr effect of -0.74 (Reiners et al. 2019), and pH, PaO_2 and $PaCO_2$ measured from the EPOC blood analyser.

Arterial oxygen-haemoglobin saturation ($cSaO_2$) was calculated according to the white rhinoceros' oxygen-haemoglobin dissociation curve function represented by the following equations (Siggaard-Andersen et al. 1984; Siggaard- Andersen et al. 1988; Reiners et al. 2019):

$$\text{Method 2 } \mathrm{cSaO_2} = \frac{\mathrm{e^y}}{(1 + \mathrm{e^y})}$$

where y is calculated using the equation $\mathrm{y} = \mathrm{y_s} + \mathrm{x} - \mathrm{x_0} + \mathrm{h} \times \tanh\left[\mathrm{k} \times (\mathrm{x} - \mathrm{x_0})\right]$, given $\mathrm{y_s} = 2.177$ (Reiners et al. 2019), $\mathrm{h} = 1.835$ (Reiners et al. 2019) and $\mathrm{k} = 1.169$ (Reiners et al. 2019). x_0 was calculated using the equation $\mathrm{x_0} = \mathrm{x_s} + \mathrm{a}$, where, $\mathrm{x_s} = \mathrm{y_s} - \mathrm{y} + \mathrm{x} + \mathrm{h} \times \tanh\left[\mathrm{k} \times (\mathrm{x} - \mathrm{x_0})\right]$ (Siggaard-Andersen et al. 1984; Siggaard- Andersen et al. 1988) [i.e., $\mathrm{x_s} = 1.431$ (Reiners et al. 2019)] and $\mathrm{a} = \mathrm{c}\beta(\mathrm{pH\text{-}7.4}) + 1.38 \ln\left(1 + \frac{\mathrm{PaCO_2}}{5.33}\right)(\mathrm{pH\text{-}7.2})$ because of the influence of pH and $PaCO_2$ on the point of symmetry of the oxygen-haemoglobin dissociation curve and where $c\beta = -1.7$ from the equation $\mathrm{c}\beta = (-1) \times \ln(10) \times \beta$ [$\beta = -0.74$; Bohr effect (Reiners et al. 2019)].

Substance fraction of methaemoglobin (MetHb or Hi), carboxyhaemoglobin (HbCO), foetal haemoglobin, body temperature, and 2.3-diphosphogycerate (2.3-DPG) were removed from the model because they have little influence on the oxygen affinity for the white rhinoceros' haemoglobin (Baumann et al. 1984; Haymerle et al. 2016; Reiners et al.2019).

Statistical analyses

The Bland-Altman analysis for multiple observations (Bland & Altman 2007) was used to determine the agreement between the calculated arterial oxygen-haemoglobin saturation (methods 1 & 2 $cSaO_2$ values) and the benchtop AVOXimeter 4000 co-oximeter SaO_2 measurements (i.e., method 1 $cSaO_2$ versus co-oximeter SaO_2 and method 2 $cSaO_2$ versus co-oximeter SaO_2). The Bland-Altman analysis determined the accuracy (bias), precision [standard deviation (SD)], and the 95% limits of agreement

(LOA) between the paired $cSaO_2$-SaO_2 measurements (Bland & Altman 2007). Bias is the mean difference between the paired measurements, precision is a measure of the variability (SD) between the paired measurements and the 95% LOA (bias ± 1.96 × SD) is an estimate of the interval within which 95% of the differences between measurements lie. An area root mean squares (ARMS), which is a combined estimate of accuracy (bias) and precision (SD), was also calculated to determine the overall agreement between $cSaO_2$ and SaO_2 measurements (Batchelder & Raley 2007). Guidelines for clinical acceptability are not available for $cSaO_2$ values, and therefore, for this study we followed the ISO performance requirements for pulse oximetry, which states that the device is clinically reliable (acceptable) only when the comparisons with co-oximetry are ≤± 3% for accuracy (bias), ≤ 3% for precision (SD) and ≤ 4% for ARMS (Batchelder & Raley 2007).

SaO_2 measured by the reference method, a benchtop co-oximeter, methods 1 and 2 $cSaO_2$ calculated from the oxygen content equation (method 1) and the $cSaO_2$ calculated from the Siggaard-Anderson algorithm (method 2) modified for white rhinoceros (Siggaard-Andersen et al. 1984; Siggaard-Andersen et al. 1988; Reiners et al. 2019) were plotted against PaO_2 measured by the EPOC blood analyser to construct oxygen-haemoglobin dissociation curves. A “specific binding with Hill slope” model was applied to determine the least squares regression fit equations from the oxygen-haemoglobin dissociation curves. Partial pressure of oxygen when haemoglobin is 50% saturated with oxygen (P_{50}) were calculated from each oxygen-haemoglobin dissociation curve using the least squares regression fit equation.

Statistical analyses were performed using GraphPad Prism version 9.3.1 for Windows (GraphPad Software, La Jolla, California 92073, USA). The data were reported as mean ± standard deviation. P value of < 0.05 was considered statistically significant.

5.4 Results

Mean [standard deviation (SD)] of blood values are summarized in Table 5.2. The PaO_2 ranged between 14.3 to 91.1 mmHg, $PaCO_2$ between 57.4 to 115.0 mmHg and pH from 7.15 to 7.39. Packed cell volumes (PCV) ranged from 19.5 to 51.5%, haemoglobin concentration [Hb] ranged from 8.9 to 17.0 $g.dL^{-1}$, and CaO_2 ranged from 5.1 to 24.4 $mL.dL^{-1}$. The mean (SD) body temperature is 37.5 (1.3)°C.

Table 5.2 Mean ± [standard deviation (SD)] for arterial oxygen-haemoglobin saturations calculated from the oxygen content equation (method 1 $cSaO_2$) and calculated from the Siggaard-Andersen algorithm (method 2 $cSaO_2$), arterial oxygen-haemoglobin saturations (co-oximeter SaO_2) measured by the benchtop AVOXimeter 4000 co-oximeter, total oxygen content (CaO_2) measured by the method of Tucker (1967), arterial partial pressures of oxygen and carbon dioxide (PaO_2 and $PaCO_2$), pH, packed cell volume (PCV), and haemoglobin concentration [Hb] in immobilized southern white rhinoceros (*n* = 8).

Blood variables	**Mean ± standard deviation**
Method 1 $cSaO_2$ (%)	77.2 ± 23.1
Method 2 $cSaO_2$ (%)	86.7 ± 12.9
Co-oximeter SaO_2 (%)	76.2 ± 18.8
CaO_2 ($mL.dL^{-1}$)	15.0 ± 4.2
PaO_2 (mmHg)	44.7 ± 13.5
$PaCO_2$ (mmHg)	71.1 ± 9.3
pH	7.30 ± 0.05
Packed cell volume (%)	41.1 ± 5.5
Haemoglobin concentration ($g.dL^{-1}$)	14.4 ± 1.4

In total, 194 paired $cSaO_2$-SaO_2 measurements were used for comparisons. Method 1 $cSaO_2$ values ranged from 21.7 to 152.2%, method 2 $cSaO_2$ ranged from 37.5% to 98.6% and the co-oximeter SaO_2 measurements ranged from 11.8% to 99.0%.

Reliability of Method 1 $cSaO_2$ using the Tucker oxygen content and its equation

Method 1 $cSaO_2$ values were accurate but imprecise, and unreliable when assessed across the entire 0-100% saturation range and within the other narrower ranges analysed (Table 5.3). Although the bias was low (average bias was roughly 1%) across the entire 0-100% saturation range and within the other ranges, the precision was poor, with the 90-100% saturation range reporting the worst precision (SD of 18%), respectively (Table 5.3).

Reliability of Method 2 $cSaO_2$ using measured blood gas variables in the Siggaard-Andersen algorithm

Method 2 $cSaO_2$ values were reliable (accurate and precise) at the 90-100% saturation range but were unreliable (inaccurate and imprecise) when assessed across the entire 0-100% saturation range and within the 70-100% saturation range, and below 70% (Table 5.3). Although precise, method 1 $cSaO_2$ values were unreliable (high bias) at the 70-79% and 80-89% saturation ranges. The highest bias of 20% occurred at saturations below 70% (Table 5.3).

Table 5.3 Performance of arterial oxygen-haemoglobin saturation calculated from the oxygen content equation (method 1 $cSaO_2$), and those calculated from the Siggaard-Andersen algorithm (method 2 $cSaO_2$), in eight immobilized southern white rhinoceros (*Ceratotherium simum simum).* Methods 1 and 2 $cSaO_2$ were compared against the arterial oxygen-haemoglobin saturation measured by a benchtop AVOXimeter 4000 co-oximeter (co-oximeter SaO_2) reference method. ARMS, area root mean squares; LOA, limits of agreement (minimum to maximum); *n* represents the sample size between paired measurements.

	Ranges	***n***	**Bias (%)**	**Precision (%)**	**ARMS (%)**	**LOA (maximum and minimum)**
Co-oximeter SaO_2 vs method 1 $cSaO_2$	0-100	194	1*	13	13	-24 to 26
	70-100†	148	1*	14	14	-26 to 28
	<70	46	1*	9	9	-17 to 19
	70-79	25	0*	14	13	-27 to 26
	80-89	83	1*	11	11	-21 to 24
	90-100	40	1*	18	18	-34 to 36
Co-oximeter SaO_2 vs method 2 $cSaO_2$	0-100	194	10	7	12	-4 to 24
	70-100†	148	7	4	8	-14 to 0
	<70	46	20	7	21	-35 to 6
	70-79	25	12	2*	12	8 to 16
	80-89	83	8	2*	8	4 to 12
	90-100	40	3*	2*	4*	-1 to 7

†The manufacturers' claimed performance range (70-100%). *Results that are acceptable according to the Food and Drug Administration (FDA) and International Organisation for Standardization (ISO) ($\leq\pm$3% for bias, $\leq$3% for precision and $\leq$4% for ARMS).

Oxygen-haemoglobin dissociation curves derived from co-oximeter SaO_2 measurements and method 1 and method 2 $cSaO_2$ values.

The P_{50} for the oxygen-haemoglobin dissociation curves derived from the co-oximeter SaO_2 is 27 mmHg, from method 1 $cSaO_2$ is 28 mmHg and from method 2 $cSaO_2$ is 20 mmHg (Fig. 5.1). The oxygen-haemoglobin dissociation curve derived from method 1 $cSaO_2$ shows a similar shift to the right (P_{50} of 28 mmHg) when compared to the curve derived from co-oximeter SaO_2 measurements (P_{50} of 27 mmHg) (Fig. 5.1). The similar shift is evident across all saturation ranges, corresponding to the small mean difference (bias 1%) at the entire 0-100% saturation range (Fig. 5.1; Table 5.3). However, at the upper flatter part of the curve (plateau region), the curve derived from method 1 $cSaO_2$ is higher than the curve derived from co-oximeter SaO_2 measurements. The plateau region of the curve derived from method 1 $cSaO_2$ corresponds to the worst precision of 18% at the 90-100% saturation range (Fig. 5.1; Table 5.3).

The oxygen-haemoglobin dissociation curve derived from Method 2 $cSaO_2$ shows a minimal shift to the right (P_{50} of 20 mmHg) compared to rhinoceros at rest (P_{50} of 15-20 mmHg) and the curve derived from co-oximeter SaO_2 measurements (P_{50} of 27 mmHg) (Fig. 5.1). The smaller shift is more evident at saturations below 90%, corresponding to the large difference (bias) found at the 80-89% and 70-79% saturation ranges and below 70% (Fig. 5.1; Table 5.3). However, at the upper flatter part of the curve (plateau region), the curve derived from method 2 $cSaO_2$ is similar to the curve derived from co-oximeter SaO_2 measurements. The plateau region of the curve derived from method 1 $cSaO_2$ corresponds to the low bias of 3% and the good precision of 2% at the 90-100% saturation ranges (Fig. 5.1; Table 5.3).

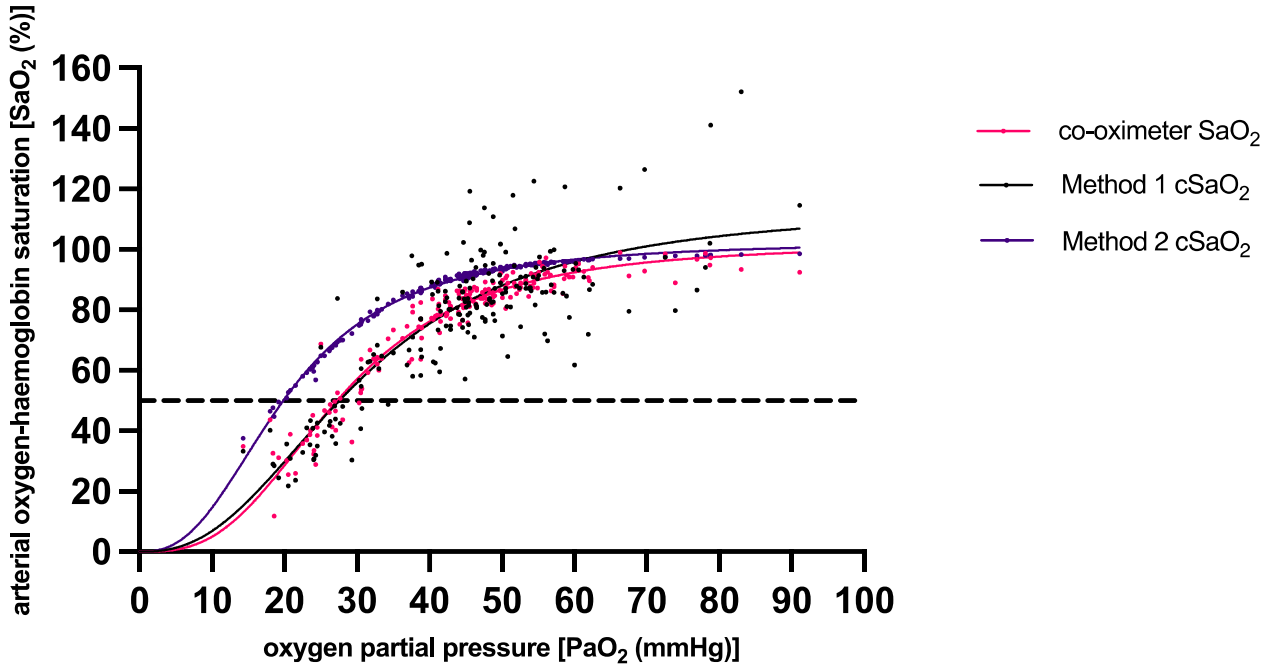

Figure 5.1 Relationship between arterial oxygen partial pressures (PaO_2) and the arterial oxygen-haemoglobin saturation measured by a benchtop AVOXimeter 4000 co-oximeter (co-oximeter SaO_2) reference method, the arterial oxygen-haemoglobin saturation calculated from the oxygen content equation (method 1 $cSaO_2$) and those calculated from the Siggaard-Andersen algorithm (method 2 $cSaO_2$) in eight immobilized southern white rhinoceros. The data were plotted using the "specific binding with Hill slope" model in GraphPad Prism version 9.4.1. The dashed line at 50% arterial oxygen-haemoglobin saturation helps visualize the P_{50} (arterial oxygen partial pressure when haemoglobin is 50% saturated with oxygen) of the curves.

5.5 Discussion

This study demonstrates that the arterial oxygen-haemoglobin saturation calculated from oxygen content measured by the method of Tucker (1967) and using the oxygen content equation (method 1 $cSaO_2$), was an unreliable estimate of SaO_2. Method 1 $cSaO_2$ values were unreliable because of the discernibly poor precision indicated by a SD of 13%, over the entire 0-100% saturation range. The P_{50} of rhinoceros at rest is between 15mmHg to 20 mmHg; the oxygen-haemoglobin dissociation curve derived from method 1 $cSaO_2$ values (P_{50} = 28 mmHg) demonstrated a similar larger shift to the right as the curve derived from co-oximeter SaO_2 (P_{50} = 27 mmHg). However, the plateau region of the curve (i.e., at the 90-100% saturation range) derived from method 1 $cSaO_2$ was higher than that of the curve derived from co-oximeter SaO_2. Arterial oxygen-haemoglobin saturation calculated from the Siggaard-Andersen algorithm (method 2 SaO_2), provided a reliable (accurate and precise) estimate of SaO_2 at the 90-100% saturation range. However, at the other saturation ranges, method 2 SaO_2 provided an unreliable (poor accuracy, precision, and ARMS) estimate of SaO_2. Method 2 $cSaO_2$ readings overestimated the co-oximeter SaO_2 readings by an average difference of 10% (bias 10%) and were also associated with discernibly poor precision indicated by a SD of 7%, over the entire 0-100% saturation range. The oxygen-haemoglobin dissociation curve derived from method 2 $cSaO_2$ values (P_{50} = 20 mmHg) demonstrated a smaller shift compared to the curve constructed using co-oximeter SaO_2 (P_{50} = 27 mmHg). However, the plateau region of the curve (i.e., at the 90-100% saturation range) derived from method 2 $cSaO_2$ was similar to that of the curve derived from the co-oximeter SaO_2. The shift of the oxygen-haemoglobin dissociation curves in the immobilized white rhinoceros, when compared the rhinoceros' curve at rest (P_{50} between 15 mmHg and 20 mmHg), were to the right because of hypercapnia ($PaCO_2$ = 71.1 mmHg) and acidosis (pH = 7.30) induced by the effects of etorphine during the chemical immobilization.

Conventionally, the CaO_2 measured by the manometric method is used to calculate arterial oxygen-haemoglobin saturation after correcting for PaO_2 (Sendroy et al. 1934; Lambertsen et al. 1952; Holmgren & Pernow 1959; Weiss & Sinha 1978). Alternatively, CaO_2 measured by the method of Tucker (1967) can be used and compares favourably with the manometric method (Tucker 1967; Bridges et al. 1979; Boutilier et al. 1984; Harter et al. 2015). In our study, arterial oxygen-haemoglobin saturation

calculated by the oxygen content equation, using CaO_2 measured by the method of Tucker (1967) was unreliable due to poor precision. There could have been several reasons that may have resulted in the lack of precision in these $cSaO_2$ values. Firstly, the method of Tucker (1967) requires extensive training and careful attention to detail. So, if it is not used correctly, it may introduce error and imprecision into our results. In this study, we did not use the gold standard method [cyanmethaemoglobin (HiCN) method] for the measurement of haemoglobin concentration. Instead, we used a regression equation ($[\mathrm{Hb}] = 0.2528 \times \mathrm{PCV} + 4.013$), devised by Boesch (2019) for the calculation of haemoglobin concentrations from PCVs of white rhinoceros. The PCV's inputted into the equation by Boesch (2019) may have introduced some error into the arterial oxygen-haemoglobin saturation calculation resulting in imprecise $cSaO_2$ values. The imprecision in these $cSaO_2$ values could have also resulted from measurement error, such as the variation in the micro-syringe blood volumes drawn, as it can be difficult to draw exact 4 μL of blood using micro-syringes. Additionally, flushing the catheter using heparinised saline may have also affected the quality of the blood samples, despite discarding the initial blood from the catheter, leading to imprecise $cSaO_2$ values. The co-oximeter used in this study is a human-specific benchtop co-oximeter that is not yet verified for rhinoceros. Therefore, using this co-oximeter as a reference method for comparison might have introduced error, resulting in imprecise and unreliable $cSaO_2$ values.

The relationship between PaO_2 and SaO_2 is well explained by the oxygen-haemoglobin dissociation curve and theoretically SaO_2 can be calculated if the position of the curve is known (Lutz et al. 1975; Severinghaus 1979; Smale et al. 1994; Anstey 2003; Serianni et al. 2003). For many years, the oxygen-haemoglobin dissociation curve has been used to construct algorithms that can estimate or calculate arterial oxygen-haemoglobin saturations as a function of PaO_2 (Lutz et al. 1975; Severinghaus 1979; Gabel 1980; Siggaard-Andersen et al. 1984; Siggaard-Andersen et al. 1988; Smale et al. 1994; Serianni et al. 2003; Dash et al. 2016). The Siggaard-Andersen algorithm for standard (human) and non-standard oxygen-haemoglobin dissociation curves provides reliable $cSaO_2$ values in humans (Breuer et al. 1989; Anstey 2000) and bovids (Detry et al. 2003). Haymerle and colleagues (2016) used this algorithm to calculate arterial oxygen-haemoglobin saturations of white rhinoceros using the white rhinoceros P_{50} and the Bohr effect reported by Baumann (1984). Later Reiners et al. (2019) performed further experiments on rhinoceros' blood to improve this algorithm. To our knowledge, our study is the first to determine the reliability of the arterial oxygen-haemoglobin saturation calculated from the

modified Siggaard-Andersen algorithm for white rhinoceros (Reiners et al. 2019), when compared to the SaO_2 measured by the reference co-oximeter method, in immobilized southern white rhinoceros. Using the white rhinoceros' distinct haemoglobin characteristic and influencing physiological variables, we found that the $cSaO_2$ values using this method, were reliable (accurate and precise) only at saturations above 90%. These results are similar to those reported in studies using other algorithms that incorporate oxygen-haemoglobin dissociation curves to calculate arterial oxygen-haemoglobin saturation (Scott et al. 2005; Duke-Novakovski 2019). These findings are not surprising given that saturation levels above 90% corresponds to the plateau region of the curve, which is similar in most species regardless of the position of the curve (Scott et al. 2005; Collins et al. 2015; Duke-Novakovski 2019).

The position of the oxygen-haemoglobin dissociation curve is shifted dynamically by changes in pH, $PaCO_2$, temperature, 2.3-diphosphoglycerate (2.3-DPG), chloride ions (Cl^-), and the presence of haemoglobin derivatives (HbCO and MetHb) (Clerbaux et al. 1993; Chu et al. 2020). An increase in H^+ ions (low pH), $PaCO_2$, temperature, 2.3-DPG, Cl^-, and haemoglobin derivatives causes the oxygen-haemoglobin dissociation curve to dynamically shift to the right, whereas a decrease causes the curve to dynamically shift to the left. The immobilized white rhinoceros' oxygen-haemoglobin dissociation curve derived from the co-oximeter SaO_2 measurements was shifted to the right (P_{50} of 27 mmHg) when compared the rhinoceros' curve at rest (P_{50} between 15 mmHg and 20 mmHg). This right shift may have facilitated oxygen offloading to the tissues, but limited the ability for the rhinoceros' haemoglobin to bind and carry oxygen to the tissues. Therefore, the rhinoceros' naturally left-shifted curve has physiological advantages for rhinoceros when they are conscious because it may facilitate oxygen loading at low PaO_2 values, however, this advantage is cancelled out during chemical immobilization.

The Siggaard-Andersen algorithm considers the dynamic shift of the oxygen-haemoglobin dissociation curve caused by the changes in some of these variables [i.e., pH, $PaCO_2$, temperature, 2.3-DPG), chloride ions (Cl^-), and the presence of haemoglobin derivatives (HbCO and MetHb)] (Siggaard-Andersen et al. 1984; Siggaard-Andersen et al. 1988). But surprisingly, Baumann et al. (1984) found that the position of the white rhinoceros' oxygen-haemoglobin dissociation curve was not significantly

altered by the presence of 2.3-DPG (Baumann et al. 1984). According to Baumann et al. (1984), this is primarily because rhinoceros haemoglobin lacks histidine, at position $\beta 2$, that is present in the human haemoglobin at the same position, which is responsible for the binding of 2.3-DPG (Mazur et al. 1982; Baumann et al. 1984). In addition, at pH < 7.20, the white rhinoceros' oxygen-haemoglobin dissociation curve did not respond to an increase in $PaCO_2$, primarily because their haemoglobin globin chains contain free N-termini that in humans are responsible for binding CO_2 (Baumann et al. 1984). Reiners et al. (2019) also reported that the effect of HbCO, MetHb and body temperature on the white rhinoceros' oxygen-haemoglobin dissociation curve is small, and therefore, these authors removed these variables (i.e., HbCO, MetHb and body temperature) from their model used to formulate the modified algorithm. The removal of these variables from the Siggaard-Andersen algorithm may have contributed to the unreliability of the $cSaO_2$ values at saturations ranges below 90%, which corresponds to the steep region of the oxygen-haemoglobin dissociation curve.

At rest (body temperature of 37°C and pH of 7.40) a healthy white rhinoceros has a P_{50} between 15 and 20 mmHg (Baumann et al. 1984; Reiners et al. 2019). White rhinoceros in this study were hypercapnic ($PaCO_2$ = 71.1 mmHg), acidaemic (pH = 7.30) and hypoxaemic (PaO_2 = 44.7 mmHg) and had a right shifted oxygen-haemoglobin dissociation curve (co-oximeter SaO_2 P_{50} = 27 mmHg). The oxygen-haemoglobin dissociation curve derived from method 2 $cSaO_2$ values had a smaller shift (20 mmHg) compared to the curve derived from method 1 $cSaO_2$ (28 mmHg). The Siggaard-Andersen algorithm, modified for white rhinoceros, is based on white rhinoceros' oxygen-haemoglobin dissociation curves measured *in vitro* (Reiners et al. 2019) and may have overlooked some factors that affect the $cSaO_2$ values in *in vivo* situations, thereby resulting in unreliable $cSaO_2$ values (method 2) and a small shift in the curve, rather than a larger shift that actually occurs during opioid-induced immobilization.

5.6 Conclusion

Respiratory compromise, associated with severe hypoxaemia, hypercapnia, and acidosis, is one of the most serious and potentially fatal complications during chemical immobilization of rhinoceros. When clinical decisions are informed by incorrect information from unreliable information related to blood

oxygenation, animals may be placed at risk of morbidity and mortality. In this study, we demonstrated that method 1 $cSaO_2$ calculated by the oxygen content equation is an unreliable estimate of SaO_2 in immobilized white rhinoceros across the entire 0-100% saturation range. Arterial oxygen-haemoglobin saturation calculated from the Siggaard-Andersen algorithm (method 2 $cSaO_2$) can be used to estimate SaO_2 reliably, but only when the saturation levels are above 90%; below 90% they should not be used as surrogates for SaO_2. If alternative SaO_2 calculations are used in immobilized rhinoceros, their reliability should be appropriately assessed. Until a reliable method of calculating arterial oxygen-haemoglobin saturation from other measured variables is found, a co-oximeter should be rather used to monitor blood oxygenation, particularly at low saturation levels that often occur in immobilized white rhinoceros.

CHAPTER 6:

General discussion and conclusions

Adequate oxygen supply to the tissues is crucial for continuous production of adenosine triphosphate (ATP) to support different biological processes of the body (Habler & Messmer 1997; Boas & Franceschini 2011; Pittman 2011). Since there are no large stores of ATP (energy) available for later use, at rest, roughly 90% of oxygen is continuously used in the tissue mitochondria to produce ~1270 kJ of energy during aerobic respiration with only ~67 kJ of energy being produced via anaerobic respiration (Habler & Messmer 1997; Boas & Franceschini 2011; Pittman 2011). Therefore, to meet the tissue's oxygen demand, continuous and adequate transport of oxygen by the blood (blood oxygenation) and oxygen supply to the tissues is crucial. Only 2-4% of the total oxygen (oxygen content) carried in arterial blood is dissolved oxygen (PaO_2), while the remaining 96–98% is bound to haemoglobin (SaO_2) (Collins et al. 2015), making SaO_2 a more informative indicator of blood oxygenation. Hypoxaemia is one of the most prevalent and problematic physiological derangements in immobilized white rhinoceros, which, if incorrectly monitored and improperly managed can increase the risk of morbidity and mortality in these animals. Therefore, it is essential to identify the most reliable and practical method for monitoring blood oxygenation and hypoxaemia in white rhinoceros. In this thesis, I evaluated the reliability of five different methods used to monitor blood oxygenation, with some designed specifically for human use. Therefore, I aimed to determine whether these human-specific blood oxygenation methods are reliable in immobilized white rhinoceros. In chapters 2 & 3, I evaluated the reliability of a Nonin 2500A PalmSAT pulse oximeter and a Masimo Radical-7 pulse co-oximeter, that both estimate SaO_2 as peripheral arterial oxygen-haemoglobin saturation (SpO_2), at different attachment sites. In Chapters 4 & 5, I evaluated the reliability of different methods used to calculate arterial oxygen-haemoglobin saturation ($cSaO_2$). In Chapter 4, arterial oxygen-haemoglobin saturation calculated by the Enterprise Point-of-Care (EPOC) blood analyser was evaluated. In Chapter 5, arterial oxygen-haemoglobin saturation is calculated by two methods, namely, the oxygen content equation using CaO_2 measured by a microrespirometer following the method of Tucker (1967) and the Siggaard-Andersen algorithm modified for the specific characteristics of rhinoceros' blood, were evaluated. Arterial oxygen-haemoglobin saturation measured or calculated from all the methods tested in this

thesis were compared against SaO_2 measured by an AVOXimeter 4000 co-oximeter; co-oximetry is considered the reference method by the US Food and Administration (FDA) and International Organization for Standardization (ISO) guidelines. For each method to be considered reliable, the measured or calculated arterial oxygen-haemoglobin saturation values must fall within the acceptable limits dictated by the FDA and ISO (bias $\leq \pm 3\%$, precision $\leq 3\%$ and ARMS $\leq 4\%$) (Batchelder & Raley 2007).

The work described in this thesis yielded important and novel findings that will significantly improve monitoring of blood oxygenation in white rhinoceros during immobilization, thereby helping to reduce risks of morbidity and mortality and improving overall conservation and management efforts. Overall, this thesis demonstrates that blood oxygenation can be monitored reliably with minimal invasiveness in immobilized southern white rhinoceros provided that appropriate methods are employed. To elaborate, I have shown that in immobilized white rhinoceros, a conventional Nonin PalmSAT 2500A pulse oximeter with a 2000T transflectance probe placed in the space between the third eyelid and sclera, and facing the third eyelid, yielded reliable SpO_2 readings at saturation ranges between 70% and 100%; corresponding to the manufacturers' claimed performance range and within the acceptable limit outlined by the FDA and ISO (bias $\leq \pm 3\%$, precision $\leq 3\%$ and ARMS $\leq 4\%$). However, below 70%, at this attachment site, this device and probe yielded unreliable SpO_2 readings. Also, the Nonin PalmSAT 2500A pulse oximeter with 2000T transflectance probes attached to the cheek, rectum, and the tail, and with the 2000SL transmission probe attached to the ear provided unreliable SpO_2 readings. But most surprisingly, the Masimo Radical-7 pulse oximeter with a LNCS TF-I AH transflectance probe attached to the third eyelid, and with a LNS YI AH transmission probe attached to the ear pinna, both in a similar way to the Nonin probes, were unreliable, which was unexpected as this device was designed to address some limitations presented in conventional pulse oximeters. Despite the lack of reliability, the 2500A Nonin PalmSAT pulse oximeter and the Masimo Radical-7 pulse co-oximeter with their probes have moderate to high sensitivity and specificity in detecting hypoxaemia ($SaO_2 \leq 92\%$) in immobilized white rhinoceros. To elaborate, when our white rhinoceros were hypoxaemic (i.e., $SaO_2 \leq 92\%$), in ≥86% of the measurement times the pulse oximeter and the pulse co-oximeter provided SpO_2 values of ≤92%, indicating that they may still be clinically useful in detecting hypoxaemia and warning clinicians of dangerously low blood oxygen levels, despite readings not necessarily being reliable (i.e., accurate and

precise). In this thesis, I also demonstrated that arterial oxygen-haemoglobin saturation calculated by the EPOC blood analyser is an unreliable estimate of SaO_2 across the entire 0-100% saturation range in our immobilized white rhinoceros. Furthermore, arterial oxygen-haemoglobin saturation calculated by the oxygen content equation, using CaO_2 measured by the method of Tucker (1967), is an unreliable estimate of SaO_2 across the entire 0-100% saturation range in our white rhinoceros. Lastly, the Sigggard-Andersen algorithm, modified for the specific characteristics of rhinoceros blood, calculates arterial oxygen-haemoglobin saturation reliably in immobilized white rhinoceros, but only at saturations above 90%; below 90%, it was unreliable. The methods used to calculate arterial oxygen-haemoglobin saturation in this thesis also failed to adequately account for the level of hypercapnia and acidosis that occurred in our immobilized white rhinoceros. Therefore, these methods should be used with caution in immobilized southern white rhinoceros.

6.1 Thesis limitations

This thesis covers a complex area of research, because it involves the direct monitoring of oxygen bound to haemoglobin, a respiratory pigment with a structure and function that unpredictably varies between species (Schmidt-Neilsen et al.1958; Severinghaus et al.1966; Dhindsa et al. 1979; Bauman et al. 1984; Gustin et al. 1988; Clerbaux et al. 1993; Cambier et al. 2005; Reiners et al. 2019). Haemoglobin structure and function varies among species because of evolutional effects, where long- and, or short-term adaptations of haemoglobin affect how different allosteric effectors [i.e., 2.3-diphosphoglycerate (2.3-DPG) and ATP, protons (H^+), chloride ions (Cl^-) and temperature] interact with haemoglobin. Because of differences in haemoglobin among species, there is currently no reference method for assessing blood oxygenation that is designed specifically for white rhinoceros, especially when they are physiologically challenged during immobilization. As a result, in my research we used a benchtop AVOXimeter 4000 co-oximeter, which is verified as a reference method for humans, but not for rhinoceros which may have been a source of error when assessing the reliability of the methods validated in this thesis. This benchtop co-oximeter uses seven wavelengths of light (i.e., 488.4, 520.1, 562.4, 585.2, 597.5, 621.7 and 671.7 nm) to measure fractional SaO_2, oxyhaemoglobin (HbO_2), carboxyhaemoglobin (HbCO), methaemoglobin (MetHb) and haemoglobin concentration in whole blood. This human-specific benchtop co-oximeter is assumed to be appropriate for use in white

rhinoceros because the absorption spectra of human and white rhinoceros' oxyhaemoglobin and deoxyhaemoglobin are similar at wavelengths between 600 to 1000 nm (Reiners et al. 2019). Although other co-oximeter SaO_2 values have been shown to be repeatable in different mammalian species (e.g., dogs, cats and horses) (Matthews at al. 2003), additional research is needed to assess the precision and repeatability of the benchtop AVOXimeter 4000 co-oximeter in white rhinoceros. In my study, I did not test for precision and repeatability (i.e., taking repeated measurements per blood sample) of the AVOXimeter 4000 co-oximeter because of the limited number of cuvettes available for the study and this might have introduced further error in our results. Nonetheless, it was important to use and test for reliability of the different methods during immobilization (i.e., in clinical or field settings) where most workers rely on a single value. The benchtop AVOXimeter 4000 co-oximeter, EPOC blood analyser and Tucker chambers (microrespirometers) were kept in a controlled laboratory environment to help reduce random and systematic error, and to control for temperature. Although most blood samples were analysed within 15 minutes, there was a longer delay before analysis for some of the samples, which might have also introduced some error in our results.

6.2 Reliability of pulse oximetry and pulse co-oximetry, at different attachment sites, in immobilized southern white rhinoceros

My findings show that the conventional dual-wavelength Nonin PalmSAT 2500A pulse oximeter is more reliable than the new multi-wavelength Masimo Radical-7 pulse co-oximeter when used at different attachment sites in immobilized white rhinoceros. These findings were unexpected because the Masimo device was developed to address some of the limitations present in conventional pulse oximeters, such as motion, light artefacts, and low tissue vascular perfusion (Masimo Corporation 2007; Causey et al. 2011; Quinn et al. 2013). Furthermore, given that the Masimo Radical-7 pulse co-oximeter measures SpO_2 and the other haemoglobin derivatives (i.e., SpHb, SpCO and SpMet) using multi-wavelength spectrophotometry, which conventional dual-wavelength pulse oximeters cannot, it was anticipated that it would be more reliable, but this was not. To the best of our knowledge, my research is the first to validate pulse oximetry and pulse co-oximetry, at different attachment sites, to monitor blood oxygenation in immobilized white rhinoceros. The findings of Chapters 2 & 3 provide a better understanding of the factors influencing the reliability of pulse oximetry and pulse co-oximetry SpO_2

readings in immobilized white rhinoceros. These findings will improve minimal-invasive monitoring of blood oxygenation and hypoxaemia, ultimately improving the health and welfare of white rhinoceros during immobilization.

The reliability of the Nonin PalmSAT 2500A pulse oximeter in white rhinoceros, only at the 70-100% saturations range, was expected given that similar conventional pulse oximeters (e.g., Nellcor, Surgi-Vet and other Noni models) are reliable in anaesthetized dogs (Matthews et al. 2003; Burns et al. 2006), impala (Mtetwa et al. 2020), llamas (Grubb & Andersen 2017), alpacas (Grubb & Andersen 2017), cynomolgus monkeys (Young et al. 2002), cattle (Coghe et al. 1999) and horses (Chaffin et al. 1996; Matthews et al. 2003; Reiners et al. 2017) across different saturation ranges that are above 70%. In addition, it has been long-established by the manufacturers that conventional pulse oximeters are typically unreliable at saturations below 70%. The unreliability may be because these devices are calibrated only in healthy individuals, mostly human patients, where testing saturations below 70% is risky, but the overall reason of the unreliability at these ranges still needs to be determined. My findings on pulse oximetry complement and extend the substantial work of other researchers by identifying the factors that influence the reliability of the pulse oximetry readings, including probe attachment site, probe type, species-specific differences, and the models of pulse oximeter or pulse co-oximeter used.

This thesis demonstrated that the pulse oximeter attachment site and probe type used significantly influence the reliability of SpO_2 readings in immobilized white rhinoceros (i.e., Chapters 2 & 3). The Nonin 2500A pulse oximeter was reliable only when the 2000T transflectance probe was attached in the space between the third eyelid and the sclera, facing the third eyelid, but was unreliable at the other attachment sites (cheek, rectum, and the tail). Furthermore, the Nonin 2500A pulse oximeter with a 2000SL transmission probe attached on the ear pinna provided unreliable SpO_2 readings in immobilized white rhinoceros. The findings on the reliability of Nonin 2500A pulse oximeter when the 2000T transflectance probe was attached to the third eyelid in Chapter 3 were consistent with those of Chapter 2, respectively. The third eyelid was chosen because its mucous membrane is well perfused with little pigmentation, and external light and movement do not interfere with the SpO_2 measurements as the probe is secured by surrounding tissues. In contrast, the unreliable SpO_2 measurements at the other

attachment sites (i.e., cheek, rectum, and the tail) using the 2000T transflectance probe and the 2000SL transmission probe on the ear pinna, may be due to the unsuitable characteristics and anatomical differences of each site. These attachment sites differ in skin thickness, pigmentation, and the level of tissue vascular perfusion, which affects the reliability of SpO_2 readings. This unreliability between attachment sites has been reported in other species (Young et al. 2002; Giguére et al. 2014; Reiners et al. 2017; Mtetwa et al. 2020). For example, the cheek is reliable in anaesthetized cynomolgus monkeys (Young et al. 2002) and horses (Reiners et al. 2017) when using a Nonin pulse oximeters at the 70-100% saturation range, but unreliable in immobilized impala (Mtetwa et al. 2020) and our rhinoceros across the entire 0-100% saturation range. In immobilized impala (Mtetwa et al. 2022), the tail is reliable only at the 90-100% saturation range, but interestingly, in our rhinoceros the tail showed a consistent underestimation of SaO_2 measurements, producing a systemic pattern (Fig. 2.2) accompanied with poor reliability across the entire 0-100% saturation range. Unreliability of SpO_2 readings and a consistent underestimation of SaO_2 across the entire 0-100% saturation range was also previously reported when the probe was attached to the tail of anaesthetized foals (Chaffin et al. 1996). The rectum was also found to be unreliable in immobilized impala (Mtetwa et al. 2020), similar to our white rhinoceros across the entire 0-100% saturation range. I also demonstrated that the ear is unreliable when using either the Nonin PalmSAT 2500A pulse oximeter or the Masimo Radical-7 pulse co-oximeter with their transmission probes across the entire 0-100% saturation range in immobilized white rhinoceros. My findings on the unreliability of the ear pinna are important because the ear is often the “go-to” attachment site for pulse oximetry in wildlife, particularly white rhinoceros, without the validation of its reliability as an attachment site (Boardman et al. 2014; Fahlman et al. 2016; Bertelsen et al. 2017; Mtetwa et al. 2020; Meuffels et al. 2022). My study is the first to accurately document the unreliability of the SpO_2 readings obtained from the ear pinna when compared against SaO_2 measured by a benchtop co-oximeter, reference method in immobilized white rhinoceros. The ear pinna may be potentially unreliable because pigmentation and tissue thickness inhibit the transmission of light through the tissue and limit its detection by the photodiode located on the opposite side of the probe. As is commonly practiced by clinicians in the field, I also scarified the ear to obtain readings, by removing the epidermal layer. This practice exposes oozing blood to air, which possibly producing contributes to the unreliable SpO_2 readings obtained. The ear is also unreliable in immobilized impala (Mtetwa et al. 2020), horse (Matthews et al. 2003) and giraffe (Bertelsen et al. 2017) at the 70-100% saturation range when

using a similar scarifying technique. Therefore, it is important that veterinarians avoid using the ear as a possible attachment site for pulse oximetry, especially if there is no research validating its reliability for a specific species. Furthermore, since the third eyelid provided reliable SpO_2 readings in our white rhinoceros, it should be tested in other species, particularly in wildlife, as it may be a better alternative than the commonly used ear pinna.

The type of probes used in our investigation also affected the reliability of SpO_2 measurements in our immobilized white rhinoceros. The differences in reliability of SpO_2 measurements when using transmission and transflectance probes at different attachment sites, was expected as it has been reported in other species (Chaffin et al. 1996; Matthews et al. 2003; Giguére et al. 2014; Mtetwa et al. 2020). I have demonstrated that our transmission probes (i.e., Nonin 2000SL lingual and a Masimo LNS YI AH SpO_2 animal multisite clip probes) attached to the rhinoceros' ear may have also contributed to the unreliability of the SpO_2 readings obtained. These probes have relatively short clips and at times did not adhere well to the large ears of the white rhinoceros, resulting in poor tissue contact and likely also a caused of unreliable SpO_2 readings. However, the Nonin and Masimo transflectance probes attached to the third eyelid were better suited. However, the Nonin 2000T transflectance probe that provided reliable SpO_2 readings was an appropriate-sized probe compared to the Masimo LNCS TF-I AH transflectance probe, which was much bigger and kept moving out of the space between the sclera and third eyelid, likely a cause of the unreliable SpO_2 readings.

Regardless of the probe type and attachment site, the different models (i.e., Nonin and Masimo) of oximeter devices also contributed to the different SpO_2 readings in our immobilized white rhinoceros. The Nonin PalmSAT 2500A pulse oximeter was more reliable than the Masimo Radical-7 pulse co-oximeter, and as noted above, it was unexpected because the Masimo pulse co-oximeters uses signal extraction technology (SET) that is not present in the Nonin device (Masimo Corporation 2007; Causey et al. 2011; Quinn et al. 2013). Signal extraction technology applies adaptive filters that separate the true arterial signal from signals caused by motion artefacts and external light by evaluating the whole signal and breaking it down into its fundamental components to obtain reliable SpO_2 readings (Masimo Corporation 2007; Causey et al. 2011; Quinn et al. 2013). However, the Masimo Radical-7 pulse co-oximeter produced unreliable SpO_2 readings when its probes were attached to both the ear pinna and

third eyelid, even when it was shown in Chapter 2 that the third eyelid is a reliable attachment site in white rhinoceros when using the Nonin 2500A pulse oximeter. The limited studies on the reliability of Masimo Radical pulse co-oximeter in other species of mammals undergoing anaesthesia are conflicting and have mostly focused on the reliability of SpHb measurements (Read et al. 2016; Kim et al. 2019; Zoff et al. 2019; Mair et al. 2020; Tayari et al. 2021; Tayari et al. 2022). Those studies that have reported reliability in the SpO_2 readings, only looked at the reliability at a narrow range, which is not enough to conclude true overall reliability (Quinn et al. 2013; Tayari et al. 2019; Zoff et al. 2019; Tayari et al. 2022). However, if Masimo Corporation designs a smaller sized transflectance probe, there is a possibility that it may provide reliable SpO_2 readings from the third eyelid of white rhinoceros.

6.3 Reliability of calculated arterial oxygen-haemoglobin saturation in immobilized southern white rhinoceros

Wildlife veterinarians routinely use Enterprise Point-Of-Care (EPOC) blood analysis to monitor the animal's ventilatory, acid-base and blood oxygenation status without knowing the reliability of the EPOC's calculated arterial oxygen-haemoglobin saturation ($cSaO_2$) values (Buss et al. 2018; Boesch et al. 2018; Semjonov et al. 2018; Gaudio et al. 2020; Mtetwa et al. 2020; Pohlin et al. 2020; Blignaut et al. 2021; Pfitzer et al. 2021; Chelepo et al. 2022; Meuffels et al. 2022). The EPOC blood analyser calculates arterial oxygen-haemoglobin saturation using a Severinghaus algorithm-derived standard human oxygen-haemoglobin dissociation curve, which has a resting P_{50} of ~ 27 mmHg (Severinghaus 1979). Compared to humans, white rhinoceros have a more left shifted oxygen-haemoglobin dissociation curve with a resting P_{50} between 15 mmHg (Reiners et al. 2019) and 20 mmHg (Baumann et al. 1984). My findings indicate that in immobilized white rhinoceros, the EPOC $cSaO_2$ values are unreliable, underestimating the co-oximeter SaO_2 by a mean difference of 6% and a precision of 5% across the entire 0-100% saturation range. My findings were different from those reported in immobilized impala, where the EPOC's $cSaO_2$ is reliable across the entire 0-100% saturation range (Mtetwa et al. 2020). The differences in the oxygen-haemoglobin dissociation curves of white rhinoceros and humans may have compromised the reliability of EPOC $cSaO_2$ values in our immobilized white rhinoceros. Even though the impala oxygen-haemoglobin dissociation curve is unknown, it might be

close to that of humans, especially as a function of body mass (i.e., mammals of similar body mass tend to have similar P_{50} values) (Schmidt-Neilsen & Larimer 1958). Oxygen-haemoglobin dissociation curves also shift dynamically in response to acute changes in pH, $PaCO_2$, temperature, 2.3-diphosphoglycerate (2.3-DPG) and chloride ions (Cl^-). Our white rhinoceros were hypoxaemic (mean PaO_2 = 44.7 mmHg), hypercapnic (mean $PaCO_2$ = 71.1 mmHg), and acidotic (mean pH = 7.30). Therefore, it was important to investigate EPOC $cSaO_2$ of immobilized white rhinoceros at these specific physiological conditions. Our immobilized rhinoceros' oxygen-haemoglobin dissociation curve derived from EPOC $cSaO_2$ shifted to the right (i.e., P_{50} of 32 mmHg), compared to their normally left shifted curve, at rest (i.e., P_{50} between 15 mmHg and 20 mmHg). Therefore, our findings demonstrate that in our immobilized rhinoceros, the EPOC blood analyser algorithm shifted its typically right-shifted curve (i.e., P_{50} of ~27 mmHg) further to the right (i.e., P_{50} of ~32 mmHg) across the entire 0-100% saturation range therefore underestimating SaO_2 and producing unreliable $cSaO_2$ values.

In this thesis, I also examined the oxygen content equation [i.e., $\mathrm{CaO_2} = (\text{Hüfner factor} \times [\mathrm{Hb}] \times \mathrm{SaO_2}) + (0.003 \times \mathrm{PaO_2})$] as a potential method to reliably calculate arterial oxygen-haemoglobin saturation in immobilized white rhinoceros. Oxygen content has traditionally been measured using the manometric method of Van-Slyke & Neill (1924), which remained a reference method for over 25 years until the Clark electrode was introduced in 1953 (Crystal & Pagel 2020). The manometric method uses the measured CaO_2 to reliably calculate arterial oxygen-haemoglobin saturation after correcting for PaO_2 (Sendroy et al. 1934; Lambertsen et al. 1952; Holmgren & Pernow 1959; Weiss & Sinha 1978). In this thesis, I used the method of Tucker (1967) that uses a Clark-type electrode to calculate CaO_2 based on direct measurement of PaO_2 before and after potassium ferricyanide releases oxygen-bound haemoglobin to the solution. The method of Tucker (1967) is just as reliable, but much quicker compared to the manometric method (Tucker 1967; Bridges et al. 1979; Boutilier et al. 1984; Harter et al. 2015). Therefore, we used the Tucker-derived CaO_2, EPOC measured PaO_2, a horse Hüfner factor of 1.383 $mL.g^{-1}$ and [Hb] ranging from 8.9 to 17.0 $g.dL^{-1}$ to calculate arterial oxygen-haemoglobin saturation ($cSaO_2$) from the oxygen content equation. However, I demonstrated that these $cSaO_2$ values were unreliable across the entire 0-100% saturation range, probably because the oxygen content equation relies on multiple variables to calculate arterial oxygen-haemoglobin saturation, and these variables are either measured or calculated using different methods, increasing the risk of propagation

of error (propagation of uncertainty). Surprisingly though, the oxygen-haemoglobin dissociation curve derived from these $cSaO_2$ values showed a similar shift (P_{50} of ~ 28 mmHg) to the curve derived from the reference method co-oximeter SaO_2 (P_{50} of ~ 27 mmHg) but only at saturation ranges below 90%, corresponding to PaO_2 of approximately ≤60 mmHg. The similar shift indicates that the $cSaO_2$ using the oxygen content equation may have accounted for the hypercapnia and acidosis observed in our rhinoceros, which is a positive finding as it reflects the animal's physiological conditions during immobilization. But above 90% saturation, the oxygen-haemoglobin dissociation curve derived from these $cSaO_2$ values was higher than the curve derived from the co-oximeter's SaO_2, corresponding to the calculated imprecision of 18% at the 90-100% saturation range. These findings were unexpected because, as explained above, the plateau part of the curve is normally similar among different species regardless of the animal's physiological conditions and the position of the curve (Scott et al. 2005; Collins et al. 2015; Duke-Novakovski 2019). The imprecision of 18% at the plateau region may have resulted from measurement error that occurred when flushing the catheter before taking an arterial sample, despite discarding the initial blood from the catheter, therefore affecting the quality of our blood samples. Also, further measurement error might have resulted from variation in the micro-syringe blood volumes drawn, as it can be difficult to draw exactly 4 μL of blood using a micro-syringe.

I also evaluated the Siggaard-Andersen algorithm that applies rhinoceros-specific haemoglobin variables (e.g., P_{50} and Bohr effect) to calculate arterial oxygen-haemoglobin saturation of white rhinoceros after correcting for $PaCO_2$, pH and temperature (Haymerle et al. 2016; Reiners et al. 2019). The Siggaard-Andersen algorithm, using human- and bovine-specific haemoglobin variables, calculates arterial oxygen-haemoglobin saturation reliably in humans (Breuer et al. 1989; Anstey 2000) and bovids (Detry et al. 2003) across different saturation ranges. In our immobilized white rhinoceros, arterial oxygen-haemoglobin saturation calculated by the Siggaard-Andersen algorithm is reliable only at saturation levels between 90-100%. These findings were expected as saturation levels above 90% correspond to the plateau part of the oxygen-haemoglobin dissociation curve that is normally similar among species, regardless of the animal's physiological conditions and their resting P_{50} value (Scott et al. 2005; Collins et al. 2015; Duke-Novakovski 2019). Since this modified algorithm uses a rhinoceros-specific curve to calculate arterial oxygen-haemoglobin saturation, it was surprising that the $cSaO_2$ values were unreliable at saturations below <90%. Also, arterial oxygen-haemoglobin saturation

calculated from this modified algorithm overestimated the co-oximeter SaO_2 readings by a difference (bias) of 10% and with a poor precision of 7% across the entire 0-100% saturation range. These rather contradictory findings may be due to the fact that Reiners et al. (2019), authors who formulated the modified algorithm for white rhinoceros' blood, removed certain variables (i.e., 2.3-DPG, HbCO, MetHb and body temperature effects) in their model used to formulate their modified algorithm. The removal of these variables is based on the knowledge that white rhinoceros haemoglobin is only partially altered by 2.3-DPG [presumably because it lacks histidine at position $\beta 2$, that is present in the same position in human haemoglobin, and is responsible for the binding of 2.3-DPG (Mazur et al. 1982; Baumann et al. 1984)], and also by changes in HbCO, MetHb and body temperature [of which the reasons are currently unknown (Reiners et al. 2019)]. Therefore, the removal of these variables from the algorithm may have contributed to the unreliability of the $cSaO_2$ values at saturations ranges below 90%, making it an unreliable method for monitoring blood oxygenation in immobilized white rhinoceros.

The white rhinoceros' oxygen-haemoglobin dissociation curve derived from these $cSaO_2$ values failed to account for hypercapnia and acidaemia observed in our immobilized study animals at saturations below 90%, corresponding to PaO_2 values of approximately ≤45 mmHg. Compared to the P_{50} of white rhinoceros at rest (i.e., which is between 15 mmHg and 20 mmHg), the P_{50} of the oxygen-haemoglobin dissociation curve derived from Siggaard-Andersen algorithm $cSaO_2$ was approximately 20 mmHg, showing an inadequate shift of the curve, which was unexpected when using this algorithm. The authors who modified the algorithm did acknowledge some limitations arising from formulating this algorithm, such as the use of a small sample size and that the modified algorithm is based on oxygen-haemoglobin dissociation curves measured *in vitro,* which could not account for any factors that may arise during *in vivo* situations (Reiners et al. 2019). For example, in *in vivo* situations, an increase in HbCO and MetHb concentrations, as well as the animal's body temperature may shift the white rhinoceros' curve further to the right (i.e., give a P_{50} >20 mmHg), but the magnitude of the shift is currently unknown. Therefore, further research is required to determine what happens *in vivo*, particularly during chemical immobilization when white rhinoceros are hypoxaemic, hypercapnic, and acidotic and have other physiological derangements (e.g., other changes from hypermetabolism). With that said, in the rhinoceros, I found low levels of MetHb (1.1 ± 0.5%), HbCO (<1%) and normothermia (37.4 ± 1.8°C), which might have had little effect on the shift of the white rhinoceros' oxygen-haemoglobin dissociation curve.

Nonetheless, the oxygen-haemoglobin dissociation curve derived in this thesis from the co-oximeter SaO_2 values facilitate a better understanding of how immobilized white rhinoceros respond when they are hypoxaemic, hypercapnic and acidotic. My findings show that rhinoceros' naturally left-shifted curve is not advantageous, or evident, when they are chemically immobilized because their SaO_2-derived curve was dynamically right-shifted in response to severe hypoxaemia, hypercapnia and acidaemia. This right shift may have facilitated the offloading of oxygen to the tissues, but limited the ability for the rhinoceros' haemoglobin to bind and carry oxygen to the tissues. Therefore, the rhinoceros' naturally left-shifted curve will have physiological advantages for rhinoceros when they are conscious, but unfortunately this advantage is cancelled out during chemical immobilization.

6.4 Future studies and recommendations

Veterinarians should use a Nonin PalmSAT 2500A pulse oximeter with a 2000T transflectance probe attached under and facing the third eyelid to monitor blood oxygenation reliably in immobilized white rhinoceros with saturation levels between 70-100%. If there is a risk of SaO_2 below 70%, and reliable monitoring is required, then a benchtop co-oximeter should rather be used for reliable measurements. Since the third eyelid is a reliable attachment site in immobilized white rhinoceros, my research has opened a gap for more research into the reliability of using this attachment site to acquire SpO_2 readings in other species. Several questions remain unanswered regarding monitoring of MetHb, HbCO, and [Hb] using non-invasive spectrophotometric methods and further research in this area would be of value. Specifically, there are gaps in our knowledge regarding the absorption spectra of white rhinoceros' haemoglobin, especially for HbCO and MetHb at the near and infrared spectra range, respectively. Also, further investigations to determine the reliability of SpHb measured by the pulse co-oximeter and [Hb] measured by the benchtop co-oximeter when compared to the reference cyanmethaemoglobin method are warranted for white rhinoceros. Furthermore, tonometry research is still needed specifically to validate the AVOXimeter 4000 co-oximeter using *in vitro* methods such as the method of Van Slyke & Neill (1924). It will also be of value to investigate the absorption spectra of rhinoceros' HbO_2 and the other haemoglobin derivatives (i.e., HHb, HbCO and MetHb) at wavelengths between 400 to 600 nm that are used in the AVOXimeter 4000 co-oximeter and Masimo Radical-7 pulse co-oximeter.

I reached the conclusion that there is still potential in using the oxygen content equation to calculate arterial oxygen-haemoglobin saturation in white rhinoceros because, although the $cSaO_2$ values were imprecise, the bias was low across the entire 0-100% saturation range. Additionally, the oxygen-haemoglobin dissociation curve derived from these $cSaO_2$ values had a similar shift to the curve derived from the co-oximeter SaO_2, both equally accounting for the effects of hypercapnia and acidosis observed in the immobilized white rhinoceros. However, it is also important to note that the method of Tucker (1967) is a complex laboratory-based method which requires careful attention to detail and will still introduce residual error in the measurements if proper and extended training is not provided. Furthermore, the method of Tucker (1967) is not easy to use in the field, it requires daily calibrations, precision in blood and chamber volumes and should be kept at a constant and known temperature to obtain reliable measurements. In future investigations, it might be possible to refine the method of Tucker (1967) to determine CaO_2 reliably and construct better oxygen-haemoglobin dissociation curves, but the $cSaO_2$ values obtained using the oxygen content equation should be interpreted with caution unless properly validated.

It is clear that the white rhinoceros' haemoglobin structure and oxygen-haemoglobin dissociation curve are different from that of human and other species, therefore, the extraction and further analysis of white rhinoceros' haemoglobin structure using protein sequencing and crystallisation technologies is still needed. Furthermore, because of these differences in characteristics of haemoglobin among species, arterial oxygen-haemoglobin saturation calculated from algorithms based on the human oxygen-haemoglobin dissociation curve should be interpreted with caution in other species. Before using any blood oxygenation monitoring method, it is important to be aware of the differences in haemoglobin characteristics among species as most blood oxygenation monitoring methods are designed for human use, or sometimes for specific domestic animal species.

Further research should also be done to investigate other possible devices or methods that can measure or calculate blood oxygenation at an extensive scale. For example, a device that can continuously measure real-time accurate and reliable measurements not only for SaO_2, but also for

[Hb], PaO_2, and total oxygen carrying capacity of blood, would be ideal. Furthermore, devices that appropriately apply species-specific variables such as P_{50}, Bohr effect and Hüfner factor would be of great benefit too. I also recommend further studies to determine the exact Hüfner factor of white rhinoceros to employ the correct value in co-oximeters and blood analysers when they are used in rhinoceros, and to improve calculations of arterial oxygen-haemoglobin saturation using the oxygen content equation. The methods explored in my thesis only monitor arterial blood oxygenation and therefore only provides information about the amount of oxygen supplied to the tissues by the blood, and no information about the tissue's oxygen demand and consumption (i.e., tissue oxygenation, perfusion, and aerobic metabolism). As discussed in the literature review (Chapter 1), there are alternative methods that measure tissue blood oxygenation, perfusion, and metabolism in real-time such as the oxygen optode sensors, oxygen electrodes, fibre-optic pulmonary artery and central venous catheters, near infrared spectroscopy (NIRS), and brain and fibre-optic reflectance oximetry (Waller et al. 1982; Nakajima et al. 1993; Schell & Cole 2000; Tànczos & Molnár 2013). A few of these methods are minimally invasive and can be used in field-settings (e.g., NIRS, fibre-optic reflectance oximetry), but they use spectrophotometry or optics that have never been validated before, even in humans (Sakr 2010). However, most of these methods are very invasive (i.e., fibre-optic or pulmonary artery and central venous catheters) or are impractical (i.e., NIRS probes may not sufficiently penetrate the brain of large body mass mammals like the white rhinoceros) and therefore are still only suitable for use in humans. So there exists a large scope for further research into looking at these devices and improving their measures of tissue oxygenation, perfusion, and metabolism in different species. Furthermore, future studies are required to design and explore methods which use combined assessments of global blood oxygen supply and tissue oxygenation using one integrated method or POC device. For example, a method or device that considers blood pressures, cardiac output, blood oxygenation (i.e., SaO_2, PaO_2), tissue oxygenation (i.e., StO_2) and perfusion, and metabolism to assess appropriate global oxygen supply, tissue oxygenation and oxygen consumption. To do so, measurements of different biomarkers of tissue oxygenation and metabolism could also be included in the method or device. For example, biomarkers such as blood lactate levels as a sign of anaerobic respiration, central or mixed venous oxygen-haemoglobin saturation (i.e., SvO_2 or StO_2) and central or mixed venous blood gas variables (i.e., PvO_2 or $PcvO_2$), because venous oxygenation is normally elevated when tissues inadequately utilize oxygen. Another potential biomarker is cytochrome C oxidase (cytochrome aa3),

which can monitor tissue oxygen consumption, because it directly reacts with oxygen at the terminus of cellular respiration (i.e., in the mitochondria) (Scheufler 2004). These methods will help detect and monitor any imbalances between oxygen supply, demand and consumption that normally occur in clinically ill-patients under anaesthesia and during immobilization, which will be beneficial for adequate management of human and veterinary patients. Furthermore, since prolonged hypoxaemia causes tissue hypoxia and cellular damage, it might be useful to explore other different biomarkers that are normally released in response to tissue hypoxia. These biomarkers could include upregulation of hypoxia-inducible factors, whose synthesis is upregulated to help maintain oxygen homeostasis. Hypoxia-inducible factors also leads to an increase in the production of other potential biomarkers like erythropoietin, angiogenic factors and vasoactive mediators (i.e., neuronal nitric oxide synthases and nitric oxide), which improve haemoglobin concentrations (i.e., increased red blood cell production) and volume and flow of blood to the tissues, improving overall tissue oxygenation (Le & Courter 2008; MacIntyre 2014). Also, the release of non-protein bound ions and down-regulation of other metabolic processes, which when coupled with tissue hypoxia form free radicals and enhance tolerance to tissue hypoxia (Perrone et al. 2002; MacIntyre 2014). The early diagnosis of inadequate tissue oxygenation, by monitoring these hypoxia biomarkers, may also help reduce the risks of mortality associated with hypoxaemia, hypermetabolism and tissue hypoxia following chemical immobilization of white rhinoceros.

6.5 Conclusion

Blood oxygenation and hypoxaemia can be monitored reliably in immobilized southern white rhinoceros. To do so, a Nonin PalmSAT 2500A pulse oximeter with a 2000T transflectance probe, attached in the space between the third eyelid and the sclera, should be used when saturation levels are between 70 and 100%; and below 70%, a benchtop co-oximeter should instead be used. When the Masimo Radical-7 pulse co-oximeter is used to measure SpO_2 with the LNCS TF-I AH animal transflectance and LNS YI AH transmission probes attached to the third eyelid and the ear pinna, it produces unreliable estimates of SaO_2 across the entire 0-100% saturation range. The EPOC blood analyser calculates arterial oxygen-haemoglobin saturation unreliably in immobilized white rhinoceros because it uses a Severinghaus algorithm-derived human oxygen-haemoglobin dissociation curve, which is different from that of white rhinoceros. Arterial oxygen-haemoglobin saturation calculated by the oxygen content

equation using Tucker-derived CaO_2 is unreliable across the entire saturation range because of measurement complexity of the method of Tucker (1967) and variables used for the calculation of arterial oxygen-haemoglobin saturation. The Siggaard-Andersen algorithm, modified for rhinoceros, calculates arterial oxygen-haemoglobin saturation reliably only at saturations above 90% and so may not be particularly useful. The information provided within this thesis will assist wildlife veterinarians in monitoring blood oxygenation and hypoxaemia reliably, continuously, and non-invasively in immobilized white rhinoceros.

References

Adair, G. S., Bock, A. V., & Field Jr, H. (1925). The haemoglobin system: VI. The oxygen dissociation curve of haemoglobin. *Journal of Biological Chemistry*, *63*(2), 529-545.

Agarwal, S., Shafi, R., Edwards, R. M., Collymore, L., & Devaraj, S. (2014). Evaluation of the analytical performance of the modified enterprise point-of-care blood gas and electrolyte analyzer in a pediatric hospital. *Point of Care*, *13*(4), 132-136.

Andersen, J. B., & Wang, T. (2002). Effects of anaesthesia on blood gases, acid–base status and ions in the toad *Bufo marinus*. *Comparative Biochemistry and Physiology Part A: Molecular and Integrative Physiology*, *131*(3), 639-646.

Anstey, C. (2000). The accuracy of in vivo P_{50} at high haemoglobin saturation. *Anaesthesia and Intensive Care*, *28*(1), 31-37.

Auckburally, A. (2016). Pulse oximetry and oxygenation assessment in small animal practice. *In Practice*, *38*(2), 50-58.

Auckburally, A., & Nyman, G. (2017). Review of hypoxaemia in anaesthetized horses: predisposing factors, consequences and management. *Veterinary Anaesthesia and Analgesia*, *44*(3), 397-408.

Ayres, D. A. (2012). Pulse oximetry and co-oximetry. In *Advanced Monitoring and Procedures for Small Animal Emergency and Critical Care* (pp. 274-285). Wiley-Blackwell, New York, USA.

Bailey, S. R., Russell, E. L., & Martinez, A. (1997). Evaluation of the AVOXimeter: precision, long-term stability, linearity, and use without heparin. *Journal of Clinical Monitoring*, *13*(3), 191-198.

Bardell, D., West, E., & Senior, J. M. (2017). Evaluation of a new handheld point-of-care blood gas analyser using 100 equine blood samples. *Veterinary Anaesthesia and Analgesia*, *44*(1), 77-85.

Baumann, R., Mazur, G., & Braunitzer, G. (1984). Oxygen binding properties of haemoglobin from the white rhinoceros (| β2-GLU|) and the tapir. *Respiration Physiology*, *56*(1), 1-9.

Bautista, N. M., Malte, H., Natarajan, C., Wang, T., Storz, J. F., & Fago, A. (2021). New insights into the allosteric effects of CO_2 and bicarbonate on crocodilian haemoglobin. *Journal of Experimental Biology*, *224*(15), jeb242615.

Barker, S. J., Hyatt, J., Shah, N. K., & Kao, Y. J. (1993). The effect of sensor malpositioning on pulse oximeter accuracy during hypoxemia. *Anesthesiology*, *79*(2), 248-254.

Barker, S. J., Shander, A., & Ramsay, M. A. (2016). Continuous noninvasive hemoglobin monitoring: a measured response to a critical review. *Anesthesia and Analgesia*, *122*(2), 565.

Bartels, H., Hilpert, P., Barbey, K., Betke, K., Riegel, K., Lang, E. M., & Metcalfe, J. (1963). Respiratory functions of blood of the yak, llama, camel, Dybowski deer, and African elephant. *American Journal of Physiology-Legacy Content*, *205*(2), 331-336.

Batchelder, P. B., & Raley, D. M. (2007). Maximizing the laboratory setting for testing devices and understanding statistical output in pulse oximetry. *Anesthesia and Analgesia*, *105*(6), S85-S94.

Benesch, R. E., Benesch, R., & Yung, S. (1973). Equations for the spectrophotometric analysis of hemoglobin mixtures. *Analytical Biochemistry*, *55*(1), 245-248.

Berenbrink, M. (2006). Evolution of vertebrate haemoglobins: histidine side chains, specific buffer value and Bohr effect. *Respiratory Physiology and Neurobiology*, *154*(1-2), 165-184.

Bertelsen, M. F., Grøndahl, C., Stegmann, G. F., Sauer, C., Secher, N. H., Hasenkam, J. M., Damkjær, M., Aalkjær, C., & Wang, T. (2017). Accuracy of noninvasive anesthetic monitoring in the anesthetized giraffe (*Giraffa camelopardalis*). *Journal of Zoo and Wildlife Medicine*, *48*(3), 609-615.

Bland, J. M., & Altman, D. G. (2007). Agreement between methods of measurement with multiple observations per individual. *Journal of Biopharmaceutical Statistics*, *17*(4), 571-582.

Blignaut, C. J., Steenkamp, G., Loock, D., Emslie, R., & Zeiler, G. E. (2021). Immobilization, cardiopulmonary and blood gas effects of ketamine–butorphanol–medetomidine versus butorphanol–midazolam–medetomidine in free-ranging serval (*Leptailurus serval*). *Veterinary Anaesthesia and Analgesia*, *48*(5), 707-715.

Boardman, W. S., Caraguel, C. G., Raath, J. P., & Van Zijll Langhout, M. (2014). Intravenous butorphanol improves cardiopulmonary parameters in game-ranched white rhinoceroses (*Ceratotherium simum*) immobilized with etorphine and azaperone. *Journal of Wildlife Diseases*, *50*(4), 849-857.

Boas, D. A., & Franceschini, M. A. (2011). Haemoglobin oxygen saturation as a biomarker: the problem and a solution. *Philosophical Transactions of the Royal Society A: Mathematical, Physical and Engineering Sciences*, *369*(1955), 4407-4424.

Boesch, J. M. (2019). Respiratory, cardiovascular, and metabolic effects of etorphine, with and without butorphanol, in white rhinoceros *(Ceratotherium simum)* (Doctoral dissertation, PhD Thesis, Department of Paraclinical Sciences, Faculty of Veterinary Science, University of Pretoria, Pretoria, South Africa).

Boesch, J. M., Gleed, R. D., Buss, P., Hofmeyr, M., Tordiffe, A., Zeiler, G., & Meyer, L. (2018). Effects of a supplemental etorphine dose on pulmonary artery pressure and cardiac output in immobilized, boma-habituated white rhinoceros (*Ceratotherium simum*): a preliminary study. *Journal of Zoo and Wildlife Medicine*, *49*(4), 849-855.

Bohnhorst, B., Peter, C. S., & Poets, C. F. (2002). Detection of hyperoxaemia in neonates: data from three new pulse oximeters. *Archives of Disease in Childhood-Fetal and Neonatal Edition*, *87*(3), F217-F219.

Boom, M., Niesters, M., Sarton, E., Aarts, L., W Smith, T., & Dahan, A. (2012). Non-analgesic effects of opioids: opioid-induced respiratory depression. *Current Pharmaceutical Design*, *18*(37), 5994-6004.

Boutilier, R. G., Heming, T. A., & Iwama, G. K. (1984). Physicochemical parameters for use in fish respiratory physiology. In *Fish Physiology* (Vol. 10, pp. 403-430). Academic Press, Massachusetts, USA.

Boyes-Watson, J., Davidson, E., & Perutz, M. F. (1947). An X-ray study of horse methaemoglobin. I. *Proceedings of the Royal Society of London. Series A. Mathematical and Physical Sciences*, *191*(1024), 83-132.

Braunitzer, G., Hilse, K., Rudloff, V., & Hilschmann, N. (1964). The hemoglobins. *Advances in Protein Chemistry*, *19*, 1-71.

Breuer, H. W., Groeben, H., Breuer, J., & Worth, H. (1989). Oxygen saturation calculation procedures: a critical analysis of six equations for the determination of oxygen saturation. *Intensive Care Medicine*, *15*(6), 385-389.

Breuer, H. W., Groeben, H., Schöndeling, H., & Worth, H. (1990). Comparative analysis of arterial oxygen saturations during exercise by pulse oximetry, photometric measurements, and calculation procedures. *International Journal of Sports Medicine*, *11*(1), 22-25.

Bridges, C. R., Bicudo, J. E. P. W., & Lykkeboe, G. (1979). Oxygen content measurement in blood containing haemocyanin. *Comparative Biochemistry and Physiology Part A: Physiology*, *62*(2), 457-461.

Brinkman, R., & Zylstra, W. G. (1949). Determination and continuous registration of the percentage oxygen saturation in clinical conditions. *Archivum Chirurgicum Neerlandicum*, *1*(3), 177-183.

Brodbelt, D. C., Pfeiffer, D. U., Young, L. E., & Wood, J. L. N. (2007). Risk factors for anaesthetic-related death in cats: results from the confidential enquiry into perioperative small animal fatalities (CEPSAF). *British Journal of Anaesthesia*, *99*(5), 617-623.

Brown, L. J. (1980). A new instrument for the simultaneous measurement of total hemoglobin,% oxyhemoglobin,% carboxyhemoglobin,% methemoglobin, and oxygen content in whole blood. *IEEE Transactions on Biomedical Engineering*, (3), 132-138.

Buerk, D. G., & Bridges, E. W. (1986). A simplified algorithm for computing the variation in oxyhemoglobin saturation with pH, PCO_2, T and DPG. *Chemical Engineering Communications*, *47*(1-3), 113-124.

Bunn, H. F. (1980). Regulation of haemoglobin function in mammals. *American Zoologist*, *20*(1), 199-211.

Bunn, H. F. (1981). Evolution of mammalian hemoglobin function. *Blood, 58*(2), 189–197.

Bunn, H. F., & Kitchen, H. (1973). Hemoglobin function in the horse: the role of 2, 3-diphosphoglycerate in modifying the oxygen affinity of maternal and fetal blood. *Blood*, *42*(3), 471-479.

Burns, P. M., Driessen, B., Boston, R., & Gunther, R. A. (2006). Accuracy of a third (dolphin voyager) versus first generation pulse oximeter (nellcor n-180) in predicting arterial oxygen saturation and pulse rate in the anesthetized dog. *Veterinary Anaesthesia and Analgesia*, *33*(5), 281-295.

Burrin, D. G., Ferrell, C. L., Eisemann, J. H., Britton, R. A., & Nienaber, J. A. (1989). Effect of level of nutrition on splanchnic blood flow and oxygen consumption in sheep. *British Journal of Nutrition*, *62*(1), 23-34.

Buss, P. E., & Meltzer, D. G. A. (2001). Changes in respiratory function following the intramuscular administration of etorphine to boer goats (*Capra hircus*). *Journal of the South African Veterinary Association*, *72*(3), 137-142.

Buss, P., Miller, M., Fuller, A., Haw, A., Stout, E., Olea-Popelka, F., & Meyer, L. (2018). Postinduction butorphanol administration alters oxygen consumption to improve blood gases in etorphine-immobilized white rhinoceros. *Veterinary Anaesthesia and Analgesia*, *45*(1), 57-67.

Buss, P., Miller, M., Fuller, A., Haw, A., Wanty, R., Olea-Popelka, F., & Meyer, L. (2016). Cardiovascular effects of etorphine, azaperone, and butorphanol combinations in chemically immobilized captive white rhinoceros (*Ceratotherium simum*). *Journal of Zoo and Wildlife Medicine*, *47*(3), 834-843.

Buss, P., Miller, M., Haw, A., Meyer, L. C., De Lange, S. S., Hofmeyr, M., & Fuller, A. (2017). Tremors in white rhinoceroses (*Ceratotherium simum*) during etorphine–azaperone immobilisation. *Journal of the South African Veterinary Association*, *88*(1), 1-10.

Buss, P., Olea-Popelka, F., Meyer, L., Hofmeyr, J., Mathebula, N., Kruger, M., Brüns, A., Martin, L., & Miller, M. (2015). Evaluation of cardiorespiratory, blood gas, and lactate values during extended immobilization of white rhinoceros (*Ceratotherium simum*). *Journal of Zoo and Wildlife Medicine*, *46*(2), 224-233.

Cambier, C., Di Passio, N., Clerbaux, T., Amory, H., Marville, V., Detry, B., Frans, A., & Gustin, P. (2005). Blood–oxygen binding in healthy Standardbred horses. *The Veterinary Journal*, *169*(2), 251-256.

Causey, M. W., Miller, S., Foster, A., Beekley, A., Zenger, D., & Martin, M. (2011). Validation of noninvasive hemoglobin measurements using the masimo radical-7 SpHb station. *The American Journal of Surgery*, *201*(5), 592-598.

Chaffin, M. K., Matthews, N. S., Cohen, N. D., & Carter, G. K. (1996). Evaluation of pulse oximetry in anaesthetised foals using multiple combinations of transducer type and transducer attachment site. *Equine Veterinary Journal*, *28*(6), 437-445.

Chan, E. D., Chan, M. M., & Chan, M. M. (2013). Pulse oximetry: understanding its basic principles facilitates appreciation of its limitations. *Respiratory Medicine*, *107*(6), 789-799.

Chelopo, N. D., Buss, P. E., Miller, M. A., & Zeiler, G. E. (2022). Cardiopulmonary responses of free-ranging African elephant (*Loxodonta africana*) bulls immobilized with a thiafentanil–azaperone combination. *Veterinary Anaesthesia and Analgesia*, *49*(3), 291-298.

Chu, Z., Wang, Y., You, G., Wang, Q., Ma, N., Li, B., Zhao, L., & Zhou, H. (2020). The P_{50} value detected by the oxygenation-dissociation analyser and blood gas analyser. *Artificial Cells, Nanomedicine, and Biotechnology*, *48*(1), 867-874.

Chung, J. H., Ji, J. Y., Kim, N. S., Seo, Y. H., Gong, H. Y., Kim, J. W., Kim, J. B., & Yoo, S. H. (2014). Efficacy of noninvasive pulse co-oximetry as compared to invasive laboratory-based hemoglobin measurement during spinal anesthesia. *Anesthesia and Pain Medicine*, *9*(4), 277-281.

Citino, S. B., & Bush, M. (2007). Reference cardiopulmonary physiologic parameters for standing, unrestrained white rhinoceroses (*Ceratotherium simum*). *Journal of Zoo and Wildlife Medicine*, *38*(3), 375-379.

Clerbaux, T., Gustin, P., Detry, B., Cao, M. L., & Frans, A. (1993). Comparative study of the oxyhaemoglobin dissociation curve of four mammals: man, dog, horse and cattle. *Comparative Biochemistry and Physiology. Comparative Physiology*, *106*(4), 687-694.

Clerbaux, T., Serteyn, D., Willems, E., & Brasseur, L. (1986). Determination of the standard oxyhemoglobin dissociation curve in horses. Effects of temperature, pH and diphosphoglycerate. *Canadian Journal of Veterinary Research Revue Canadienne de Recherche Veterinaire*, *50*(2), 188-192.

Coghe, J., Uystepruyst, C., Bureau, F., & Lekeux, R. (1999). Non-invasive assessment of arterial haemoglobin oxygen saturation in cattle by pulse oximetry. *Veterinary Record*, *145*(23), 666-669.

Collins, J. A., Rudenski, A., Gibson, J., Howard, L., & O'Driscoll, R. (2015). Relating oxygen partial pressure, saturation and content: the haemoglobin–oxygen dissociation curve. *Breathe*, *11*(3), 194-201.

Cook, S. F. (1928). The action of potassium cyanide and potassium ferricyanide on certain respiratory pigments. *The Journal of General Physiology*, *11*(4), 339.

Crystal, G. J., & Pagel, P. S. (2020). The physiology of oxygen transport by the cardiovascular system: evolution of knowledge. *Journal of Cardiothoracic and Vascular Anesthesia*, *34*(5), 1142-1151.

Cugmas, B., Štruc, E., & Spigulis, J. (2019). Photoplethysmography in dogs and cats: a selection of alternative measurement sites for a pet monitor. *Physiological Measurement*, *40*(1), 01NT02.

Dash, R. K., Korman, B., & Bassingthwaighte, J. B. (2016). Simple accurate mathematical models of blood HbO_2 and $HbCO_2$ dissociation curves at varied physiological conditions: evaluation and comparison with other models. *European Journal of Applied Physiology*, *116*(1), 97-113.

Dawson, J. A., Bastrenta, P., Cavigioli, F., Thio, M., Ong, T., Siew, M. L., Hooper, S. B., & Davis, P. G. (2014). The precision and accuracy of nellcor and masimo oximeters at low oxygen saturations (70%) in newborn lambs. *Archives of Disease in Childhood-Fetal and Neonatal Edition*, *99*(4), F278-F281.

De Rosa, R. C., Romano, G. M., Abbate, R., Corcione, A., & De Robertis, E. (2020). Accuracy and trending ability of hemoglobin measurement by the pulse co-oximeter during vascular surgery. *Journal of Clinical Monitoring and Computing*, *34*(3), 501-508.

Detry, B., Cambier, C., Frans, A., Gustin, P., & Clerbaux, T. (2003). Calculation of bovine haemoglobin oxygen saturation by algorithms integrating age, haemoglobin content, blood pH, partial pressures of oxygen and carbon dioxide in the blood, and temperature. *The Veterinary Journal*, *165*(3), 258-265.

Dhindsa, D. S., Hoverland, A. S., & Metcalfe, J. (1979). Resting hemodynamics and oxygen transport in unanesthetized adult cats. *Respiration Physiology*, *38*(2), 105-114.

Dhindsa, D. S., Metcalfe, J., McKean, T., & Thorne, T. (1974). Comparative studies of the respiratory functions of mammalian blood. XI. Pronghorn antelope (*Antilocapra americana*). *Respiration Physiology*, *21*(3), 297-306.

Dhindsa, D. S., Sedgwick, C. J., & Metcalfe, J. (1972). Comparative studies of the respiratory functions of mammalian blood. VIII. Asian elephant (*Elephas maximus*) and African elephant (*Loxodonta africana africana*). *Respiration Physiology*, *14*(3), 332-342.

Dijkhuizen, P., Buursma, A., Fongers, T. M. E., Gerding, A. M., Oeseburg, B., & Zijlstra, W. G. (1977). The oxygen binding capacity of human haemoglobin. *Pflügers Archiv*, *369*(3), 223-231.

Dominguez de Vlllota, E., Garcia Carmona, M. T., Barat, G., Estada, J., & Avello, F. (1976). The influence of carboxyhaemoglobin on the oxygen-binding capacity of blood: A comparison of manometric (Van Slyke) and optical (co-oximeter) measurements. *British Journal of Anaesthesia*, *48*(2), 111-119.

Dörfelt, R., Diels, J., & Hartmann, K. (2021). Evaluation of the performance of two new generation pulse oximeters in cats at different probe positions and under the influence of vasoconstriction. *Journal of Feline Medicine and Surgery*, *24*(10), 1098612X211063768.

Duke-Novakovski, T. (2019). Retrospective comparison of equine hemoglobin oxygen saturation measured by a human-specific co-oximeter, or derived from an algorithm using temperature-corrected and-uncorrected oxygen tension. *Veterinary Anaesthesia and Analgesia*, *46*(5), 636-642.

Epoc System Manual (2022, April 11). https://www.woodleyequipment.com/docs/system_manual_english.pdf

Erhardt, W., Lendl, C., Hipp, R., Von Hegel, G., Wiesner, G., & Wiesner, H. (1990). The use of pulse oximetry in clinical veterinary anaesthesia. *Journal of the Association of Veterinary Anaesthetists of Great Britain and Ireland*, *17*(1), 30-31.

Fahlman, A. (2008) Advances in wildlife immobilization and anaesthesia: clinical and physiological evaluation in selected species (Ph.D. Dissertation, Swedish University of Agricultural Sciences, Uppsala, Sweden).

Fahlman, Å. (2014). Oxygen therapy. In *Zoo Animal and Wildlife Immobilization and Anesthesia* (pp. 69-81). Wiley-Blackwell, New York, USA.

Fahlman, Å., Edner, A., Wenger, S., Foggin, C., & Nyman, G. (2016). Pulmonary gas exchange and acid–base status during immobilisation of black rhinoceroses (*Diceros bicornis*) in Zimbabwe. *Journal of the South African Veterinary Association*, *87*(1), 1-9.

Fahlman, Å., Pringle, J., Arnemo, J. M., Swenson, J. E., Brunberg, S., & Nyman, G. (2010). Treatment of hypoxemia during anaesthesia of brown bears (*Ursus arctos*). *Journal of Zoo and Wildlife Medicine*, *41*(1), 161-164.

Farrell, K. S., Hopper, K., Cagle, L. A., & Epstein, S. E. (2019). Evaluation of pulse oximetry as a surrogate for PaO_2 in awake dogs breathing room air and anesthetized dogs on mechanical ventilation. *Journal of Veterinary Emergency and Critical Care*, *29*(6), 622-629.

Feiner, J. R., Bickler, P. E., & Mannheimer, P. D. (2010). Accuracy of methemoglobin detection by pulse co-oximetry during hypoxia. *Anesthesia and Analgesia*, *111*(1), 143-148.

Ferrari, M., Mottola, L., & Quaresima, V. (2004). Principles, techniques, and limitations of near infrared spectroscopy. *Canadian Journal of Applied Physiology*, *29*(4), 463-487.

FDA, U. S. (2013). Pulse Oximeters-Premarket Notification Submissions [510 (k) s]: Guidance for Industry and Food and Drug Administration Staff.

Freeman, G. L., & Steinke, J. M. (1993). Evaluation of two oximeters for use in cardiac catheterization laboratories. *Catheterization and Cardiovascular Diagnosis*, *30*(1), 51-57.

Gabel, R. A. (1980). Algorithms for calculating and correcting blood-gas and acid-base variables. *Respiration Physiology*, *42*(3), 211-232.

Gaudio, E., Laubscher, L. L., Pfitzer, S., Raath, J. P., Hoffman, L. C., & De Benedictis, G. M. (2020). Immobilization quality and cardiopulmonary effects of etorphine alone compared with etorphine–azaperone in blesbok (*Damaliscus pygargus phillipsi*). *Veterinary Anaesthesia and Analgesia*, *47*(4), 528-536.

Gehring, H., Duembgen, L., Peterlein, M., Hagelberg, S., & Dibbelt, L. (2007). Hemoximetry as the "gold standard"? Error assessment based on differences among identical blood gas analyzer devices of five manufacturers. *Anesthesia and Analgesia*, *105*(6), S24-S30.

Giguère, S., Sanchez, L. C., & Shih, A. (2014). Accuracy of calculated arterial saturation in oxygen in neonatal foals and effects of monitor, sensor, site of sensor placement, and degree of hypoxemia on the accuracy of pulse oximetry. *Journal of Veterinary Emergency and Critical Care*, *24*(5), 529-535.

Goldman, J. M., Petterson, M. T., Kopotic, R. J., & Barker, S. J. (2000). Masimo signal extraction pulse oximetry. *Journal of Clinical Monitoring and Computing*, *16*(7), 475-483.

Gong, A. K. (1995). Near-patient measurements of methemoglobin, oxygen saturation, and total hemoglobin: Evaluation of a new instrument for adult and neonatal intensive care. *Critical Care Medicine*, *23*(1), 193-201.

Gorelov, V. (2004). Theoretical value of Hüfner's constant. *Anaesthesia*, *59*(1), 97-97.

Gustin, P., Clerbaux, T., Willems, E., Lekeux, P., Lomba, F., & Frans, A. (1988). Oxygen transport properties of blood in two different bovine breeds. *Comparative Biochemistry and Physiology. A, Comparative Physiology*, *89*(4), 553-558.

Grosenbaugh, D. A., Alben, J. O., & Muir, W. W. (1997). Absorbance spectra of inter-species hemoglobins in the visible and near infrared regions. *Journal of Veterinary Emergency and Critical Care*, *7*(1), 36-42.

Grosenbaugh, D. A., & Muir, W. W. (1998). Pulse oximetry: A practical, efficient monitoring method. *Veterinary Medicine, 93*(1), 60-66.

Grubb, T. L., & Anderson, D. E. (2017). Assessment of clinical application of pulse oximetry probes in llamas and alpacas. *Veterinary Medicine and Science*, *3*(3), 169-175.

Habler, O. P., & Messmer, K. F. (1997). The physiology of oxygen transport. *Transfusion Science*, *18*(3), 425-435.

Haskins, S. C. (2012). Acid-base evaluation. In *Advanced Monitoring and Procedures for Small Animal Emergency and Critical Care* (pp. 651-664). Wiley-Blackwell, New York, USA.

Haw, A., Hofmeyr, M., Fuller, A., Buss, P., Miller, M., Fleming, G., & Meyer, L. (2014). Butorphanol with oxygen insufflation corrects etorphine-induced hypoxaemia in chemically immobilized white rhinoceros (*Ceratotherium simum*). *BioMed Central Veterinary Research*, *10*(1), 1-9.

Harboe, M. (1959). A method for determination of hemoglobin in plasma by near-ultraviolet spectrophotometry. *Scandinavian Journal of Clinical and Laboratory Investigation*, *11*(1), 66-70.

Harter, T. S., Morrison, P. R., Mandelman, J. W., Rummer, J. L., Farrell, A. P., Brill, R. W., & Brauner, C. J. (2015a). Validation of the i-STAT system for the analysis of blood gases and acid–base status in juvenile sandbar shark (*Carcharhinus plumbeus*). *Conservation Physiology*, *3*(1), cov002.

Harter, T. S., Reichert, M., Brauner, C. J., & Milsom, W. K. (2015b). Validation of the i-STAT and HemoCue systems for the analysis of blood parameters in the bar-headed goose, *Anser indicus*. *Conservation Physiology*, *3*(1), cov021.

Haymerle, A., Knauer, F., & Walzer, C. (2016). Two methods to adapt the human haemoglobin–oxygen dissociation algorithm to the blood of white rhinoceros (*Ceratotherium simum*) and to determine the accuracy of pulse oximetry. *Veterinary Anaesthesia and Analgesia*, *43*(5), 566-570.

Heard, D. J., Olsen, J. H., & Stover, J. (1992). Cardiopulmonary changes associated with chemical immobilization and recumbency in a white rhinoceros (*Ceratotherium simum*). *Journal of Zoo and Wildlife Medicine*, *23*(2), 197-200.

Heinemann, G., Löschenkohl, K., & Schievelbein, H. (1979). Comparative Evaluation of Different Spectrophotometric Methods for the Determination of Small Amounts of Carboxyhaemoglobin. *Journal of Clinical Chemistry and Clinical Biochemistry*, 17, 647-651.

Hendricks, J. C., & King, L. G. (1993). Practicality, usefulness, and limits of pulse oximetry in critical small animal patients. *Journal of Veterinary Emergency and Critical Care*, *3*(1), 5-12.

Heusch, G. (1998). Hibernating myocardium. *Physiological Reviews*, *78*(4), 1055-1085.

Hill, A. V. (1910). The possible effects of the aggregation of the molecules of haemoglobin on its dissociation curves. *The Journal of Physiology*, *40*, 4-7.

Holmgren, A., & Pernow, B. (1959). Spectrophotometric measurement of oxygen saturation of blood in the determination of cardiac output. A comparison with the van Slyke method. *Scandinavian Journal of Clinical and Laboratory Investigation*, *11*(2), 143-149.

Hüfner, G. (1984). Neue versuche zur bestimmung der sauerstoffcapacitat des blutfarbstoffs. *Archives of Physiology and Biochemistry*, *18*, 130-176.

Humm, K., & Kellett-Gregory, L. (2016). Monitoring small animal patients in the intensive care unit. *In Practice*, *38*, 12-17.

Huss, B. T., Anderson, M. A., Branson, K. R., Wagner-Mann, C. C., & Mann, F. A. (1995). Evaluation of pulse oximeter probes and probe placement in healthy dogs. *Journal of the American Animal Hospital Association*, *31*(1), 9-14.

Hsia, C. C. (1998). Respiratory function of hemoglobin. *New England Journal of Medicine*, *338*(4), 239-248.

i-STAT Technical Bulletin. (2013). PO_2 and calculated oxygen saturated/sO_2. Abbott Point of Care Inc., Abbott Park, IL, USA.

ISO 80601-2-61:2011 Medical electrical equipment- part 2-61: particular requirements for basic safety and essential performance of pulse oximeter equipment (2022, April 15). http://www.iso.org/iso/catalogue_detail.htm?csnumber=51847

ITC AVOXimeter 4000 whole blood co-oximeter user manual (2022, April 11). https://www.manualsdir.com/manuals/602983/itc-avoximeter-4000-whole-blood-co-oximeter.html

Izwan, A., Snelling, E. P., Seymour, R. S., Meyer, L. C., Fuller, A., Haw, A., Mitchell, D., Farrell, A. P., Costello, M., & Maloney, S. K. (2018). Ameliorating the adverse cardiorespiratory effects of chemical immobilization by inducing general anaesthesia in sheep and goats: Implications for physiological studies of large wild mammals. *Journal of Comparative Physiology B*, *188*(6), 991-1003.

Jacobson, J. D., Miller, M. W., Matthews, N. S., Hartsfield, S. M., & Knauer, K. W. (1992). Evaluation of accuracy of pulse oximetry in dogs. *American Journal of Veterinary Research*, *53*(4), 537-540.

Jones, J. H., Longworth, K. E., Lindholm, A., Conley, K. E., Karas, R. H., Kayar, S. R., & Taylor, C. R. (1989). Oxygen transport during exercise in large mammals. I. Adaptive variation in oxygen demand. *Journal of Applied Physiology*, *67*(2), 862-870.

Jensen, L. A., Onyskiw, J. E., & Prasad, N. G. N. (1998). Meta-analysis of arterial oxygen saturation monitoring by pulse oximetry in adults. *Heart and Lung*, *27*(6), 387-408.

Jensen, L. A., & Kjelgaard-Hansen, M. (2006). Method comparison in the clinical laboratory. *Veterinary Clinical Pathology*, *35*(3), 276-286.

Jubran, A. (1999). Pulse oximetry. *Critical Care*, *3*(2), 1-7.

Karas, R. H., Taylor, C. R., Rösler, K., & Hoppeler, H. (1987). Adaptive variation in the mammalian respiratory system in relation to energetic demand: V. Limits to oxygen transport by the circulation. *Respiration Physiology*, *69*(1), 65-79.

Karis, J. H., & Lumb, P. D. (1988). Clinical evaluation of the Edwards Laboratories and oximetrix mixed venous oxygen saturation catheters. *Journal of Cardiothoracic Anesthesia*, *2*(4), 440-444.

Katz, L. M., Mooney, L. A., Gough, K., McGivney, C. L., McCoughlan, M., Hill, E. W., & Anhold, H. (2016). Evaluation of a portable analyzer for determining hemoglobin concentrations and oxygen saturation in whole-blood samples from domestic animals. *Journal of Equine Veterinary Science*, *45*, 64-72.

Keller, G., Cassar, E., Desebbe, O., Lehot, J. J., & Cannesson, M. (2008). Ability of pleth variability index to detect hemodynamic changes induced by passive leg raising in spontaneously breathing volunteers. *Critical Care*, *12*(2), 1-7.

Kim, E. H., Lee, J. H., Song, I. K., Kim, H. S., Jang, Y. E., Yoo, S., & Kim, J. T. (2019). Accuracy of pulse oximeters at low oxygen saturations in children with congenital cyanotic heart disease: An observational study. *Pediatric Anesthesia*, *29*(6), 597-603.

Kimura, S., & Haji, A. (2014). Pharmacological strategy for overcoming opioid-induced ventilatory disturbances. *European Journal of Pharmacology*, *725*, 87-90.

Kock, M. D., Morkel, P., Atkinson, M., & Foggin, C. (1995). Chemical immobilization of free-ranging white rhinoceros (*Ceratotherium simum simum*) in Hwange and Matobo National Parks, Zimbabwe, using combinations of etorphine (M99), fentanyl, xylazine, and detomidine. *Journal of Zoo and Wildlife Medicine*, *26*(2), 207-219.

Koenig, J., McDonell, W., & Valverde, A. (2003). Accuracy of pulse oximetry and capnography in healthy and compromised horses during spontaneous and controlled ventilation. *Canadian Journal of Veterinary Research*, *67*(3), 169.

Lambertsen, C. J., Bunce, P. L., Drabkin, D. L., & Schmidt, C. F. (1952). Relationship of oxygen tension to hemoglobin oxygen saturation in the arterial blood of normal men. *Journal of Applied Physiology*, *4*(12), 873-885.

Le, Q. T., & Courter, D. (2008). Clinical biomarkers for hypoxia targeting. *Cancer and Metastasis Reviews*, *27*(3), 351-362.

Lee, J. H., Park, Y. H., & Kim, J. T. (2014). Current use of noninvasive hemoglobin monitoring in anesthesia. *Current Anesthesiology Reports*, *4*(3), 233-241.

Lindstedt, S. L. (2021). Body size, time and dimensions of oxygen diffusion. *Comparative Biochemistry and Physiology Part A: Molecular and Integrative Physiology*, *252*, 110847.

Louie, A., Feiner, J. R., Bickler, P. E., Rhodes, L., Bernstein, M., & Lucero, J. (2018). Four types of pulse oximeters accurately detect hypoxia during low perfusion and motion. *Anesthesiology*, *128*(3), 520-530.

Louw, A., Cracco, C., Cerf, C., Harf, A., Duvaldestin, P., Lemaire, F., & Brochard, L. (2001). Accuracy of pulse oximetry in the intensive care unit. *Intensive Care Medicine*, *27*(10), 1606-1613.

Lutz, J., Schulze, H. G., & Michael, U. F. (1975). Calculation of O_2 saturation and of the oxyhemoglobin dissociation curve for different species, using a new programmable pocket calculator. *Pflügers Archiv*, *359*(4), 285-295.

Maas, A. H. J., Hamelink, M. L., & De Leeuw, R. J. M. (1970). An evaluation of the spectrophotometric determination of HbO_2, HbCO and Hb in blood with the co-oximeter IL 182. *Clinica Chimica Acta*, *29*(2), 303-309.

MacIntyre, N. R. (2014). Tissue hypoxia: implications for the respiratory clinician. *Respiratory Care*, *59*(10), 1590-1596.

Maikala, R. V. (2010). Modified Beer's Law–historical perspectives and relevance in near-infrared monitoring of optical properties of human tissue. *International Journal of Industrial Ergonomics*, *40*(2), 125-134.

Mair, A., Ferreira, J., Ricco, C., & Nitzan, M. (2020). Appraisal of the 'penumbra effect' using lingual pulse oximetry in anaesthetized dogs and cats. *Veterinary Anaesthesia and Analgesia*, *47*(2), 177-182.

Mallett, S., Halligan, S., Thompson, M., Collins, G. S., & Altman, D. G. (2012). Interpreting diagnostic accuracy studies for patient care. *British Medical Journal, 2, 345*.

Malte, H., Lykkeboe, G., & Wang, T. (2021). The magnitude of the Bohr effect profoundly influences the shape and position of the blood oxygen equilibrium curve. *Comparative Biochemistry and Physiology Part A: Molecular and Integrative Physiology*, *254*, 110880.

Marieb, E. N., & Hoehn, K. (2013). The respiratory system. In *Human Anatomy and Physiology* (9th edn) (pp. 1056-1061). Pearson, London, UK.

Matthews, N. S., Hartke, S., & Allen Jr, J. C. (2003). An evaluation of pulse oximeters in dogs, cats and horses. *Veterinary Anaesthesia and Analgesia*, *30*(1), 3-14.

Mazur, G., Braunitzer, G., & Wright P.G. (1982) Die Primaerstruktur des Haemoglobins vom Breitmaulnashorn (*Ceratotherium simum*, Perissodactyla): *β*2 Glu. *Hoppe Seyler's Zeitschrift für Physiologische Chemie*, *363*, S1077–1086.

McDonald, J., & Lambert, D. G. (2005). Opioid receptors. *Continuing Education in Anaesthesia, Critical Care and Pain*, *5*(1), 22-25.

Mendelson, Y., Cheung, P. W., Neuman, M. R., Fleming, D. G., & Cahn, S. D. (1983). Spectrophotometric investigation of pulsatile blood flow for transcutaneous reflectance oximetry. In *Oxygen Transport to Tissue—IV* (pp. 93-102). Springer, Boston, MA.

Merlet-Bénichou, C., Sinet, M., Blayo, M. C., & Gaudebout, C. (1974). Oxygen-combining capacity in dog. In vitro and in vivo determination. *Respiration Physiology*, *21*(1), 87-99.

Meschia, G., Hellegers, A., Blechner, J., Wolkoff, S., & Barron, D. (1960). Oxygen dissociation curves of the bloods of pregnant sheep, fetal and newborn lambs at various pHs. In *Federation Proceedings*

(Vol. 19, No. 1, pp. 379-379). Federation of American Societies for Experimental Biology, 9650 Rockville Pike, Bethesda, USA.

Meuffels, J., Bertschinger, H., Tindall, B., Pohlin, F., Luther-Binoir, I., Trivedi, S., Boshoff, C.R., & Lueders, I. (2022). Arterial blood gases and cardiorespiratory parameters in etorphine-medetomidine-midazolam immobilized free-ranging and game-farmed southern white rhinoceroses (*Ceratotherium simum simum*) undergoing electro-ejaculation. *Frontiers in Veterinary Science*, *9*, 862100.

Meyer, L. C., Fuller, A., Hofmeyr, M., Buss, P., Miller, M., & Haw, A. (2018). Use of butorphanol and diprenorphine to counter respiratory impairment in the immobilised white rhinoceros (*Ceratotherium simum*). *Journal of the South African Veterinary Association*, *89*(1), 1-8.

Meyer, L. C., Hetem, R. S., Fick, L. G., Mitchell, D., & Fuller, A. (2010). Effects of serotonin agonists and doxapram on respiratory depression and hypoxemia in etorphine-immobilized impala (*Aepyceros melampus*). *Journal of Wildlife Diseases*, *46*(2), 514-524.

Meyer, L. C. R., Hetem, R. S., Mitchell, D., & Fuller, A. (2015). Hypoxia following etorphine administration in goats (*Capra hircus*) results more from pulmonary hypertension than from hypoventilation. *BioMed Central Veterinary Research*, *11*(1), 1-9.

Miller, M., Kruger, M., Kruger, M., Olea-Popelka, F., & Buss, P. (2016). A scoring system to improve decision making and outcomes in the adaptation of recently captured white rhinoceroses (*Ceratotherium simum*) to captivity. *Journal of Wildlife Diseases*, *52*(2s), S78-S85.

Monod, J., Wyman, J., & Changeux, J. P. (1965). On the nature of allosteric transitions: a plausible model. *Journal of Molecular Biology*, *12*(1), 88-118.

Moraga, F., Monge, C., Riquelme, R., & Llanos, A. J. (1996). Fetal and maternal blood oxygen affinity: a comparative study in llamas and sheep. *Comparative Biochemistry and Physiology Part A: Physiology*, *115*(2), 111-115.

Mosing, M., Waldmann, A. D., Sacks, M., Buss, P., Boesch, J. M., Zeiler, G. E., Hosgood, G., Gleed, R.D., Miller, M., Meyer, L.C., & Böhm, S. H. (2020). What hinders pulmonary gas exchange and changes distribution of ventilation in immobilized white rhinoceroses (*Ceratotherium simum*) in lateral recumbency?. *Journal of Applied Physiology*, *129*(5), 1140-1149.

Mtetwa, T. K., Snelling, E. P., Buss, P., Zeiler, G. E., & Meyer, L. C. (2022). Reliability of pulse oximetry at four different attachment sites in immobilized white rhinoceros (*Ceratotherium simum*). *Veterinary Anaesthesia and Analgesia*, *49*(6), 650-655.

Mtetwa, T. K., Zeiler, G. E., Laubscher, L., Pfitzer, S., & Meyer, L. C. (2020). Evaluation of the reliability of pulse oximetry, at different attachment sites, to detect hypoxaemia in immobilized impala (*Aepyceros melampus*). *Veterinary Anaesthesia and Analgesia*, *47*(3), 323-333.

Nahas, G. G. (1951). Spectrophotometric determination of hemoglobin and oxyhemoglobin in whole hemolyzed blood. *Science*, *113*(2947), 723-725.

Nakajima, T., Ohsumi, H., & Kuro, M. (1993). Accuracy of continuous jugular bulb venous oximetry during cardiopulmonary bypass. *Anesthesia and Analgesia*, *77*(6), 1111-1115.

Nijland, R., Nierlich, S., Jongsma, H. W., Nijhuis, J. G., Oeseburg, B., Springer, K., & Mannheimer, P. (1997). Validation of reflectance pulse oximetry: an evaluation of a new sensor in piglets. *Journal of Clinical Monitoring*, *13*(1), 43-49.

Nixdorff, J., Zablotski, Y., Hartmann, K., & Dörfelt, R. (2021). Comparison of transmittance and reflectance pulse oximetry in anesthetized dogs. *Frontiers in Veterinary Science*, *8*, 643966.

Norton, J. R., Jackson, P. G. G., & Taylor, P. M. (1998). Measurement of arterial oxygen-haemoglobin saturation in newborn lambs by pulse oximetry. *Veterinary Record*, *142*(5), 107-109.

Novy, M. J., Hoversland, A. S., Dhindsa, D. S., & James, M. (1973). Blood oxygen affinity and hemoglobin type in adult, newborn, and fetal pigs. *Respiration Physiology*, *19*(1), 1-11.

Novy, M. J., & Parer, J. T. (1969). Absence of high blood oxygen affinity in the fetal cat. *Respiration Physiology*, *6*(2), 144-150.

Oladokun, O. O., & Atere, TG (2020). Haemoglobin: structure, synthesis and oxygen transport. In *Sickle Cell Disease: From the Laboratory to Clinical Practice* (pp. 1-12). Cambridge Scholars Publishing, Newcastle upon Tyne, UK.

Pattinson, K. T. (2008). Opioids and the control of respiration. *British Journal of Anaesthesia*, *100*(6), 747-758.

Perrone, S., Bracci, R., & Buonocore, G. (2002). New biomarkers of fetal-neonatal hypoxic stress. *Acta Paediatrica*, *91*, 135-138.

Perutz, M. F. (1983). Species adaptation in a protein molecule. *Molecular Biology and Evolution*, *1*(1), 1-28.

Perutz, M. F., Wilkinson, A. J., Paoli, M., & Dodson, G. G. (1998). The stereochemical mechanism of the cooperative effects in hemoglobin revisited. *Annual Review of Biophysics and Biomolecular Structure*, *27*(1), 1-34.

Petschow, D., Wurdinger, I., Baumann, R., Duhm, J., Braunitzer, G., & Bauer, C. (1977). Causes of high blood O_2 affinity of animals living at high altitude. *Journal of Applied Physiology*, *42*(2), 139-143.

Pfitzer, S., Meyer, L., Laubscher, L., Warren, K., Vaughan-Higgins, R., Raath, J. P., & Laurence, M. (2021). Comparison of some cardiopulmonary effects of etorphine and thiafentanil during the chemical immobilization of blesbok (*Damaliscus pygargus phillipsi*). *Veterinary Anaesthesia and Analgesia*, *48*(1), 42-52.

Pittman, R. N. (2011). Regulation of tissue oxygenation. In *Colloquium Series on Integrated Systems Physiology: From Molecule to Function* (Vol. 3, No. 3, pp. 1-100). Morgan and Claypool Life Sciences, California, USA.

Pohlin, F., Hooijberg, E. H., Buss, P., Huber, N., Viljoen, F. P., Blackhurst, D., & Meyer, L. C. (2020). A comparison of hematological, immunological, and stress responses to capture and transport in wild white rhinoceros bulls (*Ceratotherium simum simum*) supplemented with azaperone or midazolam. *Frontiers in Veterinary Science*, 790, https://doi.org/10.3389/fvets.2020.569576.

Pologe, J. A. (1987). Pulse oximetry: technical aspects of machine design. *International Anesthesiology Clinics*, *25*(3), 137-153.

Popel, A. S. (1989). Theory of oxygen transport to tissue. *Critical Reviews in Biomedical Engineering*, *17*(3), 257.

Portas, T. J. (2004). A review of drugs and techniques used for sedation and anaesthesia in captive rhinoceros species. *Australian Veterinary Journal*, *82*(9), 542-549.

Proulx, J. (1999). Respiratory monitoring: arterial blood gas analysis, pulse oximetry, and end-tidal carbon dioxide analysis. *Clinical Techniques in Small Animal Practice*, *14*(4), 227-230.

Quinn, C. T., Raisis, A. L., & Musk, G. C. (2013). Evaluation of Masimo signal extraction technology pulse oximetry in anaesthetized pregnant sheep. *Veterinary Anaesthesia and Analgesia*, *40*(2), 149-156.

Read, M. R. (2003). A Review of alpha$_2$ adrenoreceptor agonists and the development of hypoxemia in domestic and wild ruminants. *Journal of Zoo and Wildlife Medicine*, *34*(2), 134-138.

Read, M. R., Rondeau, J., & Kwong, G. P. (2016). Validation of noninvasive hemoglobin measurements using co-oximetry in anesthetized dogs. *The Canadian Veterinary Journal*, *57*(11), 1161.

Reddy, M.V.S. (1997). Probes. In *Design of Pulse Oximeters* (pp. 159-176). CRC Press, Florida, USA.

Reiners, J. K., Rossdeutscher, W., Hopster, K., & Kästner, S. B. R. (2018). Development and clinical evaluation of a new sensor design for buccal pulse oximetry in horses. *Equine Veterinary Journal*, *50*(2), 228-234.

Reiners, J. K., Hellmann, N., Schmidt, J., & Kästner, S. B. (2019). Odd haemoglobins in odd-toed ungulates: Impact of selected haemoglobin characteristics of the white rhinoceros (*Ceratotherium simum*) on the monitoring of the arterial oxygen saturation of haemoglobin. *Plos One*, *14*(12), e0226851.

Revsbech, I. G., & Fago, A. (2017). Regulation of blood oxygen transport in hibernating mammals. *Journal of Comparative Physiology B*, *187*(5), 847-856.

Reynolds, K. J., Palayiwa, E., Moyle, J. T., Sykes, M. K., & Hahn, C. E. (1993). The effect of dyshemoglobins on pulse oximetry: Part I, Theoretical approach and Part II, Experimental results using an in vitro test system. *Journal of Clinical Monitoring*, *9*(2), 81-90.

Riegel, K., Bartels, H., Buss, I. O., Wright, P. G., Kleihauer, E., Luck, C. P., Parer, J. T., & Metcalfe, J. (1967). Comparative studies of the respiratory functions of mammalian blood IV. Fetal and adult African elephant blood. *Respiration Physiology*, *2*(2), 182-195.

Robertson, S. A., & Bailey, J. E. (2002). Aerosolized salbutamol (albuterol) improves PaO_2 in hypoxaemic anaesthetized horses–a prospective clinical trial in 81 horses. *Veterinary Anaesthesia and Analgesia*, *29*(4), 212-218.

Romer, L. M., Dempsey, J. A., Lovering, A., & Eldridge, M. (2007). Exercise-induced arterial hypoxemia: consequences for locomotor muscle fatigue. In *Hypoxia and Exercise* (pp. 47-55). Springer USA.

Roughton, F. J., & Severinghaus, J. W. (1973). Accurate determination of O_2 dissociation curve of human blood above 98.7 percent saturation with data on O_2 solubility in unmodified human blood from 0 degrees to 37 degrees c. *Journal of Applied Physiology*, *35*(6), 861-869.

Sakr, Y. (2010). Techniques to assess tissue oxygenation in the clinical setting. *Transfusion and Apheresis Science*, *43*(1), 79-94.

Save the rhino (2022, November 30). https://www.savetherhino.org/rhino-info/poaching-stats/

Schell, R. M., & Cole, D. J. (2000). Cerebral monitoring: jugular venous oximetry. *Anesthesia and Analgesia*, *90*(3), 559-566.

Scherrer, M., & Bachofen, H. (1972). The oxygen-combining capacity of hemoglobin. *The Journal of the American Society of Anesthesiologists*, *36*(2), 190-190.

Scheufler, K. M. (2004). Tissue oxygenation and capacity to deliver O_2 do the two go together?. *Transfusion and Apheresis Science*, *31*(1), 45-54.

Schmidt-Nielsen, K. (1970). Energy metabolism, body size, and problems of scaling. In *Federation Proceedings* (Vol. 29, No. 4, pp. 1524-1532). Federation of American Societies for Experimental Biology, 9650 Rockville Pike, Bethesda, USA.

Schmidt-Neilsen, K., & Larimer, J. L. (1958). Oxygen dissociation curves of mammalian blood in relation to body size. *American Journal of Physiology-Legacy Content*, *195*(2), 424-428.

Schowalter, J. (1997). Calibration. In *Design of Pulse Oximeters* (pp. 159-176). CRC Press, Florida, USA.

Scott, N. E., Haskins, S. C., Aldrich, J., Rezende, M., Gallagher, R. M., & Henderson, M. M. (2005). Comparison of measured oxyhemoglobin saturation and oxygen content with analyzer-calculated values and hand-calculated values obtained in unsedated healthy dogs. *American Journal of Veterinary Research*, *66*(7), 1273-1277.

Semjonov, A., Andrianov, V., Raath, J. P., Orro, T., Laubscher, L., Pfitzer, S., & Tiirats, T. (2018). Evaluation of butorphanol–azaperone–medetomidine (BAM) in captive blesbok immobilization (*Damaliscus pygargus phillipsi*). *Veterinary Anaesthesia and Analgesia*, *45*(4), 496-501.

Sendroy Jr, J. (1932). Manometric analysis of gas mixtures: VI. carbon monoxide by absorption with blood. *Journal of Biological Chemistry*, *95*(2), 599-611.

Sendroy, Jr, J., Dillon, R. T., & Van Slyke, D. D. (1934). Studies of gas and electrolyte equilibria in blood: XIX. The solubility and physical state of uncombined oxygen in blood. *Journal of Biological Chemistry*, *105*(3), 597-632.

Serianni, R., Barash, J., Bentley, T., Sharma, P., Fontana, J. L., Via, D., Bunger, D. R., & Mongan, P. D. (2003). Porcine-specific hemoglobin saturation measurements. *Journal of Applied Physiology*, *94*(2), 561-566.

Severinghaus, J. W. (1966). Blood gas calculator. *Journal of Applied Physiology*, *21*(3), 1108-1116.

Severinghaus, J. W. (1979). Simple, accurate equations for human blood O_2 dissociation computations. *Journal of Applied Physiology*, *46*(3), 599-602.

Severinghaus, J. W., & Astrup, P. B. (1986). History of blood gas analysis. VI. Oximetry. *Journal of Clinical Monitoring*, *2*(4), 270-288.

Sharan, M., Singh, M. P., & Aminataei, A. (1989). A mathematical model for the computation of the oxygen dissociation curve in human blood. *Biosystems*, *22*(3), 249-260.

Sharan, M., & Singh, M. P. (1984). Equivalence between one step kinetics and Hill's equation. *Journal of Biomedical Engineering*, *6*(4), 297-301.

Shiao, S. Y. P. (2002). Functional versus fractional oxygen saturation readings: bias and agreement using simulated solutions and adult blood. *Biological Research for Nursing*, *3*(4), 210-221.

Shimada, Y., Nakashima, K., Fujiwara, Y., Komatsu, T., Kawanishi, M., Takezawa, J., & Takatani, S. (1991). Evaluation of a new reflectance pulse oximeter for clinical applications. *Medical and Biological Engineering and Computing*, *29*(5), 557-561.

Shimizu, S., Enoki, Y., Kohzuki, H., Ohga, Y., & Sakata, S. (1986). Determination of Hüfner's factor and inactive hemoglobins in human, canine, and murine blood. *The Japanese Journal of Physiology*, *36*(5), 1047-1051.

Shook, J. E., Watkins, W. D., & Camporesi, E. M. (1990). Differential roles of opioid receptors in respiration, respiratory disease, and opiate-induced respiratory depression. *American Review of Respiratory Disease*, *142*(4), 895-909.

Sidi, A., Rush, W., Gravenstein, N., Ruiz, B., Paulus, D. A., & Davis, R. F. (1987). Pulse oximetry fails to accurately detect low levels of arterial hemoglobin oxygen saturation in dogs. *Journal of Clinical Monitoring*, *3*(4), 257-262.

Siggaard-Andersen, O. (1977). The van Slyke equation. *Scandinavian Journal of Clinical and Laboratory Investigation*, *37*(sup146), 15-20.

Siggaard-Andersen, O., Nørgaard-Pedersen, B., & Rem, J. (1972). Hemoglobin pigments. Spectrophotometric determination of oxy-, carboxy-, met-, and sulfhemoglobin in capillary blood. *Clinica Chimica Acta*, *42*(1), 85-100.

Siggaard-Andersen, O., Wimberley, P. D., Fogh-Andersen, N., & Gøthgen, I. H. (1988). Measured and derived quantities with modern pH and blood gas equipment: calculation algorithms with 54 equations. *Scandinavian Journal of Clinical and Laboratory Investigation*, *48*(sup189), 7-15.

Siggaard-Andersen, O., Wimberley, P. D., Göthgen, I., & Siggaard-Andersen, M. (1984). A mathematical model of the hemoglobin-oxygen dissociation curve of human blood and of the oxygen partial pressure as a function of temperature. *Clinical Chemistry*, *30*(10), 1646-1651.

Smale, K., & Butler, P. J. (1994). Temperature and pH effects on the oxygen equilibrium curve of the thoroughbred horse. *Respiration Physiology*, *97*(3), 293-300.

Speers-Roesch, B., Richards, J. G., Brauner, C. J., Farrell, A. P., Hickey, A. J., Wang, Y. S., & Renshaw, G. M. (2012). Hypoxia tolerance in elasmobranchs. I. Critical oxygen tension as a measure of blood oxygen transport during hypoxia exposure. *Journal of Experimental Biology*, *215*(1), 93-102.

Storz, J. F. (2007). Haemoglobin function and physiological adaptation to hypoxia in high-altitude mammals. *Journal of Mammalogy*, *88*(1), 24-31.

Sugino, S., Kanaya, N., Mizuuchi, M., Nakayama, M., & Namiki, A. (2004). Forehead is as sensitive as finger pulse oximetry during general anesthesia, *Canadian Journal of Anesthesia*, *51*(5), 432-436.

Svedberg, T., & Fåhraeus, R. (1926). A new method for the determination of the molecular weight of the proteins. *Journal of the American Chemical Society*, *48*(2), 430-438.

Swets, J. A. (1988). Measuring the accuracy of diagnostic systems. *Science*, *240*(4857), 1285-1293.

Tánczos, K., & Molnár, Z. (2013). The oxygen supply–demand balance: a monitoring challenge. *Best Practice and Research Clinical Anaesthesiology*, *27*(2), 201-207.

Tayari, H., Flaherty, D., Schauvliege, S., La Rosa, L., & Auckburally, A. (2022). Accuracy and trending capability of haemoglobin measurement by noninvasive pulse co-oximetry in anaesthetized horses. *Veterinary Anaesthesia and Analgesia*, *49*(1), 76-84.

Tayari, H., Flaherty, D., Yamaoka, T. T., & Auckburally, A. (2021). Assessment of pulse co-oximetry technology after in vivo adjustment in anaesthetized dogs. *Veterinary Anaesthesia and Analgesia*, *48*(3), 297-304.

The Point-of-Care Coordinators online Resource (2022, November 30). http://www.pointofcare.net/vendors/avox.htm

Tucker, V. A. (1968). Oxygen dissociation curve of echidna blood. *Comparative Biochemistry and Physiology*, *24*(1), 307-310.

Tucker, V. A. (1967). Method for oxygen content and dissociation curves on microliter blood samples. *Journal of Applied Physiology*, *23*(3), 410-414.

Uystepruyst, C. H., Coghe, J., Bureau, F., & Lekeux, P. (2000). Evaluation of accuracy of pulse oximetry in newborn calves. *The Veterinary Journal*, *159*(1), 71-76.

Van Kampen, E. J., & Zijlstra, W. G. (1983). Spectrophotometry of haemoglobin and haemoglobin derivatives. *Advances in Clinical Chemistry*, *23*, 199-257.

Van Slyke, D. D., & Neill, J. M. (1924). The determination of gases in blood and other solutions by vacuum extraction and manometric measurement. I. *Journal of Biological Chemistry*, *61*(2), 523-573.

Langhout, M. V. Z., Caraguel, C. G., Raath, J. P., & Boardman, W. S. (2016). Evaluation of etorphine and midazolam anesthesia, and the effect of intravenous butorphanol on cardiopulmonary parameters in game-ranched white rhinoceroses (*Ceratotherium simum*). *Journal of Zoo and Wildlife Medicine*, *47*(3), 827-833.

Verhovsek, M., Henderson, M. P., Cox, G., Luo, H. Y., Steinberg, M. H., & Chui, D. H. (2010). Unexpectedly low pulse oximetry measurements associated with variant hemoglobins: a systematic review. *American Journal of Hematology*, *85*(11), 882-885.

Waller, J. L., Kaplan, J. A., Bauman, D. I., & Craver, J. M. (1982). Clinical evaluation of a new fiberoptic catheter oximeter during cardiac surgery. *Anesthesia and Analgesia*, *61*(8), 676-679.

Ward, J. (2006). Oxygen delivery and demand. *Surgery*, *24*(10), 354-360.

Weber, R. E. (2007). High-altitude adaptations in vertebrate hemoglobins. *Respiratory Physiology and Neurobiology*, *158*(2-3), 132-142.

Weber, R. E., & Campbell, K. L. (2011). Temperature dependence of haemoglobin–oxygen affinity in heterothermic vertebrates: mechanisms and biological significance. *Acta Physiologica*, *202*(3), 549-562.

Weber, R. E., & Wells, R. M. G. (1989). Haemoglobin structure and function. *Comparative Pulmonary Physiology*, *39*, 279-310.

Weininger, S. (2007). Effective standards and regulatory tools for respiratory gas monitors and pulse oximeters: the role of the engineer and clinician. *Anesthesia and Analgesia*, *105*(6), S95-S99.

Weiss, H. R., & Sinha, A. K. (1978). Regional oxygen saturation of small arteries and veins in the canine myocardium. *Circulation Research*, *42*(1), 119-126.

Wells, R. M. (1999). Evolution of haemoglobin function: molecular adaptations to environment. *Clinical and Experimental Pharmacology and Physiology*, *26*(8), 591-595.

Wells, R. M., Forster, M. E., Davison, W., Taylor, H. H., Davie, P. S., & Satchell, G. H. (1986). Blood oxygen transport in the free-swimming hagfish, *Eptatretus cirrhatus*. *Journal of Experimental Biology*, *123*(1), 43-53.

Wenger, S., Boardman, W., Buss, P., Govender, D., & Foggin, C. (2007). The cardiopulmonary effects of etorphine, azaperone, detomidine, and butorphanol in field-anesthetized white rhinoceroses (*Ceratotherium simum*). *Journal of Zoo and Wildlife Medicine*, *38*(3), 380-387.

West, E., Bardell, D., & Senior, J. M. (2014). Comparison of the EPOC and i-STAT analysers for canine blood gas and electrolyte analysis. *Journal of Small Animal Practice*, *55*(3), 139-144.

Whitehair, K. J., Watney, G. C., Leith, D. E., & Debowes, R. M. (1990). Pulse oximetry in horses. *Veterinary Surgery*, *19*(3), 243-248.

Wideman Jr, R. F., & Kirby, Y. K. (1995). Evidence of a ventilation-perfusion mismatch during acute unilateral pulmonary artery occlusion in broilers. *Poultry Science*, *74*(7), 1209-1217.

Winslow, R. M., Morrissey, J. M., Berger, R. L., Smith, P. D., & Gibson, C. C. (1978). Variability of oxygen affinity of normal blood: an automated method of measurement. *Journal of Applied Physiology*, *45*(2), 289-297.

World Health Organization. (2013). Pocket book of hospital care for children: guidelines for the management of common childhood illnesses. In *Oxygen Therapy* (pp. 312). World Health Organization, Geneva, Switzerland.

Wukitsch, M. W., Petterson, M. T., Tobler, D. R., & Pologe, J. A. (1988). Pulse oximetry: analysis of theory, technology, and practice. *Journal of Clinical Monitoring*, *4*(4), 290-301.

Young, S. S., Skeans, S. M., Lamca, J. E., & Chapman, R. W. (2002). Agreement of SpO_2, SaO_2 and ScO_2 in anesthetized cynomolgus monkeys (*Macaca fascicularis*). *Veterinary Anaesthesia and Analgesia*, *29*(3), 150-155.

Zaouter, C., & Zavorsky, G. S. (2012). The measurement of carboxyhemoglobin and methemoglobin using a non-invasive pulse co-oximeter. *Respiratory Physiology and Neurobiology*, *182*(2-3), 88-92.

Zeiler, G. E., & Stegmann, G. F. (2012). Anaesthetic management of a 10-month-old white rhinoceros (*Ceratotherium simum*) calf for emergency exploratory celiotomy. *Journal of the South African Veterinary Association*, *83*(1), 1-5.

Zijlstra, W. G., & Buursma, A. (1997). Spectrophotometry of hemoglobin: absorption spectra of bovine oxyhemoglobin, deoxyhemoglobin, carboxyhemoglobin, and methemoglobin. *Comparative Biochemistry and Physiology Part B: Biochemistry and Molecular Biology*, *118*(4), 743-749.

Zijlstra, W. G., & Buursma, A. (1987). Spectrophotometry of hemoglobin: a comparison of dog and man. *Comparative Biochemistry and Physiology. B, Comparative Biochemistry*, *88*(1), 251-255.

Zijlstra, W. G., Buursma, A., Falke, H. E., & Catsburg, J. F. (1994). Spectrophotometry of hemoglobin: absorption spectra of rat oxyhemoglobin, deoxyhemoglobin, carboxyhemoglobin, and methemoglobin. *Comparative Biochemistry and Physiology Part B: Comparative Biochemistry*, *107*(1), 161-166.

Zijlstra, W. G., Buursma, A., & Meeuwsen-Van der Roest, W. P. (1991). Absorption spectra of human fetal and adult oxyhemoglobin, de-oxyhemoglobin, carboxyhemoglobin, and methemoglobin. *Clinical Chemistry*, *37*(9), 1633-1638.

Zoff, A., Dugdale, A. H. A., Scarabelli, S., & Rioja, E. (2019). Evaluation of pulse co-oximetry to determine haemoglobin saturation with oxygen and haemoglobin concentration in anaesthetized horses: a retrospective study. *Veterinary Anaesthesia and Analgesia*, *46*(4), 452-457.

Zwart, A., Buursma, A., Van Kampen, E. J., Oeseburg, B., Van der Ploeg, P. H. W., & Zijlstra, W. G. (1981). A multi-wavelength spectrophotometric method for the simultaneous determination of five haemoglobin derivatives. *Journal of Clinical Chemistry and Clinical Biochemistry*, 19, 457-463.

Zwart, A., Buursma, A., Van Kampen, E. J., & Zijlstra, W. G. (1984). Multicomponent analysis of hemoglobin derivatives with reversed-optics spectrophotometer. *Clinical Chemistry*, *30*(3), 373-379.

Zwart, A., Buursma, A., & Zijlstra, W. G. (1987). A new trend in blood gas chemistry: the measurement of clinically relevant hemoglobin derivatives. Performance of the osm3 hemoximeter. *Scandinavian Journal of Clinical and Laboratory Investigation*, *47*(sup188), 57-60.

Addendums……..206

A.1 University of Pretoria animal ethics certificate……206

A.2 SANParks animal ethics certificate……...207

A.3 University of Pretoria animal ethics certificate……....208

A.4 SANParks animal ethics certificate……..209

A.5 Proof of published article……..…210

Addendums

A.1 University of Pretoria animal ethics certificate

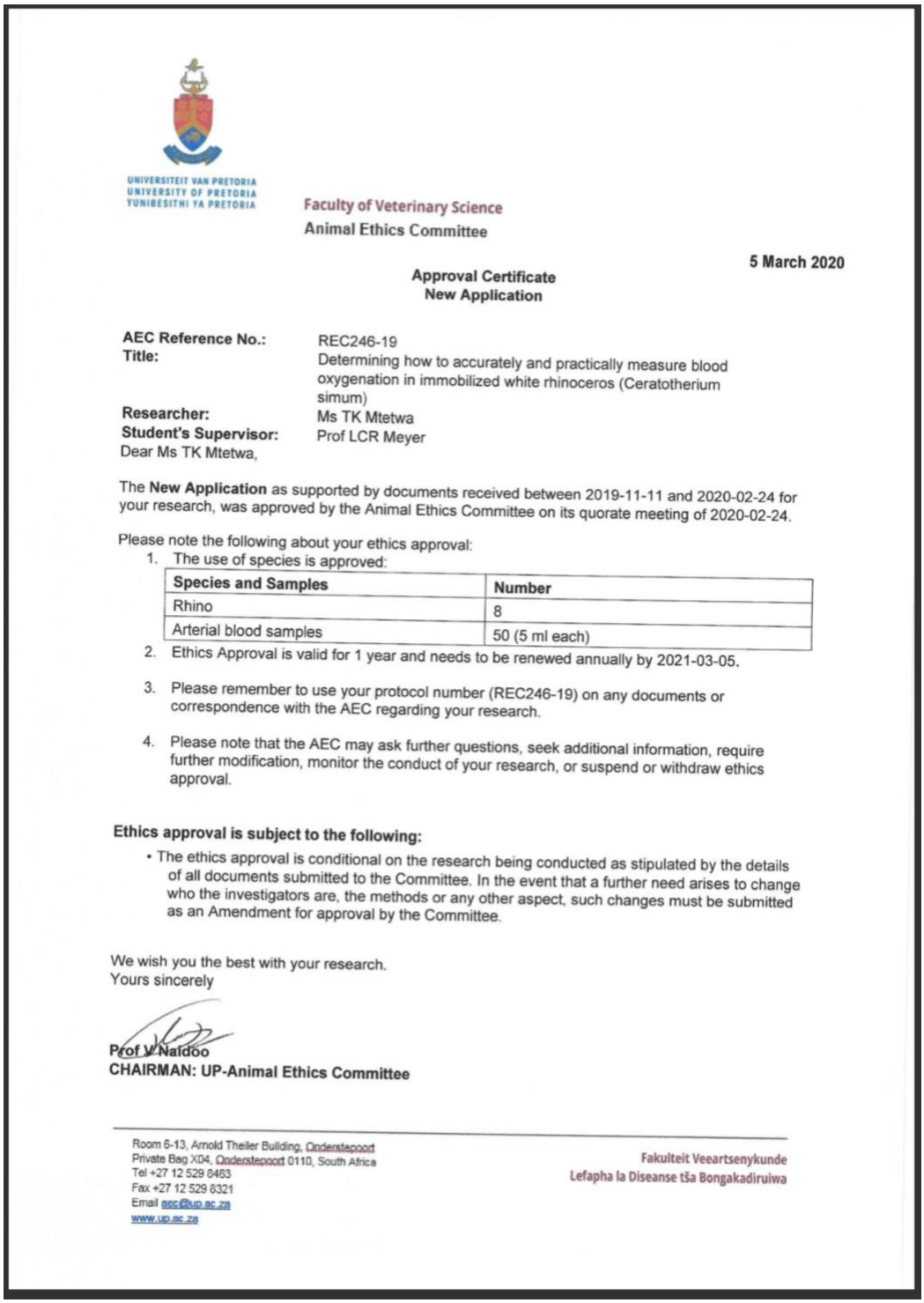

UNIVERSITEIT VAN PRETORIA
UNIVERSITY OF PRETORIA
YUNIBESITHI YA PRETORIA

Faculty of Veterinary Science
Animal Ethics Committee

5 March 2020

Approval Certificate
New Application

AEC Reference No.: REC246-19
Title: Determining how to accurately and practically measure blood oxygenation in immobilized white rhinoceros (Ceratotherium simum)
Researcher: Ms TK Mtetwa
Student's Supervisor: Prof LCR Meyer

Dear Ms TK Mtetwa,

The **New Application** as supported by documents received between 2019-11-11 and 2020-02-24 for your research, was approved by the Animal Ethics Committee on its quorate meeting of 2020-02-24.

Please note the following about your ethics approval:

1. The use of species is approved:

Species and Samples	Number
Rhino	8
Arterial blood samples	50 (5 ml each)

2. Ethics Approval is valid for 1 year and needs to be renewed annually by 2021-03-05.
3. Please remember to use your protocol number (REC246-19) on any documents or correspondence with the AEC regarding your research.
4. Please note that the AEC may ask further questions, seek additional information, require further modification, monitor the conduct of your research, or suspend or withdraw ethics approval.

Ethics approval is subject to the following:

- The ethics approval is conditional on the research being conducted as stipulated by the details of all documents submitted to the Committee. In the event that a further need arises to change who the investigators are, the methods or any other aspect, such changes must be submitted as an Amendment for approval by the Committee.

We wish you the best with your research.
Yours sincerely

Prof V Naidoo
CHAIRMAN: UP-Animal Ethics Committee

Room 6-13, Arnold Theiler Building, Onderstepoort
Private Bag X04, Onderstepoort 0110, South Africa
Tel +27 12 529 8463
Fax +27 12 529 8321
Email aec@up.ac.za
www.up.ac.za

Fakulteit Veeartsenykunde
Lefapha la Diseanse tša Bongakadiruiwa

UNIVERSITEIT VAN PRETORIA
UNIVERSITY OF PRETORIA
YUNIBESITHI YA PRETORIA

Faculty of Veterinary Science
Animal Ethics Committee

7 April 2021

Approval Certificate
Annual Renewal
(EXT1)

AEC Reference No.: REC246-19
Title: Determining how to accurately and practically measure blood oxygenation in immobilized white rhinoceros (Ceratotherium simum)
Researcher: Ms TK Mtetwa
Student's Supervisor: Prof LCR Meyer

Dear Ms TK Mtetwa,

The **Annual Renewal** as supported by documents received between 2021-03-11 and 2021-04-01 for your research, was approved by the Animal Ethics Committee on its quorate meeting of 2021-04-01.

Please note the following about your ethics approval:

1. The use of species is approved:

Species	**Number Available**
Rhino	8
Samples	
Arterial blood samples	50 (5ml each)

2. Ethics Approval is valid for 1 year and needs to be renewed annually by 2022-04-07.
3. Please remember to use your protocol number (REC246-19) on any documents or correspondence with the AEC regarding your research.
4. Please note that the AEC may ask further questions, seek additional information, require further modification, monitor the conduct of your research, or suspend or withdraw ethics approval.
5. **All incidents** must be reported by the PI by email to Ms Marleze Rheeder (AEC Coordinator) within 3 days, and must be subsequently submitted electronically on the application system within 14 days.
6. The committee also requests that you record major procedures undertaken during your study for own-archiving, using any available digital recording system that captures in adequate quality, as it may be required if the committee needs to evaluate a complaint. However, if the committee has monitored the procedure previously or if it is generally can be considered routine, such recording will not be required.

Ethics approval is subject to the following:

- The ethics approval is conditional on the research being conducted as stipulated by the details of all documents submitted to the Committee. In the event that a further need arises to change who the investigators are, the methods or any other aspect, such changes must be submitted as an Amendment for approval by the Committee.

A.2 SANParks animal ethics certificate

To develop and manage a system of national parks that represents the biodiversity, landscapes, and associated heritage assets of South Africa for the sustainable use and benefit of all.

South African NATIONAL PARKS

ANIMAL USE AND CARE COMMITTEE: APPROVAL CERTIFICATE

A. PROJECT DETAILS

Project Title	**Determining how to accurately measure blood oxygenation in immobilized white rhinoceros (*Ceratotherium simum*)**		
Researcher	**T Mtetwa**	SANParks Reference No.	**012-20**

B. CONDITIONS OF APPROVAL

- There must be an approved and signed research contract with SANParks prior to implementation of this project.
- Ethics approval is valid for the duration of the SANParks research contract.
- Any changes to the original research protocol must be submitted in the appropriate format to the AUCC for evaluation and approval.
- The AUCC must be informed of mortalities or injuries beyond those expected in the approved research protocol.

Submission Date:	30 June 2020	APPROVED
AUCC Approval Date:	06 August 2020	Signature:

Note: In accordance with the South African National Standard (SANS 10386-2008): "The Care and Use of Animals for Scientific Purposes", an animal is regarded as being "live, sentient non-human vertebrate, including eggs, foetuses and embryos, that is, fish, amphibians, reptiles, birds and mammals, including domestic animals, purpose-bred animals, farm animals, wildlife and higher invertebrates such as advanced members from the Cephalopoda and Decapoda".

addo elephant
agulhas
augrabies falls
bontebok
golden gate highlands
karoo
kgalagadi transfrontier
knysna lake area
kruger
mapungubwe
marakele
mountain zebra
namaqua
table mountain
tankwa-karoo
tsitsikamma
|ai-|ais/richtersveld
vaalbos
west coast
wilderness

643 Leyds Street
MUCKLENEUK
0002

P.O. Box 787
PRETORIA
0001

Tel: 012 426-5000

central reservations: 012 428 9111
reservations@sanparks.org
www.sanparks.org

A.3 University of Pretoria animal ethics certificate

UNIVERSITEIT VAN PRETORIA
UNIVERSITY OF PRETORIA
YUNIBESITHI YA PRETORIA

Animal Ethics Committee

Extension No. 1

PROJECT TITLE	**Cardiopulmonary effects of etorphine-based drug combinations in boma-habituated vs. free-ranging white rhinoceros *(Ceratotherium simum)***
PROJECT NUMBER	**V101-15**
RESEARCHER/PRINCIPAL INVESTIGATOR	**JM Boesch**

STUDENT NUMBER (where applicable)	**Not UP**
DISSERTATION/THESIS SUBMITTED FOR	**PhD**

ANIMAL SPECIES	**White rhinoceros *(Ceratotherium simum)***	
NUMBER OF ANIMALS	**28**	
Approval period to use animals for research/testing purposes		**November 2016-November 2017**
SUPERVISOR	**Dr. LCR Meyer**	

KINDLY NOTE:

Should there be a change in the species or number of animal/s required, or the experimental procedure/s - please submit an amendment form to the UP Animal Ethics Committee for approval before commencing with the experiment

APPROVED	Date 22 November 2016
CHAIRMAN: UP Animal Ethics Committee	Signature

S4285-15

A.4 SANParks animal ethics certificate

To develop and manage a system of national parks that represents the biodiversity, landscapes, and associated heritage assets of South Africa for the sustainable use and benefit of all.

South African NATIONAL PARKS

ANIMAL USE AND CARE COMMITTEE: APPLICATION FOR APPROVAL

A. PROJECT DETAILS

Project Title	"CARDIOPULMONARY EFFECTS OF ETORPHINE-BASED DRUG COMBINATIONS IN BOMA-HABITUATED VS. FREE-RANGING WHITE RHINOCEROS (*Ceratotherium simum*)"		
Researcher	Dr J. M. Boosch	SANParks Reference No.	001/16

B. SCIENTIFIC REVIEW STATEMENT

(Every application should be supported by a declaration that it has undergone prior scientific review through at least one of the SANParks Research Nodes.)

This research protocol has been reviewed by the Savanna and / or Arid Research Centres SANParks and has been judged to be of national importance, designed in accordance with accepted scientific practices and norms and is in the opinion of the reviewers likely to be successful in achieving its objective.

Name: [illegible] Designation: Acting M.E. Signature: [signature] Date: 10/8/2016

*As per SANParks Research Approval process

Note: In accordance with the South African National Standard (SANS 10386-2008): "The Care and Use of Animals for Scientific Purposes", an animal is regarded as being 'live, sentient non-human vertebrate, including eggs, foetuses and embryos, that is, fish, amphibians, reptiles, birds and mammals, including domestic animals, purpose-bred animals, farm animals, wildlife and higher invertebrates such as advanced members from the Cephalopoda and Decapoda".

This form should be submitted with the SANParks standard Research Project Application, and (where relevant) the following supporting documents: CVs of practitioners in support of competence to handle or treat animals, notices of approval of other ethics committees, diagrams or references illustrating the equipment and/or techniques to be applied.

For Administrative Purposes			
Submission Date	9th Dec 2015	APPROVED	DISAPPROVED
AUCC approval / Disapproval Date	10/3/2016	Signature [signature]	
Reason for Decision	The study fully meets ethical standards		

643 Leyds Street
MUCKLENEUK
0002

P.O. Box 787
PRETORIA
0001

Tel: 012 426 5000

central reservations: 012 428 9111
reservations@sanparks.org
www.sanparks.org

A.5 Proof of published article

Veterinary Anaesthesia and Analgesia 2022, **49**, 650–655 https://doi.org/10.1016/j.vaa.2022.08.006

SHORT COMMUNICATION

Reliability of pulse oximetry at four different attachment sites in immobilized white rhinoceros (*Ceratotherium simum*)

Thembeka K Mtetwa[a,b], **Edward P Snelling**[b,c], **Peter Buss**[d], **Gareth E Zeiler**[e] & **Leith CR Meyer**[a,b]

[a]Department of Paraclinical Sciences, Faculty of Veterinary Science, University of Pretoria, Onderstepoort, South Africa
[b]Centre for Veterinary Wildlife Research, Faculty of Veterinary Science, University of Pretoria, Onderstepoort, South Africa
[c]Department of Anatomy and Physiology, Faculty of Veterinary Science, University of Pretoria, Onderstepoort, South Africa
[d]Veterinary Wildlife Services, South African National Parks, Kruger National Park, Skukuza, South Africa
[e]Department of Companion Animal Clinical Studies, Faculty of Veterinary Science, University of Pretoria, Onderstepoort, South Africa

Correspondence: Department of Paraclinical Sciences, Faculty of Veterinary Science, University of Pretoria, Private Bag X04, Onderstepoort, Gauteng 0110, South Africa. E-mail: u04892497@tuks.co.za

Abstract

Objectives To determine the reliability of peripheral oxygen haemoglobin saturation (SpO_2), measured by a Nonin PalmSAT 2500A pulse oximeter with 2000T transflectance probes at four attachment sites (third eyelid, cheek, rectum and tail), by comparing these measurements to arterial oxygen haemoglobin saturation (SaO_2), measured by an AVOXimeter 4000 co-oximeter reference method in immobilized white rhinoceros (*Ceratotherium simum*).

Study design Randomized crossover study.

Animals A convenience sample of eight wild-caught male white rhinoceros.

Methods White rhinoceros were immobilized with etorphine (0.0026 ± 0.0002 mg kg^{-1}, mean ± standard deviation) intramuscularly, after which the pinna was aseptically prepared for arterial blood sample collection, and four pulse oximeters with transflectance probes were fixed securely to their attachment sites (third eyelid, cheek, rectum and tail). At 30 minutes following recumbency resulting from etorphine administration, the animals were given either butorphanol (0.026 ± 0.0001 mg kg^{-1}) or an equivalent volume of saline intravenously. At 60 minutes following recumbency, insufflated oxygen (15 L minute^{-1} flow rate) was provided intranasally. In total, the SpO_2 paired measurements from the third eyelid ($n = 80$), cheek ($n = 67$), rectum ($n = 59$) and tail ($n = 76$) were compared with near-simultaneous SaO_2 measurements using Bland-Altman to assess bias (accuracy), precision, and the area root mean squares (ARMS) method.

Results Compared with SaO_2, SpO_2 measurements from the third eyelid were reliable (i.e., accurate and precise) above an SaO_2 range of 70% (bias = 1, precision = 3, ARMS = 3). However, SpO_2 measurements from the cheek, rectum and tail were unreliable (i.e., inaccurate or imprecise).

Conclusions and clinical relevance A Nonin PalmSAT pulse oximeter with a transflectance probe inserted into the space between the third eyelid and the sclera provided reliable SpO_2 measurements when SaO_2 was > 70%, in immobilized white rhinoceros.

Keywords chemical immobilization, co-oximetry, oxygen haemoglobin saturation, pulse oximetry.

Introduction

Hypoxaemia is a life-threatening complication that often accompanies chemical immobilization of white rhinoceros (*Ceratotherium simum*) (Reiners et al. 2019). If untreated, hypoxaemia can cause organ failure, leading to morbidity and mortality. Hence, reliable and field-friendly techniques are needed to monitor hypoxaemia, for early detection and treatment in rhinoceros.

Arterial oxygen haemoglobin saturation (SaO_2) is a useful index of blood oxygenation that can be indirectly estimated by pulse oximetry, or directly measured by co-oximetry. Co-oximetry is a spectrophotometric method that directly measures SaO_2 and is regarded as a 'reference method' for humans. Although untested in the rhinoceros, the spectrophotometric